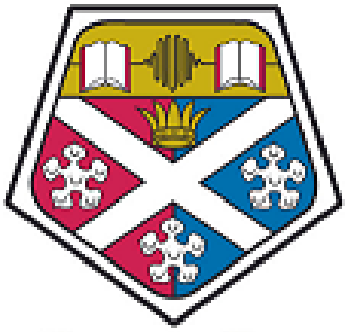

University of Strathclyde

Strathclyde Institute of Pharmacy and Bioscience

Use of time lapse microscopy in molecular genetic analysis of cardiolipin synthase homologue *SCO1389* in *Streptomyces coelicolor*.

by

Vinod Jyothikumar

A thesis presented in fulfilment of the requirements for the degree of

Doctor of Philosophy

2010

Declaration

This thesis is the result of the author's original research. It has been composed by the author and has not been previously submitted for examination which has led to the award of a degree. The copyright of this thesis belongs to the author under the terms of the United Kingdom Copyright Acts as qualified by University of Strathclyde Regulation 3.50. Due acknowledgement must always be made of the use of any material contained in, or derived from, this thesis.

Vinod Jyothikumar. Date: / / .

Dedication

To my Dad, you're someone to look up to no matter how tall I've grown.

To my best loving friend, companion, guide, to walk through life, linked hand-in-hand, my beloved wife Janani Kalyanakrishnan without your love and support this thesis would not have been written.

I remember my mother's prayers and they have always followed me. They have clung to me all my life. Finally to my brother who shares childhood memories and grown-up dreams.

Acknowledgements

SALUTATION TO TEACHER

अज्ञानतिमिरांधस्य ज्ञानांजनशलाकया।
चक्षुरुन्मीलितं येन तस्मै श्रीगुरवे नमः॥

English Translation of Sanskrit Quote:

I bow to my teacher who has opened my eyes blinded by the darkess of ignorance, with enlightening rays of knowledge.

I would like to express my respect and gratitude to my supervisor Dr. Paul Herron for his continuous guidance, support and patience. My special thanks to Prof. Iain Hunter, for providing continuous help and guidance throughout my PhD. To, Dr. Paul Hosikisson, a sincere thank you for all the discussions and patiently answering all my questions.

Big thank you to Vera Gill who helped me by providing assistance from beginning of my PhD, and made me feel comfortable and gain confidence in the lab. My sincere gratitude to all my fellow lab mates and departmental friends from over the years who provided support, friendship and intellectual debates, Thomas, Karen, Urska, Debs, Janet, Naomi, Emma.T, Russell, Laura, Leena, Badri, Maniza, James and Chris Baron. Very special thanks to Gopal valsan, Divya, Narayan, Krishna, Nishal, Lakshmi, Ram, Rob, Emma. B, Manal, Chantevy, Angzass, Dzeti and Liz for their friendship and support.

Table of Contents

Table of Figures.

Table of Tables

Abbreviations

Standard Units

°C - Degress Celsius

g – gram

k – kilo

L – litre

M – Molar

Ω- ohms

Psi – pounds per square inch

V – volt

W – Watt

σ-sigma

μ-micro

α-alpha

Φ-phi

Δ-mutant

~-more or less

β-beta

λ-lambda

DNA Bases

A - Adenine

C – Cytosine

G – Guanine

T – Thymine

U – Uracil

Textual abbreviations

am – apramycin

atc- Anhydrotetracyline

amp - amplicillin

BLAST - Basic local alignment tool

bp - base pairs

CL-cardiolipin

chl^{r}-Chloramphenicol

DNA - Deoxyribonucleic acid

DNase – Deoxyribonulease

dATP - deoxyadenisine 5'-triphosphate

dCTP - deoxycytidine 5'-triphosphate

dGTP - deoxyguanidine 5'-triphosphate

dNTP - dinucleoside 5'-triphosphate

dsDNA - double stranded deoxyribonucleic acid

dTTP - deoxythymidine 5'-triphosphate

EDTA – Ethylendiaminotetraacetic acid

Etbr-ethidium bromide

G/C – guanine/cytosine content

hyg-hygromycin

kb – kilobase

km-Kanamycin

L – litre

LB - Lennox Broth

mL – millilitre

mM – millimolar

MS - Mannitol Soya

nt – nucleotide

NA-Naldixic acid

NAO-10 nonyl acridine orange

OD - optical density

PCR - Polymerase chain reaction

PA-phosphatidic acid

PG-phosphotidylglycerol

PE-phosphatidyl ethanolamine

PI-phosphatidyl Inositol.

PL-phospholipid

PS-phosphatidyl serine

rpm - revolutions per minute

RNase - Ribonuclease

SDS - sodium deodecyl sulphate

SDW – sterile distilled water

strep^{r}-Streptomycin

spec^{r}-Spectinomycin

sp - species

ssDNA - single stranded deoxyribonucleic acid

tet^{r} – tetracycline

tsr^{r}- thiostrepton

Tm – melting temperature

Tris - Trishydroxymethylaminomethane

v/v - volume to volume ratio

w/w - weight to weight ratio

w/v - weight to volume ratio

WGA-wheat germ agglutinin

YEME - Yeast Extract-Malt Extract Medium

x-gal - 5-bromo-4chloro-3indoyl-β-D-galactoside

Abstract

Streptomycetes have a complex morphogenetic programme with formation of aerial hyphae that develop into chains of spores. After spore dispersal, environmental signals trigger dormant spores to germinate to establish a new colony. This complexity of streptomycete microcolonies makes studying the dynamic processes that contribute to growth and development a challenging procedure. In order to study the mechanisms that underpin streptomycete growth, we have developed a system for studying hyphal extension, protein trafficking, and sporulation by time-lapse microscopy. Heterogeneous distribution of phospholipids along bacterial membrane results in the formation of domains enriched in anionic phospholipids at the cell poles and at the mid cell. Cardiolipin plays a key role in organization of bacterial membranes and forms membrane domains that participate in interaction with multi-protein complexes involved in cell division, energy metabolism, and membrane transport.

This work focuses in cloning and functional characterization of the gene encoding the cardiolipin synthase -SCO1389 in the *Streptomyces coelicolor. SCO1389,* was disrupted by replacement with an apramycin-resistant gene followed by exchange with the homologous chromosomal region. Most recombinations resulted in single crossover and none had undergone the second crossover event to delete the *SCO1389* gene. *SCO1389* could not be deleted without causing lethality, except when a second *SCO1389* copy was expressed in the same cells, which implies that *SCO1389* is involved in an essential primary metabolic process, likely membrane phospholipid biosynthesis. The proper genomic disruptions were confirmed by Southern blot hybridization. Depletion of *SCO1389* caused failure in erection of aerial hyphae and severely retards growth whilst there was enough genetic evidence that *SCO1389* is essential for growth and development, it was not clear why cells cannot grow in the absence of this gene. Over expression of *SCO1389* weakens hyphal tips, mis-shaped aerial hyphae and large anucleated spores. A *SCO1389-egfp* translational fusion was constructed, which showed distinctive regions of strong fluorescence mostly in the substrate hyphae and in few young aerial hyphae. Use of the cardiolipin specific fluorescent dye 10-*N*-nonyl-acridine orange (NAO) revealed cardiolipin rich domains in the *Escherichia coli* membrane (Mileykovskaya *et al*., 2000). Staining of *Streptomyces* cells with NAO showed that there were green fluorescence domains in the branch points, substrate hyphae, hyphal tips, aerial hyphae and in spores. These fluorescence domains were scarcely detectable in cells of the *SCO1389*-disrupted mutant. The red shift fluorescence due to stacking of two dye molecules showed same results like the green shift in mutants and M145 strains. Statistical analysis shows altering the expression level in *SCO1389* affects the growth and branching in the strain RJ118b (induced by anhydrotetracycline-atc) and RJ110 (induced by thiostrepton).

Chapter 1

Introduction

1.1 Morphological development of *Streptomyces coelicolor*.

Streptomyces are multicellular, saprophytic, Gram positive, chemo-organotropic bacteria (Hodgson, 2000) and are best known for producing over two thirds of naturally derived antibiotics currently in medical or veterinary use (Challis and Hopwood, 2003). There are over 60 species of streptomycetes, classified according to the similarity of their 16S rRNA, cell wall composition, fatty acid and lipid contents (Williams *et al.,* 1989; Anderson and Wellington., 2001). Apart from their application in various industries, streptomycetes are interesting model organism to study developmental biology because of their close relationship to Gram positive pathogens and their development complexity. The completion of the sequence of the 8.7Mb linear chromosome of *Streptomyces coelicolor*, confirmed that the chromosomes contains 7825 genes (Bentley *et al.,* 2002).

Streptomycetes are generally characterised by having a high DNA percentage of guanine and cytosine (~ 72%). The genome sequencing project has provided a key step in understanding and characterising the genes involved in cell division and chromosome segregation in this complex mycelial organism. As mutations of many cell division genes are not lethal (McCormick *et al.,* 1996; Grantcharova *et al.,* 2003), *S. coelicolor* provides a very good experimental system to understand how cell division operates in actinobacteria, such as the pathogenic and experimentally intractable *Mycobacterium tuberculosis* (Cole *et al.,* 1998) and *Corneybacterium diptheriae* (Cerdeno *et al.,* 2003). The other *Streptomyces* species used as model organisms for the study of multicellular differentiation and secondary metabolism are *Streptomyces griseus* and *Streptomyces avermitilis*, due to their industrial importance, their genome has been sequenced (Haruo *et al.,* 2003**;** Yasuo *et al.,* 2008).

1.2 Growth of substrate hyphae.

Streptomyces coelicolor is by far the genetically most studied member of the genus *Streptomyces*. The life cycle (Fig. 1), starts from a spore and involves two phases: substrate and aerial mycelium. Whilst in most unicellular bacteria, cells divide and daughter cells are separated, in *Streptomyces* the growth occurs by cell-wall extension at hyphal tips and hyphal branching that leads to a matted vegetative mycelium (Prosser and Tough, 1991). The incorporation of fresh cell wall materials takes place only at the hyphal tips (Flardh, 2003b). The growth by tip extension can be visualized using fluorescent conjugates of vancomycin FL that stains the regions of the peptidoglycan precursor (Flardh, 2003a; Daniel and Errington, 2003). The pattern of staining is different from *Escherichia coli* and *Bacillus subtilis*. The vegetative mycelium contains multiple copies of the genome with irregular cross walls. The spores germinate and develop into branching hyphae that forms the substrate mycelium; some hyphae grow away into the air to from aerial hyphae and then aerial hyphae undergo septation into multiple compartments that mature into grey, pigmented, desiccation resistant spores (Chater, 1998; Kelemen and Buttner, 1998).

In *E. coli* and *B. subtilis* cell elongation is driven by the bacterial actin homologue MreB (Carballido, 2006; Thanbichler *et al.,* 2008). In these bacteria MreB directs the insertion of new peptidoglycan into lateral walls allowing cell extension and so gives shape to the bacteria. In contrast, *Streptomyces* tip extension is independent of MreB and the peptidoglycan synthesis takes place at the tips unlike in other bacteria where it is incorporate along the lateral walls. From the genome sequence two *mreB* genes have been identified in *S. coelicolor* and are involved more in sporulation in aerial hyphae and play a less significant role in tip extension (Mazza *et al.,* 2006).

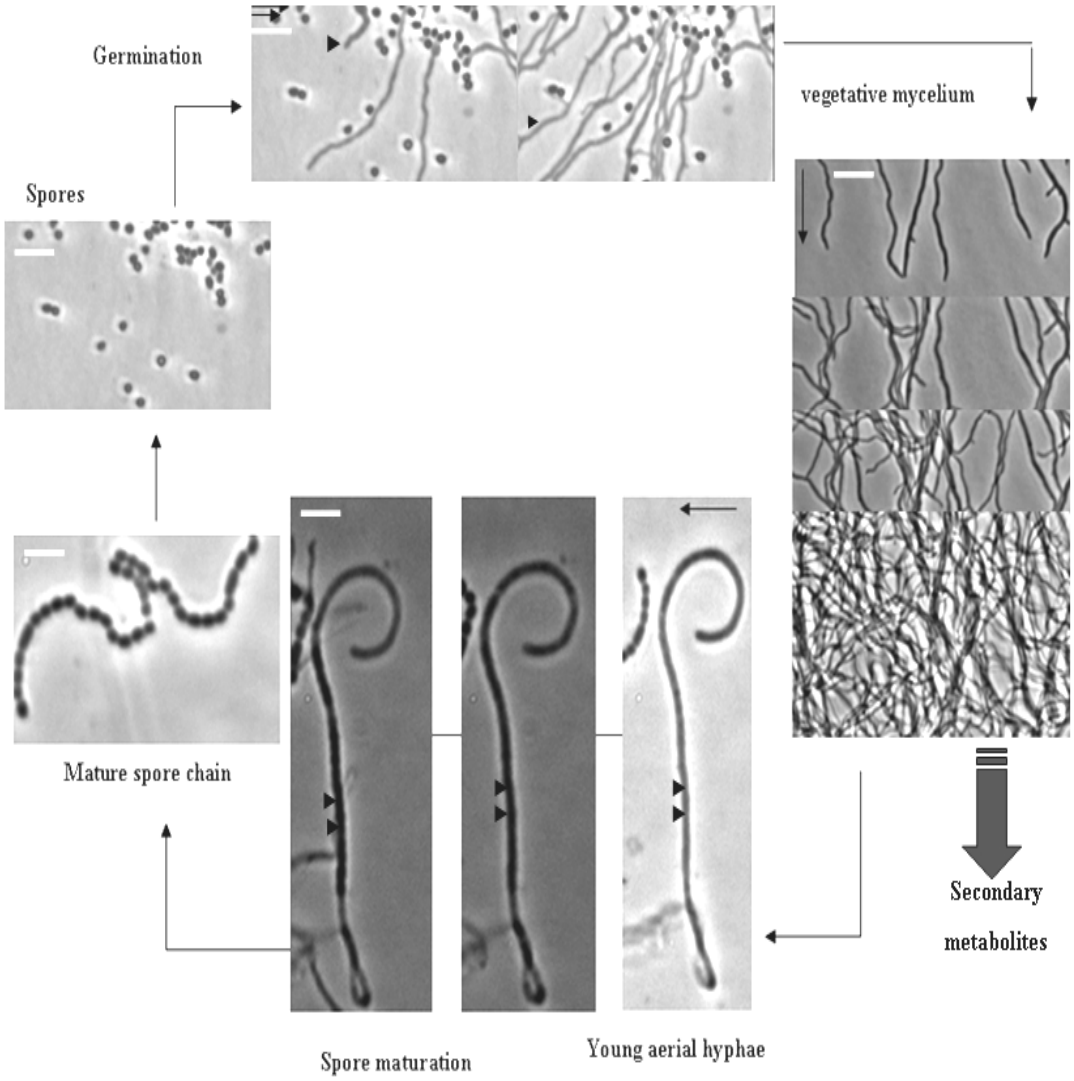

Figure 1**: Life cycle of *S. coelicolor*.**

The black arrows in germination and vegetative mycelium shows the time-lapse frames, the small arrows in young aerial hyphae and spore maturation indicates the formation of mature desiccation resistant spores and completing the cycle by germination.

There are many other actinobacteria that lack *mreB* genes, and follow a similar growth pattern to *Streptomyces* by growing apically and incorporating cell wall material at the poles (Daniel, 2003; Mazza *et al.,* 2006; Nguyen *et al.,* 2007; Letek *et al.,*2008; Hett *et al.,*2008). The protein that drives tip extension in *Streptomyces* and other actinobacteria was identified as DivIVA, a coiled coil protein (Flardh, 2003a). All the new tips and lateral branchs, that originates needs to be filled in with new chromosomes. *Streptomyces* chromosome replication takes place along the vegetative and aerial hyphae, although the rapidly extending apical compartments of the aerial mycelium have more active replication than any other compartments. (Osmiałowska *et al*., 2006). DivIVA is essential and shows a strong effect on tip extension and cell shape. In *Coryneybacterium* and *Mycobacterium* species the orthologues of DivIVA have similar localization and activity as *Streptomyces*. However, depletion of DivIVA in *Coryneybacterium* leads to loss of cell wall assembly and changes to spherical cell shape. This suggests that DivIVA is required for *mreB*-independent cell wall extension in all actinobacteria (Letek *et al.,* 2008, Hempel *et al.,* 2008, McCormick *et al.,* 1994). The hyphal tips are probably important for cellular processes functions during growth and development. Recently, cellulose synthase like protein cellulose synthase (CslA) was found at the hyphal tips and interacting with DivIVA and may be involved in deposition of a β-linked glucan during cell wall extension (Xu *et al.,* 2008).

1.3 Growth of aerial hyphae.

After the growth of substrate mycelium, *S. coelicolor* develops morphologically and erects aerial hyphae (Chater, 1993). The surface of the colonies is covered by a thick mat of white aerial mycelium that grows away from the substrate mycelium into the air. At this point, aerial hyphae obtain nutrients from the degradation of the vegetative mycelium (Challis and Hopwood, 2003; Miguelez., 1999). The formation and initiation of aerial hyphae erection is the result of a complex intracellular signalling cascade and is consistent with the switch from primary to secondary metabolism with production of antibiotics (Chater, 1998; Willey *et al.,* 2006). On a rich media, *S. coelicolor* produces the lantibiotic like peptide, SapB. These molecules contribute to a hydrophobic coating on spores (Willey *et al.,* 1993; kodani *et al.,* 2004). The gene cluster responsible for the synthesis of SapB is the *ram* cluster, which contains *ramR*, a gene that encodes for the response regulator that directly activates the *ramCSAB* operon (Kodani *et al.,* 2004; Keijser *et al.,* 2000; Nguyen *et al.,* 2002; Connor *et al.,* 2005 and 2002). Over expressing *ram* genes in *S. coelicolor* induces rapid erection of aerial hyphae (Ma *et al*., 1994). In *S. griseus* deletion of the *ram* gene causes the loss of aerial hyphae formation on a rich media, leading to a 'bald' phenotype (Keijser *et al.,* 2002; Nguyen *et al.,* 2002; Connor *et al.,* 2005; Capstick *et al*., 2007; Ueda *et al*., 2002). From biochemical evidence it was shown that RamC was similar to lantibiotic synthetases. On analysing the structure of SapB, it was shown that it is peptide derived from a 42-amino acid *ramS*-encoded pre-peptide and further modified by RamC (Kodani *et al.,* 2004). On minimal media it was noticed that although *S. coelicolor* produces aerial hyphae, no SapB was produced, indicating that *S. coelicolor* switched over to a SapB-independent pathway for aerial hyphae formation (Claessen *et al.,* 2003). This alternative pathway that produces a hydrophobic sheath for erection of aerial hyphae, involves chaplins and rodlins proteins. There are eight chaplins proteins secreted in *S. coelicolor*, *chp A, B, C, D, E, F, G* and *H*. All these proteins share a conserved hydrophobic domain of ~ 50 amino acids called the chaplin domains (Claessen *et al.,* 2003; Elliot *et al.,* 2003; Berardo *et al.,* 2008).

The chaplins are classified in two types, short and long chaplins. The five short type chaplins found in *S. coelicolor*, are *chp D, E, F, G, H* with a chaplin domain and a Sec (secretion) signal peptide. The long chaplins consist of *chp A, B,* and *C*, and have an amino terminal and a Sec signal peptide. The mechanism for the erection of aerial hyphae is through the assembly of chaplins into amyloid like filaments at the air-water interfaces. Here the short chaplins are anchored to the surface of aerial hyphae through hetero-polymerization and the long chaplins anchored to the cell wall, to form hydrophobic filaments. On rich and poor media the expression of *chp* genes was activated before the erection of aerial hyphae. However, on deletion of *chp* genes, *S. coelicolor* cannot produce aerial filaments on minimal media and is severely affected on rich media (Claessen *et al*., 2004). The other protein which contributes to the hydrophobic sheath is the rodlin proteins; RdlA and RdlB (Claessen *et al.,* 2002). Mutants that lack both *rdlA* and *rdlB* still form hydrophobic sheath and normal aerial hyphae. However, strains that cannot produce both SapB and chaplins are 'bald' under all growth conditions (Capstick *et al.*, 2007).

1.3.1 Role of *bld* genes during aerial hyphae formation.

During genetic screening studies in *S. coelicolor*, a number of mutants were isolated that were blocked in aerial mycelium formation (termed *bld* mutants for their bald colony appearance) or in the spore chain maturation process (termed as *whi* mutants for their white colony coloration). At least 10 *bld* loci, *bldA*, *bldB*, *bldC*, *bldD*, *bldF*, *bldG*, *bldH*, *bldI*, *bldK*, and *bld261*, have been found in *S. coelicolor* (Champness, 1988; Merrick, 1976, Nodwell *et al.,* 1996; Willey *et al.,* 1991,1993) and blocked at an early stage in the initiation of development. From the standard genetic code, one of the six codons for leucine (UUA) has no G or C residues, and is codon is rarely used in streptomycetes. The *bldA* codes for the gene leucyl-tRNA that recognizes the UUA codon (Lawlor *et al*., 1987; Leskiw *et al*., 1991). It has been suggested that this tRNA is involved in the translation of regulatory genes, which is involved in antibiotic production and morphogenesis (Fernandez *et al.,* 1991; Leskiw *et al.,* 1991a, 1991b).

However, mutations in *bldA* do have phenotypic effects; the most obvious are bald colonies that are devoid of pigmented secondary metabolites (Merrick, 1976). Expression of *bldA* increases during initial growth development and the gene is active during vegetative growth (Wezel *et al.,* 1997). Microscopic examination of colonies of *bldA* mutants reveal that they are covered with malformed, aberrant hyphae (Merrick, 1976), which are probably defective aerial hyphae. The complexity of this phenotype suggests that *bldA* may have a regulatory role in many aspects of developmental biology. A *bldA*-like tRNA locus is present in all actinobacteria. However, TTA codons are more frequent in the genomes of other actinobacteria. In *S. coelicolor*, 22% of TTA codons occur in the first 10 codons, compared to 9% in *N. farcinica* (Fuglsang, 2005). The frequent observation on effects of *bldA* mutations on antibiotic production are mostly exerted directly via UUA codons (Chater & Horinouchi, 2003; Chater, 2006). The *bldA* mutant phenotype is carbon source dependent; on glucose or cellobiose, or in the presence of glucose in a mixture of carbon sources, colonies are bald, whereas a carbon source, such as maltose, galactose, or mannitol, the bald phenotype is suppressed and sporulation occurs (Piret *et al.,* 1985). Similarly, growth on mannitol rescues both sporulation and antibiotic production in *bldH* mutants (Champness, 1988). These observations strongly suggest that there is a direct connection between the regulation of carbon utilization and the initiation of morphogenesis in streptomycetes. During screening for mutants defective in catabolite control some mutants were identified that were resistant to glucose repression, but defective in the regulation of antibiotic production and are *bld* (Pope *et al.,* 1996).

One of the 11 TTA-containing genes common to *S. coelicolor* and *S. avermitilis* is *adpA*, or *bldH* (*SCO2792*) - (Nguyen *et al*., 2003; Takano *et al*., 2003). This gene was first studied in *S. griseus* (Ohnishi *et al*., 2005), where it contains a TTA codon, as in the other two orthologues. In *S. coelicolor*, this TTA codon is the major route through which *bldA* influences development; while in *S. griseus* the influence of *bldA* on antibiotic production is partially mediated via *adpA*. This shows the role of *adpA* in *Streptomyces.*

Thus, in *S. griseus*, *adpA* expression is directly regulated by a repressor protein called ArpA ('A-factor receptor protein'); on the other hand *adpA* repression is removed by an extracellular accumulation of the γ-butyrolactone A-factor (see section 1.3.2). Production of SapB is impaired in *bld* mutants and aerial mycelium formation could be restored at the edges of *bld* mutant colonies, when grown close to nearby SapB-producing colonies. Interestingly, when two *bld* mutants were grown together the production of aerial hyphae was restored at the edges of colonies and the cells started to sporulate. This suggests that differentiation was governed by a hierarchical cascade of intercellular signals (Nodwell *et al.*, 1996, Willey *et al.,* 1993). This extracellular complementation is always unidirectional, with one *bld* mutant acting as a "donor" and the other as a "recipient." All *bld* mutants can be restored in the order as follows: *bldJ-bldKbldL-bldA*, *bldH-bldG-bldC-bldD-bldM*, eventually causing the *bldD*-dependent production of SapB, which allows aerial hyphae to overcome surface tension and grow into the air (Nodwell *et al*. 1996, 1998, 1999; Willey *et al.,* 1993; Elliot, *et al.,* 1998).

BldD mutant was capable of complementing all of the other *bld* mutants and is at the top of the hierarchy. There is also evidence that a covalently modified oligopeptide rescues development in a *bldJ* mutant in a *bldK*-dependent manner (Nodwell *et al*. 1996). BldK (Nodwell *et al.* 1996) is an oligopeptide transporter and is perhaps responsible for the import of an extracellular signal required for the initiation of morphogenesis. BldB mutants form very smooth colonies, leathery in texture, apparently composed only of substrate mycelium. Eight independent *bld* mutants have been assigned to *bldB,* (Merrick, 1976; Champness, 1988), and are of special interest because their phenotype is the most pleiotropic of all *bld* mutants and are completely defective in antibiotic production (Champness, 1988). The *bldB* mutants are also defective in the regulation of carbon utilization (Pope *et al.,* 1996; Merrick, 1976). Out of all the *bld* mutants, *bldB* phenotype is not rescued by different carbon sources or by extracellular complementation (Champness, 1988, Merrick, 1976, Pope *et al.,* 1996). BldC gene encodes a small protein, with similarity to MerR family DNA-binding proteins in *S. coelicolor* and *S. avermitilis*, (Hunt *et al*., 2005).

The *bldG* gene encodes an anti-σ factor (Bignell *et al*., 2000). The interaction between BldG proteins depends on the phosphorylation state of an anti-anti-σ factor (BldG). The phosphorylation state of the BldG is determined by the three factors, the availability of phosphorylated form of BldG, the kinase activity of the anti-σ factor and the dephosphorylation state of BldG (Hesketh *et al*., 2002; Bignell *et al*., 2003). BldD is a regulatory protein that possesses a putative DNA binding domain similar to those of Xre-like regulators (Elliot *et al*., 1998). It represses its own expression and that of several other developmental genes including *bldN* and *whiG* (Elliot & Leskiw, 1999; Elliot *et al*., 2001). A whiK null mutant was bald, as a consequence of the null mutant phenotype, *whiK* was renamed *bldM*, that encodes a response regulator, a class of proteins involved in signal transduction, typically in conjunction with a membrane-localized, cognate sensor kinase (Molle and Buttner, 2000). Recent reports show that a *bldM* null mutant when grown near to other *bld* mutants; aerial mycelium formation was restored in *bldJ*, *bldK*, *bldA*, *bldH*, *bldG* and *bldC* mutants. In contrast, *bldM* failed to restore aerial mycelium formation to a *bldD* mutant, and the *bldD* mutant also failed to restore aerial mycelium formation to *bldM*. BldM therefore fits into the proposed hierarchy and is a member of the *bldD* extracellular complementation group (Willey *et al.*, 1993; Nodwell *et al*., 1996; 1999; Nodwell and Losick, 1998).

The gene *bldN* encodes a member of the extracytoplasmic function (ECF) subfamily of RNA polymerase sigma factors and has a unique N-terminal extension of approximately 86 residues that is not found in other sigma factors. σ_{BldN} is required for the transcription of one of two promoters of *bldM* (Bibb *et al*., 2000). An important consequence of the expression of *bldM* is the activation of the *chp* genes encoding the morphogenetic chaplin proteins (Elliot *et al*., 2003). Interestingly, some *bldM* and *bldN* alleles give rise to a white aerial mycelium phenotype (Ryding *et al*., 1999), suggesting that they are both needed for development.

The *bldN* orthologue in the *S. griseus* is 84% identical to *adsA*, which is a direct target of AdpA (Yamazaki *et al*., 2000); and *bldN* transcription is also *bldH*-dependent in *S. coelicolor* (Bibb *et al*., 2000). However, it is not clear if AdpA and BldD both interact with *bldN* in *S.coelicolor*. A second BldD-binding site in *bldN* corresponds to the segment of the promoter region that is expected to interact with RNA polymerase (Elliot *et al*., 2001), which is highly conserved among the actinobacteria.

1.3.2 Role of A-factor in development of aerial hyphae.

A-factor (2-(6`-methylheptanoyl)-3R-hydroxymethy-4 butanolide) triggers both aerial mycelium formation and streptomycin biosynthesis in *S. griseus*. A-factor is a γ-butyrolactone signalling molecule, which leads to initiation of aerial mycelium formation in *S. griseus*. In streptomcetes, γ-butyrolactone is widely produced, but their roles vary from species to species (Nishida *et al*., 2007; Takano, 2006; Chater *et al.,* 2003). A low concentration of A-factor is needed for the effects on *Streptomyces* growth. Therefore it has been deemed as a "microbial hormone". A-factor expresses its regulatory function by binding to A-factor binding protein leading to regulation of genes that are important for secondary metabolism and sporulation. (Horinouchi, 2002; Kato *et al*., 2002; Takano *et al*., 2003; Takano *et al*., 2005). In *S. griseus*, other than the repression effect of A-factor on *adpA,* the other direct targets of AdpA includes the genes as σ^{AdsA}, Extracytoplasmic factor-ECF, SsgA (a protein that influences septum formation) and AmfR (a response regulator that influences septum formation) controls the *amfTSBA* operon (Yamazaki *et al.,* 2000, Yamazaki *et al.,* 2003a & 2003b). However in *S. griseus adpA* is autoregulatory, contributing to its own transcriptional repression (Kato *et al*., 2005). Four out of six of the AdpA-binding sites of the *adpA* promoter of *S. griseus* are conserved in the *adpA* promoter regions of *S. coelicolor* and *S. avermitilis* (Kato *et al*., 2005). Although AdpA orthologues are known only in streptomycetes, AdpA belongs to a subfamily within the family of activator/repressor proteins whose best-known member is AraC of *E. coli* (Yamazaki *et al*., 2004; Kato *et al*., 2005).

1.4 Sporulation of aerial mycelium.

After the erection of aerial mycelium (Fig. 1), the apical part of the aerial hyphae stops growing and the hyphae undergo multiple septation, which results in formation of unigenomic spores. Through genetic screening a group of genes was identified, the *whi* genes, which regulate sporulation (Chater, 1972). White mutants forms two groups, the early *whi* mutants that fail to produce sporulation septa (Chater, 1972, McVittie, 1974), while the late *whi* mutants are defective during subsequent spore maturation (Chater, 1993; Davis and Chater, 1990; Kelemen *et al.,* 1998). The *whi* genes are involved in a network of developmental check points and in sporulation (Chater, 2000, 2001, 2006). The family of early *whi* genes consists of *whiG*, *whiA*, *whiB*, *whiH*, and *whiI*.

whiG (*SCO5621*) genes of several other streptomycetes play a role in erection of aerial hyphae and sporulation. These genes carry highly conserved coding regions that are characterized by BldD-binding sites in *S. coelicolor* (Soliveri *et al.,* 1993; Kormanec *et al.,* 1994; Elliot *et al.,* 2001; Catakli *et al.,* 2005). *whiG* encodes an sigma factor, σ^{whiG} , required for the initiation of the sporulation program (Tan *et al.,* 1998; Mendez & Chater, 1987; Chater *et al.,* 1989). The *whi*G promoter is repressed by the BldD developemental regulator, which shuts off many developmental genes during vegetative growth (Elliot *et al.,* 2001). This dependence of *whiG* expression on BldD is the first evidence of a link between *whi* and *bld* genes. σ^{whiG} RNA polymerase holoenzyme transcribes the early sporulation genes *whiH* (Ryding *et al.,* 1998) and *whiI* (Ainsa *et al.,* 1999; Ryding *et al.,* 1999).

These two sporulation regulatory genes, *whiH* (*SCO5819*) and *whiI* (*SCO6029*) are well established targets for σ^{WhiG} RNA polymerase holoenzyme (Ryding *et al.,* 1998; Ainsa *et al.,* 1999; Kormanec *et al.,* 1999). Each gene encodes a member of regulatory DNA-binding proteins. WhiH belongs to GntR superfamily, a class of transcriptional regulators that typically respond to metabolite effector molecules. WhiH responds to a change in concentration of such a metabolite during aerial mycelium growth (Fig. 1) (Ryding *et al.,* 1998).

WhiH appears to induce the strong developmentally controlled *ftsZ* promoter to bring about sporulation septation (Flardh *et al.,* 2000). WhiI resembles the response regulators associated with bacterial two-component systems (Ainsa *et al.,* 1999). There is circumstantial evidence that different genes are induced or repressed by different forms of WhiI, and it also responds to a phosphorylated intermediary metabolite rather than being phosphorylated by a histidine protein kinase. WhiI may be involved in the chromosome condensation that accompanies sporulation (Ainsa *et al.,* 1999). *whiA* (*SCO1950*) and *whiB* (*SCO3034*) are two genes which are expressed during the early stages of sporulation and are independent of *whi*G expression. *whiA* and *whiB* mutants both have unusually long and curly aerial hyphae that completely lack sporulation septa (Flardh *et al.,* 1999). The developmentally controlled expression of *whiA* and *whiB* in *S. coelicolor* (Soliveri *et al.,* 1992; Ainsa *et al.,* 2000) and in *S. aureofaciens* (Soliveri *et al.,* 1992) appears to be largely independent of *whiG*. The *whiA* gene is located in a cluster that shows significant conservation across all Gram-positive bacteria. *whiA* is expressed at a low level throughout growth and is strongly upregulated during aerial hyphal development, (Ainsa *et al.,* 2000).The distribution of *whiB*-like (‘*wbl*’) genes is quite different from that of *whiA* homologues. They are members of a substantial family of generally small (80–120 aa) proteins whose major conserved features are a set of four cysteine residues and a short glycine- and tryptophan-rich segment (Soliveri *et al.,* 2000). Several WhiB like proteins are widespread among actinobacteria. Several *wbl* genes and their products have been studied experimentally in streptomycetes and mycobacteria. One of these, *whiD*, is a late sporulation gene in *S. coelicolor* (Chater, 1972; Molle *et al.,* 2000). The physiological stimulus for the activity of Wbl proteins is generated by a redox change which associated with four conserved cysteine residues (Soliveri *et al.,* 2000); and the idea of redox sensing has received support from evidence that WhiD contains an oxygen-sensitive 4Fe-4S cluster (Jakimowicz *et al.,* 2005; Alam *et al*.,2007). *whiD* mutants formed sporulation septa but failed to go on to produce mature spores. These spores are unpigmented, thinwalled, and showed frequent lysis (McVittie, 1974; Molle *et al.,* 2000). However, there are many other loci identified for developmental genes that are involved during sporulation in *S. coelicolor* (Potuckova *et al.,* 1995; Ryding *et al.,* 1999).

The *whiE* locus (SCO5314–5321) is a cluster of eight genes, most of which encode recognizable enzymes of polyketide biosynthesis (Davis and Chater, 1990). Importantly, *whiE* gene specifies the grey spore pigment which acts as an excellent marker for genetic analysis during sporulation (Fig. 1). Mutations in *whiE* genes cause a loss of spore pigment or a change in spore colour (Shen *et al.,* 1999; Moore & Piel, 2000). The *whiE* genes have two transcription units, both of which are switched on only during sporulation. The promoters of *whiE* genes are dependent on all the early *whi* genes (Kelemen *et al*., 1998). Remarkably, the genome of *S. griseus* does not contain a *whiE* gene cluster. Moreover, *whiE* mutants do not appear morphologically defective (Davis *et al*., 1990; Kelemen *et al.,* 1998; Chater, 2006).

1.4.1 Other genes affecting sporulation in *Streptomyces*.

The σ factor encoded by *sigF* (*SCO4035*) is required for the late stages of sporulation (Potuckova *et al.,* 1995; Kormanec *et al.,* 1996; Kelemen *et al.,* 1996). A *sigF* mutant undergoes sporulation septation, but the resulting spore chains are irregular, thin-walled and more or less unpigmented, and contain uncondensed DNA. Interestingly, σ^F is a member of the same subgroup of Gram-positive-specific σ factors, called σ^B belonging to *B. subtilis* stress-response. There are nine σ^B like stress response sigma factors in *S. coelicolor;* one of them is *sigF*. Evidence shows that *sigF* controls one of the promoters of *whiE* gene cluster. The other σ factors that affect the development and stress response are σ^B and σ^H. σ^B is a master regulator for osmotic stress response in *S. coelicolor*, governing induction of more than 280 genes. σ^B is regulated at transcriptional level for its synthesis and post-translationally for its activity through interaction of its antisigma factor (RsbA) with an antianti-sigma factor (RsbV), involving phospho-relay mechanism (Lee *et al* ., 2004). σ^H is regulated at levels of transcription, translation start site selection, protein processing and possibly interaction with an antisigma factor (PrsH/UshX) (Sevcikova *et al.*, 2001; Sevcikova and Kormanec, 2002; Viollier *et al* ., 2003a,b). σ^I increases rapidly upon osmotic stress, most likely via increased transcription (Viollier *et al*., 2003a). σ^B, σ^H, σ^F and σ^{WhiG} have been also implicated in controlling proper differentiation (Chater *et al*., 1989; Potuckova *et al*., 1995; Cho *et al*., 2001; Sevcikova *et al*., 2001).

The *ssgA* gene was first identified in *S. griseus* (*SAV4267*) as a hypersporulating mutant (Kawamoto *et al.,* 1997), and is required for correct sporulation septation of *S. griseus* (Jiang & Kendrick, 2000; Traag *et al.,* 2004). *S. coelicolor* has six other *ssgA* (*SCO3926*) paralogues and *S. avermitilis* five (SALP-SsgA-like proteins). One of the paralogues in *S. coelicolor*, *ssgB* (*SCO1541*), is also involved in sporulation the mutant of this gene was white and completely defective in sporulation and septation, and, large-colony phenotype (Keijser *et al.,* 2003). *ssgB* is not necessary for *ssgA* expression. Analysis of mutants on *ssgA*-like genes of *S. coelicolor*, have shown to affect the peptidoglycan biosynthesis, sporulation, septation and spore morphogenesis (Noens *et al.,* 2005).

Another interesting gene that affects sporulation and aerial mycelium in *Streptomyces* is *crgA* (Del Sol *et al.,* 2003). This protein encodes a small, membrane-bound protein that inhibits premature sporulation septation in *S. coelicolor*. A *crgA* mutant showed premature aerial mycelium growth and sporulation, as well as early production of the blue antibiotic actinorhodin. On the other hand, a *crgA* mutant of *S. avermitilis* had white, coiled, non-sporulating aerial mycelium. Over expression of *crgA* in both species gave white colonies in which the aerial hyphae did not undergo sporulation septation. The disruption of *samR* (SCO2935) causes colonies to produce fluffy, nonsporulating aerial mycelium similar to that of a *whiG* mutant (Tan *et al.,* 1998). The product of *samR* is a member of the IclR family of transcriptional regulators, and has no orthologues outside of streptomycetes. On solid agar medium glycogen accumulates in two distinct locations. Phase I deposits are found in a substrate mycelium region bordering the developing aerial mycelium, by GlgBI Phase II deposits occur in the upper regions of aerial hyphae, in long tip cells that are dividing into unigenomic prespore compartments. Their formation involves a second branching enzyme isoform, GlgBII, which is regulated (directly or indirectly) by *whiG* (Schneider *et al.,* 2000; Yeo & Chater, 2005).

Recent studies have identified more developmental mutants in the new *cmdABCDEF* gene cluster. Deletions of this cluster showed over-production of actinorhodin, defective sporulation and especially abnormalities in chromosome segregation, indicating that *cmdABCDEF* are new genes that affects the antibiotic production and differentiation of *S. coelicolor* (Xie *et al.,* 2009).

The morphological changes associated with development involve several other proteins that are associated with sporulation septation (Fig. 1). These include FtsZ and ParAB, which are expressed during vegetative growth and differentiation (Flardh *et al.,* 2000; Jakimowicz *et al.,* 2006). During growth cessation it is thought that *whiI* and *whiH* activate signals which in turn regulate FtsZ and DNA condensation mechanisms and finally leads to sporulation septation. Nucleoid condensation and septation takes place through a cascade of signalling events (Flardh, 2003) which results with in polymerization of the tubulin homologue FtsZ into Z ring (Schweddock *et al.,* 1997; Grantcharova, 2005).

1.5 A general overview of bacterial cell division.

Bacteria undergo binary fission, where one cell divides into two progeny cells. The complete process is called cytokinesis, which is highly regulated in time in order to achieve a successful partitioning of the chromosome. Cytokinesis starts with the assembly of the prokaryotic tubulin homologue, FtsZ, in a ring like structure at the mid of the cell (Bi and Lutkenhaus, 1991; Lowe and Amos, 1998). The Z ring is assembled in the midcell and utilizes the energy released by GTP hydrolysis (de Boer *et al*., 1992). During this process, the Z ring recruits a number of proteins required to complete the cell division. FtsZ is a highly conserved protein. It is the main cell division protein in most bacteria and in the archaea. FtsZ contains four protein regions; a variable N-terminal segment, a highly conserved core region, a variable linker, and a C-terminal tail (Margolin, 2005; Vaughan *et al*., 2004). The C-terminal tail of *E. coli* FtsZ binds to the two cell division proteins, FtsA and ZipA (Ma and Margolin, 1999; Pichoff and Lutkenhaus, 2002). The Z ring is remarkably dynamic, it is able to assemble and disassemble quickly (Addinall *et al*., 1997; Sun and Margolin, 1998). During the cell cycle of *E. coli* the Z rings goes through a series of phases of assembly, steady state turnover and disassembly. The assembly of the cell division machinery, the divisome, begins with the formation of a Z ring which recruits a set of other proteins to the division site (Errington *et al*., 2003; Margolin, 2005; Weiss, 2004). The number of protein partners that assemble at the divisome varies significantly between species. In *E. coli* the divisome comprises at least 12 proteins. These proteins that are recruited by the divisome have multiple functions throughout cell division. The assembly of FtsZ is modulated by FtsA, ZipA & ZapA. Anchoring of the Z ring to the membrane involves FtsA and ZapA, coordination of the division and chromosome segregation, FtsK. Peptidoglycan synthesis is carried out by FtsI and FtsW; whilst the other known proteins involved during cell division are FtsEX, FtsQ, FtsB, FtsL, and FtsN. The proteins of the divisome are engaged in multiple interactions during cell division. It has been shown that FtsA and ZipA in *E. coli* interact directly with C-terminal of FtsZ (Pichoff and Lutkenhaus, 2002), which are required for stabilizing the Z ring assembly.

The ZapA protein from *B. subtilis* also binds directly to FtsZ (Gueiros-Filho and Losick, 2002). Once FtsA and ZipA are bound to the Z ring the remaining proteins are recruited in a defined and hierarchical order (Buddelmeijer and Beckwith, 2002) as follows:

FtsE+FtsX → FtsK → FtsQ → FtsL+FtsB → FtsW FtsI → FtsN ▸ AmiC

Cell division normally follows each round of chromosome replication in *E. coli* (Donachie, 2001). It has been suggested that assembly of the Z ring is coupled to chromosome replication in *E. coli*, *B. subtilis* and *C. crescentus* (Blaauwen *et al*., 1999; Harry *et al*., 1999; Quardokus and Brun, 2002; Regamey *et al*., 2000). However, blocking the initiation of DNA replication does not prevent the Z ring assembly (Gullbrand and Nordstrom, 2000; Harry *et al*., 1999; Sun and Margolin, 2001). The spatial regulation of cell division is determined by the site for Z-ring placement and is controlled by the Min system in *E. coli* which consists of three proteins. MinC acts as the inhibitor of FtsZ assembly (Hu *et al*., 1999). MinD forms a complex with MinC that oscillates from one cell pole to other causing FtsZ depolymerisation (Raskin and Boer, 1999b). MinE determines the specific site for the mode of action of MinCD complex (Raskin and Boer, 1999a). MinE is also capable of displacing MinC from the membrane –bound MinCD complex (Hu *et al*., 2003; Ma *et al.*, 2004; Suefuji *et al*., 2002). MinE binds to MinD and stimulates the ATPase activity which leads to dissociation of MinD from the membrane. MinD-ADP then travels to the other end of the cell pole, where the concentration of MinE is low and associate to form MinD-ATP and assembles back into the membrane (Hu and Lutkenhaus, 2001; Huang *et al*., 2003; Suefuji *et al*., 2002). This oscillatory behaviour of MinCD complex maintains the concentration of MinC at the poles and regulates the assembly the Z- ring during cell division. The MinCD complexes of *B. subtilis* are static and anchored to both poles via the DivIVA protein (Marston *et al*., 1998). However, in many bacterial species like *Caulobacter crescentus* and *S. coelicolor* lack a Min system, showing that these proteins are not universally conserved.

1.5.1 A detailed note on role of FtsK during cell division in bacteria.

FtsK/SpoIIIE proteins belong to AAA+ super family of proteins that are involved in a wide range of functions, use ATP as the source of energy and include a range of family members, such as DNA translocases, helicases, motor proteins, clamp loaders and other ATP dependent enzymes (Greg *et al.,* 2005). The other proteins with similar functions are TraSA of *Streptomyces ambofaciens* (Possoz *et al.,* 2001), SpoIIIE of *B. subtilis* (Sigal *et al.,* 2003; NaiJia *et al.,* 2006), FtsK in *E. coli* (Begg *et al.,* 1995). FtsK in *E. coli* is a bi-functional protein (Liu *et al.,* 1998), its N terminal membrane domain is localised to the division septum (Wang *et al.,* 1998; Yu *et al.,* 1998) and is necessary for septal formation (Draper *et al.,* 1998; Chen *et al.,* 2001). While its C-terminal motor domain ($FtsK_c$) is implicated in chromosome dimer resolution (Possoz *et al.,* 2001; Aussel *et al.,* 2002) and chromosome segregation (Liu *et al.,* 1998; Yu *et al.,* 1998; Capiaux *et al.,* 2002; Corre *et al.,* 2002). The newly formed chromosomes are prone to recombination that produces a dimer. Prior to segregation, these dimers must be resolved into monomeric chromosomes. The resolution in *E. coli* occurs at a specific locus, known as *dif* sites (deletion induced filamentation) along with XerC and XerD. XerC and XerD belong to the lambda integrase family. Individually, the XerD protein acts as a type I topoisomerase and relaxes the super coils by nicking one strand of the *dif* site (Draper *et al.,* 2002; Bigot *et al.,* 2005; Lesterlin *et al.,* 2004). Subsequently the resolved chromosomes are translocated through the division septum by $FtsK_c$ (Yu *et al.,* 1998; Donachie, 2002; Lau *et al.,* 2003; Lavy *et al.,* 2005; Paul *et al.,* 2005). SpoIIIE is the FtsK counterpart in *B. subtilis* and also plays a vital role in its assembly during cell division. The translocation of DNA by SpoIIIE prevents chromosome trapping by the division septum (Ben *et al.,* 2003). As a result, DNA anchoring is responsible for the assembly of SpoIIIE and other DNA translocase like proteins to remove the trapped chromosomes from the division septum and allow the cells to resume binary division. SpoIIIE is also responsible for the transport of the chromosome into the small polar pre-spore compartment during sporulation (Bath *et al.,* 2000). Recent evidence shows that SpoIIIE DNA translocase participates in membrane fusion during cytokinesis and engulfment (Liu *et al.,* 2006).

1.6 Introduction to cell division in *S. coelicolor*.

The complex life cycle of streptomycetes imparts a unique cell division process to this group when compared to other bacterial systems. Cell division in streptomycetes is different with respect to septal morphology, chromosome segregation (Flardh and Wezel, 2003). In the multicellular mycelium the individual cell compartments sizes are limited by the cross wall and contain multiple copies of the chromosome. The hyphal cells of *S. coelicolor* grow by tip extension, where nascent peptidoglycan is incorporated at the tips of the growing hyphal cells (Flardh, 2003; Gray *et al*., 1990; Miguelez *et al*., 1992). Cell division only occurs during sporulation and needs to be co-ordinated with chromosome replication and segregation in order to maintain a systematic partitioning of DNA in the spores. Cell division in *S. coelicolor* starts with the assembly of FtsZ at the division sites (Flardh and Wezel, 2003; Schwedock *et al*., 1997). Although FtsZ is essential for cell division, deletion mutants are viable with non-septated branching of hyphae (McCormick *et al*., 1994). *S. coelicolor* is unique among most of bacterial species as it is able to survive deletion of *ftsZ*, and thus making it an excellent model for genetic studies. Several cell division proteins are encoded in the highly conserved *dcw* gene cluster (division and cell wall synthesis) in many bacterial species (Mingorance *et al*., 2004). In *S. coelicolor*, *dcw* consists of *ftsL, ftsI, ftsZ, ftsQ* and *ftsZ*. FtsQ is a cytoplasmic membrane protein which is required throughout cell division in *E. coli*. FtsQ is dispensable for growth of *S. coelicolor* but is required for the efficient subdivision of aerial filaments into uni-nucleoid spores (McCormick *et al.,* 1996). FtsZ in *S. coelicolor* is required for both vegetative cross walls and sporulation septation and Z rings are formed in both cases for efficient controlled cell division in sporogenic hyphae (Grantcharova *et al.,* 2003; Grantcharova *et al.,* 2005). It has been postulated that nucleoids migrate in *Streptomyces*, such that the chromosome move in relation to the cell envelope tip and populate the extending tips and lateral branchs (Flardh, 2003). Deletions of major divisome genes like *ftsI, ftsK, ftsL, ftsW* and *divIC* in *S. coelicolor* showed some variable defects on sporulation and none affected the cell division organism (Bennett *et al*., 2002; McCormick, 2001).

Most of the cell division proteins that contribute to the assembly of the Z ring and it's anchoring in the membrane in *E. coli* and *B. subtilis* are absent in streptomycetes. On the contrary, FtsZ in *mycobacteria* interacts with C-terminal tail of the protein FtsW, there by stabilizing the membrane anchoring of Z ring (Datta *et al*., 2002; 2004). Recent studies show the role for putative FtsW-FtsI and their interaction with Z-ring assembly in *S. coelicolor* (Mistry *et al*., 2008).

The exact manner of nucleoids migration in *Streptomyces* is still unknown. In *Streptomyces* there is no Min system in contrast to rest of the bacterial family. In *E. coli* the Min system involves three proteins MinCDE and two proteins MinCD in *B. subtilis* along with DivIVA (functional homologue of MinE). In contrast, *Streptomyces* growth involves hyphal extension at the tips; this type of tubular growth extension in bacteria is not unique to *Streptomyces*. DivIVAsc (Section 1.2) the *Streptomyces* homologue of the *B. subtilis* protein DivIVA is essential for the tip extension and polar growth in *S. coelicolor* (Flardh, 2003). In B.subtilis the C-terminal of MinD is essential for membrane localization; the protein undergoes dynamic oligomerization on the membrane surface and direct interaction with membrane lipids (Mileykovskaya and Dowhan, 2005). The membrane targeting sequence (MTS) is conserved in all MinD homologues. The MTS of *E. coli* has been shown to bind preferentially to anionic phospholipids and several of the hydrophobic residues within this sequence insert into the cell membrane lipid bilayer (Mileykovskaya *et al*., 2003). The MTS of *B. subtilis* MinD is three amino acid residues longer than the MTS of *E. coli* MinD, indicating a possible higher affinity for the membrane (Szeto *et al*., 2002; Barak *et al*., 2008). Protein lipid interactions have been dealt in detail in section 1.7.5.

1.6.1 Genes involved in chromosome segregation in *S. coelicolor*.

The sporogenic cells contain many copies of the linear chromosome in each hyphal compartment. The DNA that segregates into unigenomic spores undergoes a step wise development until the final stages of septation (Flardh, 2003). This orderly process forms unigenomic spores during sporulation and involves many genes including *parAB* and *ftsK*. *S. coelicolor parAB* is similar to many other bacterial systems, and encodes actin like ATPase, *ParA* and the DNA binding protein *ParB* , which specifically binds to *parS* sites (Flardh, 2003; Katharine *et al*., 2006). Mutants that lack one or both genes produce spores with irregular DNA content, but have no other overt defects (Kim *et al*., 2000; Jakimowicz *et al*.,2007) The *parAB* operon has two promoters, one of which is strongly upregulated in sporogenic hyphae (Jakimowicz *et al*., 2007). Mutants that are defective in chromosome partitioning often have irregularly sized spores, indicating that chromosome segregation influences the placement of Z rings and sporulation septa (Kim *et al*., 2000; Wenner *et al*., 2003). FtsK homologues are present in most, but not all, bacteria (Iyer *et al*., 2004). The *S. coelicolor ftsK*-like gene *SCO5750* termed $ftsK_{SC}$ here, encodes a 929-amino-acid (aa) protein with 45% identity in a 552-aa overlap with FtsK of *E. coli*. *S. avermitilis* also contains such a gene (84% amino acid identity to $FtsK_{SC}$) from the genome sequencing data (Ikeda *et al*., 2003). *S. coelicolor* FtsK is localized to sporulation septa, and is not required for Z-ring assembly or sporulation septation (Wang *et al*., 2007; Ausmees *et al*., 2007). Interestingly, *ftsK*-null mutant's show increased genetic instability, after sporulation, around 20% of *ftsK*-null mutant colonies were shown to have an abnormal appearance that correlated with the appearance of large deletions near the termini of the linear chromosome. These findings are consistent with a role of FtsK-mediated chromosome segregation in *E. coli*; where FtsK shows directionality of DNA transfer and promote the translocation (Section 1.5.1). The large deletions near the termini could lead to genetic instability of *Streptomyces* that is often associated with large deletions in the end regions of the linear chromosomes (Chen *et al*., 2002; Volff *et al*., 1998). Such deletions can result in linear chromosomes becoming circular, and displaying further instability in the offspring, without major effects on viability.

Another developmentally regulated FtsK-family ATPase, SffA, is found at sporulation septa in *S. coelicolor* (Ausmees *et al*., 2007). SffA accumulates within the cell and is dependent on the product of a co-transcribed gene, the small membrane protein SmeA (Rudner *et al*., 2002). SffA is first protein that is seen during early sporogenic hyphae, before it accumulates specifically at constricting sporulation septa. In a *smeA* mutant, SffA remains distributed over the cell periphery even after septation. There was no overlapping function reported between *ftsK* and *sffA*.

Spore maturation involves the production of a thick desiccation and lysozyme-resistant spore wall. The correct assembly of the spore wall depends on MreB (Mazza *et al*., 2006), that resembles the actin family of proteins (Carballido *et al.*, 2006). Deletion of *mreB* in *S. coelicolor* leads to defective and often swollen spores with irregular, thin walls. EGFP localization studies did not reveal any helical MreB structures, as seen in many other bacteria in which MreB orchestrates assembly of cell walls. However, MreB clearly has a role in *Streptomyces* spore-wall assembly. We speculate that these proteins may interact with the membrane phospholipids, specifically cardiolipin.

1.7 Introduction to lipids.

During stationary phase *Streptomyces* produces secondary metabolites many of which have antimicrobial activities (Challis and Hopwood, 2003). Many of these well characterized antibiotics and lantibiotics are synthesized by assembling acetyl-CoA and amino acid derivatives to form the complex polyketide and polypeptide structures (Davis, 1990). Acetyl CoA is also an important precursor for the biosynthesis of lipids like fatty acids, triacylglycerols and phospholipids (Fig. 2). This metabolite acetyl-CoA is formed by oxidative decarboxylation of pyruvate, the oxidative degradation of amino acids and β–oxidation of long chain fatty acids. Lipids are macro-complex biological substances which are soluble in organic solvents such as chloroform and methanol. Lipids display essential roles in several biological functions in both eukaryotic and prokaryotic organisms (Kates, 1960). Lipids functions as structural components of membranes, storage and transport of metabolic fuel, protective coating on the surface and species specific markers for cell recognition and immunological detection (Eoin *et al.,* 2005). *E. coli* has always been the first choice in exploring the biochemical pathway in bacteria. Initially lipid metabolism was studied in detail in *E. coli* because of its simple lipid composition (Thomas and Cronan, 1989).

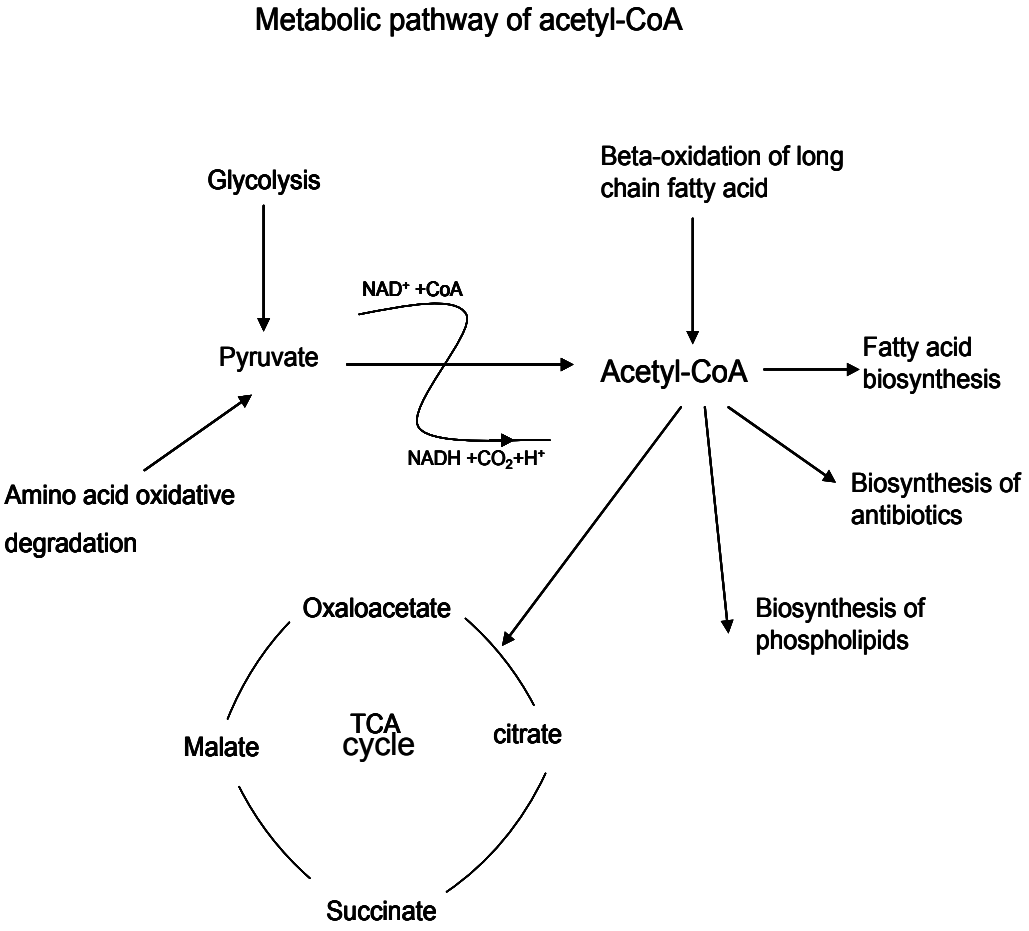

Figure 2 : Schematic representation of the metabolic pathway of acetyl –CoA.

The pathway illustrates the metabolism of acetyl-CoA. Both glycolysis and β-oxidation of fatty acids produce acetyl CoA as the end product, which serves as the important precursor for fatty acid, polyketides and TCA cycle.

1.7.1 Fatty acid biosynthesis in streptomycetes.

Extensive knowledge of the *E. coli* fatty acid biosynthesis pathways has been very useful in studies of a variety of bacteria and higher organisms. Fatty acid profiling of microorganism is one of the main factors that contribute to taxonomic classification of actinobacteria (Lechevalier *et al.,* 1971). Fatty acids are the simplest form of lipids which are important precursors for several metabolic pathways. In *Streptomyces* the branchd chain iso-and anteiso-fatty acids are abundant (Verma, 1983). These fatty acid ranges from C_{12} to C_{18} in all *Streptomyces* species. The subcellular distribution of lipids in *Streptomyces* is focused in membrane, cell wall and cytosolic globular lipids. Acyl carrier protein (ACP) plays an important role in fatty acid synthesis. It helps in building fatty acid chains resulting in acyl-ACP which is formed via a thioester linkage. This resulting acyl- ACP is the acyl donor in the synthesis of phospholipids and lipid-A (Cronan, 1979; Anne *et al.,* 1969). In *S. coelicolor* three sets of ACP were identified and found to be involved in fatty acid biosynthesis. Two of the ACP's in *S. coelicolor*, SCO2389 and SCO4744 are known to be involved in the synthesis of the aromatic polyketides during different stages of the life cycle (Revill, *et al.,* 1996; Florova *et al*., 2002; Zhou *et al*., 1999). Recent studies show that streptomycetes have a type II FAS, a multienzyme complex commonly found in bacteria and plants (Revill *et al.*, 1991; 1996; Summers *et al*., 1995). *Streptomyces* synthesize the majority of their fatty acids from branchd starters such as isobutyryl, isovaleryl, and anteisovaleryl units to give odd- and even-numbered fatty acids with a methyl branch at the ω-terminus (80 to 90% of total fatty acid content); the others are synthesized from straight chain such as acetyl and butyryl units (Kaneda *et al*., 1991; Wallace *et al*., 1995).

A *fabD* gene encoding a malonyl-CoA acyl carrier protein transacylase-(MAT) has been identified in both *S. glaucescens* and *S. coelicolor*. The MAT appears to be responsible for catalyzing the production of malonyl-ACP that is required for each successive elongation step in fatty acid biosynthesis. The *fabD* gene is clustered with three other genes, *fabH*, *fabC*, and *fabB*, which encode proteins with high sequence similarity to the following components of the *Escherichia coli* type II FAS: the FabH

b-ketoacyl-ACP synthase III (KASIII), the FabC ACP, and the FabB KASI. In *E. coli*, FabH catalyzes the first step in fatty acid biosynthesis, which involves condensation of the acetyl-CoA starter unit with the first extender unit, malonyl-ACP, to form acetoacetyl-ACP. *E. coli* FabH also has acetyl- CoA: ACP transacylase (ACAT) activity, which catalyzes the formation of acetyl-ACP from acetyl-CoA and ACP (Tsay *et al*., 1992; Choi, *et al*., 2000; Han *et al.,* 1998).

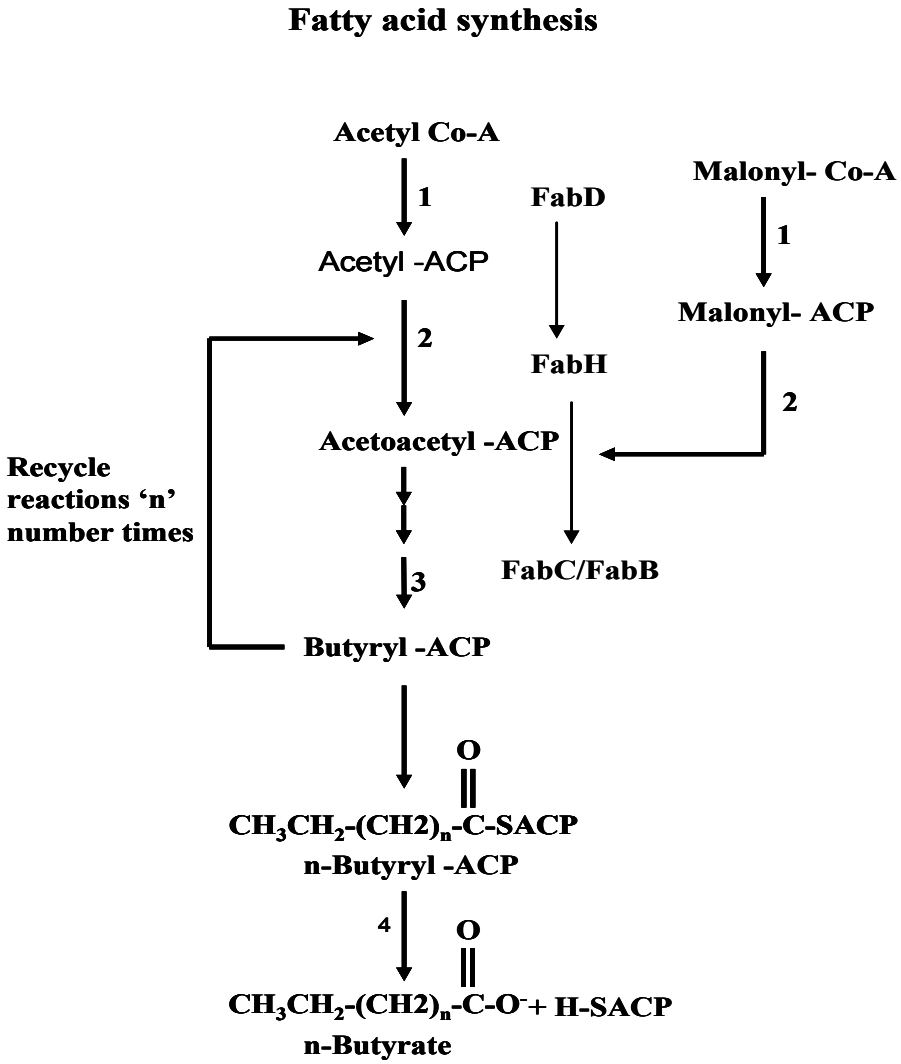

Figure 3 : Fatty acid biosynthesis.

Initiation of chain assembly in type III fatty acid synthase (FAS). 1-Malonyl/acetyl-CoA-ACP transacylase (MAT) coded by *fabD*; 2-β-ketoacyl-ACP synthase (KS) encoded by *fabH*. Further the chain was extended by the addition of β-ketoacyl-ACP reductase (KR) followed by β-hydroxyacyl-ACP dehydrase (DH) and 3-enoyl-ACP reductase (ER) to form butyryl-ACP. Finally, thio ester ACP was cleaved by 4-n-Butyrate thioestarase (TE) to form free fatty acid.

1.7.2 Biosynthesis of glycerophospholipids in bacteria.

Glycerophospholipid metabolism has been extensively studied in plant and animal systems (Frentzen *et al.,*1994). Bacterial membrane lipids recently have gained lot of focus for various metabolic functions as well as their potential as drug targets (Mattila *et al.,*2007). All microbial cells contain lipid fractions, in additions to their other cellular components. However, actinobacteria which are Gram-positive organism have exceptionally high cellular lipid content in comparison to other bacteria (Verma *et al.,* 1983). In eukaryotes and eubacteria the polar head group is present at the *sn*-3 position and in archeabacteria the *sn*-1 of the glycerol backbone which acts as the polar head group (Eoin *et al.,* 2005). Three main anionic phospholipids studied in *E. coli* are phosphotidyl ethanolamine; phosphatidylglycerol and cardiolipin. Apart from these regular phospholipids streptomycetes contain phosphatidyl-myo-inositol mannosides (PIMs) (Shaw, 1974) which are specific for actinobacteria. All major phospholipids pathway originates form the precursor simple phospholipid, phosphatidic acid (PA). The diversification of the polar head group takes place at the phosphoric moiety of the PA, which forms phosphodiesters.

The first step of the pathway, the synthesis of *sn*-glycerol 3-phosphate (G3P) from dihydroxyacetone phosphate, is catalyzed in *E. coli* by GpsA (G3P dehydrogenase) (Clark *et al*., 1980), and a similar protein is encoded in *S. coelicolor* genome, *SCO0670* (*glpD*). The GpsA reaction is the backbone of most bacterial phospholipid synthesis. In *E. coli*, phosphatidic acid formation is initiated by the acylation of sn-glycerol-3-phosphate (G3P) by PlsB, the G3P acyltransferase. PlsB of *E. coli* has been extensively characterized and utilizes either acyl- ACP (Fig. 5B) or acyl-CoA thioesters to acylate the 1-position of G3P (Green *et al*., 1981; Lightner *et al*., 1980). PlsB is responsible for the selection of fatty acids incorporated into membrane phospholipids and is a key regulatory point in the pathway (Heath *et al*., 1994; Rock *et al*., 1981). However, most bacteria lack a *plsB* gene, and the pathway for the acylation of G3P is unknown.

In some Gram-negative bacteria, the *plsB* gene is not essential (Jacobs *et al*., 2003), this shows that there might be an alternate pathway to synthesize acyl-G3P. Subsequently, the gene *plsX* was idenetified, (Larson *et al*., 1984) which encodes an acyltransferase and was involved in G3P metabolism (Fig. 4A). However, another acyltransferase gene was identified, PlsC (Coleman, 1992), which is universally expressed in bacteria and completes the synthesis of PA by transferring a fatty acid to the 2-position of acyl-G3P via acyl- ACP or acyl-CoA. The PlsX/Y system is the most widely distributed pathway for membrane phospholipid formation in bacteria. The next step of the pathway in *E. coli* is catalyzed by PlsC (acyl-ACP: 1- acyl-*sn*-glycerol-3-phosphate 2-O-acyltransferase) (Coleman *et al*., 1990). This enzyme catalyzes the attachment of the second fatty acid to the G3P backbone to form the key intermediate, phosphatidic acid (Fig. 4). However, *S. coelicolor* genome has several PlsC homologues SCO1759, SCO1085, SCO0920, and SCO1228; but lacks PlsB, PlsX and PlsY homologue's. Further, when the amino acid sequence of SCO1759 (pfam: PF01553 acyltransferase) was used as the template in BLAST on genome data base it revealed few more potential putative acyltransferases genes, *SCO5558, SCO3325* and *SCO5899*. Although not widely distributed in bacteria, PlsC homologues are found in eukaryotes and expression of several plant and animal homologues (Cronan, 2003). PlsB, PlsC, and PlsD share common sequences and some of the conserved residues are required for acyltransferase activity (Heath *et al*., 1998).

A new gene was identified; *plsD* from *Clostridium butryicum* and the protein sequence was similar to PlsC than to PlsB. This gene complemented PlsB/X mutant strain of *E. coli* (Heath *et al*., 1997). The *S. coelicolor* homologues of PlsD from protein BLAST search are SCO1566, SCO2122, SCO5558, SCO1228, SCO1085 and SCO1759. The last three hits overlaps with the PlsC hits (described above). All these genes code for putative acyltransferases, which we speculate that these genes might play a role in the formation of PA. However, the exact mechanism of PlsD involved during the phospholipid biosynthetic pathway is unclear.

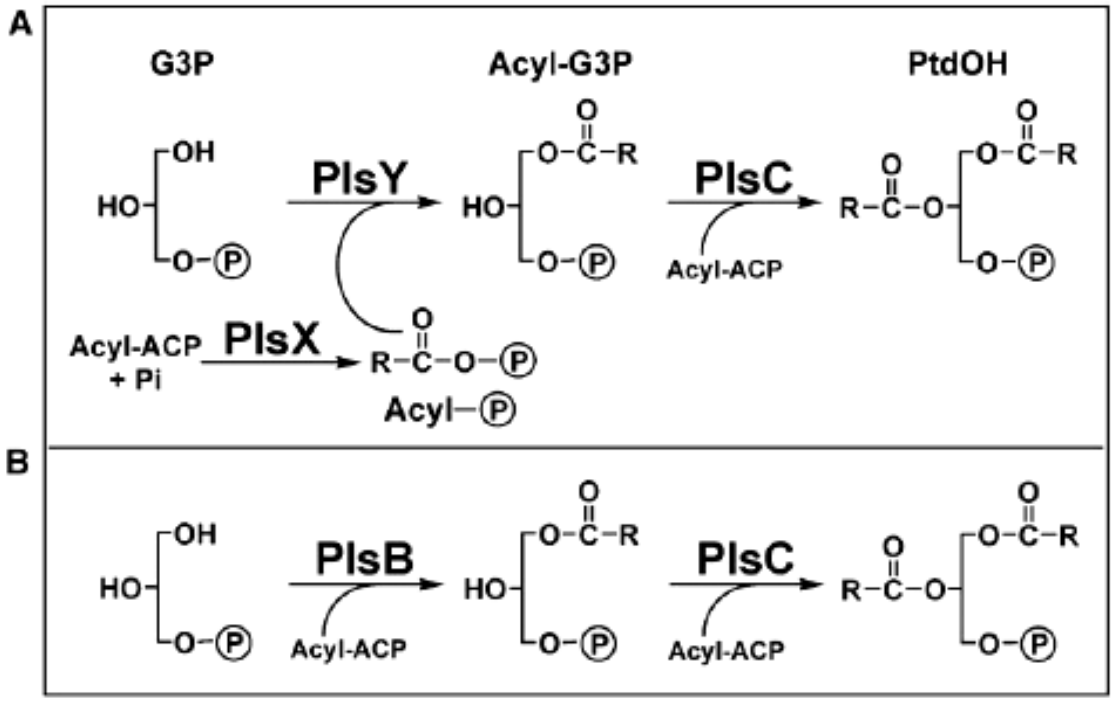

Figure 4 : The PlsX/Y and PlsB/C -pathway for phosphatidic acid formation

(A) Formation of phosphatidic acide by PlsXY pathway. The acyl-ACP end product of fatty acid synthesis is converted to acyl-phosphates by PlsX. Next step PlsY transfers the fatty acid from the acyl-phosphates to G3P. Acyl- G3P is then converted to phosphatidic acid (PA) by PlsC using acyl-ACP as the acyl donor. (B) Formation of phosphatidic acid through PlsB pathway. This catalyzes the transfer of a fatty acid to G3P from acyl-ACP (or acyl-CoA) followed by the acylation of acyl-G3P by PlsC and completes the pathway.

Most of the enzymes involved during phospholipid (PL) synthesis are intrinsic membrane proteins or associated with lipid bilayer. PL synthesis begins with CDP-diglyceride synthase (CTP: phosphatidate cytidylyltransferase), this *E. coli* enzyme is encoded by the *cdsA* gene (Dowhan, 1997) and catalyzes the conversion of phosphatidic acid to the activated intermediate, CDP-diglyceride (CDP-diacylglycerol), which can then be utilized in the synthesis of phosphatidlyethanolamine, phosphatidylglycerol and cardiolipin (Fig. 5). The pathway, which leads to PG and CL, begins with the *pgsA*-encoded CDP-diacylglycerol-glycerol-3-phosphate 3-phosphatidyltransferase, which, like GpsA and Cds, is conserved protein in all bacteria. The next step involves the removal of the phosphate moiety from PG-phosphate; this is an intermediate step before the hydrolysis reaction (Dillon *et al*., 1996). The condensation of two molecules of phosphatidylglycerol to give cardiolipin and glycerol is catalyzed in *E. coli* by the *cls* gene product, CL synthase (Nishijima *et al*., 1988; Tropp, 1997). The other enzymes identified in *E. coli* for phospholipid synthesis, are *yihC*, *ynbB*, and *ybjG* encode proteins similar to PlsC, CdsA, and PgpA/B; and two cardiolipin synthase homologs, YmdC and YbhO, are also found (Guo *et al*., 2000). The other step (Fig. 5) involves the transfer of serine with cytosine monophosphate (CMP) by phosphatidyl serine synthase (*PssA*). The resulting product, phosphatidyl serine (PS) is readily decarboxylated by phosphatidyl serine decarboxylase (*Psd*) to generate phosphatidyl ethanolamine. Screening *S. coelicolor* genome data base for genes involved in phospholipid synthesis revealed eight genes encoding for putative CDP-alcohol phosphatidyltransferases were identified in the *S. coelicolor* genome using BLAST searches: *SCO1389, SCO1527, SCO3457, SCO5753, SCO6467, SCO6647, SCO6752* and *SCO6755*.

The gene *SCO1527* is similar to *pgsA1*, the phosphatidylinositol synthase gene from *M. tuberculosis* (Jackson *et al*., 2000); *SCO5753* appears to be a homologue of *pgsA3*, which encode for a phosphatidylglycerol phosphate synthase (PgsA); PssA from *B. subtilis* (Okadat *et al.*, 1994) is the homologue of *SCO6467* in the *S. coelicolor* genome.

The gene *SCO6468* has been described as putative Phosphatidylserine decarboxylase from the annotation in *S. coelicolor* genome data base, which might be involved in the biosynthesis of phosphatidylserine (PS).

In eukaryotes the type II Cls belongs to the CDP-alcohol phosphatidyl transferases super family that forms cardiolipin, by generating CMP from the reaction between CDP-DAG and PG. A recent study, in *S. coelicolor*, *SCO1389* represents the class II *cls* which produces cardiolipin from a eukaryotic pathway. Recent evidence shows that *SCO1389* codes for cls and confirmed its function by complementing the *Rhizobium etli* mutant and restoring cardiolipin formation. Further, biochemical analysis have shown that *SCO1389* can produce cardiolipin from CDP-diacylglycerol and phosphatidylglycerol as donors this is very similar to the eukaryotic pathway (Sandoval *et al*., 2009). Bioinformatics studies show that the orthologues of putative CDP-phosphatidyl transferases super family is conserved in most of the actinobacteria. From BLAST searches in *S. coelicolor* genome, the gene *SCO7081* scores for phospholipase D (PLD), a multifunctional protein which catalysis both phosphatase and phosphatidyl transferases reaction. It can be speculated that *SCO7081* might be the alternative pathway for synthesis of cardiolipin in *S. coelicolor.*

.

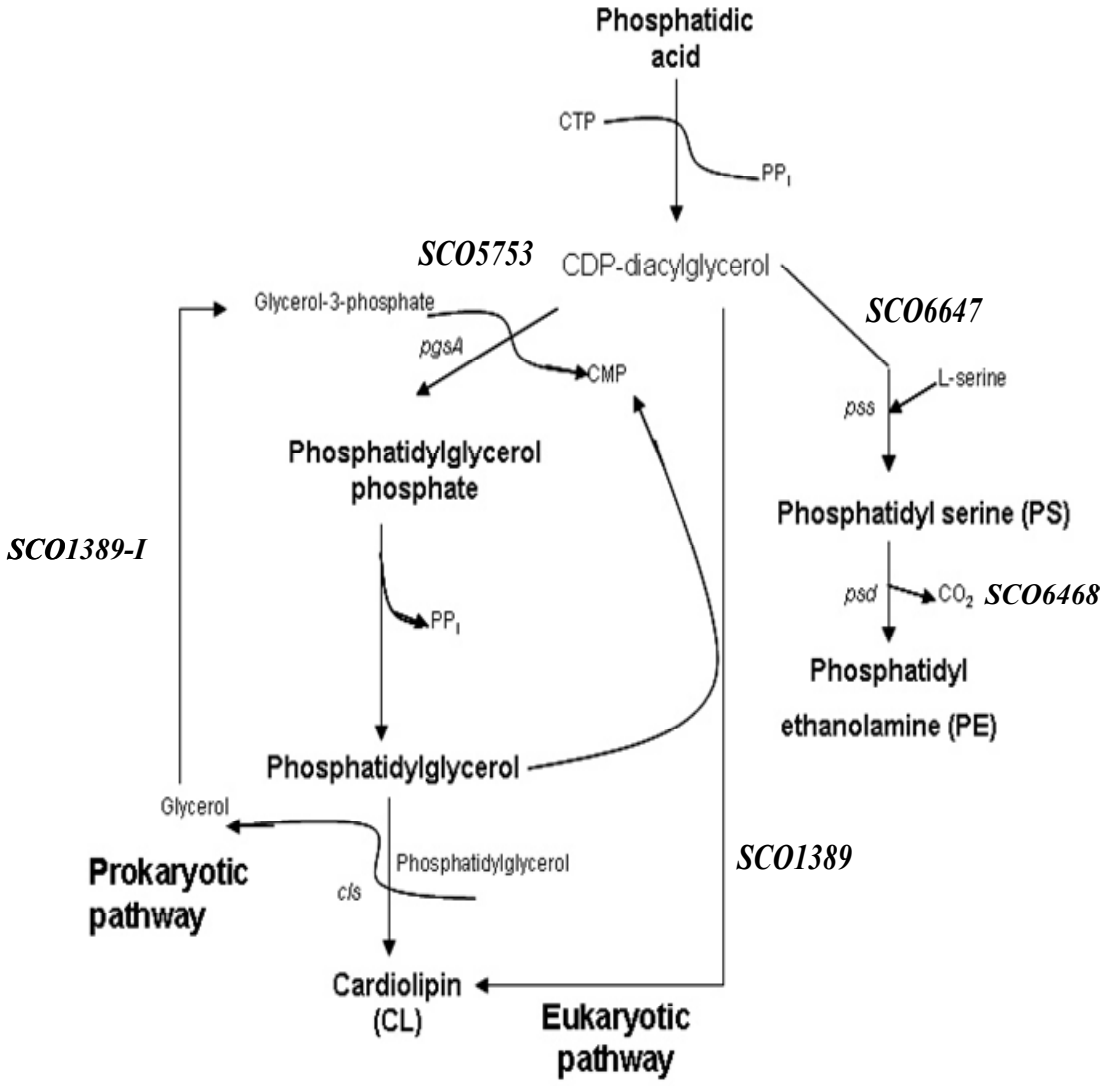

Figure 5 : Biosynthesis pathway of cardiolipin

CDP-DAG, cytidine diphosphatediacylglycerol; PE, phosphatidylethanolamine; PI, phosphatidylinositol, PG, phosphatidylglycerol; PS, phosphatidylserine; PG-P, phosphatidylglycerol-3-phosphate; CMP, cytidine monophosphate; Pss, phosphatidylserine synthase; Psd, phosphatidylserine decarboxylase; PgsA, phosphatidylglycerol-3-phosphate synthase; Cardiolipin synthase, *SCO1389* (eukaryotic like gene) and *SCO1389-I* (prokaryotic origin).

1.7.3 Introduction to cardiolipin.

Cardiolipin is a unique phospholipid with dimeric structure, carrying four acyl groups and two negative charges. It is exclusively found in bacterial and mitochondrial membranes, which are designed to generate an electrochemical potential for substrate transport and ATP synthesis. Treatment with phospholipase D yields two phospholipid products, namely phosphatidic acid (PtdOH) and phosphatidylglycerol (PtdGro). Each phosphate group of cardiolipin contains one acidic proton (Kates *et al*., 1993). The structure of cardiolipin (Fig. 6) has two chemically distinct phosphatidyl moieties, even in the presence of four identical acyl residues; there are two chiral centers on the structure of cardiolipin (Schlame *et al*., 2000).

Cardiolipin synthases require Mg^{2+}, Mn^{2+}, or Co^{2+} as a cofactor (Schlame *et al*., 2000). In mammals and *Neurospora crassa*, Co^{2+} is the most potent activator. Mammalian cardiolipin synthase accepts liponucleotides other than phosphatidyl-CMP, but enzyme activity is low with such substrates (Van *et al*., 1991). Cardiolipin synthase is also inhibited by some divalent cations, such as Cd^{2+}, Zn^{2+}, Ca^{2+}, and Ba^{2+} (McMurray *et al*.,1980), as well as other lysophospholipids. Cardiolipin synthase activity of *E. coli* is about ten-fold increased during the stationary growth phase (Hiraoka *et al.*, 1993). Mutation of cardiolipin synthase leads to low viability, prolonged doubling time and low cell density (Hiraoka *et al*., 1993). Evidence shows that the enzyme activity is regulated at the transcriptional level (Tropp *et al*., 1995). There is potential regulation by membrane lipid composition of cardiolipin and phosphatidic acid. (Guo *et al*., 1998). In the presence of mannitol, cardiolipin synthase from *E. coli* produces diphosphatidylmannitol, the mannitol analogue of cardiolipin (Shibuya *et al*., 1985).

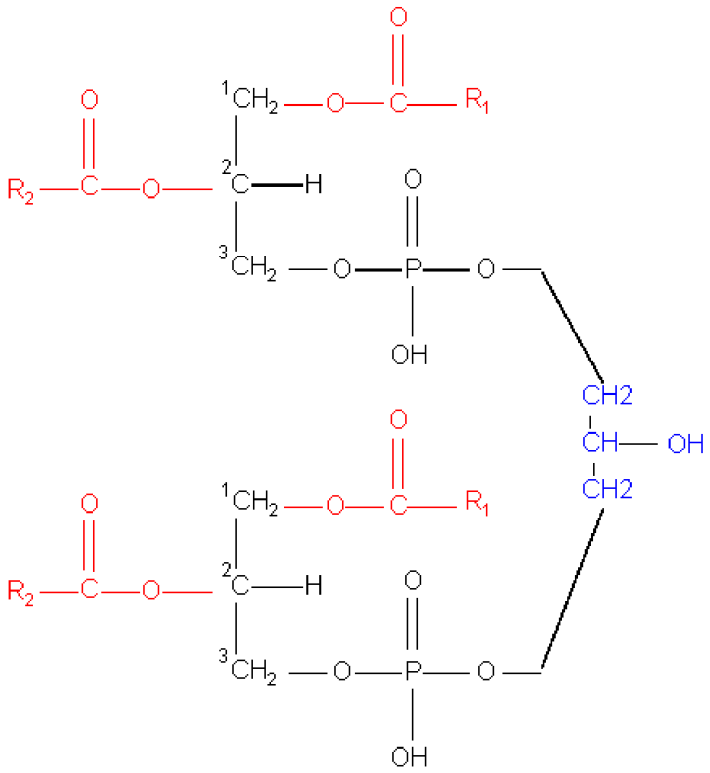

Figure 6: Structure of cardiolipin.

Two chemically distinct phosphatidyl moieties with different acyl chains R1 R2 R3 R4 on the structure of cardiolipin

1.7.4 Distribution of phospholipids in membranes.

Cardiolipin-rich domains were visualized with the cardiolipin-specific fluorescent dye 10-*N*-nonyl acridine orange (NAO) in membrane (Mileykovskaya and Dowhan 2000). The NAO inserts between the phosphate groups at the hydrophobic surface generated by the two outer acyl chains of cardiolipin (Mileykovskaya *et al*., 2001). The dye forms an array of parallel stacks on the surface of the (four per molecule) acyl chains of cardiolipin (Matsumoto *et al*., 2006). Septal and polar localization of the fluorescent domains was observed in *B. subtilis* (Kawai *et al*., 2004). In sporulating *B. subtilis*, fluorescent domains were clearly observed in the polar septal and engulfment membranes and subsequently in forespore membranes at different stages during the course of sporulation. Interestingly, spore membranes have quite high cardiolipin content (Kawai *et al*., 2006). Localization of phosphatidylethanolamine was studied with the cyclic peptide probe Ro09-0198 (Ro), which binds specifically to PE (Emoto and Umeda, 2001). In addition, the use of a fluorescent probe, filipin, indicated sterol localization to the site of cell division in the fission yeast (Wachtler *et al*., 2003).

Lipid molecules are heterogeneously distributed in bacterial membranes, and these domains are easily visible by using fluorescent lipophilic probes. By using the lipophilic fluorescent styryl dye FM4-64, uneven distribution of the fluorescence, of heterogeneous distribution of phospholipids was reported in *E. coli* membranes (Fishov *et al*., 1999).

1.7.5 Interaction between cardiolipin and protein.

Biological protein lipid membranes partition cells and organelles and support a wide range of important metabolic processes, including energy transduction, solute transport, protein transport, signal transduction, and motility. Anionic phospholipids such as phosphatidyl glycerol and cardiolipin play an important role in contributing to the membrane and their interactions with proteins (Dowhan, 1997). Anionic phospholipids have a particularly important function in energy transducing membranes such as the bacterial cytoplasmic membrane and the inner mitochondrial membrane (McAuley *et al*., 1999). In particular, cardiolipin is a key factor in the maintenance of optimal activity of a number of major integral membrane proteins. The best studied interactions are between the cytochrome *c* oxidase and cardiolipin (McAuley *et al*., 1999).

1.7.6 Role of cardiolipin in bacterial cell division.

Cardiolipin is found virtually in all bacterial membranes and is abundantly found in mitochondrial membrane of eukaryotic cells. In *E. coli*, extensive biochemical and morphological evidence exists for association of the genome with the membrane at the initiation, elongation, and termination sites (Firshein *et al*., 1989). *In vitro* evidence supports the interaction of anionic phospholipids with DnaA protein during initiation of DNA replication (Crooke *et al*., 1992). Formation of a functional DnaA–ATP complex capable of opening the DNA duplex occurs only in the presence of both anionic lipid and *oriC* (Dowhan *et al*., 2004). Activation of DnaA protein by domains of anionic lipids was demonstrated *in vitro* (Mizushima *et al*., 1996). *In vivo* evidence of anionic phospholipid interaction with DnaA was observed in *E. coli* by regulating the expression of the *pgsA* gene (Dowhan *et al*., 2004; Pogliano *et al*., 2003).

Formation of a cardiolipin domain at the midcell allows initiation of DNA replication by DnaA, followed by assembly of the replisome. During replication of DNA the origins migrate towards the cell poles, leaving the anionic phospholipid domain at the centre, for interaction with FtsZ and other early cell division proteins.

During growth of *E. coli* and *B. subtilis*, the FtsZ-ring forms at mid-cell and the cells divide. The two distinct mechanisms that contribute to the assembly of divisome are the Min system and nucleoid occlusion (Harry, 2001; Barák and Wilkinson, 2007). The concentration gradient in the Min system proteins (section 1.5) defines the mid-cell site of cell division. In *E. coli*, the Min protein oscillates from pole to pole (Hu and Lutkenhaus, 1999; Raskin and Boer, 1999; Shih *et al*., 2003). In *B. subtilis*, DivIVA directs MinCD to the cell poles, along with MinE (Edwards and Errington, 1997; Szeto *et al*., 2002; Hu and Lutkenhaus, 2003). This membrane targeting sequence (MTS) is conserved in all MinD homologues. The MTS of *E. coli* has been shown to bind specifically to anionic phospholipids and several of the hydrophobic residues within this sequence insert into the cell membrane lipid bilayer (Mileykovskaya *et al*., 2003). The MTS of *B. subtilis* MinD is three amino acid residues longer than the MTS of *E. coli* MinD, indicating a possible higher affinity for the membrane (Szeto *et al*., 2002). Lipid spirals interact with MinD in *B. subtilis* demonstrating a new model for selection of cell division site in bacterial divisome assembly (Barak *et al*., 2008). Association of amphitropic proteins like DnaA, SecA, protein kinases C (Johnson *et al.*, 1999) and MinD (Dowhan *et al*., 2004) with the membrane requires interaction with phospholipids, suggesting a role for phospholipids during FtsZ polymerization at the division site. Dynamic polymerization of FtsZ on the cell membrane is the first step in the assembly of the divisome. *In vitro* studies on FtsZ have shown that, it forms mini-rings and/or thin sheets of protofilaments in the presence of GTP or GDP when adsorbed to a zwitterionic lipid monolayer (Erickson *et al*., 1996).

Investigation of FtsZ interaction with a Langmuir film composed of dilaurylphosphatidylethanolamine and dipalmitoylphosphatidylglycerol showed that FtsZ assembled at the interface between these two phospholipids, but when cardiolipin was introduced, FtsZ assembly occurred preferentially within cardiolipin domains and at the interface of the other two phospholipids. Still, there is no direct evidence for a specific lipid-interacting domain in FtsZ, however, the mutational study on the hydrophobic loop in FtsZ, decreased its affinity for the cytoplasmic membrane (Koppelman *et al*., 2004). In *E. coli* FtsZ localization to the membrane is supported by the two early cell division proteins ZipA and FtsA (Raychaudhuri, 1999; Margolin *et al*., 2000). Recently it has been shown that FtsZ and its membrane-anchoring partner, FtsA, form helical structures in *B. subtilis* cells (Peters *et al*., 2007). FtsA, like MinD, has an amphipathic positively charged a-helix that is required for localization to the membrane (Yim *et al*., 2000). SecA and SecY exhibit spiral patterns of localization, which in the case of SecA is dependent on the presence of acidic phosphatidylglycerol phospholipids (Campo *et al*., 2004). Variability in structure and lipid composition may therefore be a general factor in shaping the interactions of membranes and proteins.

From recent studies it has been demonstrated that lipid interacts with the amphitropic proteins, and forms dynamic oligomerization on the membrane surface, and membrane phospholipids. Evidence broadens the scope and help in understanding the lipid involvement in the process of cell division. Recognition of defined lipid domains in the bacterial membrane and their association with the division machinery provide a starting point for studies of lipid dynamics in the bacterial cell division process.

1.8 Introduction to time-lapse microscopy

A revolutionary new perspective of the cell biology of prokaryotic mycelial organism is arising as a result of using live-cell imaging techniques to analyse molecular markers dynamics at high spatial resolution. This has become possible because of the development of a wide range of fluorescent probes (vital dyes and fluorescent proteins that can be used to non-invasively interrogate living cells), new microscope technologies, and powerful computer software and hardware for digital image processing and analysis. Fluorescence microscopy has revolutionized our understanding of the bacterial cell and provided new opportunities to investigate the behaviour of cell division proteins and chromosome dynamics in bacteria (Lamothe *et al*, 2008).

Time-lapse microscopy is a key tool in understanding the cellular dynamic events in multinucleate streptomycetes such as patterns in nucleoid and protein trafficking during hyphal growth. Recently, using time-lapse microscopy, spatial and temporal localization of cephamycin C biosynthesis in *S. Clavuligerus* was demonstrated (Han *et al*., 1999); however successful imaging of the complete growth and development of *Streptomyces* has not been done. The primary objectives of the thesis is to (a) provide a brief overview of time-lapse microscope construction for imaging living *Streptomyces* cells at high spatial resolution; (b) application of the vital fluorescent dyes which are proving useful for analysing the cell biology of prokaryotic mycelial organism with the inverted fluorescent microscope; (c) briefly indicate future directions for live-cell imaging of filamentous Gram positive bacteria, *Streptomyces*.

1.8.1 Why develop time-lapse microscopy?

Biological systems are dynamic in nature and a proper understanding of the cellular and molecular processes underlying living organisms is one of the major challenges of current cell biology research. Driven by substantial improvements in optics hardware, electronic imaging sensors, fluorescent probes and labelling methods, microscopy has, over the past decades, matured to the point that it enables sensitive time-lapse imaging of cells and even single molecules. These developments have had a profound impact on how research is currently being conducted in the life sciences. The morphological and differentiation of *S. coelicolor* is complex and presents many technical difficulties associated with imaging. Early growth studies of the filamentous *S. coelicolor* on solid medium were investigated through a series of snap shots in regular intervals of time, to monitor its growth kinetics, total mycelial length and the number of branchs and expressed as constant hyphal growth unit (Allan and Prosser, 1983).

Until recently, microscopic studies of cell division in streptomycetes consisted of snapshot images of hyphae or spores. These images have limited information on protein and nucleoid movement in real time, and, as a result, the exact order of intracellular events during hyphal growth and sporulation in *Streptomyces* is still largely unknown. The main reasons for this are the technical challenges associated with carrying out time-lapse microscopy of the model organism, *S. coelicolor*. These include oxygen dependence, a developmentally heterogeneous mycelium, the three-dimensional pattern of hyphal growth, and an inability to sporulate in the absence of a solid support. Time-lapse imaging studies consists two steps: 1) planning of the experiment and acquisition of the image data, and 2) analysis of the data by detecting and tracking the objects relevant to the biological questions underlying the study.

1.9 Scope of the present work.

The aims of this work were divided into two main parts.

Part I- To design and optimize time-lapse microscopy with applications of fluorescent probes.

Part II- Molecular investigation of cardiolipin synthase gene (SCO1389).
To characterize the *SCO1389* gene, PCR mediated gene replacement, mutational analysis, and construction of depletion strain under inducible promoter was carried out. Further, to investigate the distribution of cardiolipin and localization *SCO1389* by live cell imaging, fluorescent probes and green fluorescent protein was used.

Chapter 2

Materials and Methods

2.1. Bacterial strains and vectors.

Bacterial strains are listed in Table 1 and 2, vectors in Table 3

Table 1 : Streptomycete strains

Strain	Characteristics	Source/reference
S. coelicolor M145	Wild type, SCP1$^-$, SCP2$^-$, Pgl$^+$.	Kieser *et al.* 2000
S. coelicolor pIJ8600	M145::pIJ8600, am^r	Sun *et al.*1999
S. coelicolor pMS82	M145::pMS82, hyg^r	Gregory, *et al, 2003*.
S. coelicolor pSET152	M145::pSET152, am^r	Bierman, *et al.,* 1992.
S. coelicolor RJ100	M145ΔSCO1389::Tn*5062*, am^r, km^r	This work
S. coelicolor RJ103	RJ100::pMS82 , am^r, km^r , hyg^r	This work
S. coelicolor RJ102	M145::pCLS105, hyg^r.	This work
S. coelicolor RJ104	RJ100::pCLS105, am^r, hyg^r	This work
S. coelicolor RJ107	M145::pCLS108B, hyg^r	This work
S. coelicolor RJ110	M145::pCLS113A, am^r,tsr^r	This work
S. coelicolor RJ111	M145ΔSCO1389::pIJ773, am^r, km^r	This work
S. coelicolor RJ112	RJ111::pMS82 , am^r, km^r , hyg^r	This work
S. coelicolor RJ113	RJ111::pCLS108B, am^r, hyg^r	This work
S. coelicolor RJ114	RJ111::pCLS105, am^r, hyg^r	This work
S. coelicolor RJ115	M145::pCLS117B1, hyg^r	This work
S. coelicolor RJ116	M145::pCLS117B2, hyg^r	This work
S. coelicolor RJ117	M145::pAVIIb, hyg^r	This work
S. coelicolor RJ118b	RJ111::pCLS117B1, am^r, hyg^r	This work
S. coelicolor RJ118a	RJ111::pCLS117B1, am^r, hyg^r, km^r	This work
S. coelicolor K113	M145::*ftsZegfp*, am^r	Grantcharova *et al.*2005
S. coelicolor VJ101	M145ΔSCO5750::pIJ773, am^r	This work

Table 2: *Escherichia coli* strains

Strain	Characteristics	Source/reference
DS941	*recF143, proA7, str31, thr1, Leu,tsx33,mt12,ris4,argE3,lac Y+, lac ZΔM15,lacI ^{q},gal K^{2},ara 14 ,sup E44 , xy 15*	Sherrat, *et al*.,1988
JM109	*recA1, endA1, gyrA96, thi, hsdR17, supE44, relA1, Δ(lac-proAB)/F' [traD36, proAB^{+}, lacI^{q}, lacZΔM15*	Yanish perron et al, 1985
ET 12567	*F- dam-13::Tn9,dcm-6,hsd M,hsd R,Rec F143, Tn10, gal T 22, ara14, lac Y 1, xy 1-5,leu B6, thi-1 ,tonA31, rpsL 136, hisG4, tsx-78, mtl-1, gln44, supE, hsd Δ5, thi Δ(lac pro AB)*	Kieser *et al*. (2000)
BW25113	*rrnB3 ΔlacZ4787 hsdR514 Δ(araBAD)567 Δ(rhaBAD)568 rph-1*	Gust *et al.* (2003).
NovaBlue Singles™	*endA1 hsdR17 supE44 thi-1 recA1 gyrA96 relA1 lac F'[proA^{+}B^{+} lacI^{q}ZΔM15::Tn10] (Tet^{R})*	Novagen

Table 3: Vectors

Plasmid	Characteristics	Source/reference
pIJ773	Gene replacement vector, am^r	Gust *et al.*, 2003.
pIJ790	λ- RED (*gam, bet, exo*), *cat, araC, rep101*^{ts}.	Gust *et al.*, 2003.
pUZ8002	*tra*, RP4, km^r	Paget, *et al.*, 1999.
pMS82	Integrating vector $attP_{\Phi BT1}$, hyg^r.	Gregory, *et al,* 2003.
pSET152	Integrating vector $attP_{\Phi C31}$, am^r.	Bierman, *et al.,* 1992.
pIJ8600	Over expression vector,*tipA*, $attP_{\Phi C31}$, $am^r.tsr^r$	Sun *et al.* 1999
pEGFP-N1	*E. coli* vecotor containing *egfp* km^r.	Clonetech lab Inc
pALTER I	*E. coli* cloning vector, tet^r.	Promega
pT7Blue	*E. coli* blunt cloning vector (Kit), amp^r	Novogen
St1A8A	Cosmid containing *SCO1389* ,km^r, amp^r	Redenbach *et al*.1996
St1A8A.2.B10	St1A8AΔ *SCO1389*::Tn*5062*, am^r, km^r, amp^r	Bishop *et al*.,2004
St1A8A.2.EO5	St1A8A:: Tn*5062* insertion downstream *SCO1389* am^r, km^r, amp^r	Bishop *et al*.,2004
StA8A.RJ1	St1A8A,Δ *SCO1389*::pIJ773, am^r, km^r, amp^r	This work
pCLS102	pALTERI,*SCO1389* with native promoter, am^r, tet^r.	This work
pCLS105	pMS82, *SCO1389* with native promoter, hyg^r.	This work
pCLS106	PCR 1030 bp fragment containing *SCO1389*, amp^R.	This work
pCLS112	PCR 673bp fragment containing *SCO1389*, amp^R.	This work
pCLS107	pEGFP-N1 carrying *SCO1389* with native promoter, km^r.	This work
pCLS113A	pIJ8600: *SCO1389*, $am^r.tsr^r$	This work
pCLS108-B	pMS82: *SCO1389egfp* - (native promoter), hyg^r.	This work
pAVIIB	pMS82, *tcp830*, hyg^r.	Rodriguez *et al*,2005; Vargeese unpublished
pCLS117B1	pAVIIb, *SCO1389* in sense orientation, hyg^r.	This work
pCLS117B2	pAVIIb, *SCO1389* in anti-sense orientation, hyg^r.	This work
pALVJ I	pALTERI,*SCO5750* with native promoter, am^r, tet^r.	This work.
SC7C7	Cosmid containing *SCO5750* ,km^r, amp^r	Redenbach *et al.* 1996
SC7C7.VJ1	SC7C7,Δ *SCO5750*::pIJ773, am^r, km^r, amp^r	This work.

2.2 Chemicals and antibiotics.

Chemicals and antibiotics used in this study are listed in Tables 5 and 4 respectively. Unless otherwise stated chemicals and antibiotics were purchased from Sigma Aldrich, Fischer Scientific, and BDH chemicals Ltd. Antibiotics (Table 4) were stored at -20°C.

2.3 Preparation of media, chemicals and antibiotics

Media were prepared according Table 6, and antibiotics prepared according to Table 4, where appropriate solutions were sterilised by passing through a 0.22µm filter unit. All media and buffers were autoclaved for 15 minute sat 121ºC to achieve sterilisation, unless otherwise stated.

Table 4: Antibiotics

Antibiotics	Stock concentration (mg/ml)	Working concentration (µg/ml)
Apr[1]	100	50
Amp [1]	100	50
Chlr[2]	25	25
Kan [1]	50	25
NA[1]	20	25
Tet [2]	25	12.5
Str[1]	25	25
Spec [1]	50	50
Atc [2]	3	0.1 1.5
Tsr[3]	50	12
Hyg[2]	50	50

[1] Prepared in SDW.
[2] Prepared in absolute ethanol.
[3] Prepared in DMSO.
All antibiotics stored at -20°C unless otherwise stated.

Table 5: Chemicals and reagents used

Reagent	Per litre
Alkaline lysis solution I	2M Glucose; Tris Cl (pH8); EDTA (pH8).
Alkaline lysis solution II	4M NaOH; 20% (w/v) SDS.
Alkaline lysis solution III	8M Potassium Acetate; Glacial acetic acid; SDW.
10xTE-buffer	100mM Tris (pH8); 10mM EDTA.
50xTAE-buffer	2M Tris; Glacial Acetic acid; 0.05M EDTA.
Agarose	0.8% (w/v) in 1x TAE buffer
DNA marker dye	50mM EDTA; 0.5% (w/v) SDS; 0.25% (w/v) Bromophenol Blue; 15% (v/v) Ficoll.
RNase A Solution	10mgs RNase A; 1 M Tris-HCl (pH7.8); 1M $MgCl_2$.
Lysozyme solutions	25mM Tris- pH8; lysozyme (2mg/ml); RNase A (10mg/ml).
SDS solution	0.3 M NaCl; 20% SDS (w/v).
Phenol reagent	Phenol-chloroform in equal volume mixture.
Phosphate-buffer saline (PBS)	0.8% (w/v) NaCl; 0.02% (w/v) KCl; 0.4% (w/v) Na2HPO; 0.4% (w/v) KH2PO; pH to 7.4 with HCl, make up to 1000ml in SDW.
GTE solution	50mM Glucose; 20mM Tris-HCl (pH 8.0); 20mM EDTA.
Glutaraldehyde	25% (v/v)-stock solution
Formaldehyde	40% (v/v) - stock solution.
TFB1	30mM potassium acetate, 10mM CaCl2, 50mM MnCl2, 100mM RbCl, 15% (v/v) glycerol, and adjust pH to 5.8 with 1M acetic acid.
TFB2	100mM MOPS (pH 6.5), 75mM $CaCl_2$, 10mM RbCl, 15% (v/v) glycerol, and adjust the pH to 6.5 with 1M KOH.

Table 6: Media used for growing bacterial strains

Media	Constituents per litre
MS	Mannitol-20 g, Soya bean flour-20 g, Agar- 20 g Tap water-1 L.
LB broth/agar	Trypyone-10 g, Yeast Extract-5 g, NaCl-10 g, pH-7.2 in SDW, Agar-3.75g/250ml into bottles.
YEME	Yeast extract-3 g, Peptone-5 g , Malt extract-3 g Glucose-10 g, Sucrose-340 g, *Sterile 2.5M $MgCl_2$ 2ml, SDW-1L.
M9 medium	Water-90ml/80ml, Agar-1.5%, * Glucose 20%-2ml *Thiamine 1M-100µl, *M9 salts 5x,*Di sodium Hydrogen Phosphate- 6.4%, *Di Hydrogen Potassium Phosphate-1.5%, *Sodium Cholride-0.25%, *Ammonium Cholride-0.5%.
SOB medium	Tryptone-20 g, Yeast Extract-5 g, NaCl-0.5 g, *2M $MgCl_2$ -5ml.
SOC medium	Prepare SOB, then add *1M glucose-20ml/ltr
R2YE	Sucrose-103 g, K_2SO_4-0.25 g, $MgCl_2.6H_2O$-10.12g Glucose-10 g, Difco casaminoacids-0.1 g, SDW-800ml, Add 2.2 g of agar to 80ml of the above solution in 250ml bottle and autoclaved, *KH_2PO_4(0.5%)-1ml, *$CaCl_2.2H_2O$(3.68%)-8ml *L-Proline (20%)-1.5ml, *TES buffer, (5.73%,adjusted to pH 7.2)-10ml, *Trace element solution -0.2ml, *NaOH (1N) (Unsterilized is OK)-0.5ml, *Yeast extract (10%)-5ml.
SMM	Difco Casaminoacids-2g TES buffer-5.73g (25mM final) Water-1L,pH the solution to 7.2 with 5N NaOH 3g of lab M agar to 200ml of the solution in 250ml bottle and autoclave, *NaH_2PO_4+K_2HPO_4 (50mM each)-2ml (1mM final), *$MgSO_4$ (1M), *Glucose (50%) (w/v) , *Trace elements -0.2ml.
2YT	Difco bacto tryptone- 16g, Difco bacto yeast extract-10g NaCl-5g, SDW-1L.

*** Added after autoclaving separately.**

% is in w/v ratio.

2.4 Standard microbiological techniques for *Escherichia coli*.

All DNA manipulation was carried out according to Sambrook *et al*., 1989 unless otherwise stated. Chemicals and media used are described in sections 2.2 and 2.3.

2.4.1 Growth conditions for *Escherichia coli*.

Liquid cultures of *E. coli* strains from which plasmids were to be isolated were grown in L-broth (Table 6) with appropriate antibiotic selection. The volume of broth inoculated dependent on the quantity of plasmid required. Mostly, 5ml and 100ml cultures were used for small and large scale plasmid preparations, respectively. All cultures were incubated at 37°C in an orbital shaker at 250 rpm. *E. coli* strains were also propagated on L-agar or Minimal medium agar plates with appropriate marker selection. Plates contained *ca*. 25ml of agar and were incubated overnight at 37°C.

2.4.2 Preservation of *Escherichia coli* strains.

E. coli strains were stored in glycerol. An 800µl aliquot of an overnight culture was mixed with equal volume of 40% (v/v) glycerol, 2% (w/v) peptone and frozen at -80°C. The strains were revived by scraping the surface of the frozen suspension with an inoculating loop and streaking onto an agar plate to isolate single colonies.

2.4.3 Introduction of plasmid DNA into *Escherichia coli*.

Two methods of preparing competent cells were routinely carried out for chemically treated competent cells and electroporation competent cells. All competent cells prepared were stored at -80°C. An efficiency of 10^6-10^7 transformants per µgm of plasmid was typically achieved using either method. A single colony was inoculated into LB-broth containing appropriate antibiotics and incubated at 37ºC, 250 r.p.m. overnight. The next morning 1/100 dilution of the culture was re-incubated in LB-broth and its optical density was monitored until it reached 0.4-0.6 $O.D_{600}$.

A) Preparation of competent cells by $CaCl_2$ method treatment.

The pellet was gently resuspended in 0.4 original volume of ice-cold TFB1. The cells were incubated on ice for 5 minutes at 4°C. The cells were pelleted by centrifugation at 4,500 rpm for 5 minutes at 4°C. 1/25 volume of ice-cold TFB2 was used to gently resuspend the cells. The cells were incubated on ice for 15–60 minutes, and then dispense 50µl aliquots were frozen in liquid nitrogen, and stored at -80ºC.

B) Preparation of Electro competent cells.

Cells were kept on ice for approximately 30 min then centrifuged (4000 r.p.m., 4ºC for 5 min). The pellet was washed twice with 15ml and 10ml of ice-cold 10% glycerol (v/v) and centrifuged (4000 r.p.m., 4ºC for 15 minutes). Finally, the pellet was resuspended with 2ml ice-cold 10% (v/v) glycerol, 50µl aliquots were frozen in liquid nitrogen, and stored at -80ºC.

2.4.3.1 Transformation with plasmid DNA.

A) Transformation of $CaCl_2$ treated cells.

Plasmid DNA (1-100ng) in a volume less than 10µl, was added to 50 µl aliquots of the competent cells, mixed gently by inverting the Eppendorf tube and incubated on ice for 30min. The cells were heated to 42ºC for 50 sec and returned to ice for a further 2min. A 1ml aliquot of SOC broth was added and the cell suspension incubated at 37ºC for 90 min. Then the cells were plated on LB-agar plates with appropriate antibiotics for the selection of transformants.

B) Transformation of Electrocompetent cells.

Plasmid DNA (1-100ng) in a volume of 1µl, was added to 50 µl aliquots of the competent cells, mixed gently by inverting the Eppendorf tube and incubated on ice for 30minutes. The mixture then transferred to a electroporator cuvette (0.1mm), both the cuvette and the holder was dried thoroughly and placed into the GenePulser apparatus which was set, to ECI. A 1ml aliquot of SOC broth was added and the cell suspension incubated at 37ºC for 90 min. Then the cells were plated on LB-agar plates with appropriate antibiotics for the selection of transformants.

2.4.4 Isolation of plasmid DNA from *Escherichia coli* .

The alkaline lysis protocol was followed for isolation of plasmid DNA from *E. coli* cells. With appropriate antibiotic selection, *E. coli* cells were grown overnight and 1 ml of the culture was centrifuged (13,000 r.p.m.) at room temperature. The pellet was resuspended in 100 µl alkaline lysis solution I and 200µl of solution II was added to the tube and gently inverted 5 times. Finally 150 µl of alkaline lysis solution III was added and mixed by inverting the tube 10 times. The tube was centrifuged (13,000 r.p.m.) at room temperature for 10min. The supernatant was carefully transferred to a clean Eppendorf tube and 400 µl of phenol/chloroform was added and vortexed for 2min. The aqueous phase was transferred to another tube after centrifugation (13,000 r.p.m) at room temperature for 5min. DNA was ethanol precipitated; the pellet was dried and dissolved in 1x T.E. buffer (Table 5).

2.4.5 Phenol-chloroform extraction of DNA.

An equal volume of saturated phenol was added to the DNA mixture along with equal volume of chloroform in an Eppendorf. This mixture is vigorously vortexed for 2 min. The emulsion then centrifuged at 13000 rpm for 5min at room temperature. The upper, aqueous, layer was carefully removed by avoiding the interface between layers.

2.4.6 Ethanol precipitation of DNA.

Precipitation of DNA was carried out using 2-2.5 volumes of absolute ethanol in the presence of (1/10 volume) 3M sodium acetate pH 5.2 and incubated at -20^{o}C for at least 30 minutes. The DNA suspension was then centrifuged for 30 minutes, 13,000 rpm at 4˚C and the supernatant removed. The pellet was then washed with 1ml 70% (v/v) ethanol centrifuged as above, followed by air drying. The dry nucleic acid residue was then ready for further use as required.

2.4.7 Agarose gel electrophoresis.

0.8% Agarose gels were prepared using 1xTE buffer. 1µl of ethidium bromide solution (10mg/ml) was added to 100ml of agarose. The gels were immersed in 1xTAE buffer (running buffer). $1/5^{th}$ volume DNA sample loading dye (Table 5) was added to the DNA sample. The gel along with DNA molecular markers (Table 9) the voltage was set at 70V for small gels and 100V for larger gels. Photography of the agarose gel was taken by a Syngene 302nm ultra violet transilluminator and DNA visualized in gels with the aid of GeneSnap (Syngene version 6.08).

2.4.8 Extraction of DNA fragments from agarose gels.

DNA fragments of interest were extracted and purified from agarose gels using a Qiagen gel extraction kit. Using a sterile sharp scalpel, the band was excised from the gel. A 1.5ml Eppendorf was weighed before adding gel for calculating the amount of agarose in the tube. The agarose was solubilised at 50˚C water before the mixture was transferred to the spin column, and the DNA was purified according to the manufacturer's instruction.

2.4.9 DNA band sizing and quantification

DNA was quantified by signal intensity visualised on a gel by comparison to known concentrations of DNA from a HindIII digested λ marker; typically, 500ng of λ HindIII DNA was used as a ladder on all agarose gels. The band sizes and concentrations are described in the Table 9. Other ladders used included:
Promega 1kb standard: fragments sizes were 10Kb, 8Kb, 6Kb, 5Kb, 4Kb, 3Kb, 2.5Kb, 2Kb, 1.5Kb, 1Kb, 750bp, 500bp and 250bp, and Promega 100bp standard: fragment sizes were 1.5Kb, 1Kb, 900bp, 800bp, 700bp, 600bp, 500bp, 400bp, 300bp, 200bp and 100bp.

Table 7 : λ HindIII ladder

Band sizes in (bp)	Amount of DNA ng
23130	240
9416	97
6557	68
4361	44
2322	24
2027	21
564	6
125	-

2.4.10 Novagen perfectly Blunt cloning kit.

The gene of interest was PCR amplified and the PCR products were purified using PCR purification Quiagen kit (Table 8). The PCR product was converted to blunt ends using end-conversion mix provided in the kit and heat inactivate. To this mixture, the linear 1µl (100ng) blunt ended vector was added and ligation reaction was set up according to the manufacturer's guide. The reaction mixture was incubated at room temperature for 10 minutes. 1-2 µl of the sample was used to transform into NovaBlue SinglesTM Competent Cells.

2.4.11 Use of Blue/White screening for identifying clones.

X-Gal (20mg/ml) was used with IPTG (0.1 M) in order to identify colonies containing desired recombinant clones within multiple cloning sites of vectors carrying the *lacZ* gene. Colonies were coloured blue due to the activity of ß-galactosidase. Colonies containing recombinants plasmids yielded white colonies.

2.4.12 Restriction enzyme digestions and other DNA modifying enzymes.

Restriction enzyme digestions were performed by incubating 100ng of DNA with 2µl of buffer (10x) as recommended by the supplier made up to 19 µl with sterile distilled water and finally added 1 µl of an appropriate restriction enzyme, and incubated at recommended temperature for 1 hour, as specified by the manufacturer. Double digestion was carried out when two different enzymes could be used in the same reaction provided there is 100% activity using a single buffer. When there was no compatibility between the enzymes and the buffer. Digestions were carried out individually using the most suitable reaction buffer for each enzyme, precipitating the DNA between reactions. BSA was added for appropriate reactions. Enzymes used to modify DNA were obtained from New England Biolabs, Promega, Invitrogen, or Fermentas. All DNA modifying enzymes as shown below followed the appropriate conditions as described by the manufacturers' guides.

Table 8: Modifying enzymes

Enzyme	Use	Source
DNA Taq Polymerase	PCR	Fermentas
Expand Hi-Fidelity DNA polymerase	PCR	Roche
T_4 DNA ligase	Ligation	Fermentas, Promega, Invitrogen

Table 9: DNA modification kits.

Kit*	Use	Source
Qiagen Gel Extraction	DNA purification from agarose gels	Qiagen Ltd., Germany
Qiagen PCR clean up	DNA purification from PCR reaction	Qiagen Ltd., Germany
Promega Wizard plasmid prep	Preparation of cloning grade plasmid DNA	Promega
DIG-DNA Labelling Kit	Hybridization	Roche
Hi-Bond-N nitrocellulose membrane	Hybridization	Amersham Biosciences Ltd.

*All kits used according to manufactuer's guides.

2.5 Standard microbiological techniques for *Streptomyces*.

All procedures were based on "Genetic Manipulation of Streptomyces: A laboratory manual "(Hopwood *et al*., 1985), unless otherwise stated.

2.5.1 Media for propagation of *S. coelicolor*.

Streptomyces were grown on MS agar, Minimal medium agar, R2YE agar and YEME broth (Table 6).

2.5.2 Preparation of *S. coelicolor* spore suspensions.

Streptomyces were grown on MS agar for three days at 30˚C. The spores then scraped out from plates by addition of 10ml SDW. The mixture was then filtered through a non -porous cotton plug. The resulting filtrate was centrifuged at 4000 r.p.m the supernatant was discarded and the spore pellet resuspended with 20 % (w/v) glycerol and stored at -20 ºC.

2.5.3 Pre-germination of *S. coelicolor* spores

A spore suspension was prepared and spores pelleted in a bench top centrifuge. Spores were recovered in 5ml of TES buffer and heated to 50°C for 10mins. The tube was cooled quickly under a cold tap. Dense spore suspension of *Streptomyces* was added into 50ml 2xYT for 6-10 hours. Cells were pelleted at 3,000rpm for 10min. 10-12ml SDW was used to resuspend the pellet. The optical density of the growth was monitored at 450nm, and the cells were diluted according the readings from the spectrophotometer. The reading was then used to calculate the volume of inoculum needed to maintain constant inoculum strength $3x10^6$ pregerminated spores (gs).

2.5.4 Growth of *Streptomyces* mycelium.

Ehrlenmeyer flasks containing sterile springs (acting as baffles) and YEME were used for growing liquid cultures of *Streptomyces*. The volume of culture depended on the final use of the mycelium. For genomic DNA isolation, 50ml-100ml of broth were used, keeping the volume of the flask at least 5 times the volume of the broth to facilitate good aeration when incubated in an orbital shaker at 30°C at ca. 250 rpm.

2.5.5 Introduction of DNA to *S. coelicolor* by conjugation.

Spores of *S. coelicolor* were resuspended in 2YT medium and then incubated at 50 ºC for 10min. *E. coli* ET 12567/pUZ8002, containing the plasmid of interest was grown till 0.5-0.6 $O.D_{600}$ and pelleted. Wash the cells twice with an equal volume of LB (to remove antibiotics that might inhibit *Streptomyces*). The cells were mixed with the heat activated approximately 10^8 *Streptomyces* spores, pelleted briefly and the resulting mixture plated on to MS media. After 16 hrs of incubation exconjugants were selected by the addition of nalidixic acid and the appropriate antibiotic. Then the plates were incubated for 3 days to allow growth of primary exconjugants.

2.5.6 Isolation of genomic DNA from *S. coelicolor*.

200 µl of a *S. coelicolor* spore suspension was inoculated in 25ml of YEME medium (Table 5) and incubated for 3 days at 30ºC shaker (250r.p.m.). The culture was centrifuged at 10,000 r.p.m. for 5 min at room temperature. The pellet was then resuspended in 3ml of 25mM Tris- pH8 contains lysozyme (2mg/ml) and RNase A (10mg/ml). The tube was incubated for 30min at 37ºC, followed by the addition of 5ml of 0.3 M NaCl with 20 % SDS (w/v), after brief vortexing 6ml phenol-chloroform solution was added, and the solution also mixed by vortexing. After centrifugation at 10,000 r.p.m. for 5min, the aqueous phase was transferred to a clean Oakridge tube. This process was repeated until the top aqueous layer became transparent. The aqueous phase was then transferred to a sterile tube.

10ml of absolute ethanol was added and the tube was inverted 3 times. The DNA was spooled out from the solution using a bent Pasteur pipette wiping away the drops of ethanol and dried at room temperature for 10mins. Finally the DNA was dissolved in 500µl T.E. buffer and stored at -20 ºC.

2.6. Polymerase chain reaction.

All primers used for the study were obtained freeze dried from MWG-Biotech A.G. Primers were reconstituted with appropriate volumes of sterile distilled water to an overall concentration of 400pmol/µL primers were stored at -20°C.The PCR reaction was set up in a 0.5ml Eppendorf tube. The reaction mixture was set up as in Table 10 $MgCl_2$ was added according to the manufacture's instructions. Fermentas *Taq* polymerase and Roche high fidelity DNA polymerase were used for different reactions conditions. Using an Eppendorf Mastercycler gradient PCR machine, the PCR reaction was carried out. PCR products were purified using a Qiagen PCR clean up kit (Table 9). Different programmes were used for different PCR products. The primers used in this work are explained in Table 11 and the PCR programmes used to derive the products are explained in detail in subsequent chapters (3, 4, 5 & 6).

2.6.1. Preparation of dNTPs.

Nucleotide bases are prepared from a stock of 100mM diluted to a working concentration of 1.25mM and stored at -20˚C.Sterile deionized distilled water was used for dilution. The same concentration was used for both PCR and probing DNA for Southern blot.

Table 10: PCR reaction mixture

PCR reaction mix	Volume in µl
Buffer 10X	10
dNTP's(1.25mM)	8
DMSO	2.5
Primer 1 (100pM)	1
Primer 2 (100pM)	1
Template DNA	1
DNA Taq Polymerase	0.5
Water	26
Total volume	50

SCO1389-egfp **primers for native promoter**	
CL100	CCCAAGCTTGGATCCAATCGGCTGCGAC
CL101	GGGACTAGTCATATGTCTAGATGTGTATAAGAGACAGTCTGG
SCO1389 **primers for over expression**	
CL102	GGGATATCCATATGAGCATCATTGGCTCGTT
CL103	CCCAAGCTTCTAGATCAATCGGCTGCGACGT
SCO1389**-PCR mediated mutagenesis' primers**	
CL104	CGAGAGCCAGAGCTTTTTTGCGTTGAGGTAAGGTCAGTGATTCGGGGGATCCGTCG
CL105	GGCCATCCGGCCACCGGGACCGCGCAATCGGCGAGTTCATGTAGGCGTGAGCTG
SCO1389-egfp **primers for over expression.**	
CL106	GGGATATCCATATGAGCATCATTGGCTCG
CL107	CCCAAGCTTCTAGATTACTTGTACAGCTCGTCCATG
SCO5750**-PCR mediated mutagenesis' primers**	
FtsK-1	GAGGGGCGACACGAACGGGTGAAGCGGTAGGCACACGTCATTCCGGGGATCCGTCGAC
FtsK-2	GGCGGATCGTCGGCGGAACCCTTCTCCTACCCGCCCCTATCATGTAGGCGTGAGCTG

Table 11: Oligonucleotides used in this study.

Restriction sites (CL100, CL101, CL102 & CL103) and homologous regions to am^r (pIJ673; Güst *et al*., 2003) are underlined (CL104 ,CL105 and FtsK-1,FtsK-2).

2.6.2. PCR programmes for different primers.

(A) Redirect PCR-mediated gene replacement (chapter 4 and 5).

PCR reaction conditions were followed from Gust *et al.,* (2003); denaturation at 94°C for 2 min, then 10 cycles with denaturation at 94°C for 45 s, annealing at 50°C for 45 s, and extension at 72°C for 1 min 30 s, were followed by 15 cycles with the annealing temperature increased to 55°C. A last elongation step was done at 72°C for 5 min. The PCR product was analyzed by gel electrophoresis and purified by using a PCR Purification kit. The expected sizes are 78 bp larger than the sizes of the disruption cassette pIJ773 because of the 2 x 39 bp 5´-primer extensions. The PCR product was purified using the Qiagen PCR purification kit.

(B) Construction of *SCO1389* depletion strain (chapter 6).

The PCR reaction conditions that were followed for amplifying the *SCO1389* gene were; denaturation at 94°C for 2 min, then 10 cycles with denaturation at 94°C for 45 s, annealing at 54.9°C for 45 s, and extension at 72°C for 1 min 30 s, were followed by 15 cycles with the annealing temperature increased to 61.4°C. A last elongation step was done at 72°C for 5 min. The PCR product was analyzed by gel electrophoresis and purified by using a PCR Purification kit.

(C) Construction of over-expression strain of *SCO1389* (chapter 7).

PCR reaction conditions: denaturation at 94°C for 2 min, then 10 cycles with denaturation at 94°C for 45 s, annealing at 54.9°C for 45 s, and extension at 72°C for 1 min 30 s, were followed by 15 cycles with the annealing temperature increased to 61.4°C. A last elongation step was done at 72°C for 5 min. The PCR product was analyzed by gel electrophoresis and purified by using a PCR Purification kit.

2.7 Southern hybridization.

Southern hybridization (Kiesar *et al.*, 2000) was performed to confirm mutations constructed by PCR mediated mutagenesis. DIG-labelled (digoxygenin) DNA probes were used (DIG-DNA Labelling Kit from Roche) along with Hybond-N+ nitro-cellulose membranes (Amersham Biosciences Ltd.).

2.7.1 Probe synthesis by random primed DIG DNA labelling.

Using Klenow enzyme, DIG-dUTP's are incorporated into the DNA fragment to be used as the probe. 10µl DNA (1µg) in SDW was denatured by boiling for 10 minutes and placed immediately on ice for at least 1 minute and centrifuged briefly. To this solution 2µl hexanucleotide mix, 2µl d-NTP labelling mix (1mmol/l dNTPs) and 1µl Klenow enzyme (1U/µl) were added and gently mixed by pipetting .The reaction was incubated at 37^{o}C overnight and stopped by the addition of 2µl 0.2M EDTA. The probe was then boiled for 10 minutes and cooled on ice for 1 minute before hybridization at 42^{o}C overnight.

2.7.2 Binding DNA to nitrocellulose membrane.

DNA was isolated as mentioned in sections 2.5.4 and 2.6.7 for analysis by Southern. DNA was concentrated by ethanol precipitation. Lambda DNA digested with HindIII was used as a standard marker to identify bands used during Southern bloting. Further, all DNA samples were separated by electrophoresis on 0.8% agarose gel over night at 25V. The nitrocellulose membranes used to bind the DNA were washed thoroughly with deionised distilled water and then pre incubated in 10XSSC buffer for 15minutes along with filter paper. The filter paper was then transferred to a Vacugene XL blotting unit in the following order; filter paper, nitrocellulose membranes followed by agarose gel and plastic mesh. The vacuum pump inlet was connected to the blotting apparatus and the vacuum pressure was set between 50-60 mbar.

The gel was washed in deionised H2O before being immersed in depunaturation solution for 15 minutes twice. Afterwards, it was rinsed with deionised H2O. The gel was then immersed in denaturation solution and left for 15 minutes, this was then repeated, as before, and rinsed with deionised H2O.Then, the gel was covered in neutralization solution for 30 minutes. Finally, 20 x SSC was used to cover the gel and left for 1 hour to allow efficient blotting. Following this, the membrane was baked at 80°C for 2 hours.

2.7.3 Hybridization of DNA.

Membranes were rolled and placed inside the hybridization tube and incubated with prehybridization solution for 2hr. The solution was then decanted before adding the DIG labelled probe in hybridization solution. Before addition the probes were placed on boiling water bath for 10min and cooled immediately on ice for 2 min and hybridization was carried out overnight at 42°C in a hybridization oven.

2.7.4 Detection of the hybridized DNA

Membranes were washed gently with 2xSSC and 0.1% (w/v) SDS twice for 15min at 68°C in a hybridization oven. This was repeated with 0.2xSSC and 0.1%SDS under the same conditions. After consecutive washes the membranes were now ready for detection. The detection step was carried out with the hybridization oven kept open. The following washes were carried out separatley in order to develop the membrane. Initially, membranes were incubated in buffer I for 1min, followed by buffer II, for 30min. A quick wash in buffer I for 2min was followed by the addition of 3µl of antidigoxygenin AP (antibody conjugate) to 15ml of buffer I to the membrane before incubation for 30min-45min.Before developing, the membrane was washed in 10ml of buffer III for 2mins. The membranes were then transferred to a sealed plastic bag. 10ml of NBT solution (NBT Tablets dissolved in buffer III) was added and incubated in the dark for 1-2hr. To stop the reaction the bag was cut open and the membrane washed 5-10 times in running water and stored in the dark for further analysis.

2.8. Preparation of the samples for microscopy.

2.8.1 Growing cultures on cellophane.

Cellophane discs were placed on moist filter paper in glass Petri dishes, and sterilised by autoclaving for 15min. Cover slips sterilised with ethanol. Using sterile forceps the cellophane discs were transferred onto cover slips. These cover slips were then placed at acute angle on agar plates. 10µl of a 10^{-2} dilution from a *S. coelicolor* spore suspensions was added to the acute angle between the cover slips and the agar plate before being incubated at 30°C for 1-2 days. Similar protocol was carried out for setting up cultures on cover slips without cellophane.

2.8.2 Methanol fixation of *Streptomyces* for microscopy.

Cells were grown on cover slips as mentioned in section 2.9.1 for 48hr at 30°C. These cover slips then carefully removed from the agar plate and dipped in methanol to fix the cells. The cover slip was air dried, 8µl of 40% (w/v) glycerol in phosphate buffer saline (Table 5), added and the cover slip was pressed against the microscopic slide. Using tissue paper, excess glycerol was removed and the cover slips and slide were sealed using nail varnish before visualizing by microscopy for EGFP fusions.

2.8.3 Fluorescein –WGA/Propidium iodide staining

For the detection of nucleic acid and peptidoglycan of *Streptomyces* cultures, WGA/propidium iodide staining (Table 11) was carried out. The cells were anchored on cover slips using the 500µl of fixative solution (Table 5) for 15 min at room temperature. The cells were washed twice with PBS to remove any traces of fixative then air dried. The cells were rehydrated with PBS for 5 min, and then incubated with 2mg/ml lysozyme in GTE for 1 min at room temperature.

The cover slips were washed with PBS and 2% BSA (w/v) in PBS was added to the cells and incubated for 5 min at room temperature. All subsequent steps were carried out in the dark. Fluorescein WGA in PBS with 2% BSA was added to the cover slips and incubated for 2-4 hrs at room temperature. Then the cover slip was washed 10 times with 10µg/ml propidium iodide in PBS. Before the addition of slow fade solution to the cover slip, the cells were washed twice with equilibration solution (Molecular probes, solution C) for 5 min at room temperature. 8µl of slow fade solution was added and the cover slip was mounted on the slide and sealed with nail varnish.

2.8.4 10-Nonyl acridine orange staining.

NAO was added to a final concentration of 100 nM to the cover slips that was harvested after 3 days the cells were viewed by using an inverted fluorescence microscope (Nikon). Green fluorescence (with excitation at 495 nm and emission at 525 nm) from NAO was detected by using a standard GFP(R)-BP filter unit (excitation at 460 to 500 nm and emission at 510 to 560 nm). The exposure times for green NAO were 2 to 8 seconds.

2.8.4 Live cell imaging.

All live cell imaging were all carried out in a µdish (ibidi® Integrated BioDiagnostics). This is a small version of a normal Petri dish which can be mounted on a heated stage of the microscope. In order to minimize focal drift, the microscope stage and imaging chamber were allowed to equilibrate for 1 hour with respect to temperature before the start of microscopy. Imaging in *Streptomyces* was very difficult because of its heterogeneticity and 3D structure. To overcome this, images were acquired by a series of sections along the optical (z) axis of the microscope. These images then further used to construct three dimensional images or compressed to a single plane using IPLab software.

The cultures grown on cellophane (section 2.9.1.), and carefully stripped from the cover slip. The strip was then transferred to μdish creating a sandwich of the culture between the cellophane and the base of the dish. Using the sterile forceps 2% (w/v) agar plug was placed on top of the cellophane which hydrates and pass on the nutrients to culture through the cellophane. The complete set up was then mounted on the heated stage at 30˚C and observed under the microscope (Fig. 8).

2.8.5 Use of fluorescent dyes in time-lapse microscopy.

Fluorescent dye such as FM4-64; NAO, Fluorescein-WGA, propidium iodide, Vancomycin FL and Syto 42 from Invitrogen (Molecular probes) were used in this study (Table 12). The dye concentration were optimized and then applied to the cells to be observed by fluorescence microscopy. Samples were studied using a Nikon TE 2000 Eclipise inverted fluorescent microscope with 100X oil N.A. 1.3 objective lens, and images were captured bu Hamamatse camera.

Images were then processed using IPlab 3.7 bioimaging processing software (B.D. Biosciences Bioimaging, Rockville, M.D). For 3 dimensional image constructions, we used 0.5μ Z sections of both phase contrast and fluorescent images. The images were captured at 15minutes interval. For fluorescent microscopy studies the dye with the optimal concentration was then added over the agar plug and air dry for 15min then transferred to the μdish (Fig. 8). Filters used for different probes are described in table 13

2.8.6 Movie making.

One of the major advantages of live-cell imaging is to perform time-lapse experiments and make movies of time-lapse imaging. This can provide an extraordinary insight into the dynamics of labelled macro molecules in living bacterial cells. Typically images were capture 20–145 images at 5–30 minutes intervals in a time course. These images may then be processed and imported into a movie-making software package (that is present within IPLab software) in which they can be compressed, and saved into audio video interleave file (avi).

Table 12: Fluorescent stains

Dye	Stock	Working concentration	Filters used
Fluorescein-WGA	1 mg/ml	2 µg/ml	FITC
Propidium iodide	25 mg/ml	10 µg/ml	TRITC
Syto-42	5mM	1µM	DAPI
FM4-64	1 mg/ml	1 µg/ml	TRITC
NAO	21mg/ml	100nM	FITC & TRITC
Vancumycin FL	5mM	1µM	FITC

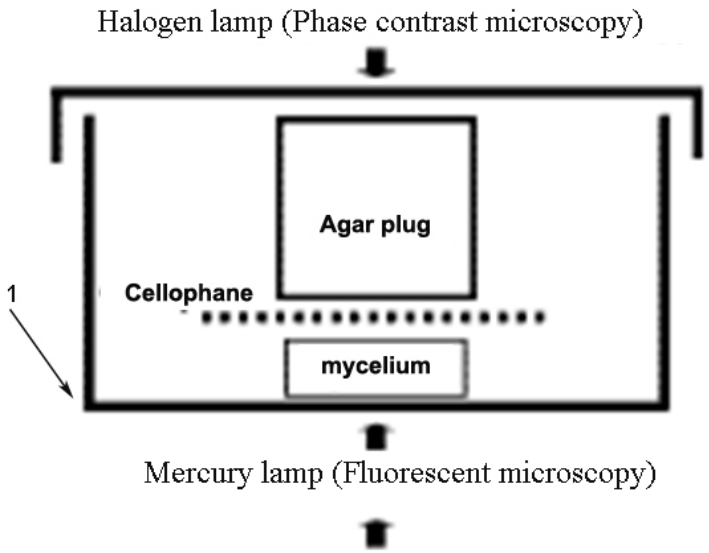

Figure 7: Live cell imaging set up

Imaging of *Streptomyces* on solid agar surface. Pre-germinated spores of about 6-8hrs of time was grown on cellophane disks before before being inverted and transferred to the µ-dish (1) imaging chamber. Subsequently, a cylinder of 3MA was applied to the cellophane µdish and the imaging chamber transferred to the incubation chamber set to 30°C and allowed to equilibrate for 1 hour before commencement of imaging.

2.9 Bioinformatics tools

2.9.1 Analysis of the genome sequences through BLAST.

All analysis of nucleotide and amino acid sequences was achieved by the Basic local alignment tool (BLAST). This allowed for the alignment of sequences against a publicly available database at the National Centre for Biotechnology Information Genebank. The programs BLASTP (Altschul *et al.*, 1997) were used for protein-protein analysis.

2.9.2 ClustalW2.

The DNA or protein sequences of specific gene of interest from one organism can be used to compare with different species and higher organisms using ClustalW2. This programme aligns multiple sequence data to show their identities, similarities and differences between the sequences. This programme can be accessed from European Bioinformatics Institute (EMBL-EBI) at http://www.ebi.ac.uk/Tools/clustalw2.

2.9.3 Cloneman version 6.

Clone-manager software can be used to do virtual experiments using DNA sequences for various activities like vector construction, alignment studies, primer designing, cloning and ligation. This programme is provided by Scientific & Educational Software. This software mainly focuses on controlling all DNA file handling, molecule viewing, sequence editing and general utility functions for molecular biology programme.

2.9.4. SMART protein analysis.

Using amino acid sequences protein structure and their functional group can be predicted using SMART (Simple Modular Architecture Research Tool). SMART programme identifies homologues, PFAM domains, signal peptides and internal repeats. This software can be accessed from http://smart.embl-heidelberg.de.

Chapter 3

Application of fluorescent probes and time-lapse microscopy in *S. coelicolor*.

3.1 Visualization of cell wall and nucleoids in fixed cells

Previously, *S. coelicolor* cell wall was visualized after lysoyme treatment and staining with fluorescent conjugates of letin wheatgerm agglutinin (WGA). WGA binds to oligomers of N-acetylglucosamine and N-acetylmuramic acid and therefore binds to lysozyme treated cells (Schwedock *et al*., 1997). Nulcleoids were stained with propidium iodide (Fig. 8B1 and B2). It was found that WGA stains strongly the tips than the hyphae, suggesting that it binds strongly to the newly formed cellwall than the lysozyme treated cell wall. The figure 8 shows the staining pattern of WGA and PI in M145 *S. coelicolor.* This stain is commonly used to visualize the cell wall and DNA in *Streptomyces*; however this is a dead cell staining method. With more new fluorescent probes, we now can explore the staining of cell walls and DNA in live cells together with protein EGFP tagged studies.

3.2 The pattern of FM 4-64 staining seems to reflect heterogeneity of phospholipid distribution in the membrane

Recent biochemical and physiological studies in *E. coli* have shown that the membrane lipids are actively involved in major cell cycle events (Funnel, 1993; Nanninga, 1998; Fishov *et al*., 1999). Anionic phospholipids, such as phosphatidylglycerol, in the fluid phase are required for rejuvenating the replication initiator protein, DnaA by facilitating an exchange of tightly bound ADP with ATP (Crooke *et al*., 1991; Castuma *et al*., 1993). Nucleoid associations with the membrane have been observed indirectly using a variety of techniques (Schaechter *et al.*, 1991). Membrane proteins have been proposed to be involved in the regulation of DNA replication and segregation and cell division through the formation of specific lipid domains (Norris, 1992; 1995; Woldringh *et al*., 1995; Binenbaum *et al*., 1999). It has been speculated that phospholipid defects may affect the correct interaction of FtsZ with the cell membrane and alter the ring structure (Mileykovskaya *et al.*, 1998)

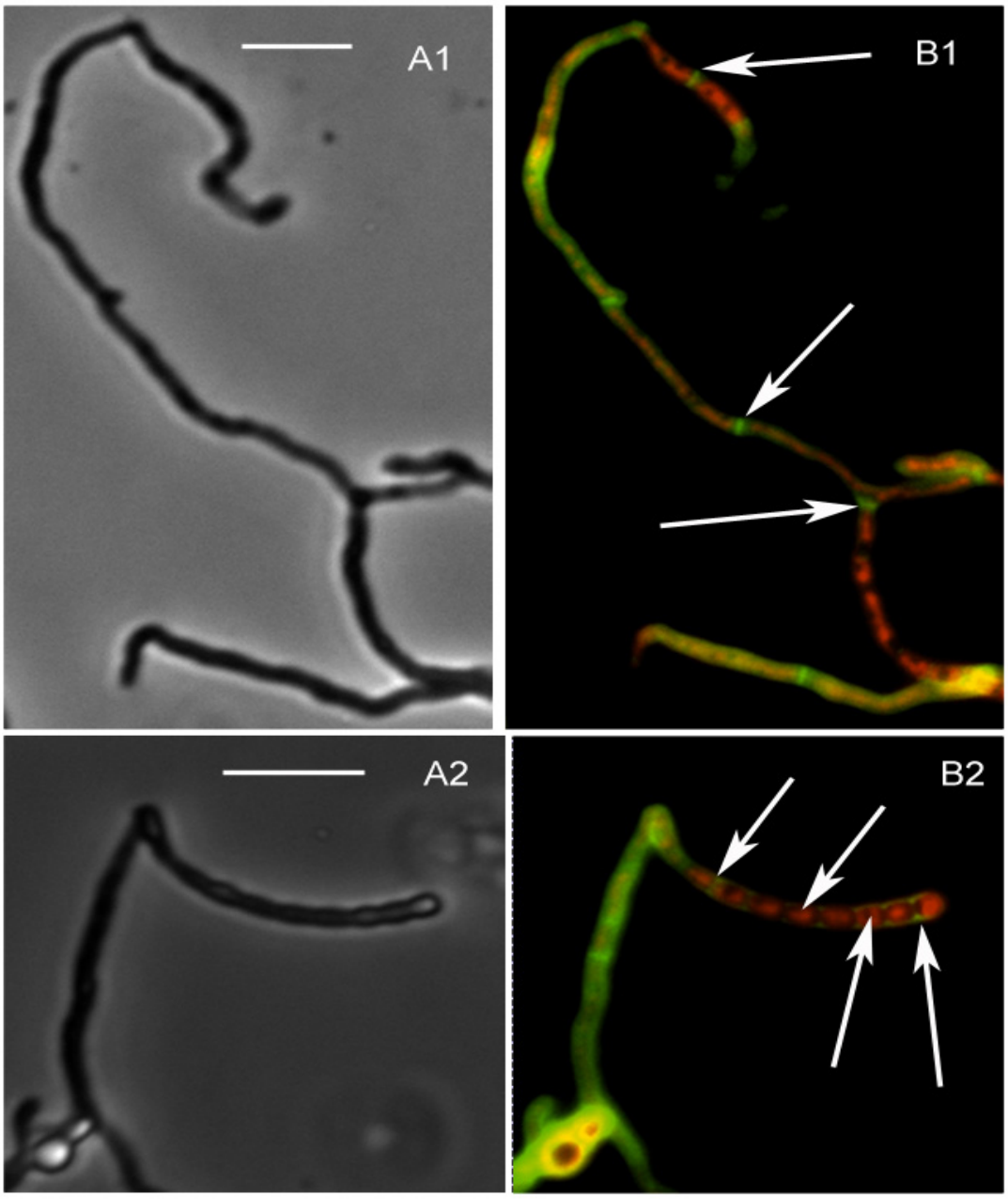

Figure 8: Visualization of DNA and cell wall in M145.

M145 was stained with WGA and PI, staining cell wall (green) and DNA (red). A1 and A2 are the phase contrast images, B1 and B2 are fluorescent images, and the arrows indicate the cross walls in substrate hyphae (B1) and aerial hyphae in (B2). Size bar 10μm.

In spite of these examples from *E. coli*, heterogeneity in the *Streptomyces* membrane, either in its phospholipid or in its protein components, has not yet been observed. Here, we used the vital membrane dye FM 4-64 for the visualization of *S. coelicolor* membrane. It has a bright red fluorescence and could thus be used for multiple staining with Syto42 for nucleoid display.

Amongst the most commonly used fluorescent dyes for live cell imaging of fungal cells are the styryl-based dyes FM4-64 (Parton *et al*., 2000). The probe FM 4-64 has a rigid hydrophobic tail containing the fluorophor and a positively charged head. In yeast, this dye only appears in vacuolar membranes (Vida and Emr, 1995), this shows that the dye seems to have higher affinity for membranes rich in basic phospholipids. The predominant phospholipids in *S. coelicolor* are Phosphatidylethanolamine (zwitterionic), phosphatidylglycerol and cardiolipin (both negatively charged) (Verma, 1983). The staining pattern developed and gradually disappeared on long incubation. The majority of cells showed a clear banding pattern, as shown in Fig. 9 B2. The most distinct dark bands occurred in the anucleated regions of the mycelium, branch points and hyphal tips. To determine the banding pattern correlating with the position of nucleoids in the mycelium, we used Syto42 stain, which binds to DNA and emits in blue (435nm) on excitation under UV light (340nm) (Table 13). In Fig. 9A and B, shows the distinct lipid domains in between the nucleoids. To conclude, whatever the nature of FM 4-64 distribution heterogeneity, we demonstrate for the first time a membrane pattern in live *S. coelicolor* in relation to the position of the nucleoids.

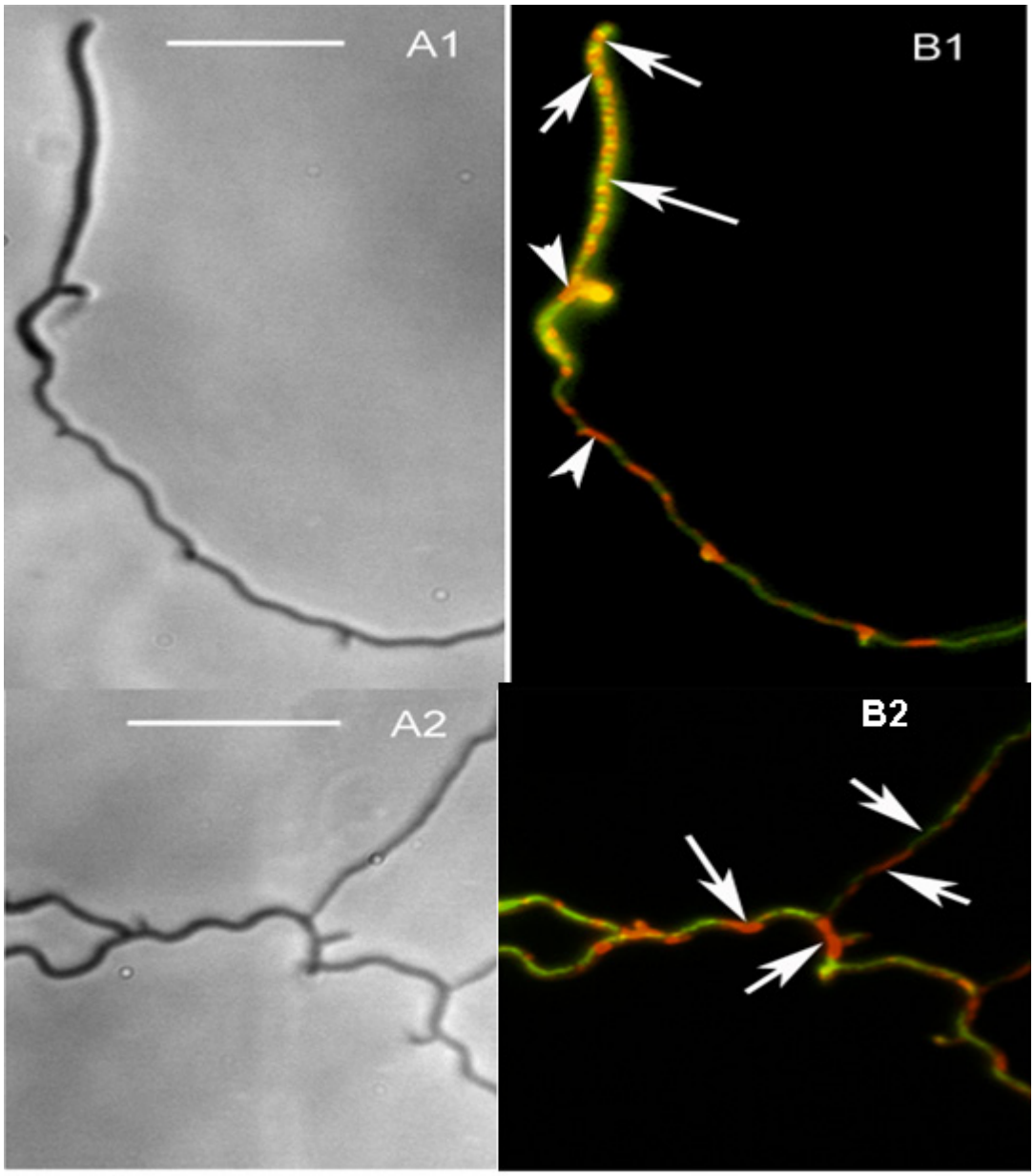

Figure 9: Visualization of lipid domains and nucleoids in M145.

M145 was stained with FM4 64 and Syto42, staining DNA (green) and lipid domains (red). A1 and A2 are the phase contrast images, B1 and B2 are fluorescent images, and the arrows indicate the lipid domains sandwiched between nucleoids in the substrate mycelium and the localization near branch points and aerial hyphae, (B1) and aerial hyphae in (B2). Size bar 10µm.

3.3 Cardiolipin domains in *S. coelicolor* membranes.

In *Streptomyces*, the protocol was adapted from Mileykovskaya, and Dowhan, (2000); NAO was added to a final concentration of 100 nM to the cover slips that were harvested after 3 days. After incubation at room temperature for 20 min, the cells were viewed by using an inverted fluorescence microscope (Nikon). Green fluorescence (with excitation at 495 nm and emission at 525 nm) from NAO was detected by using a standard GFP(R)-BP filter unit (excitation at 460 to 500 nm and emission at 510 to 560 nm). To minimize the toxicity of high-energy emission light, the focus was set under phase-contrast conditions. The exposure time for green of NAO was 0.2 to 0.8 seconds. In our work, we obtained evidence of heterogeneous distribution of cardiolipin in the gram-positive bacterium *S. coelicolor*. The cardiolipin rich domains were found in the branch points, hyphal tips and aerial hyphae (Fig. 10 B1 and B2). These accumulations of cardiolipin domains were consistent to the staining pattern of FM4 64, but using NAO more specific domains were seen in mycelium.with less than 1μm in length. The biological significance of the cardiolipin domains in sporulation was illustrated by using mutants with defective in erection of aerial hyphae, frequency of branching, dividing tips, swollen hyphal tips and mycelium (explained in subsequent chapters 6 & 7). What is the role of the cardiolipin rich domains in these membranes? We speculate a distinct role played by cardiolipin-rich domains within membranes. Cardiolipin could contribute to recruitment of peripheral membrane proteins to localize to specific regions of the cell membranes, and it could also contribute to maintenance of the optimal activity of these proteins. Recent studies shows that MinD, localizes in a horseshoe structure on the membrane at the poles of *E. coli* cells (Raskin *et al*., 1999, Suefuji *et al*., 2002). MinD, with its C-terminal amphiphilic α helix bound to liposomes containing anionic phospholipids, has a higher affinity for cardiolipin enriched liposomes (Mileykovskaya *et al*., 2003, Szeto *et al*., 2002). The other essential interactions of cardiolipin with integral membrane proteins (e.g., cytochrome *c* oxidase) are well known (Dowhan, 1997). Hence, some of the sporulation and apical extension specific proteins involved in *S. coelicolor* (Flardh, 2003; Tseng *et al*., 2006; Noens *et al*., 2005) could require cardiolipin dependent localization and/or maintenance for optimal activity.

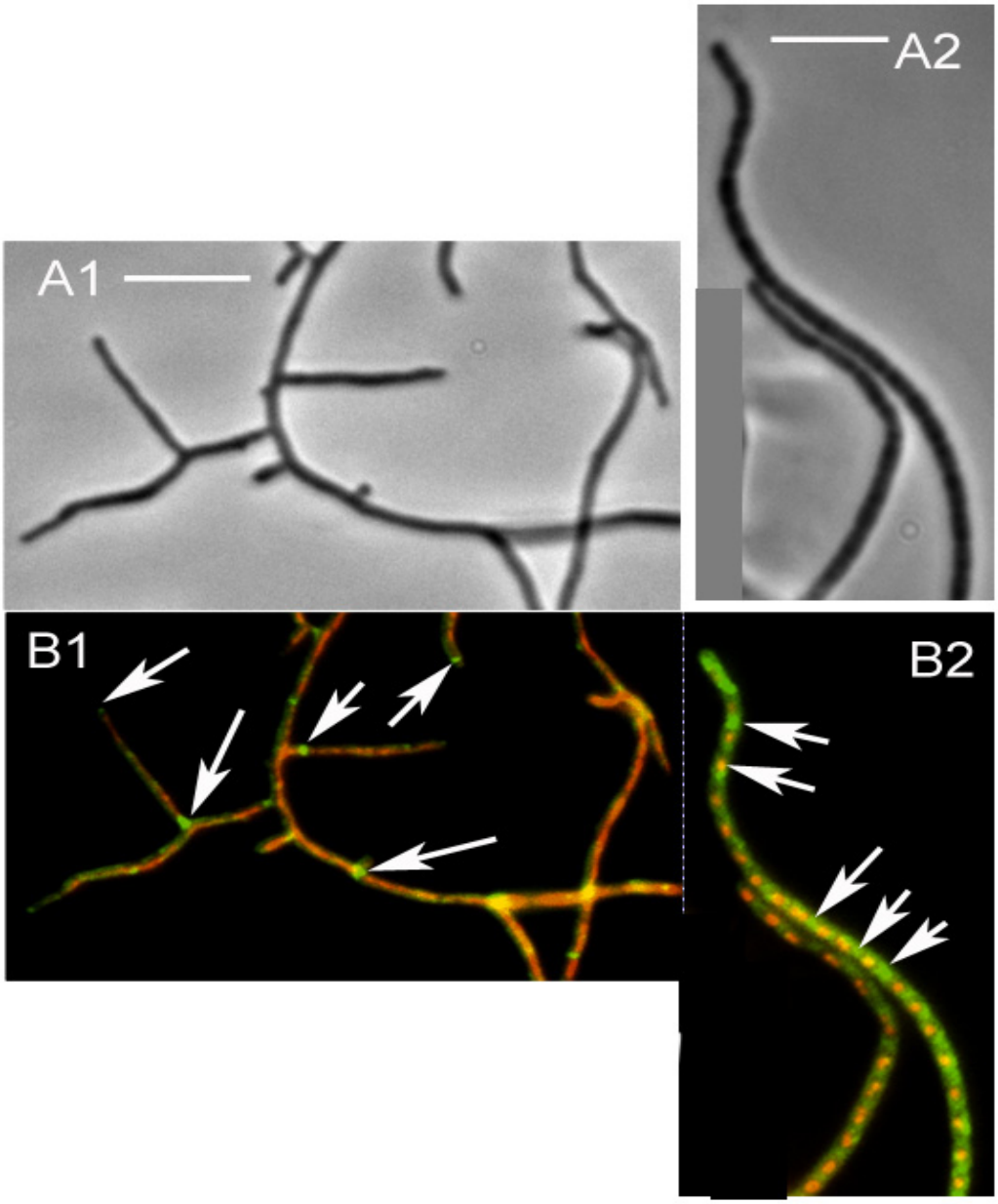

Figure 10 : Visualization of cardiolipin domains and nucleoids in M145.

M145 was stained with NAO and Syto42, staining DNA (red) and cardiolipin domains (green). A1 and A2 are the phase contrast images, B1 and B2 are fluorescent images, and in B2 arrows indicate the lipid domains sandwiched between nucleoids in aerial hyphae and B1 shows localization near branch points, hyphal tips and anucleated regions in substrate mycelium size bar 10µm.

3.4. Conception and implementation of time-lapse microscopy.

The Nikon TE 2000 inverted fluorescent microscope (IFM) is a 3D deconvolution microscope. Live-cell imaging requires cells to be in normal growth conditions (like temperature and availability of oxygen) and the use of low-dose techniques (e.g. using dyes at low non-cytotoxic concentrations with levels of light irradiation at non-harmful visible wavelengths). To monitor the temperature, ibidi® Integrated BioDiagnostics, have designed a unique heating stage that allows an easy temperature control. The heating device has been coupled with the microscopy stage and can hold the oxygen permeable ibidi μ-dishes (35mm Petri dish with a tin bottom for high end microscopy).

3.4.1 Multiple labelling living cells.

Multiple labelling is often possible with living Streptomyces cells. We have used different fluorescent probes combine together. In this chapter we use FM4-64 as a general membrane stain (Vida et al. 1995), Syto42 for staining DNA (Rowan et al., 2007), and vancomycin FL (Daniel and Errington, 2003) for peptidoglycan (Table. 13). Labelling proteins with enhanced green fluorescent protein (EGFP) (Sun et al., 1999) was used to monitor protein trafficking within cells (Table. 13). Triple labelling is also possible with proteins labelled EGFP, membrane stained with FM4-64 and DNA stained with Syto42. Certain combinations of dyes, however, are sometimes incompatible and can result in increased phototoxicity and cytotoxicity during live cell imaging e.g. propidium iodide and wheat germ agglutinin FL (Schweddock et al, 1997). 10-nonyl acridine orange is also used in live cells to localize specific membrane anionic lipid, cardiolipin.

Stain	Ex	Em	Filters used	Excited colour	Overall colour
FM4-64	558	734	TRITC	Green	Red
Syto42	433	460	DAPI	UV	Blue
Vancomycin-FL	504	511	FITC	Blue	Green
10 nonyl acridine orange	525 495	640 519	TRITC FITC	Green Blue	Red Green
Wheatgerm agglutinin	496	524	FITC	Blue	Green
Propidium iodide	535	617	TRITC	Green	Red
Green fluorescent protein	395	509	FITC	Blue	Green

Table 13: Fluorescent probes and their respective filter selection.

3.5 Phase contrast cinephotomicrography of life cycle in *S. coelicolor*.

Streptomycetes are multicellular bacteria that undergo a series of regulated developmental processes including germination, vegetative mycelial growth (Fig. 11) and secondary metabolite synthesis and eventually spore morphogenesis (Chater, 1993). In the initial stages of germination (Fig. 11), undefined signals trigger influx of water into spores, resulting in an increase in size and decreased phase brightness followed by germ-tube emergence (Hardisson *et al*., 1978). Unlike unicellular bacteria, in which chromosome replication is followed by cell division, Streptomyces genomes remain associated in branching filaments, thereby generating a dense interconnected mycelial colony (Allan and Prosser, 1985). Subsequently, discontinuous growth kinetics has been observed in *S. hygroscopicus* and *S. griseus* species (Holt *et al*., 1992; Neumann *et al*., 1996).

Despite several attempts to grow *S. coelicolor* on agar sandwiched between glass and coverslips, the oxygen levels in these environments can vary considerably. Although *S. coelicolor* cannot grow in the complete absence of oxygen, it is capable of microaerobic growth and remains viable in the absence of oxygen for long periods of time (Van Keulen *et al*., 2007). The spores took 5-6 hours to germinate, and another 4 hours to produce germtubes. In the frame figure 11A, 39 spores were analyzed of which 82% of them germinated. On an average around 85% of spores swelled and became phase dark prior to germ tube emergence (Jyothikumar *et al.*, 2008). It was impossible to describe accurately each spore germination pattern because of the difficulty of overlapping of the hyphae from a neigbhouring spore and also due to spore clumping. It was noticed some growth arrest between two germtubes from a single spore. These have been shown with statistical evidence that, germination in *S. coelicolor* is heterogeneous and displays apical dominance (Jyothikumar *et al*., 2008). After germination, the hyphal tip extends out and starts to branch to form a vegetative mycelium.

Filming vegetative mycelia (for 4 hours) was an easy step forward in documenting the growth in *Streptomyces* (Fig. 11B). The rate of hyphal tip extension calculated under normal growth parameters was 18.83 (2.13) μm/ hour and the branches formed on an average 10.23 (2.65) μm behind hyphal tips. Most of the substrate hyphae branched more than once and within few hours developed into a matted layer over one another (Fig. 11B 10-13).

This is the major problem encountered frequently in time-lapse imaging for more than 14 hours. The neighbouring cells start to outgrow the selected frame and the original focal point was lost. The average associated with branch-to-branch distances is relatively large standard deviation suggests that *S. coelicolor* shows great variability in branch placement with respect to the location of other branchs. After the growth of substrate mycelium the *S. coelicolor* develops morphologically and erects aerial hyphae (Chater, 1993). At this point aerial hyphae obtain nutrients from the degradation of the vegetative mycelium (Challis and Hopwood, 2003; Miguelez., 1999). The formation and initiation of aerial hyphae erection is the result of a complex intracellular signalling cascade and is consistent with the switch between the primary metabolisms to secondary metabolism with production of antibiotics (Champness, 2000; Chater, 1998; Willey *et al.,* 2006).

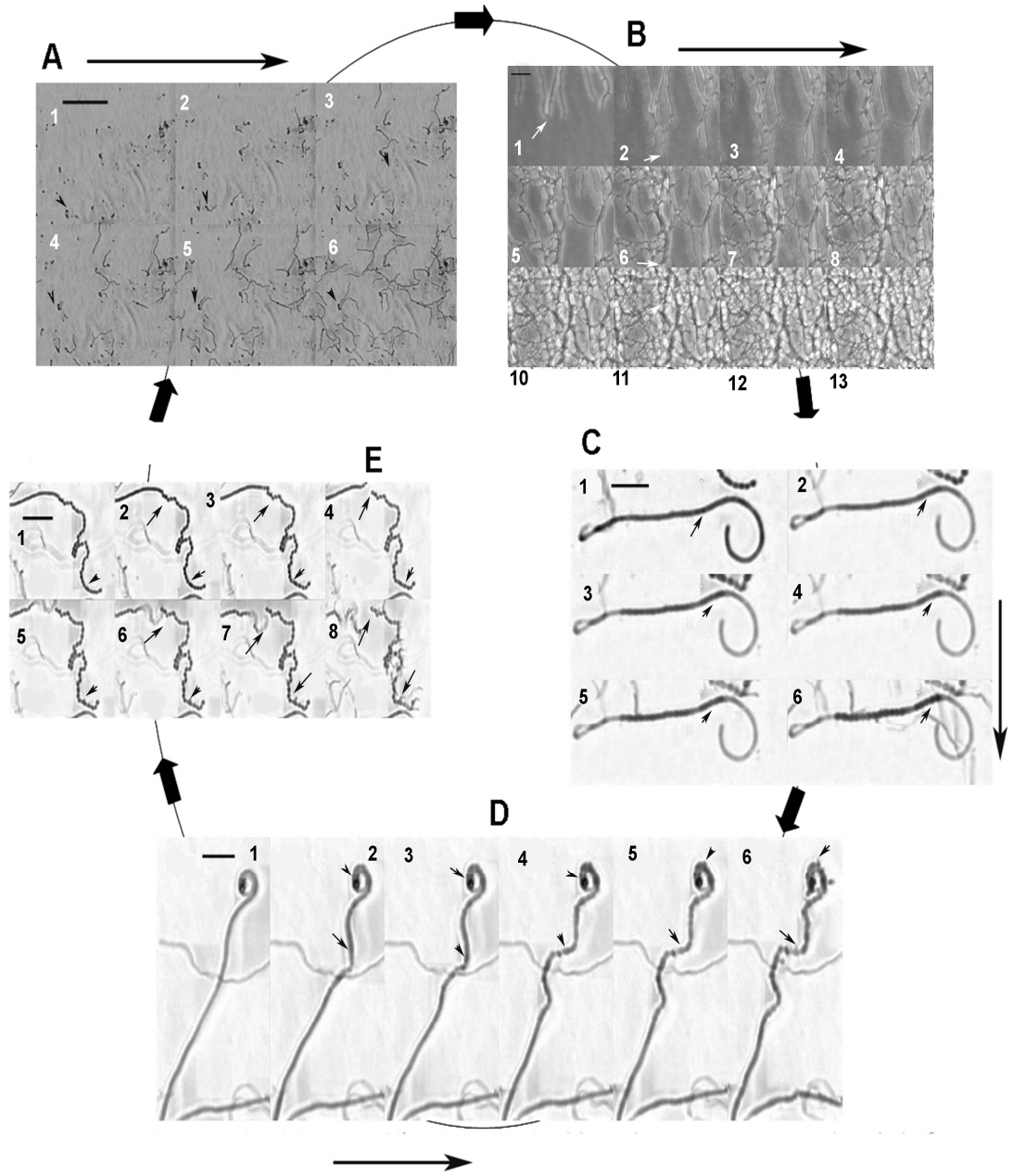

Figure 11: Time-lapse microscopy of life cycle in M145.

A-germination the black arrow indicates the germ tube extension, B-development of substrate hyphae and white arrows shows hyphal tip extension, C-young aerial hyphae goes to sporulation, black arrow shows the phase change from grey to black dense spore, D- aerial hyphae through half way in sporulation and black arrow shows germination site, E-spore chains swells and undergoes germination, the arrows shows the swelling and diassociation of the spore chain and germination. The horizontal white bar represents 10 μm.

Growth of aerial hyphae was observed in real time by coverslip-cellophane-grown cultures of *S. coelicolor*, and transferred to an imaging chamber (section 2.8.1 and 2.8.4). Aerial hyphae was identified by phase-contrast microscopy and subjected to timelapse microscopy at 15-min intervals. During filming aerial mycelium, the neighbouring substrate mycelium grew over the frame and made it very difficult for imaging. Imaging was successful in recording the key stages involved in aerial hyphae inspite of frequent growth of substrate mycelium. In figure 11.C young aerial hyphae underwent a change from phase light to dark to form mature condensed spores. However, the formation of unigenomic spores stopped before the tip of the aerial hyphae. This may be due to hyphal dehydration or phototoxicity (Fig. 11 C5-6). However, in order to maintain viability of aerial hyphae, it was necessary to apply a plug of tap water agar (Fig. 7). As mentioned earlier the experiment was conducted on low nutrient source agar as the sole carbon source. In spite of nutrient downshift substrate hyphae outgrows the selected imaging field, this was because of the agarase gene (*dagA*) in *S. coelicolor* that utilizes agar as sole carbon source (Bibb *et al.*, 1987). However, some sacrifices have to be made during live cell imaging with *S. coelicolor*.

3.5.1 Disassembly of FtsZ-EGFP in aerial hypahe.

After the successful imaging of life cycle through phase contrast set up, it was interesting to move on to excite the cells with a different wavelength of light to visualize fluorescence of the tagged proteins. For this study we are thankful to Dr. Klas Flardh, who was kind in giving us the strain *S. coelicolor* K113, *ftsZ-egfp*. *S. coelicolor* K113 (Flardh, *et al*., 2000) was grown on cellophane disc as described before (section 2.8.1 and 2.8.4).

In order to study the positioning and movement of FtsZ-EGFP in aerial hyphae, the cover slip-cellophane-grown cultures of *S. coelicolor* K113 were transferred to an imaging chamber, and aerial hyphae were identified by phase-contrast microscopy and subjected to time-lapse microscopy at 15-min intervals. In order to maintain viability of aerial hyphae, it was necessary to apply a plug of tap water agar. As seen before the growth of substrate hyphae was initiated and outgrew the aerial hyphae. This switching from aerial hyphae to substrate hyphae suggests that aerial hyphae monitors its environment and senses the slightest change and some how decides not to continue sporulation, and switches back to mycelial growth. In the section above we saw the halt in aerial hyphae development and germ tubes emergence in halfway through aerial hyphae development. Here, K113 aerial hyaphe senses conditions inappropriate for sporulation and prevent its completion; either directly or indirectly, through the depolymerisation of FtsZ-EGFP spirals (Fig. 12).

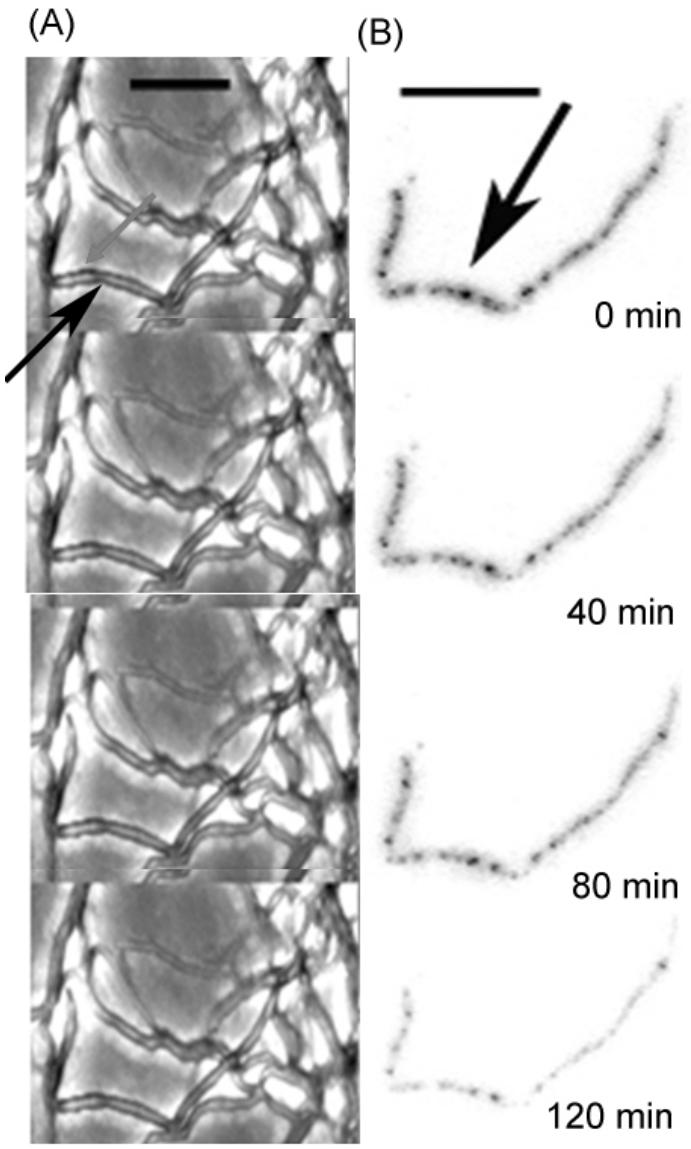

Figure 12: Time-lapse video of disassembly of FtsZEGFP in aerial hyphae.

The mosaic image is composed of images taken at 40-min intervals; A –Phase contrast images and B show the fluorescence images with inverted greyscale to clearly visualize the signals.The horizontal white bar represents 10 μm.

3.5.2 Application of FM4 64 and Syto 42 probes in time-lapse microscopy.

As explained in section 3.4 and 3.4.1, time-lapse microscopy was established. We noticed that whenever we use z section for fluorescent images, prolonged exposture quenched the intensity of fluorescence. Z-sections are sequential of optical slice acquired at different depth perpendicular to the z-axis. The section was collected by step-by-step changes in the fine focus of the microscope with sequential image capture at each step.

The experiment was designed to film different stages of the life cycle in *S. coelicolor*. Due to continous excitation of high energy photons (523-553 nm and emission at 590-650nm), the growth was arrested due to photolysis of the growing hyphae. Germination and erection of aerial hyphae was not captured due to preliminary growth arrest due to high excitation frequency of the light source. However, without z series, long time intervals (20minutes /frame), and short fluorescent light exposture (FM4 64-0.04 seconds and Syto 42-0.02 seconds) time-lapse of substrate hyphae stained with fluorescent probes was captured. But, no lipid domains were seen as discussed in earlier section. There was uniform fluorescence seen throughout hyphae at all times, including the emergence of new hyphae (Fig. 13 A2 and A3). Following the acquisition of images and processing them using the software, for the first time real –time imaging with fluorescent probe was achieved.

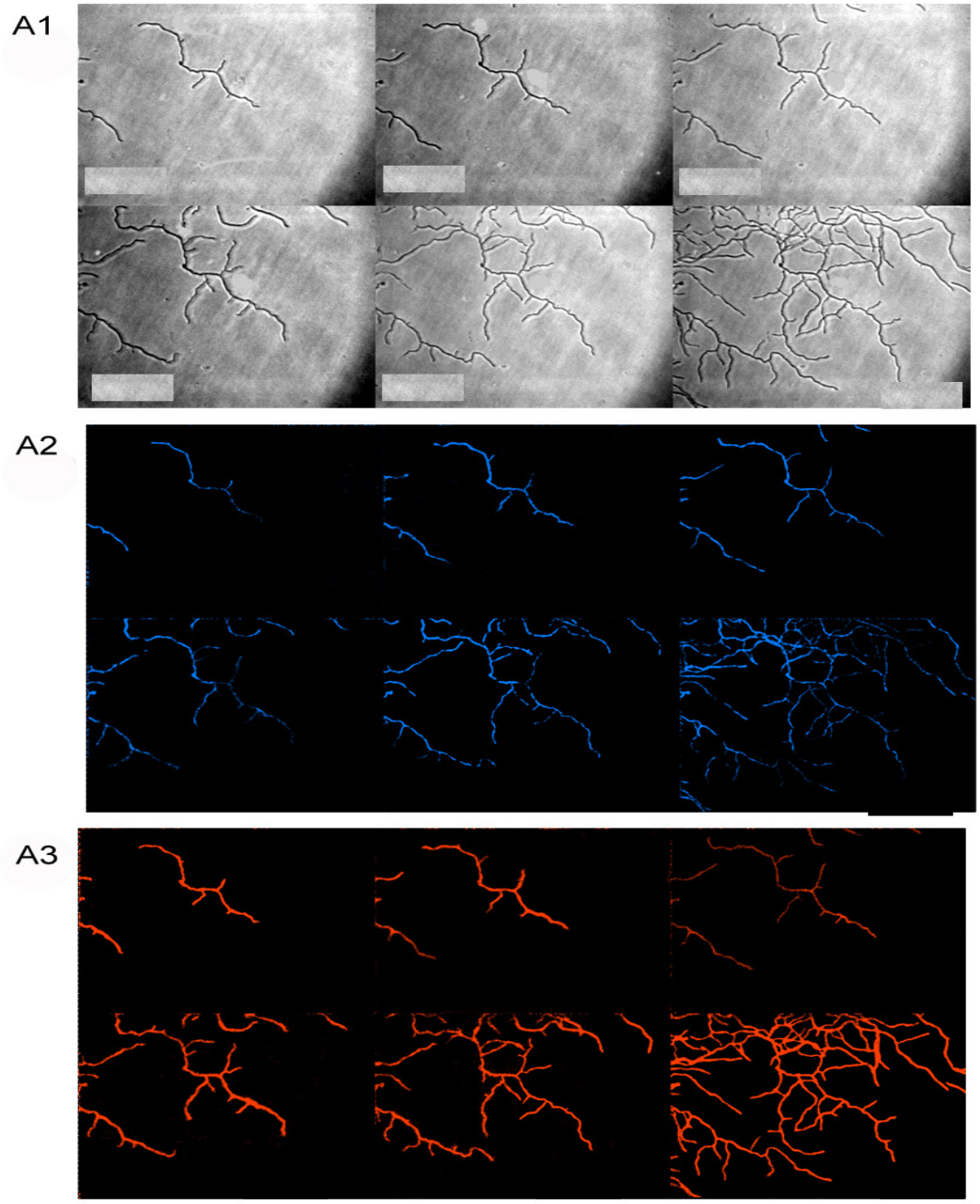

Figure 13: Time-lapse video of M145 probed with FM4 64 and Syto 42.

M145 was stained with FM4 64 and Syto42, lipid domains (red) and staining DNA (blue). A1 is the phase contrast time-lapse images; A2 stained DNA blue with syto42 and A3 with FM4 64 indicating membrane in red.Size bar 10µm.

3.6 Conclusions.

Time-lapse microscopy of *S. coelicolor* presents many challenges through its oxygen dependence, focal depth, mycelial heterogeneity, and agar-dependent sporulation. Compared to other streptomycetes, *S. coelicolor* is more adaptable to imaging systems and capable of producing movies, which is essential for understanding the cell biology of this model organism. However, while we could track down most of the growth and development in *S. coelicolor*, we were still unable to image the erection of aerial hyphae and we expect this problem to remain constant due to repressive effects of the agar plug on the formation of aerial hyphae and the stimulatory effect on substrate hyphae following the transfer of cover-slip-grown cultures to imaging chambers. Presumably the nutrients that supported growth of substrate hyphae in tap water agar came from action of the Dag protein that allows *S. coelicolor* to use agar as a nutrient source. Breaking of the surface tension by the action of SapB is required for the erection of aerial hyphae by *S. coelicolor*, and it is not known whether aerial hyphae can be formed when they are trapped within the liquid phase; we are still to answer this question.

We have also shown the application of fluorescent probes like FM4 64, Syto 42, and NAO in live cell staining of *S. coelicolor*. FM4 64 staining revealed the distinct lipid domains within *S. coelicolor*, which persuaded us to move on to use more specific marker, stain NAO to localize the anionic phospholipid cardiolipin within mycelium. Lipids until recently have been considered an inert hydrophobic environment for the action of membrane proteins. The idea that proteins perform all active tasks in the cell division process still dominates thinking. However, recent experiments with the Min system demonstrate that interplay exists between the amphitropic protein MinD, which undergoes dynamic oligomerization on the membrane surface, and membrane phospholipids. This finding was significant because it broadens the scope of lipid involvement in the process of cell division. Moreover, the use of fluorescent probes in live cell imaging seems to be very promising (depends on exposture times) which can be coupled along with EGFP tagged proteins to study the exact localization of the proteins during growth and development.

Chapter 4

A $Ftsk_{sc,}$ null mutant does not affect distribution of cardiolipin domains.

4.1 Introduction

Dynamic polymerization of FtsZ on the cell membrane is the first step in the assembly of the divisome. *In vitro* studies on FtsZ have shown that, it forms mini-rings and/or thin sheets of protofilaments in the presence of GTP or GDP when adsorbed to a zwitterionic lipid monolayer (Erickson *et al*., 1996). In *E. coli* FtsZ localization to the membrane is supported by the two early cell division proteins ZipA and FtsA (Raychaudhuri, 1999; Margolin *et al*., 2000). Recently it has been shown that FtsZ and its membrane-anchoring partner, FtsA, forms helical structures in *B. subtilis* cells (Peters *et al*., 2007). FtsA, like MinD, has an amphipathic positively charged α-helix that is required for localization to the membrane (Yim *et al*., 2000). FtsK in *E. coli* is a bi-functional protein (Liu *et al.,* 1998), its N terminal membrane domain is localised to the division septum (Wang *et al.,* 1998; Yu *et al.,* 1998) and is necessary for septal formation (Draper *et al.,* 1998; Chen *et al.,* 2001). While its $FtsK_c$ C-terminal motor domain; is implicated in chromosome dimer resolution (Possoz *et al.,* 2001; Aussel *et al.,* 2002), and chromosome segregation (Liu *et al.,* 1998; Yu *et al.,* 1998; Capiaux *et al.,* 2002; Corre *et al.,* 2002). From all above evidence we attempted to characterize *ftsk*$_{sc}$ (*SCO5750*), cell division gene in *S. coelicolor* together with cardiolipin localization using NAO.

4.2 Bioinformatic analysis on $FtsK_{sc}$ protein.

BLAST searches on StrepDB with *E.coli* and *B.subtilis* FtsK/SpoIIIE protein sequence, revealed hits in number genes of which *SCO5750* scored better than *SCO4508*. This suggested *SCO5750* encodes *ftsK* in *S. coelicolor* (Fig. 14-A). Recent publications have shown that *SCO5750* codes for *ftsK* and is not essential for growth and development in *S. coelicolor*. (Wang, *et. al*., 2007; Ausmees *et al*., 2007; Kois *et al*., 2009; Dedrick *et al.*, 2009). In Figure 14B, the 'N' terminal 216-230 amino acid sequence of the protein FtsK under the ClustalW alignment shows the conserved domains of AAA super-family.

(A)

Sequences producing significant alignments: using *E. coli ftsk*		Score (bits)	E Value
SCO5750 SC7C7.05, SCO5750	SCO5750 CAA19851.1 SC7C7.05 SCO5750 ...	375	e-104
SCO4508 SCD35.15c, SCO4508	SCO4508 CAB77299.1 SCD35.15c SCO450...	87	2e-17
SCO5717 SC3C3.03c, SCO5717	SCO5717 CAA20252.1 SC3C3.03c SCO571...	76	3e-14
SCO5734 SC3C3.20c, SCO5734	SCO5734 CAA20269.1 SC3C3.20c SCO573...	67	2e-11
SCO3934 SCD78.01, SCO3934	SCO3934 CAD55466.1 SCD78.01 SCO3934 ...	67	2e-11
SCO1554 SCL11.10c, SCO1554	SCO1554 CAB76073.1 SCL11.10c SCO155...	63	2e-10
SCO2974 SCE50.02c, SCO2974	SCO2974 CAB87324.1 SCE50.02c SCO297...	61	1e-09
SCO2960 SCE59.19c, SCO2960	SCO2960 CAB72206.1 SCE59.19c SCO296...	60	1e-09
SCO3257 SCE39.07c, SCO3257	SCO3257 CAB40315.1 SCE39.07c SCO325...	57	2e-08
SCO5339 SCBAC5H2.08, SCO5339	SCO5339 CAC33903.1 SCBAC5H2.08 SC...	57	2e-08

(B)

Sequences producing significant alignments: using *B. subtilis spoIIIE/ftsK*		Score (bits)	E Value
SCO5750 SC7C7.05, SCO5750	SCO5750 CAA19851.1 SC7C7.05 SCO5750 ...	443	e-125
SCO4508 SCD35.15c, SCO4508	SCO4508 CAB77299.1 SCD35.15c SCO450...	89	3e-18
SCO5734 SC3C3.20c, SCO5734	SCO5734 CAA20269.1 SC3C3.20c SCO573...	72	2e-13
SCO3934 SCD78.01, SCO3934	SCO3934 CAD55466.1 SCD78.01 SCO3934 ...	70	1e-12
SCO5633 SC6A9.34, SCO5633	SCO5633 CAA19919.1 SC6A9.34 SCO5633 ...	64	6e-11
SCO3257 SCE39.07c, SCO3257	SCO3257 CAB40315.1 SCE39.07c SCO325...	64	7e-11
SCO5339 SCBAC5H2.08, SCO5339	SCO5339 CAC33903.1 SCBAC5H2.08 SC...	62	4e-10
SCO4620 SCD39.20c, SCO4620	SCO4620 CAC08273.1 SCD39.20c SCO462...	61	6e-10
SCO2975 SCE50.03, SCO2975	SCO2975 CAB87325.1 SCE50.03 SCO2975 ...	48	4e-06

Figure 14: FtsK sequence analysis in *Streptomyces* data base.

BLAST-P search on *Streptomyces* genome data base with conserved FtsK/SpoIIIE domains from (A) *E.coli* and (B) *B.Subtilis*. The red box indicates the best homologue genes based on *ftsk/spoIIIE* sequences, SCO5750 is studied in this work.

These AAA+ proteins are involved in a wide range of functions and use ATP as the source of energy and include a wide range of family members, such as DNA translocases, helicases, motor proteins, clamp loaders and other ATP dependent enzymes (Greg *et al.*, 2005). The Phylogenetic tree was constructed based on BLOSUM62 (Fig 15-C). From recent study it showed that SCO4508 mutants (33.1% identity in a 245-aa overlap with *E. coli* FtsK), showed no genetic instability or any other distinct phenotype compared with the parent wild-type strain (Wang *et al*., 2007). Informatics analysis of functional domains suggests that the SCO4508 product has a coiled-coil domain and three ATPase domains, so it may be a YukA-like transporter protein, a crucial component of the gram-positive type IV secretion system (Wang *et al*., 2007).

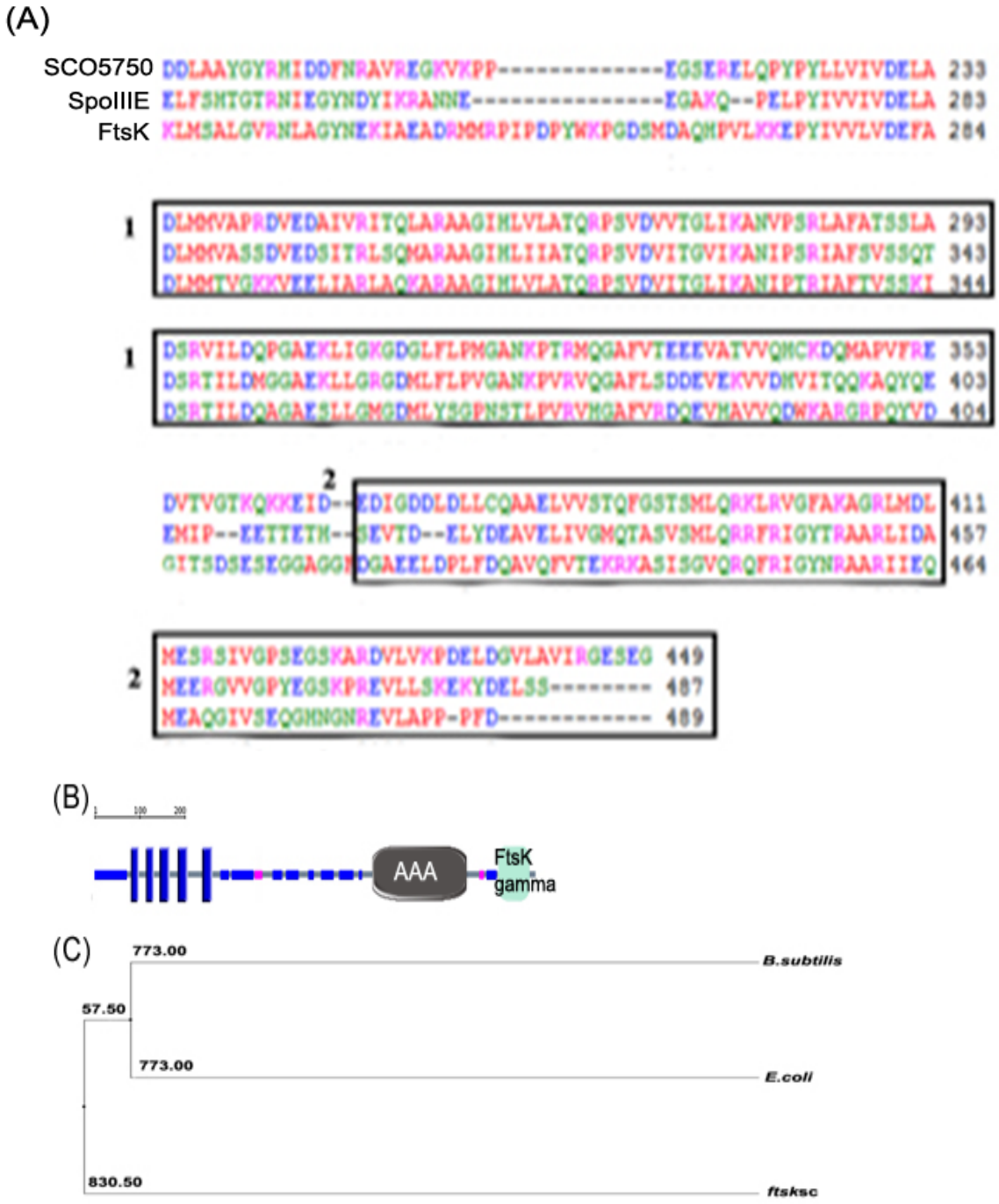

Figure 15: Sequence alignment and phylogenetic tree construction of FtsK proteins from different bacteria.

(A) sequence alignment on 'N' terminal sequence of FtsK/SpoIIIE, 1-shows the conserved domains of AAA+ super family of proteins and 2- indicates the FtsK-gama conserved region(SM00843-directs oriented DNA translocation and forms a winged helix structure);(B)- structure prediction from SMART-protein analysis sofware (C) Phylogentic tree on average distance using BLOSUM62.

4.3. Construction of *ftsK* null-mutant in cosmid.

A Null mutant of *SCO5750* was generated using PCR mediated gene replacement technology. The PCR-targeting procedure described by Gust *et al.,* (2003) was used to replace *SCO5750* on cosmid SC7C7 with a resistance marker. Oligonucleotides FtsK1 and FtsK2 (Table 11) were designed so that the 3'-ends would prime amplification of the apramycin resistance cassette from pIJ773 (Gust *et al.,* 2003), whereas the 5'- ends were 50 bp tails that would be homologous to sequences flanking *SCO5750*. These primers were used to amplify the *aacIV* cassette, which confers resistance to apramycin (1382 bp *Eco*RI/*Hin*dIII fragment). The PCR product (section 2.6.3) was used to transform to *E. coli* strain BW25113 (Datsenko and Warnner, 2000) carrying cosmid SC7C7 and the λRed system induced as described previously (Gust *et al.,* 2003). Among apramycin-resistant transformants, one was identified which had the expected gene replacement, as confirmed by restriction mapping (Fig. 16 B). This cosmid carrying Δ*SCO5750* was designated SC7C7VJ1.

SC7C7VJ1 was confirmed by restriction analysis using *HindIII*, *SstI* and *XhoI*. The presence of apramycin cassette was confirmed by *SstI*, 751 bp internal fragment within the disruption cassette, which is distinct band seen in mutagenised cosmid (Fig. 16.B).

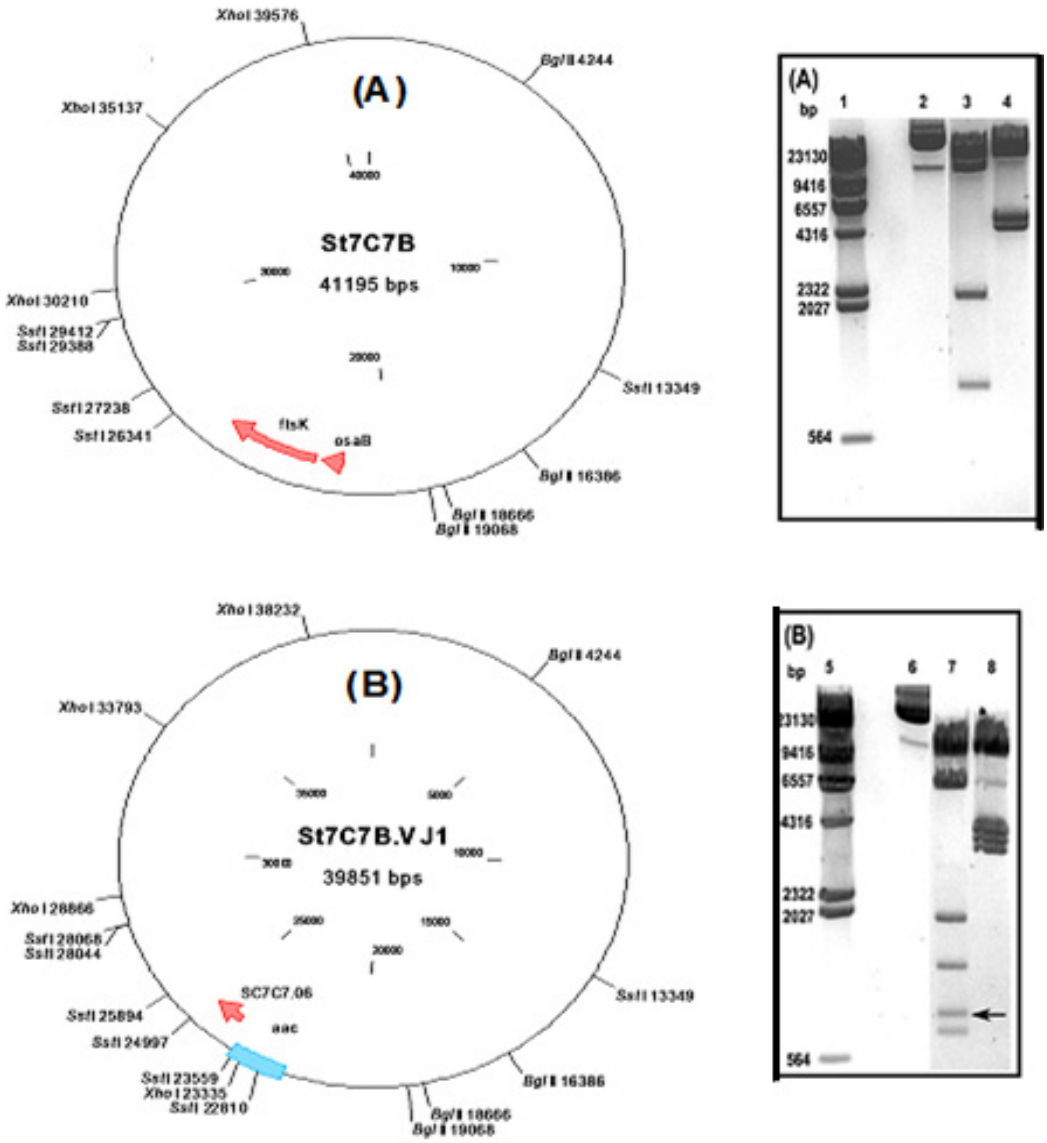

Figure 16: Confirmation of Δftsk$_{sc}$ mutant cosmid by restriction analysis.

(A) St7C7B wild type cosmid- *ftsk$_{sc}$* and (B) St7C7B.VJ1 mutant cosmid- Δ *ftsk$_{sc}$*. Restriction analysis (A) Lane 1-λ *Hind*III marker; lanes 2 - Uncut cosmid DNA, lane 3 -*SstI*; lane 4 –*XhoI*. Confirmation of the mutant cosmid St7C7B.VJ1 by restriction analysis, (B) Lane 5-λ *Hind*III marker; lanes 6- Uncut cosmid DNA, lane 7 -*SstI*; lane 8 –*Xho*I digesst. The black arrow show in B-lane 7 the 749bp fragment and confirming gene replacement.

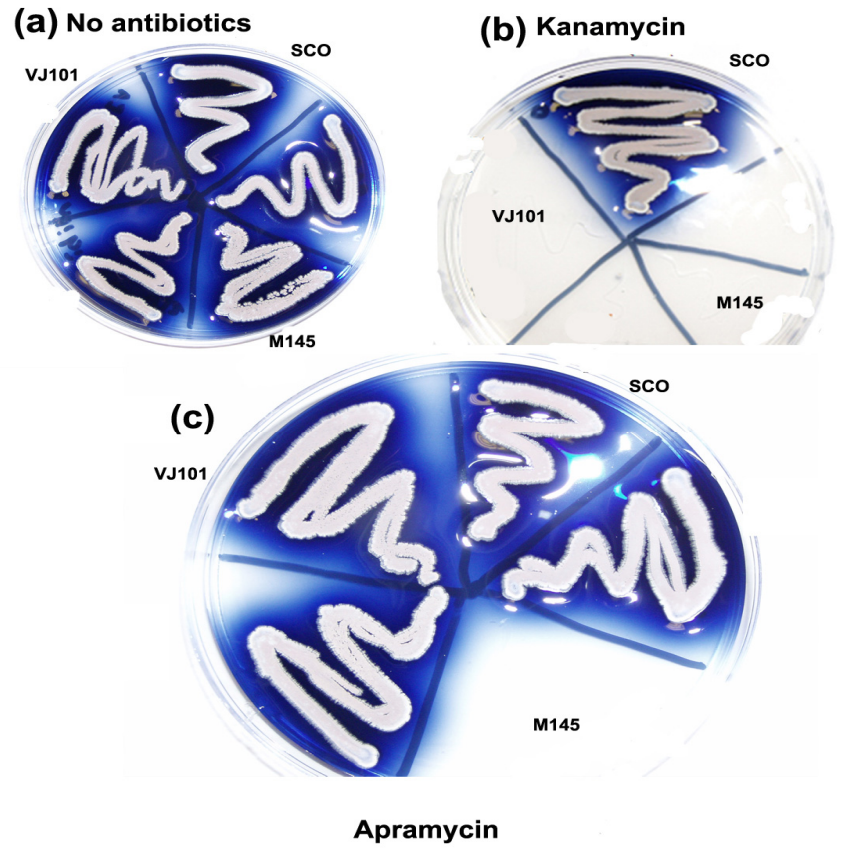

Figure 17: Screening of VJ101 on R2 media.

S. coelicolor $ftsk_{sc}$ mutants grown on R2 medium, M145 wild type and a potential single cross-over was used as the control strains for the selection markers.

4.4 Disruption of the chromosomal copy of the gene.

St7C7B.VJ1 cosmid was passaged through *E. coli* strain ET12567, and was conjugated to *S. coelicolor* (Gust *et al.,* 2003); apramycin-resistant double crossovers and putative single crossover recombinants with both am^r and km^s screened (Fig. 17). 135 colonies were screened under replica plating for apramycin colonies. About 8 colonies resulted in double cross-over (refer chapter 5 for mechanisms of double cross over). The likely interpretation of this result is that *ftsK* is non-essential. One of the 2 colonies was chosen, VJ101 and verified by Southern hybridization (Fig. 18-B, lanes 5 &7) using *ftsk* gene probe from plasmid pD82. All DNA samples were digested with *XhoI* and *BglII* restriction enzymes and the following fragment sizes have been detected using the gene probe. pD82 digested with *BglII* , 4.174 kb was used as gene probe. VJ101 was propagated through two rounds of growth and sporulation on a medium containing apramycin, 50 µg/ml.

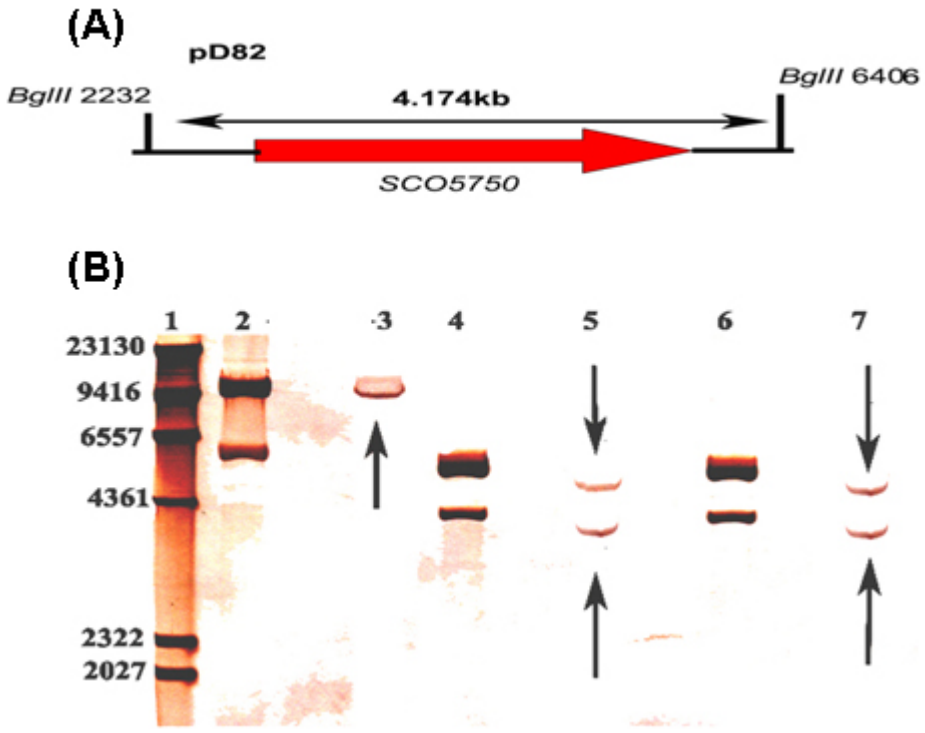

Figure 18: Southern analysis of Δ*ftsK*$_{sc}$.

All DNA samples were digested with *BglII* and *XhoI*. The arrows in the figure show the similar restriction pattern as seen in the vectors which used as controls. Southern blot confirms the *ftsk*$_{sc}$ mutant strains generated by PCR mediated gene replacement. 1-λHindIII marker, 3-gDNA M145; 5 & 7- gDNA VJ101; 2- St7C7B; 4 & 6 - St7C7B.VJ1. The arrow heads in lanes 5& 7 shows the chromosomal Δ *ftsK*$_{sc}$; 5.5kb and 4.2 kb bands. In lane 2 & 3 intact copy of *ftsK*$_{sc}$ generates a; 11.142 kb band.

4.5 Visualization of the cardiolipin rich domains using NAO.

Using PCR mediated gene replacement null mutant of *ftsKsc* in *S. coelicolor* was achieved with no major visible phenotypic effect on MS and minimal medium. Cardiolipin domains were also visualized with NAO in B. subtilis (Kawai *et al*, 2004; Matsumoto *et al*., 2006). NAO fluorescence reflects a spatially heterogeneous distribution of cardiolipin in bacterial membranes. In this chapter we obtained evidence of heterogeneous distribution of cardiolipin in the mutant VJ101 (Fig. 19 B). Although the mutant exhibited irregular nucleiod arrangement the distribution of cardiolipin was no different from the wild type M145 (Fig. 19 A). The results from staining showered some insight on the phospholipid metabolisms in *S. coelicolor*. The ability of lipids to promote formation of membrane subdomains with unique protein and lipid composition provides a mechanism to compartmentalize and regulate biological processes. In next subsequent chapters we will be focusing on the important membrane anionic phospholipid cardiolipin biosynthesis enzyme cardiolipin synthase (SCO1389). Cardiolipin, with its unique dimeric molecular structure in which two phosphatidyl moieties are linked by a glycerol, is a major participant in the formation of membrane domains in bacteria and mitochondria. Due to the four acyl chains and a small headgroup, cardiolipin can organize into domains.

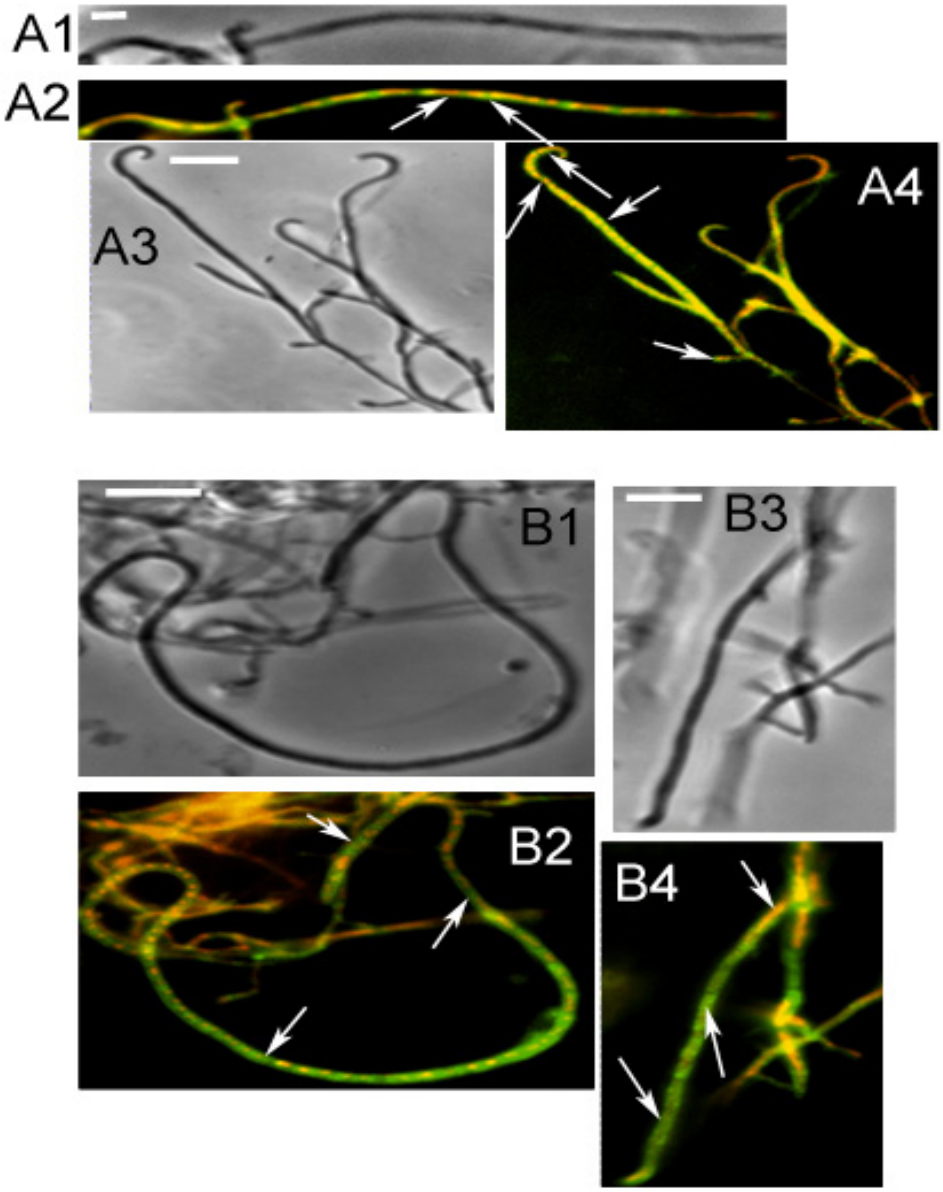

Figure 19: Normal distribution of cardiolipin domains in VJ101 and M145.

Both M145 (A) and VJ101 (B) were stained with NAO and Syto42, staining DNA (red) and lipid domains (green). A1, A3, B1 and B3 are the phase contrast images, A2, A4, B2 and B4 are fluorescent images, and in B2 & B4 arrows indicate the irregular organization of nucleoids in aerial hyphae but the distribution of cardiolipin was similar to M145 (Size bar 10μm).

Chapter 5

SCO1389 is an essential gene in *S.coelicolor*.

5. *S. coelicolor* homologue of cardiolipin synthase is an essential gene.

In the Gram negative model organism *E. coli*, extensive studies have been carried out in studying glycerophospholipid metabolism. Subsequently, mutational studies reported on cardiolipin synthase display only minor growth differences in phenotypes, despite decreased levels of cardiolipin (Satomi *et al*., 1988). As a result the *cls* gene is not essential in *E. coli* cells for growth. To determine whether the *SCO1389* (*SCO1389*) gene is essential in *S. coelicolor* and to analyze the physiological roles, if any, of this gene, an attempt to obtain a null mutation of this gene seemed most useful. This chapter describes the construction, by genetic manipulations, of *SCO1389* mutants and their characteristization.

5.1. *In Silico* functional genomics of *cls* like genes in *S. coelicolor*.

Proteins of the CDP-alcohol phosphatidyltransferase superfamily are involved in phospholipid biosynthesis and catalyze the transfer of a phosphate group, other than diphosphate or nucleotidyl residues, from one compound (donor) to a another (acceptor). There are a number of enzymes that share this common reaction pattern and belong to this super family. These enzymes are ethanolamine-phosphotransferase, diacylglycerol choline-phosphotransferase, phosphatidylglycerophosphate synthase or CDP-diacylglycerol-- glycerol-3-phosphate 3-phosphatidyltransferase, Phosphatidylserine synthase or CDP-diacylglycerol--serine O- phosphatidyltransferase, phosphatidylinositol synthase or CDP-diacylglycerol--inositol 3-phosphatidyltransferase.

BLAST analysis of the *S. coelicolor* genome sequence for putative genes encoding CDP-alcohol phosphatidyltransferase activity revealed eight genes *SCO1389*, *SCO1527*, *SCO3457*, *SCO5753*, *SCO6467*, *SCO6647*, *SCO6752*, and *SCO6755* (Sandoval *et al*., 2009). Seven of these proteins contain the motif DGX_2AR$X_{8/7}$GX_3DX_3D (PROSITE accession: PS00379). This motif is a characteristic feature for this protein super family, whereas protein SCO6755, presents a motif that differs in one amino acid. Further, BLAST search on StrepDB with eukaryotic cardiolipin synthase protein sequence, from *yeast* and *arabdidopsis thialiana* revealed hits on only two proteins of which SCO1389 scored better than SCO5753. This narrowed down to *SCO1389* as the best candidate to encode for cardiolipin synthase activity in *S. coelicolor*. Recent evidence showed that *SCO1389* from *S. coelicolor* condenses CDP-DAG with phosphatidylglycerol yielding cardiolipin which mimics the same reaction as eukaryotic cardiolipin synthase (Sandoval *et al*., 2009). Unlike eukaryotes most bacterial cardiolipin synthase belongs to the phospholipase D (PLD) phosphodiesterases super family. All members of this superfamily of phosphodiesterases contain the sequence motif H-x-K-x(4)-D-x(6)-G-S-x-N or otherwise known as 'HKD' (PROSITE accession: PS50035). This enzyme reacts at the ester bonds between the phosphoryl groups of the head moiety. Two molecules of phosphatidyl glycerol condense to form one molecule of cardiolipin by transphosphatidylation reaction. BLAST search on StrepDB showed SCO7081 as highest score hit against the cardiolipin synthase protein from *E. coli* and *B subtilis*. So, this gene can be speculated as 2nd cardiolipin synthase involved in synthesis of cardiolipin by the prokaryotic pathway. However, in *S coelicolor* it has been clearly shown with biochemical activity that *SCO1389* shares the eukaryotic reaction mechanism to synthesize cardiolipin (Sandoval *et al*., 2009).

5.1.1. Phylogenetic analysis of *cls* like genes in *S. coelicolor*.

The sequences of putative genes encoding for CDP-alcohol phosphatidyltransferases were retrieved by BLAST using *SCO1389* as query and confirmed to have this domain using the PROSITE databases. The sequence alignment was performed with the multiple alignment software ClutalW2 using the default parameters (Fig 20 A). Both the CDP-alcohol phosphatidyltransferase superfamily and phospholipase D (PLD) phosphodiesterases super family pattern are shown in black boxes.

A phylogenetic analysis was performed involving homologues of cardiolipin synthase proteins from different species (Fig. 20 B). The sequences compared with four well-studied model organisms, Gram positive organisms, *B. subtilis* (low G+C content) and *Mycobacterium* (high G+C content); Gram negative representing *E. coli* and eukaryotes *A. thaliana* and *yeast*. The Phylogenetic tree was constructed based on BLOSUM62 representing on average distance between the samples. Distance methods were used to construct from the sequence query set describing the distance between each sequence pair.

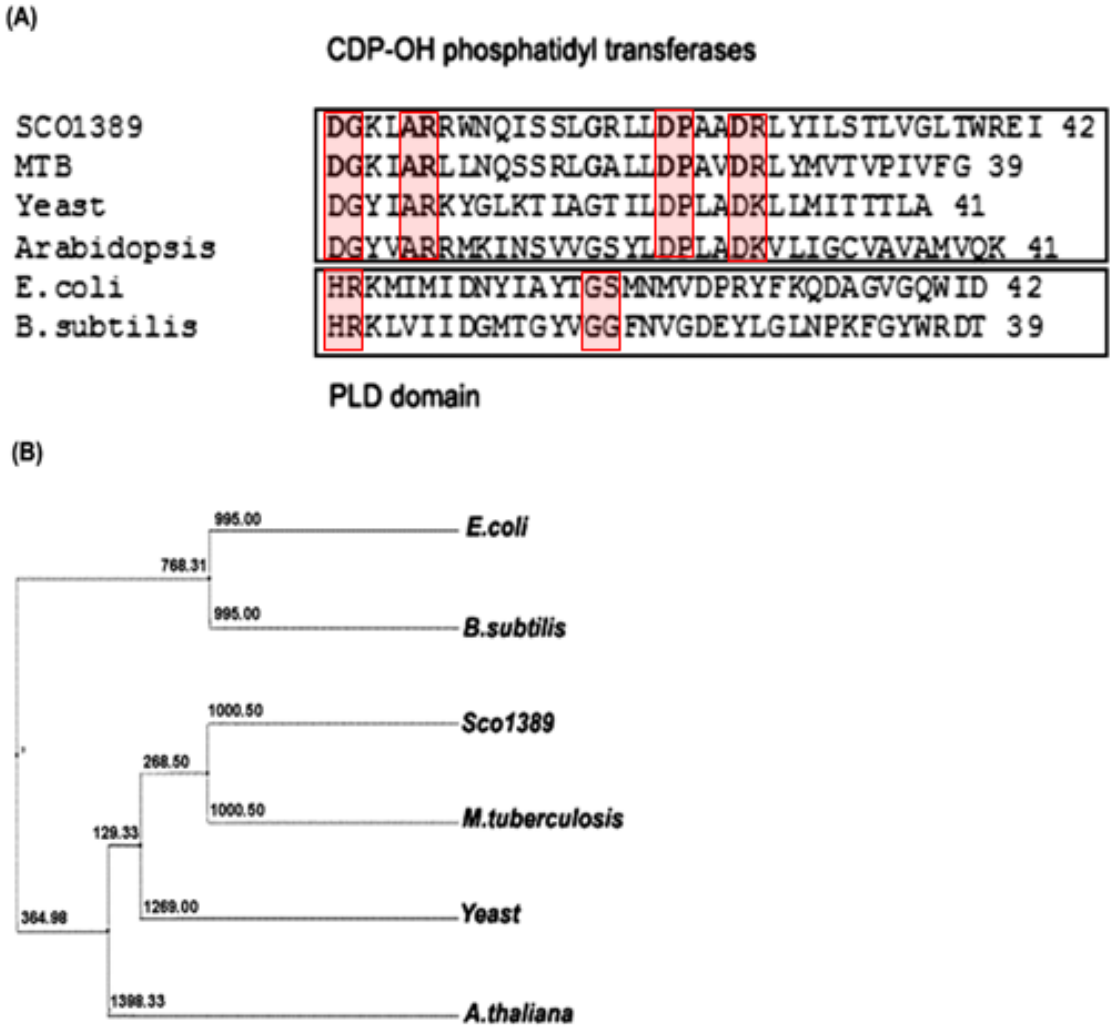

Figure 20: Conserved sequences of selected homologues of cardiolipin synthase.

(A) The alignment was generated ClustalW software. The top two sequences represents the Gram positive family, *S.coelicolor* CLSI (Accession number: Q9KZP3) and Mycobacterium Bovis *(*Accession number: C1AP99). Followed by two eukaryotic family proteins *Saccharomyces cerevisiae* (Baker's yeast) (Accession number: Q07560; P82260) and Arabidopsis thaliana (Mouse-ear cress) (Accession number: Q93YW7). The alignment was completed with two well studied model prokaryote organism, Gram negative *Escherichia coli* BW2952 (Accession number: C4ZTU1) and Gram positive (low GC) *Bacillus Subtilis* (Accession number: P71040). **(B)** Phylogenetic tree of proteins of Cls from different organisms. Gram positive organisms, *B. subtilis* (low G+C content) and *Mycobacterium* (high G+C content); Gram negative representing *E. coli* and eukaryotes *A. thaliana* and *yeast*.

5.2. *S. coelicolor SCO1389* is essential for viability.

SCO1389 from the *S. coelicolor* shares strong CDP-alcohol phosphatidyltransferase superfamily protein signature that is similar to the eukaryotic cardiolipin synthase (Sandoval *et al*., 2009). From the biochemical evidence this protein is likely to be involved with phospholipid synthesis, but its importance is unknown. In order to determine the role of this gene, initially experiments were carried on transposon insertion mutants constructed by using mutated cosmid generated by *in vitro* transposition (Bishop *et al*., 2004). To construct the mutant, we chose Tn*5062* insertions close to the start of the gene; the insertion at 1468280 was chosen to study *SCO1389* function, being aware with the fact that there would be little translated product in the mutants. St1A8A.2.B10 (Table 3) cosmid was passaged through *E. coli* strain ET12567/PUZ8002, and was conjugated to *S. coelicolor*; through homologous recominbation (Fig. 23) am^r double crossovers and putative single crossover recombinants with both am^r and km^r was screened. About 1128 colonies were screened by replica plating for am^r and km^r colonies. All of them were derived from a single cross-over event where all colonies resistant to both antibiotics (Fig 23-A). The likely interpretation of this result is that *SCO1389* is essential, but as it was insertional mutant, we speculated that the gene may not be completely non-functional.

As a result, we decided to construct a null mutant of *SCO1389* using PCR mediated gene replacement technology. The PCR-targeting procedure described by Gust *et al.,* (2003) was used to replace *SCO1389* on cosmid StA8A with a resistance marker. Oligonucleotides CL104 and CL105 (Table 11) were designed so that the 3'-ends would prime amplification of the apramycin resistance cassette from pIJ773 (Gust *et al.,* 2003), whereas the 5'- ends were 50 bp tails that would be homologous to sequences flanking *SCO1389*. These primers were used to amplify the *aacIV* cassette (Fig 21-B), which confers resistance to apramycin (1382 bp *Eco*RI/*Hin*dIII fragment).

PCR reaction conditions were followed from Gust *et al.,* (2003). The PCR product was analyzed by gel electrophoresis and purified by using a PCR Purification kit. The expected sizes are 78 bp larger than the sizes of the disruption cassette pIJ773 because of the 2 x 39 bp 5′-primer extensions (Fig. 21-B). The PCR product was purified using the Qiagen PCR purification kit (Chapter 2). The PCR product was finally eluted and checked by restriction analysis using *SacI* (Fig. 21-C). The PCR product was used to transform to *E. coli* strain BW25113 (Datsenko and Warnner, 2000) carrying cosmid StA8A and the λRed system induced as described previously (Gust *et al.,* 2003). Among apramycin-resistant transformants, one was identified which had the expected gene replacement, as confirmed by restriction mapping (Fig. 22-B). This cosmid carrying Δ*SCO1389* was designated StA8A.RJ1.

The restriction sites used for verification of StA8A.RJ1 were HindIII, *SstI* and *XhoI*. HindIII generates the linear form of the cosmid DNA. However, using *XhoI* generates very close band shift on StA8A.RJ1 DNA ,therefore *SstI* is preferred as it generates a 751 bp internal fragment within the disruption cassette, which is distinct band seen in mutagenised cosmid (Fig. 22-B lane 7).

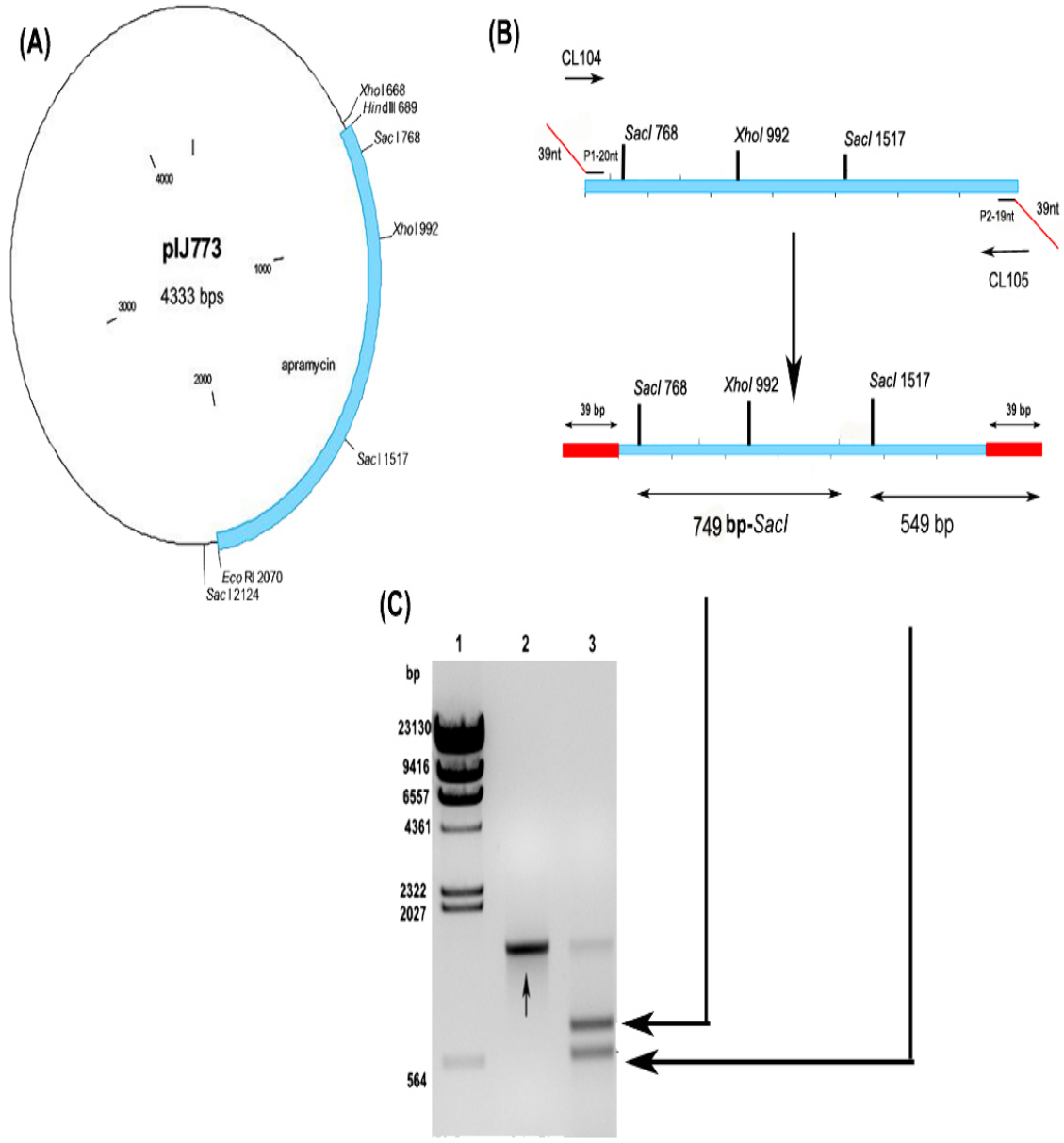

Figure 21: Confirmation of *SCO1389* PCR amplicon

(A) Template plasmid containing the apramycin resistance gene *aac(3)IV* (B) Schematic representation of *SCO1389* PCR product.Two long PCR primers (58 nt-CL104 and 59 nt-CL105) are designed. Each has at the 5´end 39 nt matching the *S. coelicolor* sequence adjacent to the gene to be inactivated, and a 3´sequence (19 nt or 20 nt) matching the right or left end of the pIJ773. The precise positioning of the 39 nt sequence as indicated is important for creating inframe deletions by FLP recombinase-induced excision of the resistance marker (Gust *et al.,* 2003). (C)-Agarose gel confirmation shows the amplified fragments of the apramycin cassette fragment 1382-bp of pIJ773 with the flanking region of *SCO1389*, Lane 1-λ HindIII marker; lane 2- PCR product of 1382 bp and lane 3- *SacI* restriction and digestion generating 749bp (internal fragment of the cassette) and 549bp.

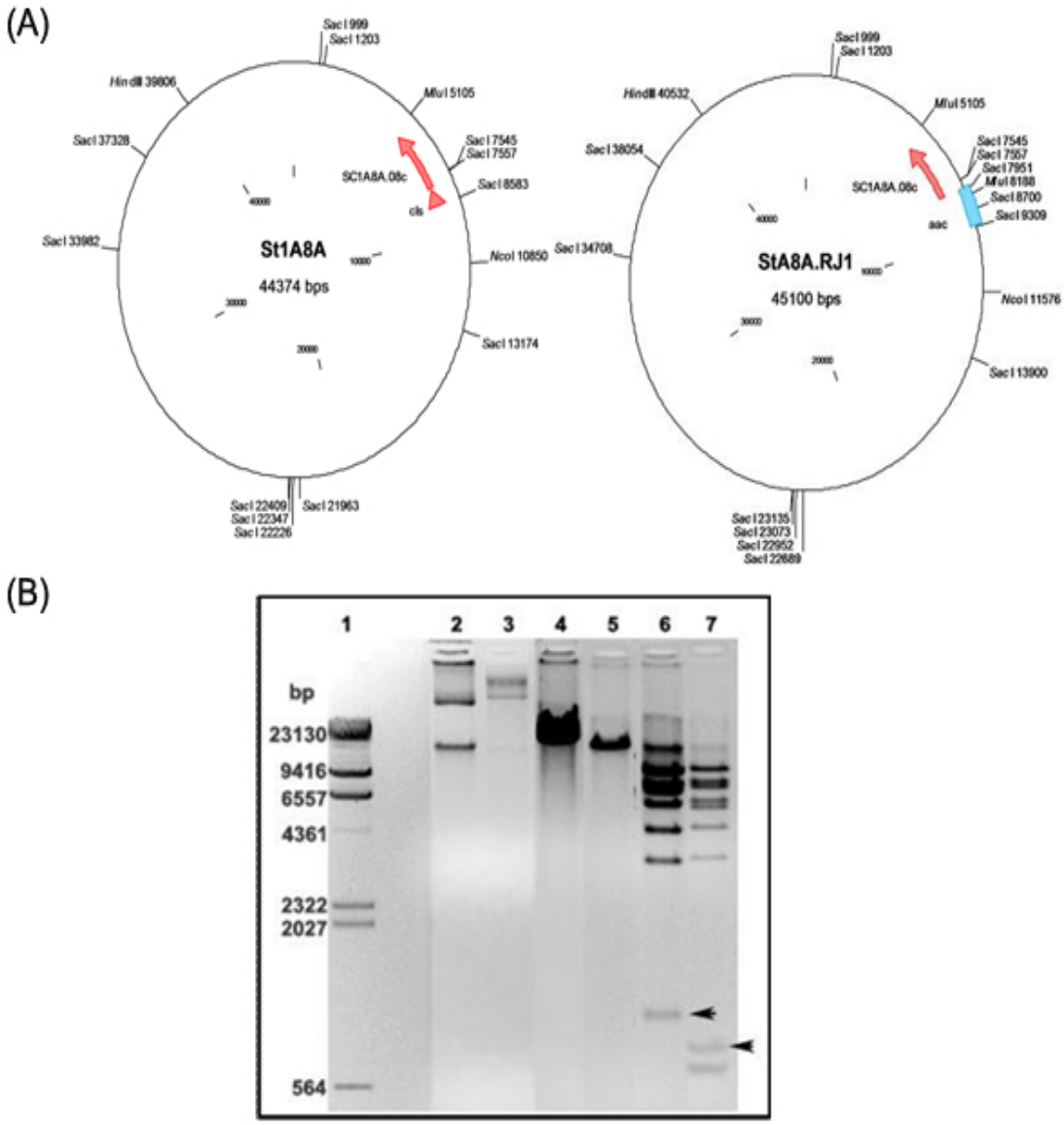

Figure 22: Confirmation of *SCO1389* gene replacement in wild type cosmid.

(A) Both cosmid's, St1A8A and St1A8A.RJ1 was constructed on supercos backbone, with St1A8A carrying functional copies of *SCO1389* and St1A8A.RJ1 carrying Δ*SCO1389* and resistant to apramycin. (B) Confirmation of the mutant cosmid St1A8A.RJ1 by restriction analysis. Lane 1-λ HindIII marker; lanes 2 & 3- Uncut cosmid DNA, lanes 4 & 5 -*HindIII* digest; lanes 6 & 7 –*SacI* digest. Lanes 2, 4 & 6 represents the wild type cosmid DNA St1A8A and lanes 3, 5 & 7 represent the disrupted cosmid St1A8A.RJ1. The black arrows show the 1026bp band in lane 6 and the band shift to 749bp and 609bp in lane 7; confirming the presence of Δ*SCO1389*.

5.3 Disruption of the chromosomal copy of *SCO1389*.

StA8A.RJ1 (Table 3) was introduced into *E. coli* ET12567/pUZ8002 by electroporation and then transferred to *S.coelicolor* by conjugation. The exconjugants were screened for am^r km^s that would indicate a double-crossover allelic exchange in *S. coelicolor*. About 938 colonies were screened under replica plating for am^r km^s. All were single cross-over and the results were consistent with transposon mutagenesis. One of the 938 colonies was chosen, RJ111 and verified by Southern hybridization (Fig. 31 lane 4); none had undergone the second crossover event to delete the *SCO1389* gene. This suggests that *SCO1389* is essential.

5.3.1. Mechanism of double cross over.

Using the apramycin resistant cassette, the cloned copy of the target gene was replaced, by PCR targeted gene replacement. Homologous recombination takes place by introducing the resistant cassette carrying the overhangs of the gene of interest The mutant formed is then used to replace the chromosomal copy of the target gene via two crossovers, and selection with one marker (Fig. 25 B), resulting in a stable irreversible double crossover mutant. These two crossovers can occur simultaneously, giving rise to a stable gene replacement, or may occur consequently proceeding *via* single cross over intermediate (Fig. 25 A), where the entire vector integrates within the chromosome and is selectable by both of the markers apramycin and kanamycin.

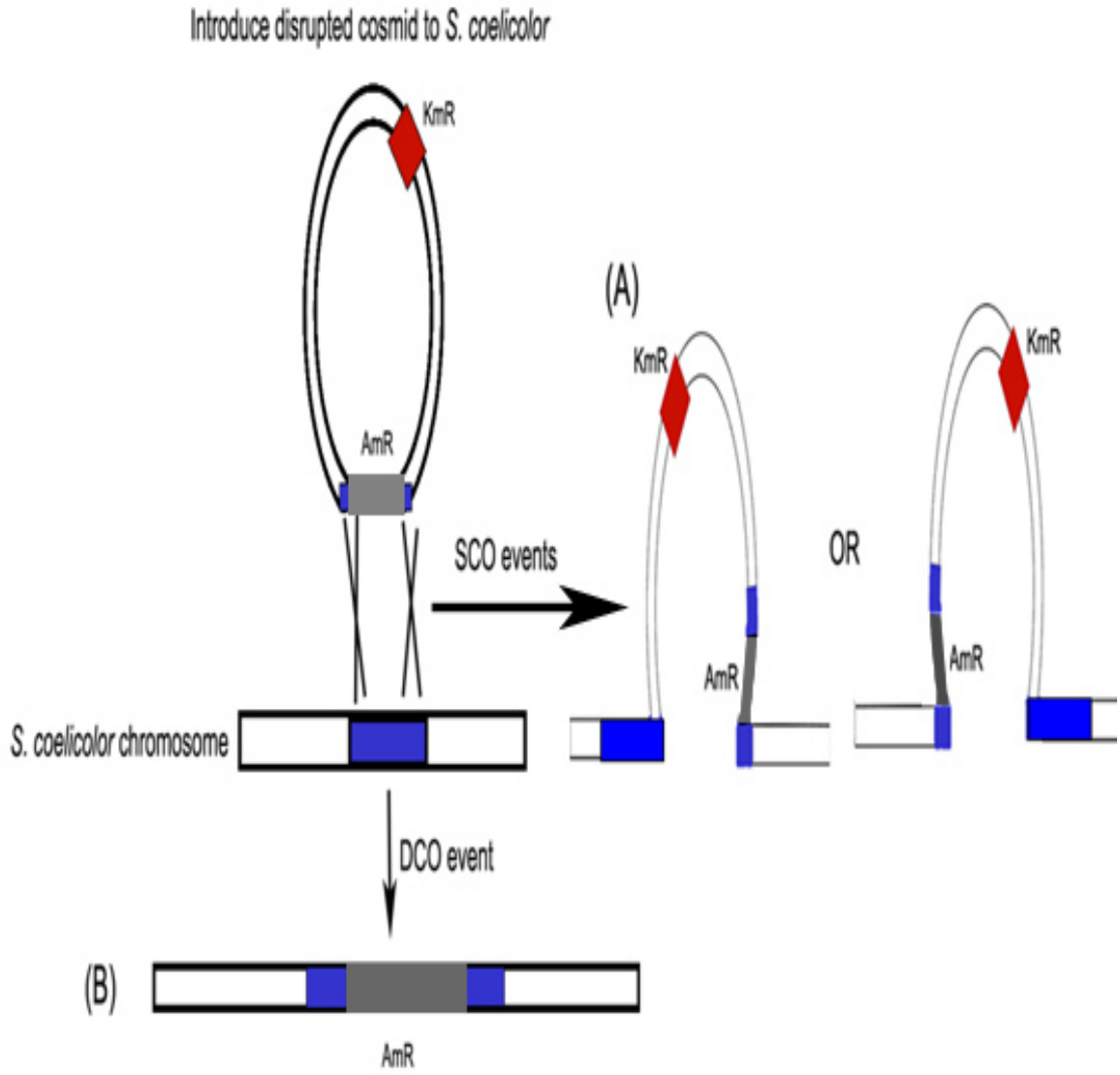

Figure 23: Mechanism of formation of double and single cross over events.

(A)- Two types of single cross over formation and (B) shows the double crossover replacing the gene within *S. coelicolor* chromosome. The exconjugants screened for *SCO1389* results only in single crossover, and they were grown through one or more rounds selecting for apramycin and kanamycin resistance markers. After successive passaging of the cells the exconjugants remained only in single crossovers, indicating that the gene *SCO1389* is essential.

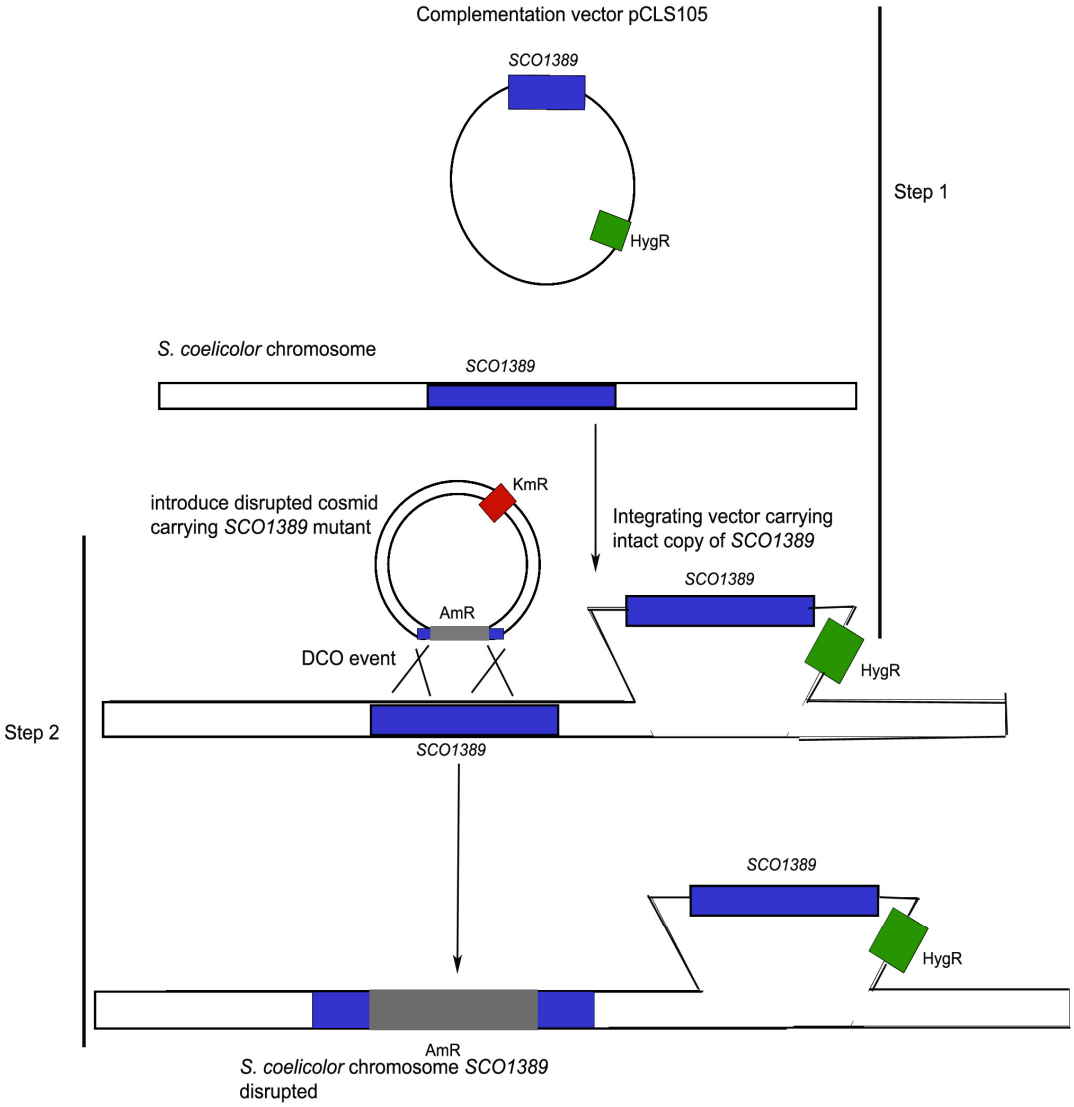

Figure 24: Deletion of chromosomal *SCO1389* by *trans* complementation.

In step 1, an extra copy of *SCO1389* was introduced to M145 (wild type) through pCLS105, resulting in RJ102, strain carrying two functional copies of *SCO1389*. To RJ102, the disrupted cosmid StA8A.RJ1 was introduced and screened for double cross over, indicating chromosomal copy *SCO1389* was replaced by apramycin cassette, we could achieve only double crossover of the target gene, when the phenotype was complemented in *trans*

5.4 Creation null mutant of *SCO1389* by *trans* complementation.

Most of the colonies didnot undergo the second crossover event to delete the *SCO1389* gene, to address this issue, a second copy of *SCO1389* was introduced into strain M145 on pCLS105 (Fig. 26, section 5.4.1) such that it would be expressed under the native promoter. The resulting strain, RJ102 (Table 1), was confirmed by Southern hybridization to contain the second copy of *SCO1389* integrated at the ΦBT1 *attP* site (Fig. 29, lane 7). RJ102 was propagated through one round of growth and sporulation on a medium containing hygromycin at 50 µg/ml. StA8A.RJ1 (Table 3) cosmid was passaged through *E. coli* strain ET12567, and was conjugated to *S. coelicolor* strain RJ102 (Table 1); apramycin and hygromycin-resistant transconjugants were tested for kanamycin sensitivity. About 10% showed kanamycin sensitivity; One of the colonies was chosen, RJ114 and verified by Southern hybridization (Fig. 29, lane 6); had undergone the second crossover event to delete the *SCO1389* gene. This demonstrated that *SCO1389* can readily be deleted from the chromosome to yield a viable strain, but only if a second copy of *SCO1389 is* available to complement the deletion.

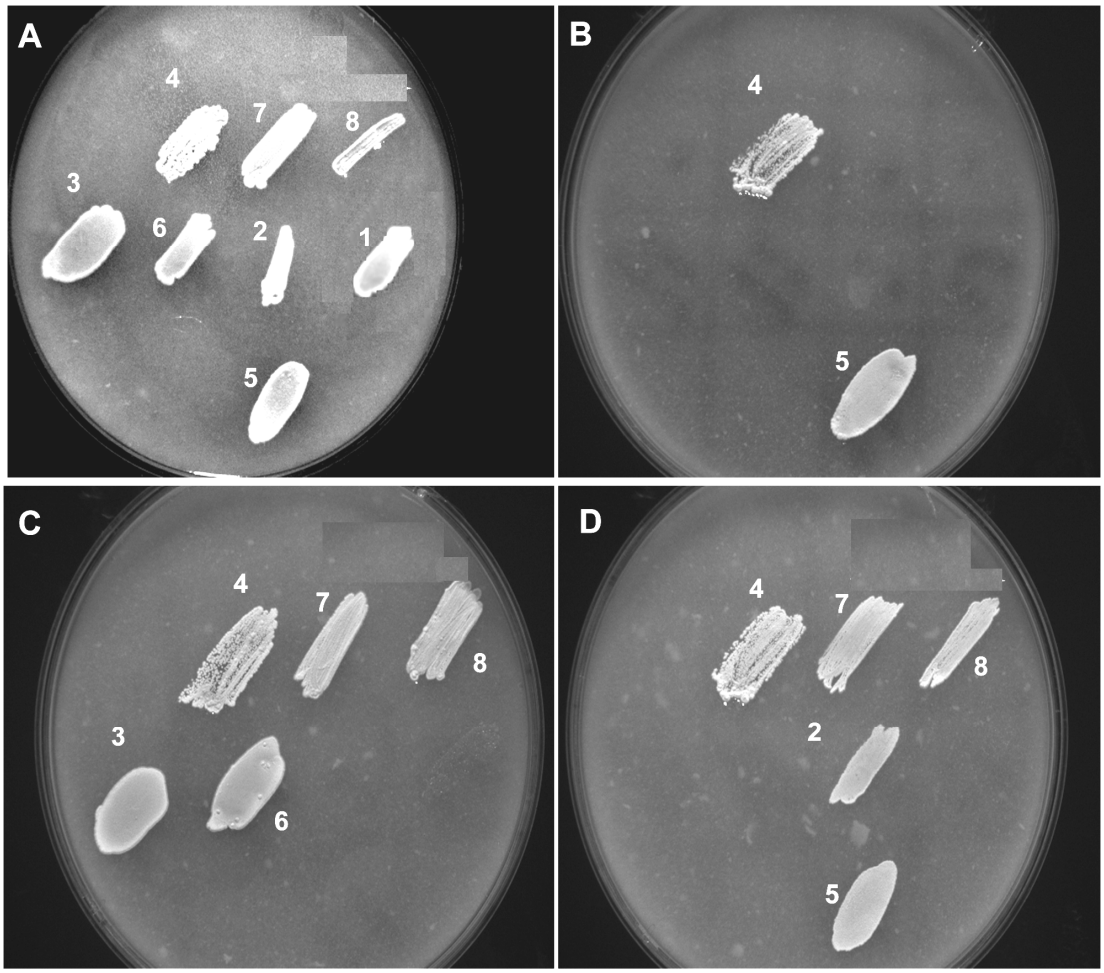

Figure 25: MS plates confirm the presence of *SCO1389* null mutant by *trans* complementation.

The plates contain A-no antibiotics, B-kanamycin, C-hygromycin, D-aparamycin. The strains used are 1-M145, 2-control for double crossover VJ101, 3- control vector *S. coelicolor* pMS82, 4- RJ111, 5-RJ100, 6-RJ102, 7-RJ104 and 8-RJ114. The strains marked 4 and 5 grow on all four plates, indicates the single crossover, 7 and 8 on A, C and D shows indicates double crossover on *trans* complementation, 3 and 6 on A and C shows the presence of integrating vector, 2 on A and D confirms control strain for double crossover that grows on apramycin only and 1 on A confirms parent strain M145.

5.4.1. Construction of complementation vector pCLS105

The cardiolipin synthase homologue of *S. coelicolor* was obtained from cosmid SC1A8A.2.EO5 (Bishop *et al*., 2004) containing a Tn*5062* insertion downstream of *SCO1389*. Initial Sub-cloning of *SCO1389* with its native promoter (4.5 kb-fragment) was isolated using *EcoRI* restriction; and then cloned into *EcoRI* linearised pALTERI generating pCLS102. The resulting plasmid pCLS102 acts as the precursor vector for next cloning step. An integration vector has been designed that integrates into a ΦBT1attB site rather than ΦC31 site. The ΦBT1 *attB* site lies approximately 1 Mb to the right of *oriC* compared to the ΦC31 *attB* site, which is approximately 90 kbp to the left of *oriC*. The ΦBT1 *attB* site lies within *SCO4848* coding for a putative integral membrane protein. This gave the potential to new range of vectors that can be used during genetic engineering in *Streptomyces* (Smith *et al*., 2003). The vector, pMS82 coding for hygromycin resistance was used in this study. Subsequent cloning involved pMS82 restriction with HindIII and 1.5Kb fragment (carrying functional *SCO1389* with native promoter region) from pCLS102 digested with HindIII. After ligation reaction, the complementation vector is generated was named, pCLS105 (Fig. 28, 29 and 30).

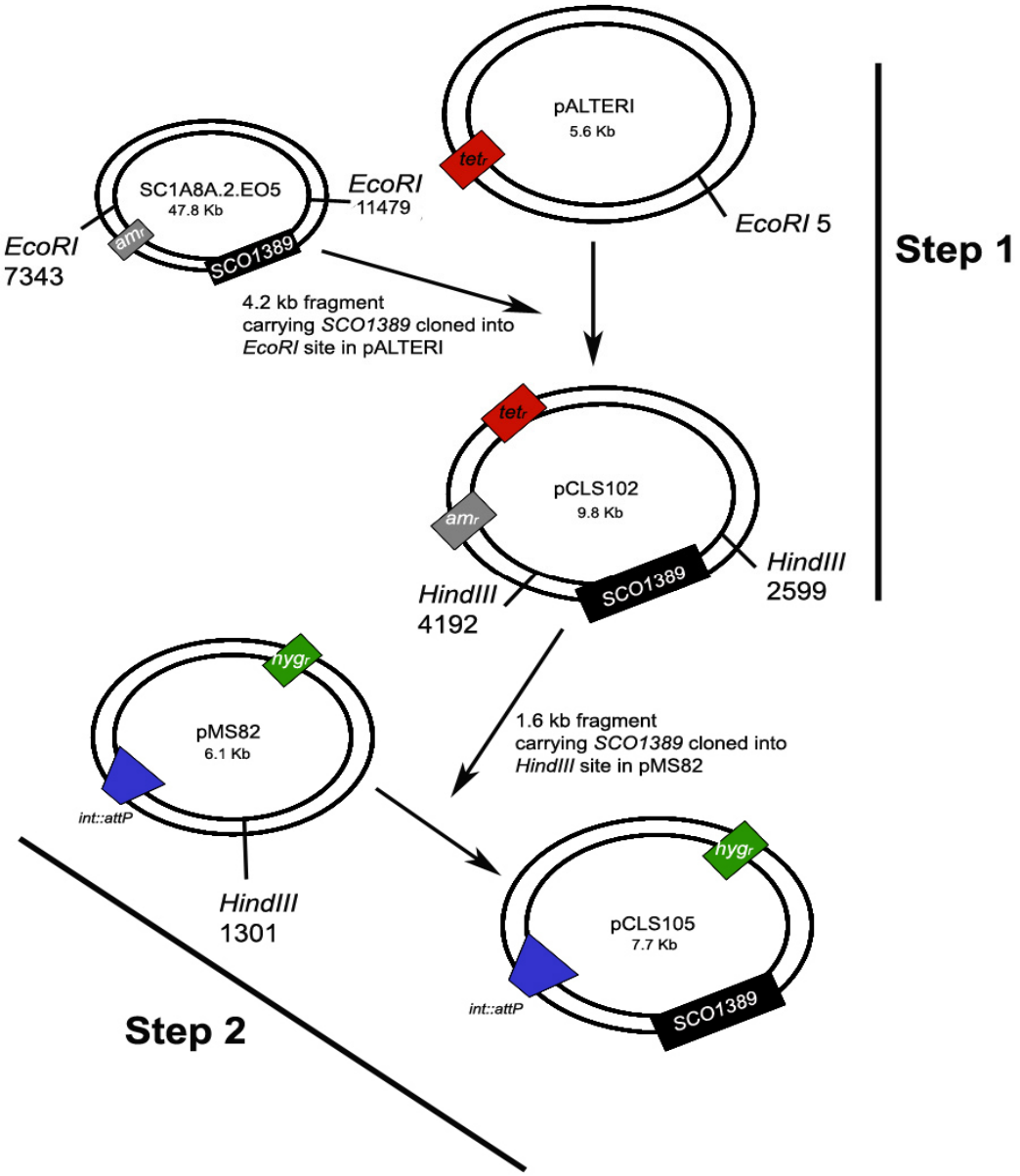

Figure 26: Cloning steps involved in construction of complementation vector pCLS105.

Cosmid St1A8A.EO5 carries a Tn*5062* insertion in the position 1468850 upstream of SCO1389 in the genome. This was used for easy sub-cloning with two selection markers. Plasmids pALTER-I codes for tetracycline resistance, and used as shuttle vector for sub-cloning reactions, and pMS82 is an integrating vector (attPΦBT1, hyg^r) in Streptomyces chromosome.

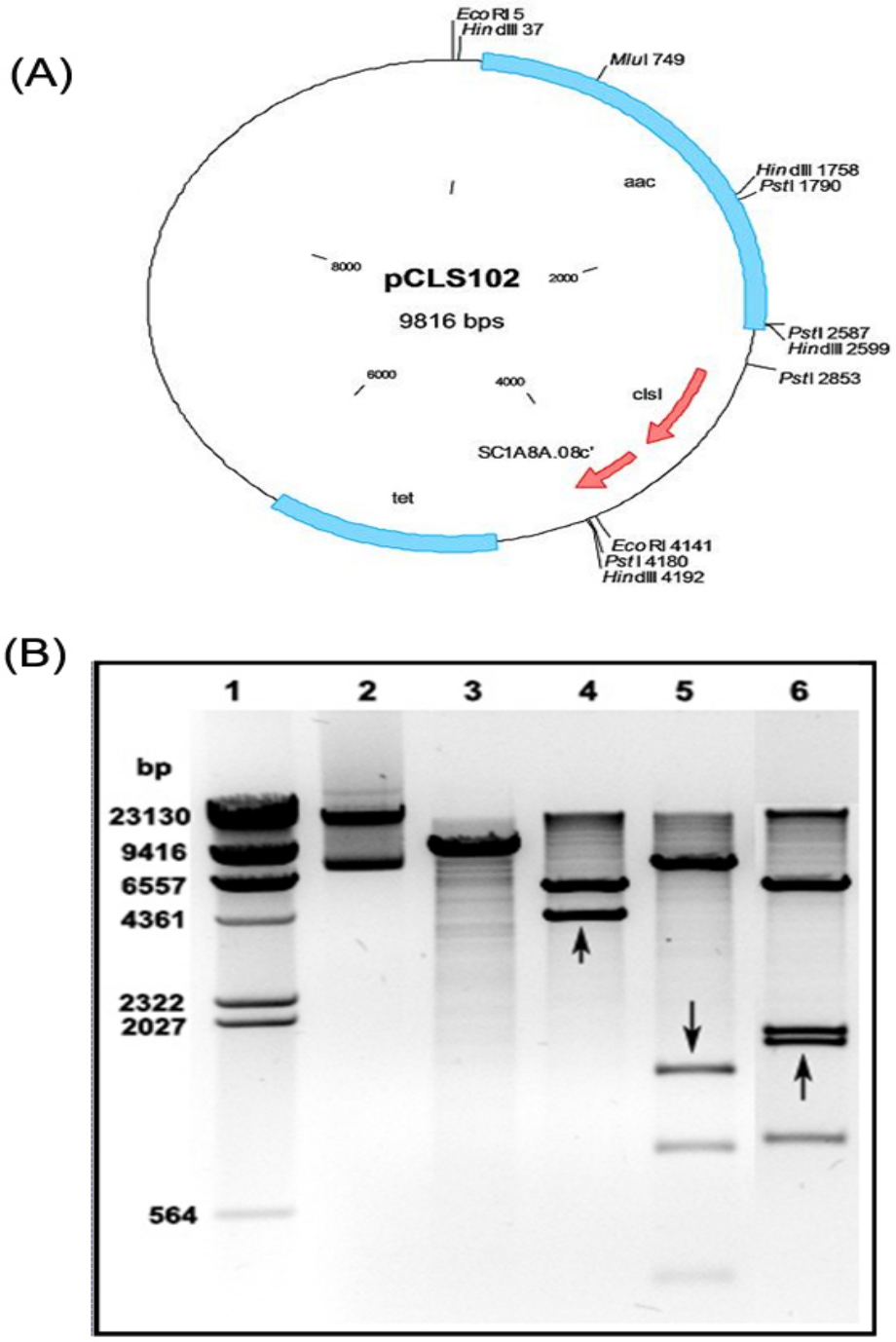

Figure 27: Confirmation of pCLS102 (Step 1 cloning reaction refer figure 4).

(A) pCLS102 plasmid map was constructed by ligating 4.2 Kb *EcoRI* fragment into pALTERI **,** the clone carries functional copy of *SCO1389* with native promoter. (B) Confirmation of the plasmid pCLS102 by restriction analysis. Lane 1-λ *HindIII* marker; lanes 2 - Uncut plasmid DNA, lanes 3 - *MluI* digest; lanes 4 – *EcoRI* digest; lanes 5- *PstI*; lanes 6- *HindIII*. The black arrow shows the fragments contain *SCO1389*.

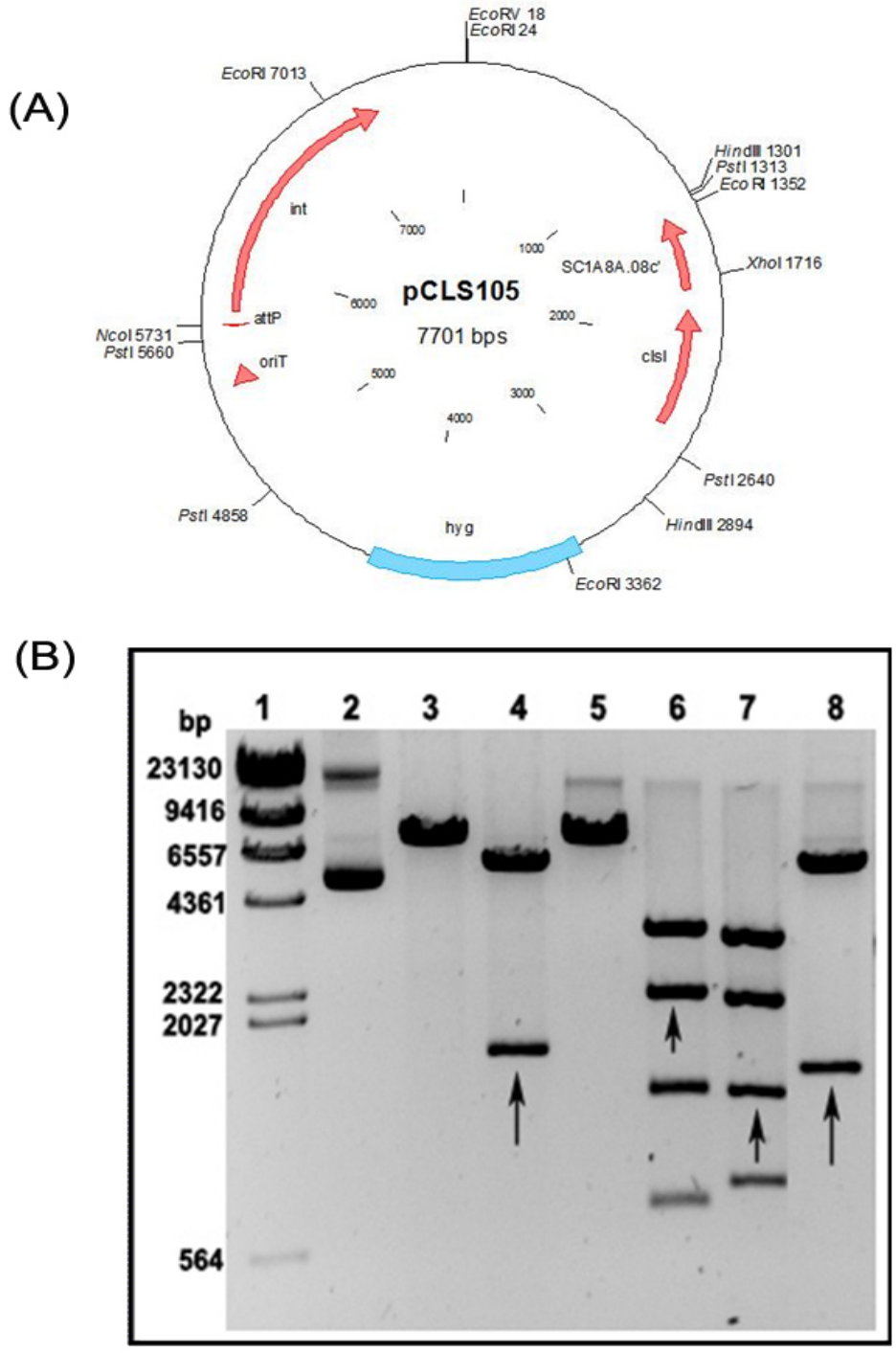

Figure 28: Confirmation of pCLS105 (Step 2 cloning reactions refer figure. 4).

(A) pCLS105 plasmid map was constructed by ligating 1.6Kb *HindIII* fragment from pCLS102 into pMS82. pCLS105 , the clone carries functional copy of *SCO1389* with native promoter. (B) Confirmation of the plasmid pCLS105 by restriction analysis. Lane 1-λ *HindIII* marker; lanes 2 - Uncut plasmid DNA, lanes 3 - *EcoRV* digest; lanes 4 – *EcoRV* and *XhoI*; lanes 5- *XhoI*; lanes 6- *EcoRI*; lanes 7- *PstI*; lanes 8- *HindIII*. T The black arrows show the fragments contain *SCO1389*.

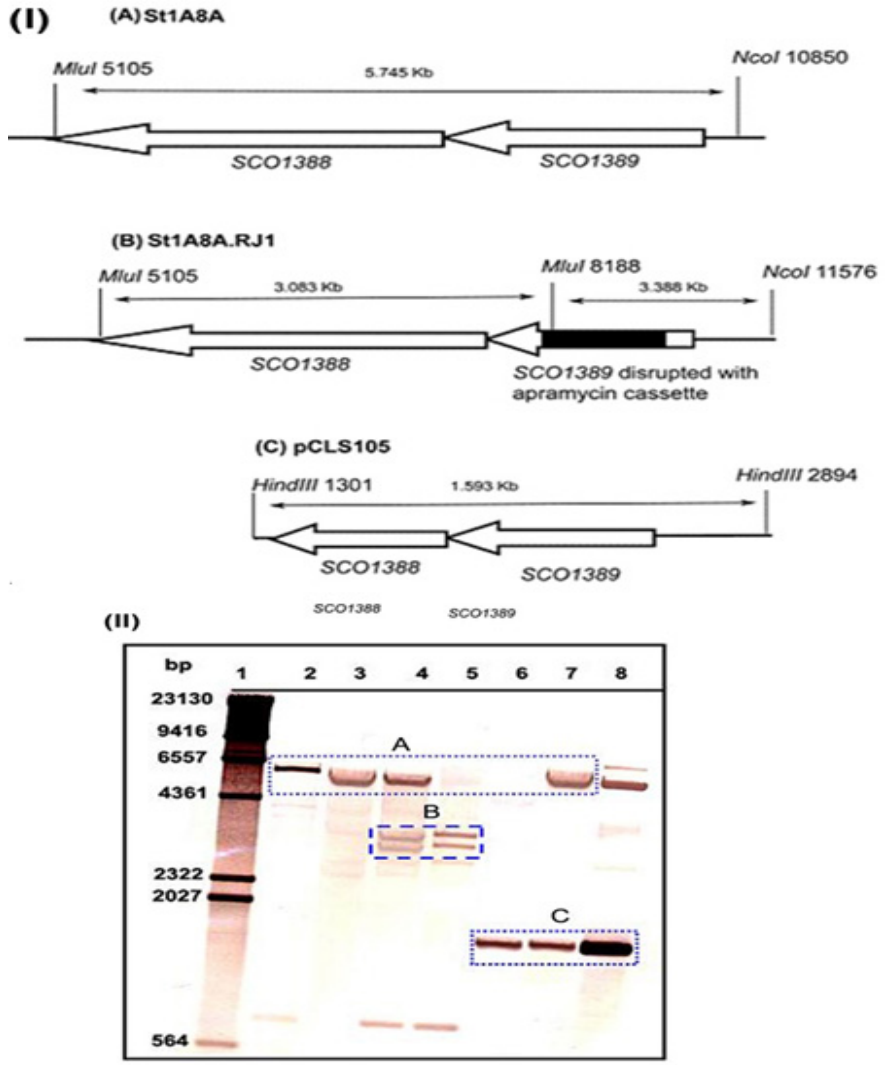

Figure 29: Southern analysis of Δ*SCO1389.*

(**I**) Schematic sketch of the cosmid and plasmid maps with restriction sites that supports the grid boxes in the Southern blot. (**II**) Lane 1-λHindIII marker-wt DNA, lane 2- StA8A cosmid ,lane 3-gDNA M145,lane 4-gDNA RJ111 ,lane 5- StA8A.RJ1 cosmid, lane 6-gDNA RJ114,lane 7-gDNA RJ102,lane 8-pCLS105 plasmid DNA. Samples were treated with *MluI*, *HindIII* and *NcoI*. Blue Box (A) highlights the fragment size 5.745 bp (*SCO1389)* in lanes 2, 3, 4 and 7; lane 5-disrupted cosmid StA8A.RJ1 and lane 6 -conditional double cross over mutant (RJ114); Box (B) highlights the fragment size 3.388 bp and 3.083 bp in lanes 4 (single crossover RJ111) and 5 represents the disrupted cosmid (StA8A.RJ1); Box (C) highlights the fragment size 1.593 bp in lanes 6 (RJ114) , 7(RJ102-M145 carrying the extra copy of *SCO1389* gene) and 8 (pCLS105 vector carrying *SCO1389*gene). 1.59 Kb fragment of pCLS105 is the gene probe.The other bands in the blot correspond to λ DNA probe.

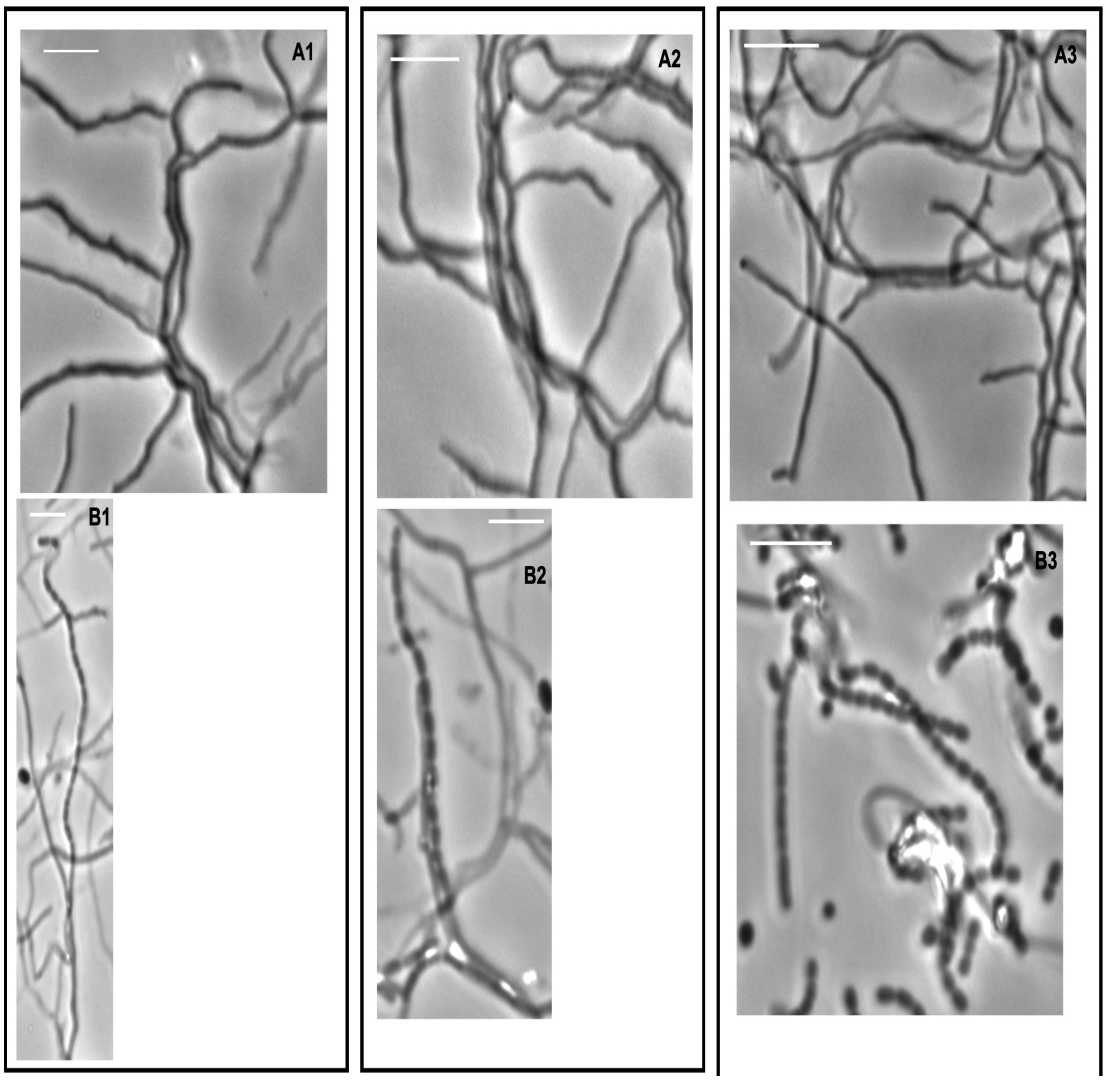

Figure 30: Complemented mutant RJ114 and single cross over RJ111 are identical to M145.

The phase contrast images shows that there is no difference between the aerial hyphae and substrate mycelium in all the strains, A1 and B1 –M145 wt; A2 and B2 – RJ111; A3 and B3- RJ114.

5.5. Mutants screened are morphologically identical to M145.

The strains RJ111, RJ114 and M145 was analysed microscopically for any phenotypic evidence. The cultures were inoculated onto a cover slip and grown on MS agar as previously explained in section 2.9.1. The culture then fixed by methanol and analysed under the microscope Nikon TE-2000 eclipse. On analysis of the slides, it was noticed that there was no striking difference between the exconjugants , single crossovers-RJ111, conditional double crossovers- RJ114 and wild type M145 (Fig. 30).

5.6. Conclusions.

Cardiolipin is an anionic phospholipid thought to be involved in numerous cellular processes. To gain further insight into its role in the cell, we undertook the characterization of gene *SCO1389* involved in cardiolipin biosynthesis in *S. coelicolor*. We have presented definitive evidence that *SCO1389* cannot be deleted without causing lethality, only when a second *SCO1389* copy is expressed in the same cells, implying that *SCO1389* is involved in an essential primary metabolic process, likely membrane phospholipid biosynthesis. This result does not rule out alternative mechanisms for cardiolipin biosynthesis in *S. coelicolor*, the other homologues of *SCO1389* that have been identified as part of the *S. coelicolor* genome project; *SCO7081* might bypass the action of *SCO1389*. It merely shows that, if the alternative pathway for cardiolipin synthesis exists, their activities are insufficient to suppress the effect of a deletion of *SCO1389.*

Chapter 6

Depletion of SCO1389 inhibits growth and development in *S. coelicolor*.

6. Introduction.

Despite important roles of cardiolipin in DNA replication and cell division (Mileykovskaya and Dowhan, 2005), reports shows that cardiolipin deficiency on *E. coli* has no specific effect other than, slightly reduced growth in standard media and reduced survival during stationary phase (Cronan, 2003). Since, we have already reported that *SCO1389* is essential in *S. coelicolor* (chapter 5). It is important to create a depleting strain of *SCO1389* under an inducible promoter, in order to visualize the growth and development of the cell in the absence of cardiolipin. A system for the tetracycline-inducible regulation of gene expression was used in this work. This system was adapted from the *E coli* transposon Tn10-TetR which has been successfully used as a tool for regulating gene expression in many organisms (Stebbins *et al.*, 2001). This system is based on regulatory elements of the Tn10-TetR specified tetracycline-resistance operon of *E. coli*, in which transcription of resistance mediating genes is negatively regulated by the tetracycline repressor (TetR). In the presence of the antibiotic tetracycline TetR does not bind to its operators located within the promoter region of the operon and allows transcription (Gossen *et al*., 1995).

In *S. coelicolor*, this regulatable system from transposon Tn10 was used and the vector contains a synthetic Tc controllable promoter (tcp), tcp830, which was active in a wide range of *Streptomyces* species (Rodrıguez *et al*., 2005). This chapter describes the construction, by genetic manipulations, of *SCO1389* mutants under the control of *tcp830* inducible promoter.

6.1. Construction of depletion strains.

The *SCO1389* gene was placed under an inducible synthetic anhydrotetracycline (ATC) controllable promoter (tcp), *tcp830* (Rodrıguez *et al*., 2005). The pPC830 plasmid was modified to a new plasmid pAVIIB (Vargeese *et al*., unpublished), containing, two transcription terminators, tmmr, *tfd* and the *tetRiS* gene, *ΦBT1* integration site with a hygromycin resistant marker. Two types of vectors were constructed on *SCO1389* under *tcp830* promoter, one in 'sense' and other in 'antisense' directions. For the first time, expression of a gene in the antisense direction was shown in *Streptomyces*. In order to deplete *SCO1389* from *S. coelicolor* a plasmid was constructed from pAVIIB. The plasmids pCLS117B1 and pCLS117B2 was constructed by amplifying *SCO1389* from plasmid pCLS105 using *Pfu* DNA polymerase and primers CL102 and CL103 (Table 11), digesting the product with *XbaI* and *EcoRV* followed by modification with Klenow DNA polymerase, and cloning the 673 bp fragment (Fig. 33 D) in to the *EcoRV* site of pAVIIB. In pCLS117B1, the orientation of *SCO1389* was in the 'sense' direction, which was placed under the control of the ATC-inducible promoter *tcp830*. A similar protocol was followed for pCLS117B2; the only difference was the *SCO1389* gene was in 'antisense' direction. The vectors were verified by restriction analysis (Fig. 34B and 34C).

By conjugation from *E. coli* strain ET12567 containing the driver plasmid pUZ8002 (Kieser *et al*., 2000), pCLS117B1 was transferred into *S. coelicolor* strain RJ111 where it integrated into the ΦBT1 attachment site. For conjugation of pCLS117B1 the strain RJ111 was preferred over M145, by doing this we save a step, and move ahead. RJ111 is a single crossover mutant resulted by the introduction of disrupted copy of *SCO1389* in the cosmid StA8A.RJ1 (section 5.3). The conjugation was carried out in the presence of atc (1.5µg/ml); since we used RJ111 it was easy to create the null mutant by the expression of *SCO1389* in *trans* from *tcp830* inducible promoter. The resulting strain, RJ118 (Table 1), contain the functional copy of *SCO1389*.

Transconjugants were screened for am^r, hyg^r and km^s. Two of them resulted in double cross-over; one of the two colonies was chosen, RJ118b, which had undergone a second crossover event to delete the chromosomal copy of *SCO1389* gene, this strain grows only in the presence of atc (Fig. 35 & 36). Three exconjugants was screened for am^r, hyg^r and km^r; resulted only in single cross over event leaving behind a partial deletion of the chromosomal copy of *SCO1389* gene, and one of them was choosen, RJ118a. Both the strains RJ118b and RJ118a carry the second copy of *SCO1389* under an inducible promoter, *tcp830*. Conjugation of pCLS117B2 to M145 resulted in the strain RJ116 that carries *SCO1389* in the opposite orientation, the exconjugants were screened for hyg^r (Fig 37) was propagated on a medium containing hygromycin (50 μg/ml).

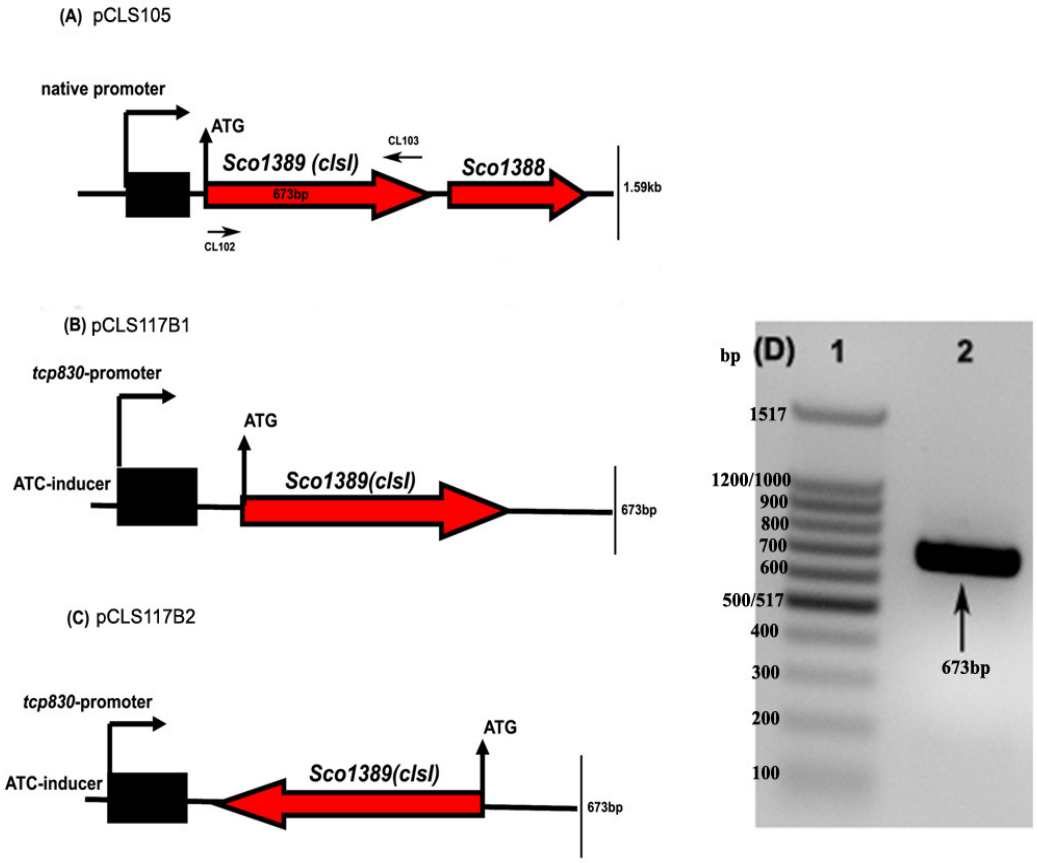

Figure 31: Vector diagram for the *SCO1389* depleting strains:

A- Represents the expression of *SCO1389* on native promoter, which acts as the template for the primers CL102 and CL103. D- Shows the PCR product 673bp, containing only *SCO1389* with start codon. B- Represents the *SCO1389* on *tcp830* promoter expressing functional copy of the gene. C- Shows the expression of "antisense" *SCO1389* on *tcp830* promoter.

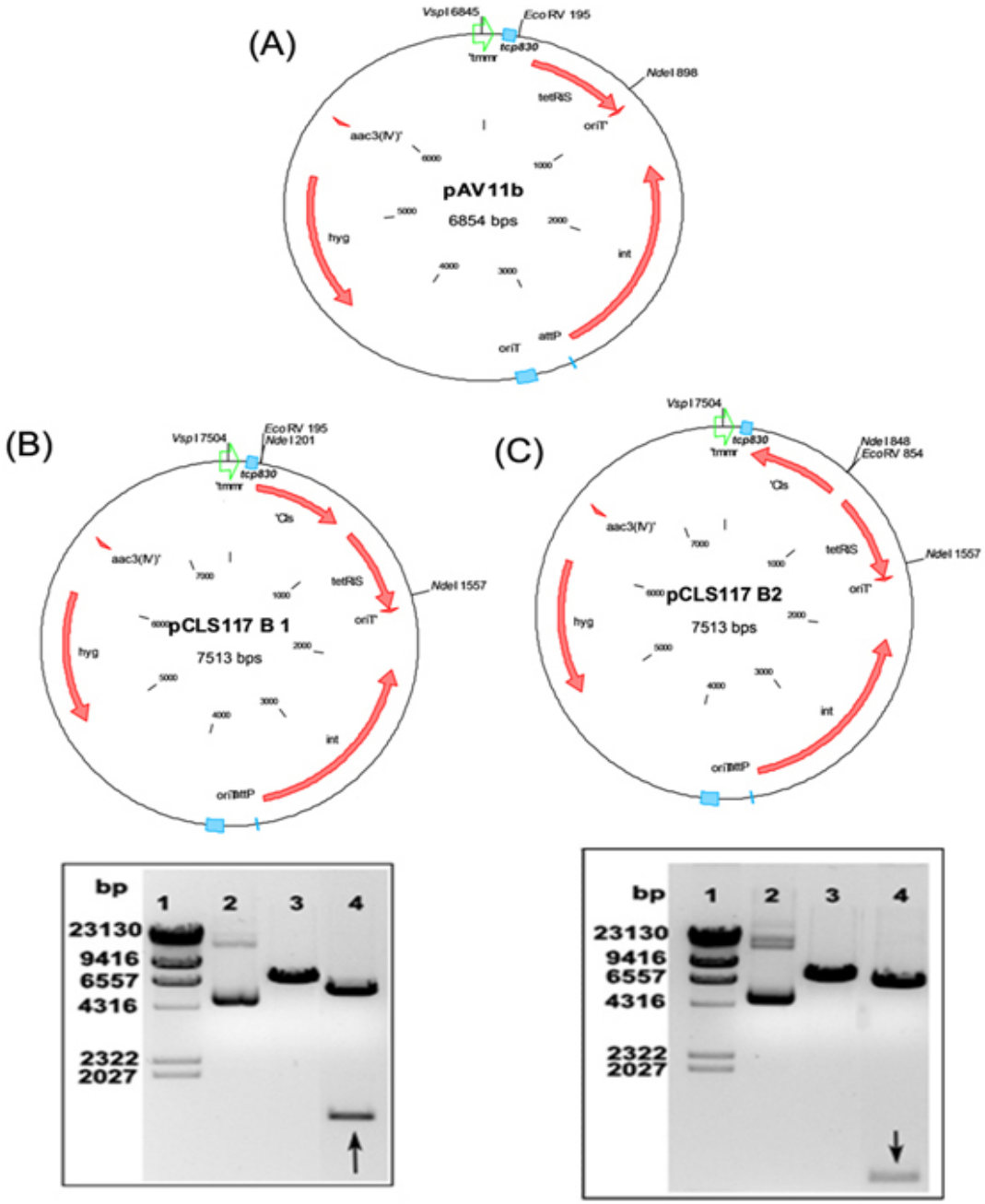

Figure 32: Confirmation of depletion vectors pCLS117B1 and pCLS117B2 by restriction analysis.

(A) pAVIIb plasmid map codes for hygromycin resistance, *tcp830* promoter induced by anhydrotetracycline, integrating vector in *Streptomyces* chromosome (Vargeese *et al*. unpublished). (B) pCLS117B1 carries "sense strand" of *SCO1389* under *tcp830* promoter. (C) pCLS117B2 carries "anti-sense strand" of *SCO1389* under *tcp830* promoter. Gel analysis, starts from lanes 1-λ *HindIII* marker; lanes 2 - Uncut plasmid DNA, lanes 3 - *EcoRV* digest; lanes 4 – *NdeI.* Lane 4 in (B) indicates 1.4 Kb *NdeI* fragment confirms pCLS117B1 and in (A) indicates 703bp *NdeI* fragment that confirms pCLS117B2.

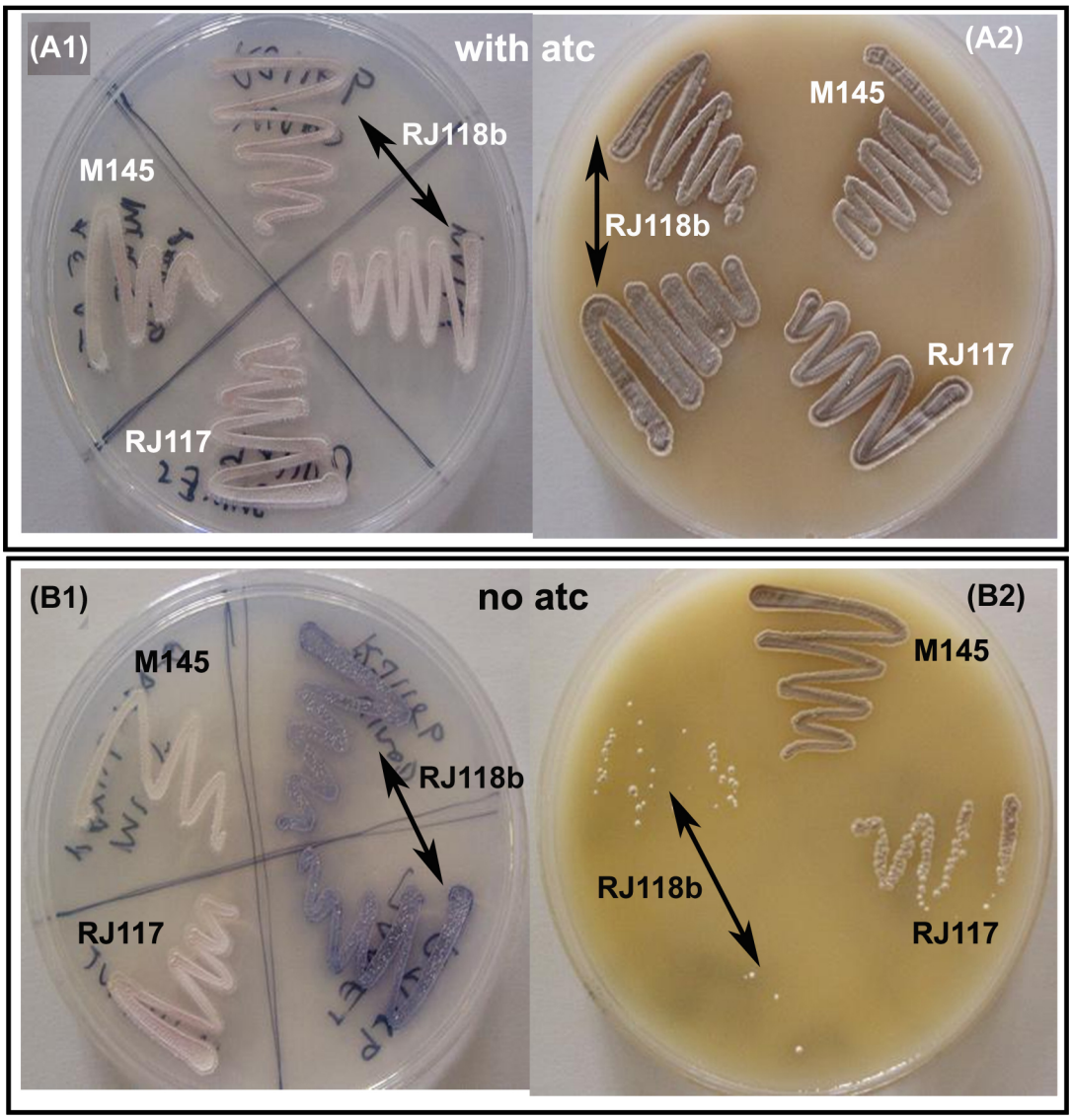

Figure 33: ATC dependent growth of RJ118b.

The plates A1, B1 are minimal media agar plates; A2, B2 are MS agar plates. Plates A1 & A2 are with atc and plates B1 & B2 are without atc. The growth of RJ118b is severely affected on minimal media plate (B1) with poor growth and no aerial hyphae, in contrast majority of no visible growth seen in MS agar plates.

6.2. Complete growth arrest in rich media (MS).

The strains RJ118b, RJ117 and M145 were grown on MS and minimal manitol medium to check if any visible phenotypic differences existed between the strains (Fig. 33). RJ118b, failed to visible grow at all on a MS medium in the absence of atc (1.5µg/ml), but when grown on minimal medium under the same conditions, there was a slight visible growth but no erection of aerial hyphae. Bioinformatic analysis of the *S. coelicolor* genome identified *SCO0253* as the closest match to Tn10 TetR regulatory protein, which may encode an innate Tc-responsive repressor that can interact with the tetO sequences in the synthetic *tcp*'s. As we know that in the presence of the antibiotic tetracycline, TetR does not bind to its operators located within the promoter region of the operon and allows transcription (Gossen *et al*., 1995). However in minimal media with no atc the promoter *tcp830* is expressed weakly *SCO1389*, supporting weak growth on the plates (Fig. 33B1). This suggests that the modified tetracycline repressor within pAVIIB, *tetRiS* does not bind completely to the *tetO* region, to stop transcription of the gene. Although, *tetRiS* was expressed from a strong constitutive promoter *S. ghanaensis* phage I19 (Labes *et al*., 1997), *SF14* in pAVIIB the expression of *tetRiS* seems to be affected when grown in different media. Morever, the innate TetR (SCO0253) has been reported to interact with the *tetO* sequences in the synthetic *tcp*, (Rodrıguez et al., 2005) with all these evidence we speculate that there can be some other factors involved during the mechanisms of *tetRiS* binding to *tetO* or there might be some interference from the innate *tetR* Contrary, in MS media the promoter *tcp830* is tightly regulated in the absence of atc suggesting that *tetRiS* completely binds to the *tetO* sequence in *tcp830*. Overall this study confirms that *tetRis* is more tightly regulated in MS agar media than in minimal media.

6.3. Depletion of *SCO1389* affects the growth and sporulation in *S. coelicolor*.

As no *SCO1389* null-mutant could be obtained, the function of the gene was investigated by partial depletion of SCO1389. Spores of strains RJ118b, RJ118a, M145, RJ111 and RJ116 were inoculated on a gradient plate with final concentration at one end of the plate 1.5µg/ml atc. The strains then streaked using a sterile toothpick from the opposite end of the highest concentration of ATC. So, that this avoids of any traces of ATC carried to the other end of the gradient plate. The plates were monitored for growth for three days at 30°C. Using a sterile cover slip, culture impressions were taken by gently pressing against the culture on the medium. The cover slip impression was taken from the different zones of the plate along the gradient (Fig. 34). To the cover slip 8µl 40% (w/v) glycerol was added and the slides were prepared. Then the slides were analysed by phase contrast microscopy. On observation there was clear evidence that RJ118b was atc dependent for its growth and development. Lane 4 (Fig. 34) shows that the growth was severely affected and there was no aerial hyphae formation on the gradient plate. The phase contrast images show aberrant substrate hyphae (Fig. 34). Weak growth of RJ118b in the absence of atc was due to the slight leakiness of this promoter, showing minimal expression of *SCO1389* was sufficient enough to support growth of substrate hyphae; although this strain was unable to grow and sporulate. From the images, on careful examination, the cardiolipin content within the cell decreases it affects the streptomycete development. The strain that carries integrated copy of antisense SCO1389, RJ116 was unaffected on the gradient plate; we speculate that this might be due to the time difference in mRNA expression levels between the integrated copy of antisense *SCO1389* and the functional copy *SCO1389* present within the chromosome. The growth of other strains was unaffected in the presence of atc including M145 wild type.

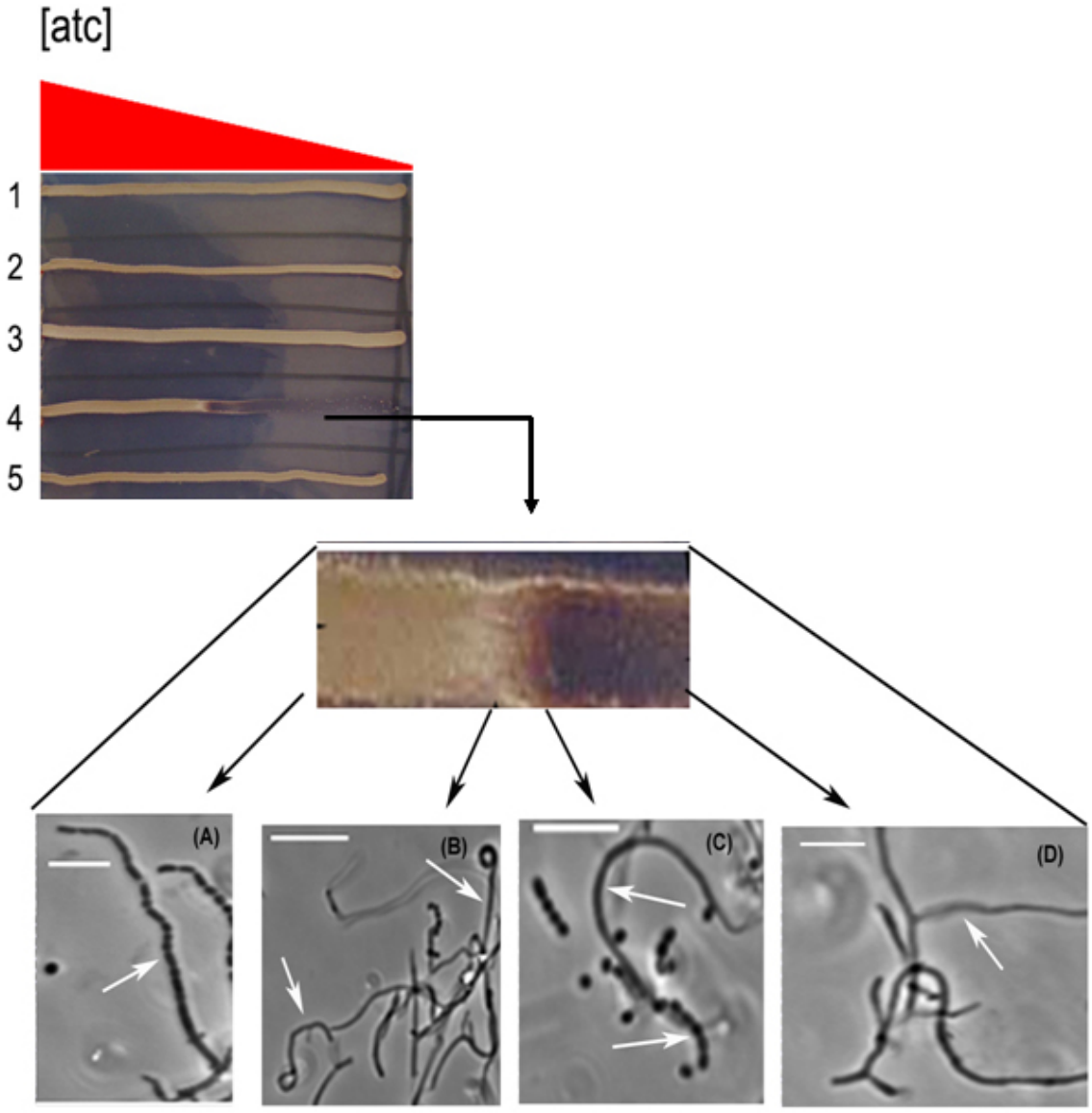

Figure 34: Decrease in cardiolipin affects growth and sporulation in S. coelicolor

SCO1389 depletion arrests development. RJ116 (1), RJ111 (2), RJ118a (3) RJ118b (4) & M145 (5) were plated along a gradient of atc (0-1.5 µg/ml). The black arrows show the phase contrast images of RJ118b along the gradient plate. A-shows normal spore chains, B-normal erection of aerial hyphae, C-the start of the depletion zone, causes less brancing and less spores and D-growth supported by the transient expression of *SCO1389* from *tcp830*, with less branching and no erection of aerial hypahe Scale bar 5µm.

6.3.1. Inducible antisense RNA of *SCO1389* affects the growth in liquid cultures.

Interference of mRNA expression with antisense RNA has been used effectively in eukaryotic systems to inhibit gene expression (Burne *et al*., 1999). Recently, this approach has also been used with *Staphylococcus aureus* (Ji *et al*., 2001), mycobacteria (Parish *et al*., 1997) to identify essential genes and virulence factors as well as to study gene functions of microorganisms (Zhang *et al*. 2000). The strain, RJ116 carries the copy of *SCO1389* in the antisense orientation (Fig 35) under the control of *tcp830* promoter induced by anhydrotetracycline. The spores were propagated through one round of growth and sporulation on a medium containing hygromycin (50 µg/ml). However, it was observed that in solid media, there was no effect on growth was seen on induction with atc. In order to verify if the behaviour of this strain changed in liquid broth; it was grown in liquid YEME media. Standard growth curve experiments were performed using M145 wild type, RJ116 and RJ117. The cells were grown in 200ml YEME broth in 2L flasks. 5ml of samples were collected every 3hrs till the stationary phase. In the mid log phase (after 9hrs) 1.5µg/ml atc was added to each flask and the samples were collected every 3hrs. The cells were filtered through pre weighed Whatman filter paper, and the filtrate was washed with SDW three times. The filter paper was dried at 60°C for 14hrs and subsequently weighed. The data were processed and using the average dry cell biomass, the growth curve was plotted against time (hrs). Interestingly the growth of RJ116 was arrested, on induction with atc. There was an average reduction in the overall cell biomass by 0.7mg/ml. However, in solid agar plates we did not see any inhibitory effects on the cell; carrying *SCO1389* in antisense orientation. This is one of the recent approaches used to study the gene function, especially those genes involved in essential cell functions through the utilization of antisense RNA to manipulate the expression levels of target genes. It was also reported that size limitations on antisense RNA has some effects on inhibition of the translation of the target genes (Wang *et al*., 2005). From, evidence we speculate that the low inhibitory effect of *SCO1389* in RJ116 may be due to the size of the antisense RNA or there is another activator gene which enables to counter effect the antisense mRNA during growth.

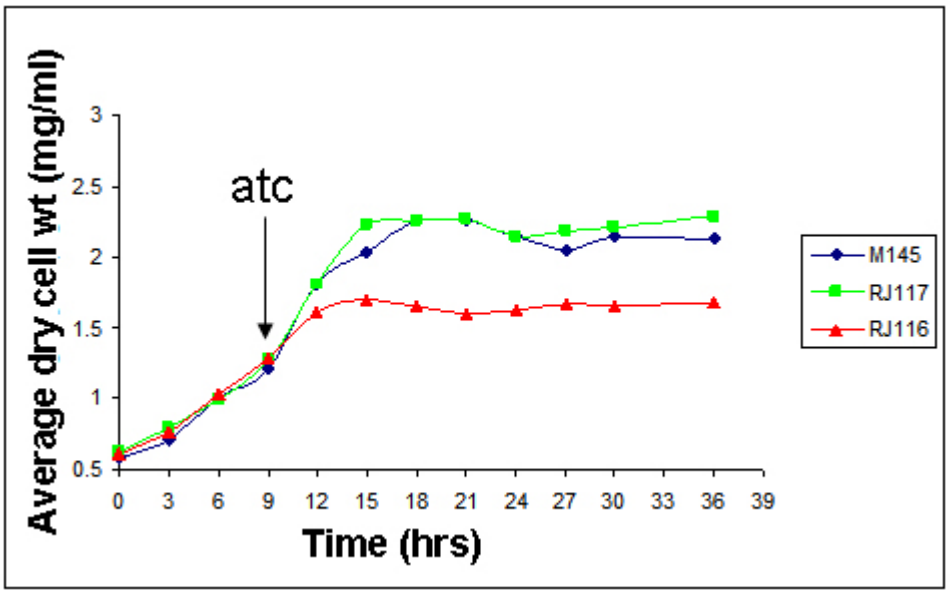

Figure 35: Antisense RNA decreases the growth in liquid culture.

A growth curve was done in liquid YEME media with the strains RJ117, M145 and RJ116 grown till mid log phase and adding 1.5µg/ml ATC (final concentration). The growth curve was measured by dry cell weight in triplicates.

6.4. NAO staining of mutant cells with a disrupted allele of *SCO1389* coding for cardiolipin synthase.

The fluorescent probe (NAO), specific for cardiolipin was used to demonstrate distribution of CL in *E. coli* membranes, which were observed mostly in the septal regions and at the poles of the cells (Mileykovskaya *et al*., 2000; 2001). *S. coelicolor* has one gene coding for cardiolipin synthase, *SCO1389* (Sandova *et al.*, 2009). We have presented definitive evidence that *SCO1389* cannot be deleted without causing lethality, only when a second *SCO1389* copy is expressed in the same cells, implying that *SCO1389* is involved in an essential primary metabolic process, likely membrane phospholipid biosynthesis. Further partial depletion of *SCO1389* appeared to cause growth arrest with no erection of aerial hyphae, short substrate mycelial growth with reduced in thickness, less branching, less frequency of curved hyphae, which are unusual in *Streptomyces*. However, it was also possible that under expression of *SCO1389* could cause alterations of cell division patterns. On the basis of this finding and these mutants were subjected to staining with NAO, to see if any detectable cardiolipin was present and Syto42 stain the DNA within the strain, RJ118b, and M145 wild type. The cells were grown as described in material methods and stained with 100 nM NAO (Molecular Probes) for 20 min at room temperature to visualize cardiolipin. Fluorescence images DAPI/FITC were taken by using the UV-2E/C filter unit (excitation at 340-380nm and emission 435-485nm), FITC (HQ) filter unit (excitation at 460 to 500 nm and emission at 510 to 560 nm). The exposure times used for the fluorescence and phase-contrast images were 0.3 and 0.02 s, respectively. The arrows indicate in figure 36-A4 and 5 shows the cardiolipin domains in branch points, hyphal tips and in substrate hyphae, in A6 distinct fluorescent foci and a blanket masking over the nucleoids are seen in the spore chains. On other hand in figure 36-B 4, 5 and 6 the arrows shows no localization of cardiolipin domains in branch points, substrate or in hyphal tips. It has already been discussed that RJ118b cannot erect aerial hyphae.

RJ118b shows no detactable cardiolipin seen compared to M145. In C there was no differences seen in the staining pattern in the presence of atc, however, in D4 and 6 we can see the growth in RJ118b was restored back and the cardiolipin are localized, in D6 it clearly shows the accumulation of cardiolin in the curved regions in substrate hyphae. In D5 aerial hyphae has been restored and displays a similar staining pattern to M145.

In RJ118b *SCO1389* disruptant cells fluorescence was scarcely detectable (Fig. 36), as expected because of the lack of cardiolipin. However, in M145 we can see cardiolipin domains localized in substrate hyphae, branch points, tips and in aerial hyphae. There are some weak spots seen in RJ118b (as discussed before this may be due to leaky expression of *SCO1389* from *tcp830*). The fluorescent foci were counted from hyphal tips, branch points and anucleated regions from the substrate hyphae and expressed in percentage distribution using a dot plot graph (Fig. 37).

RJ118b showed 8.3% & 11.7% of tips and branch points possessed cardiolipin fluorescent foci, compared to 92.7 % & 89% seen in M145. But, in the presence of atc there was no significant difference between M145 and RJ118b in cardiolipin domains accumulation in the anucleated regions. Around 36.8 % was seen in RJ118b to 46.1 percent of M145. In the presence of inducer atc, growth was restored in RJ118b showed similar fluorescent foci distribution as M145.

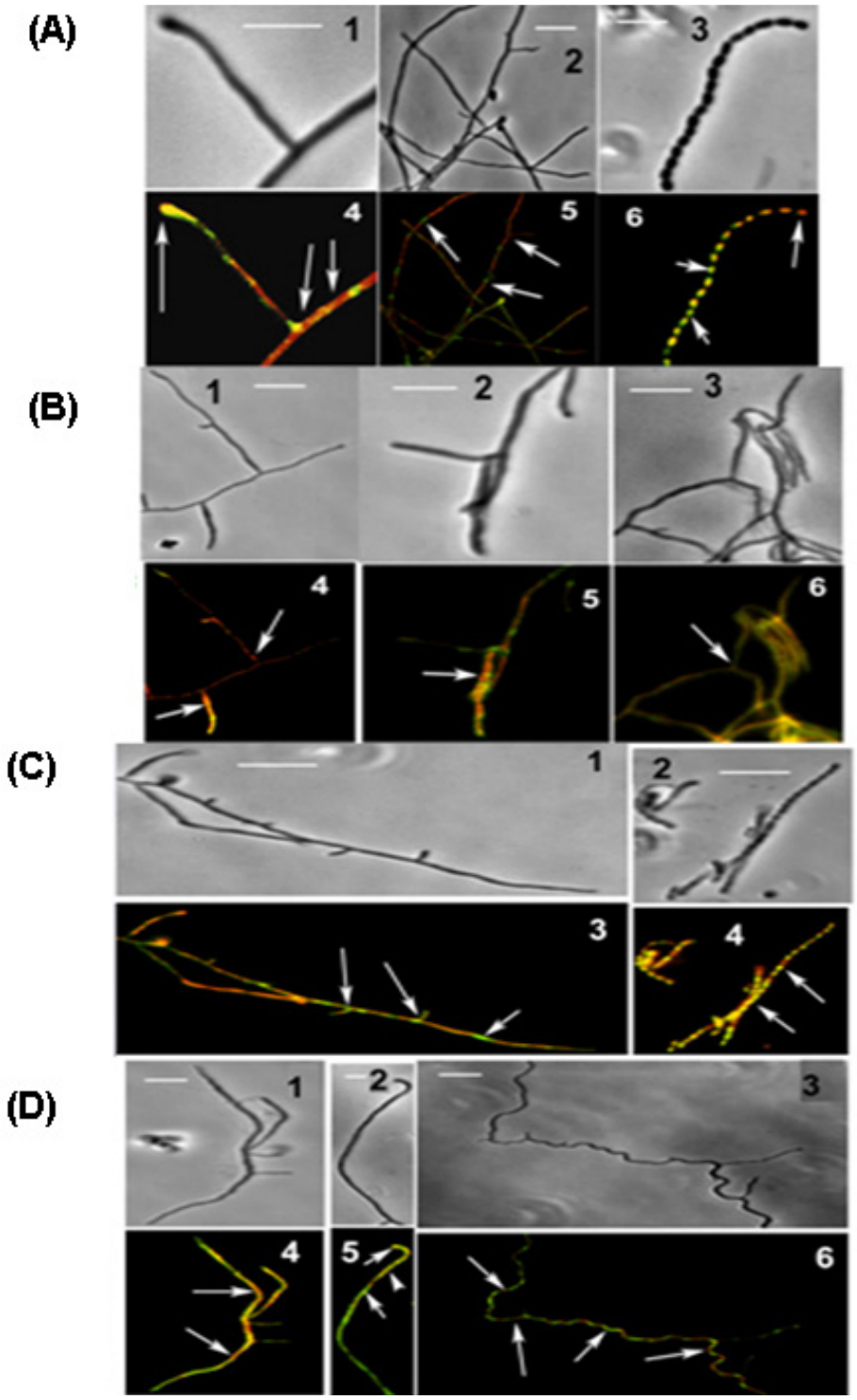

Figure 36: Effect of atc on distribution of cardiolipin

The strains marked A and C-M145, B and D- RJ118b. Both A and B are grown in absence of atc, C and D in presence of atc. The fluorescent images are shown in, A (4-6), B (4-6), C (3,4) and D (4-6) are captured in both DAPI and FITC filters, RED highlights DNA and GREEN shows cardiolipin. Corresponding phase-contrast images, A (1-3), B (1-3), C (1, 2) and D (1-3) are also shown size bar, 10 μm.

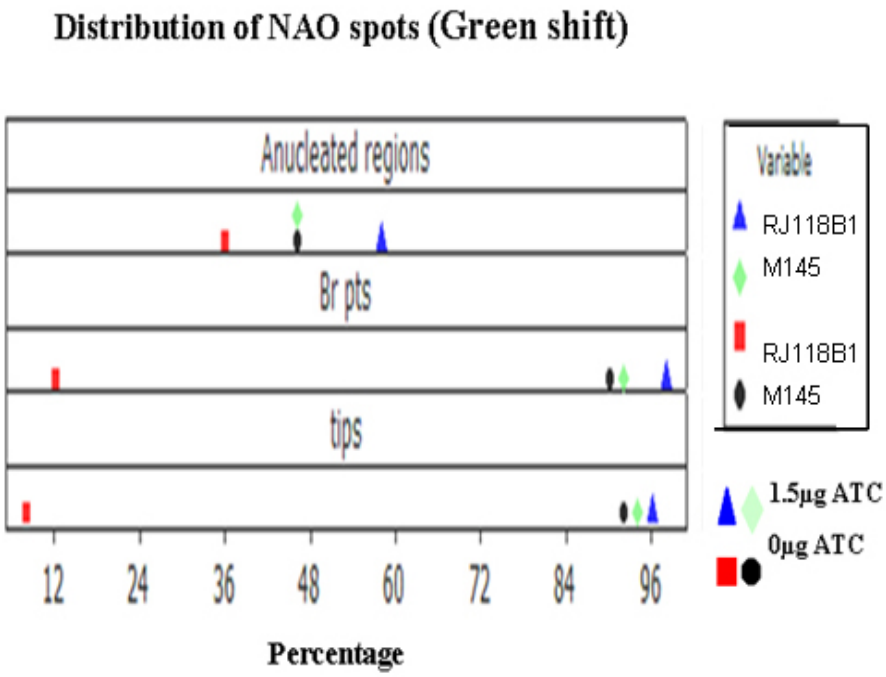

Figure 37: Percentage distribution of cardiolipin NAO spots.

The graph shows the dot plot distribution of cardiolipin NAO spots in hyphal tips, branch points and anucleated regions (within substrate hyphae) in RJ118b and M145 on induction with atc.

6.5 Depletion of CL causes altered morphology in growth.

To study the effects of depletion of *SCO1389*, spores of RJ118b were allowed to germinate and grow on the gradient plate of anhydrotetracyline for 3 days. It was observed that decrease in cardiolipin content within the cell, affects many parameters that could be used to quantitatively describe growth and development of *S. coelicolor*. The parameters used in this study (Fig. 38) are as follows: P1-branch angles; P2-branch/μm; P3-width of branch points; P4-width of substrate hyphae (sectioned at every 1μm); P5- width of the tips P6- spore size distribution; P7- spore chain length (μm) and P8- aerial hyphae width.

Statistical analysis was carried out using two sample‘t’-test with 95% confidence limit and tested for null hypothesis. Total of 5 different field were considered, and each of them was tested for the significance difference of ‘p’ value <0.05. RJ118b and M145 were grown in minimal media in the presence and absence of atc to study nycellial morphology quantitatively. From, figure 39 it was clearly evident that in absence of atc RJ118b was significantly affected in following variables P1 decrease in branch angles by 10.53° compared to 111.61° of M145. Length between two branch points was increased from 6.23 μm in uninduced M145 to 7.65μm in induced RJ118b. Substrate width was decreased from 0.53776 μm in uninduced M145 to 0.50766 μm in uninduced RJ118b. Although, there was no visible aerial hyphae, staining with Syto42 (chapter 3) showed some hyphae stacked with nucleoids (Fig 36-B4 and 5) which resembles the conclusions made by Sir David Hopwood as abberant aerial hyphae (1960). In uninduced RJ118b width was increased to 0.646 μm from 0.4710 μm in M145. From time-lapse microscopy it was seen that most of the *Streptomyces* species grown in solid culture, change direction during hyphal extension. In this study it was speculated that the change in direction may be contributed by CL.

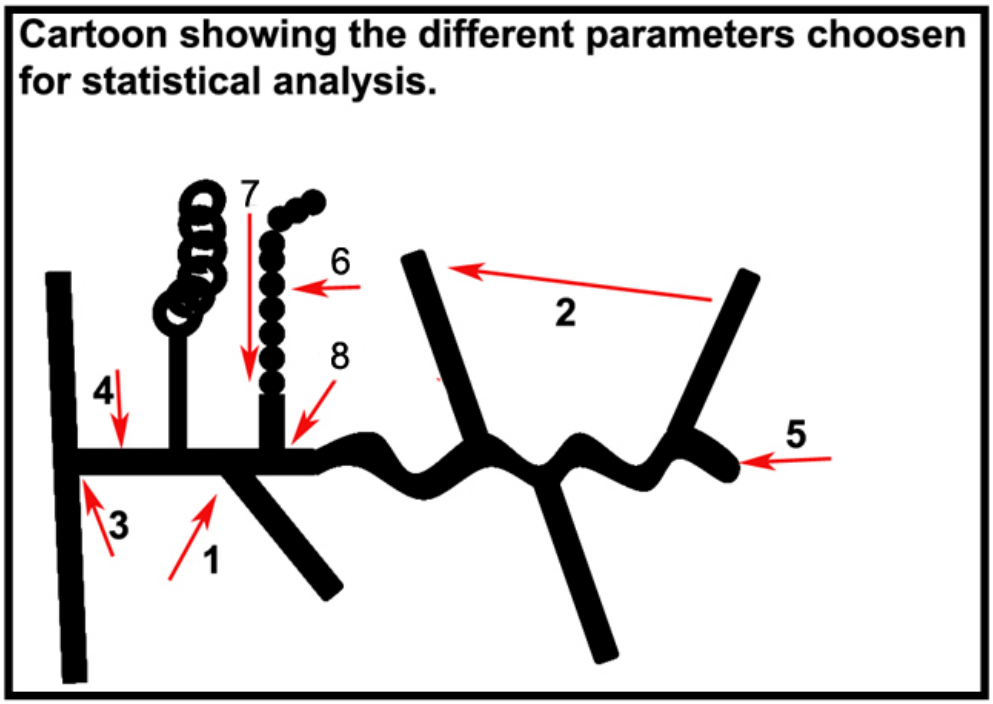

Figure 38: The cartoon shows the different parameters choosen from statistical analysis.

P1-branch angles; P2-branch/µm; P3-width of branch points; P4-width of substrate hyphae (sectioned at every 1µm) ; P5- width of the tips P6- spore size; P7-spore chain length (µm); P8- aerial hyphae width.

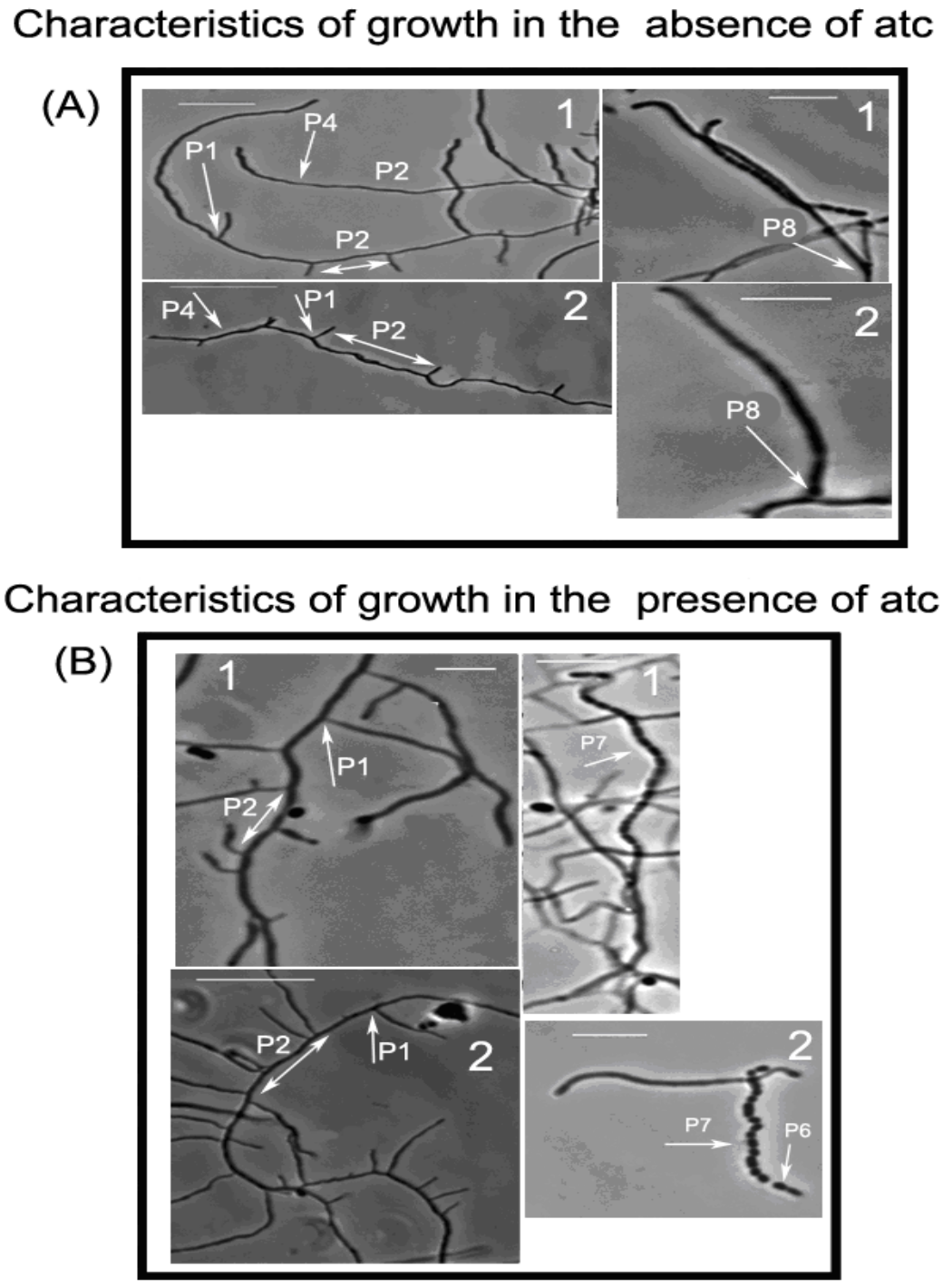

Figure 39: Growth defects due to decrease in cardiolipin production.

Images marked 1-M145 and 2-RJ118b. The white arrows show the parameters that indicates significant differences in absence and presence of atc on growth of *S. coelicolor*. 1- Branching angles, 2- Branch/µm, 4- width substrate (for every µm), 6- Spore size, 7- Spore chain length, 8- Aerial hyphae width (Scale bar 10µm).

P	Characteristics'	0-µg ATC		1.5µg ATC	
		M145[1]	RJ118b[2]	M145[3]	RJ118b[4]
1	Branching angles	111.61 (5.69)	101.08 (3.95)	114.28 (6.81)	93.0 (16.6)
2	Branch/µm	6.23 (1.63)	13.88 (4.97)	5.182 (0.966)	2.876 (0.641)
3	Branch pt width	0.5745 (0.0596)	0.5392 (0.0469)	0.5715 (0.0394)	0.6184 (0.0267)
4	Substrate width(for every µm)	0.53776 (0.00758)	0.5066 (0.0126)	0.5616 (0.0255)	0.665 (0.158)
5	Tip width	0.5558 (0.0438)	0.5203 (0.0503)	0.5610 (0.0404)	0.5620 (0.0453)
6	Spore size	0.9554 (0.0216)	-	0.9517 (0.0207)	1.027 (0.154)
7	Spore chain length	6.07 (1.59)	-	6.78 (1.54)	7.11 (1.55)
8	Aerial hyphae width	0.4710 (0.0266)	0.646 (0.134)	0.4712 (0.0334)	0.5053 (0.0205)

Table 14: Effect of atc on growth parameters.

The table shows the average mean and standard deviation of each parameter in presence and absence of atc.

P	Characteristics'	Depletion strain –*tcp830*/ATC			
		1,2	3,4	1,3	2,4
1	Branching-angles	S	S	NS	NS
2	Branch/µm	S	S	NS	S
3	Branch pt width	NS	NS	NS	S
4	Substrate width(for every µm)	S	NS	NS	NS
5	Tip width	NS	NS	NS	NS
6	Spore size	-	NS	NS	-
7	Spore chain length	-	NS	NS	-
8	Aerial hyphae width	S	NS	NS	NS

Table 15: Distribution of 'P' value during growth defects.

The 'P'-value table, when $P<0.05$ it is significant (S) and $P>0.05$ it is non-significant (NS).

In the presence of atc growth was restored back in RJ118b. However, branch angle decreased to 93° in RJ118b compared to 114.28° in M145 and intra branch distances decreased to 2.866 μm in RJ118b compared to 5.182 μm M145 these changes may be due to the strong induction of *SCO1389* from *tcp830* promoter (Rodrıguez *et al*., 2005).

In bacteria, the cell wall defines the overall shape of the membrane (Scheffers *et al*., 2006), but on the molecular scale the membrane shape is likely to be influenced by the different chemical structures of bacterial phospholipids. The difference in curvature between the poles and the cylindrical region in between is often invoked to explain the polar localization of proteins (Stahlberg *et al*., 2004). It has been shown that cardiolipin localization is driven purely by lipid phase segregation (Huang *et al*., 2006). Using, fluorophore labelled phospholipids it has been observed that they phase segregate in giant unilamellar vesicles into micron-scale domains, often with different curvatures (Baumgart *et al*., 2003; 2005).

Recent reports also documented that a lipid with a headgroup crosssectional area much smaller than that of its lipid tail, it will be attracted to the high curvature of the poles, out of the three dominant bacterial lipids (cardiolipin, phosphatidylglycerol, and phosphatidylethanolamine), cardiolipin is the most likely to seek high curvature based on head-to-tail ratio (Huang *et al*., 2006).

6.6 Conclusions

Cardiolipin-rich domains were visualized with the cardiolipin-specific fluorescent dye 10-*N*-nonyl acridine orange (NAO) in the branch points, hyphal tips and in the substrate hyphae. The mechanism of cardiolipin-specific staining shows the nonyl group of NAO inserts between the phosphate groups at the hydrophobic surface generated by the two outer acyl chains of cardiolipin (Mileykovskaya *et al*., 2001). Septal and polar localization of the fluorescent domains was observed in *B. subtilis* cells during exponential growth, but not in cells carrying a *clsA* null mutation blocking cardiolipin synthase and lacking measurable levels of cardiolipin (Kawai *et al*., 2004). In partially depleted cells of *SCO1389,* growth was arrested with no erection of aerial hyphae, short substrate mycelial growth with reduced in thickness, less of branching, less frequency of curved hyphae, which are unusual in *Streptomyces*. In RJ118b *SCO1389* disrupted cells fluorescence was scarcely detectable (Fig. 38), as expected because of the lack of cardiolipin. However, in M145 we can see cardiolipin domains localized in substrate hyphae, branch points, tips and in aerial hyphae. There are some weak spots seen in RJ118b (as discussed before this may be due to leaky expression of *SCO1389* from *tcp830*. Decreased CL affected P1-branch angles; P2-branch/μm; P4-width of substrate hyphae (sectioned at every 1μm) P8-width of aerial hyphae. However, P3-width of branch points and P5-tip width was not affected in uninduced RJ118b. These statistical analyses found to support the evidence reported of CL localization to the high curvature of the poles, based on head-to-tail ratio (Huang *et al*., 2006).

Chapter 7

Over-expression of *SCO1389* causes abnormal growth and cell death in *S. coelicolor*.

7.1 Introduction

Phospholipid composition in some bacteria varies when bacteria are grown in media that differ in salinity and/or osmolality. Recent studies show that increasing cardiolipin content is a key player in bacterial adaptation to osmotic stress (Romantsov *et al*., 2007). This work showed *SCO1389* is essential for the viability of the cell, and depletion of *SCO1389* appeared to causes deficiency in growth and development of the mycelium. In this work we are going to see what happens when *SCO1389* is overexpressed from an inducible promoter under normal growth condition in *S. coelicolor*. Moreover, to support this objective, there was evidence from the statistical data analysis from previous chapter showed increase alteration in cardiolipin production has effect on the growth and development in *S. coelicolor*. TipA promoters are widely used for inducible overexpression of cloned genes in *Streptomyces* (Takano *et al*., 1995; Yu&Hopwood, 1995). This promoter controls the synthesis of an mRNA transcript of its own, which encodes two different proteins, the 31 kDa TipAL and 17 k Da TipAS (Murakami *et al*., 1989; Holmes *et al*., 1993). The TipAL is a transcriptional activator that specifically binds thiostrepton, a cyclic peptide produced as a secondary metabolite. Thiostrepton can induce expression of the *tipA* gene by covalent binding to TipAL, thereby increasing the affinity for binding of the transcriptional activator to regions within *ptipA* (Chiu *et al*., 1996, 1999).

Therefore, to understand the effect of over production of cardiolipin, *SCO1389* was placed under an inducible *tipA* promoter in pIJ8600 (Ali N *et al*., 2002). Where, *tipA* is flanked by transcriptional terminators, for expressing genes inserted in host chromosomes. This vector integrates into the ΦC31 attB site in the chromosome. By adding 10 mg/ml of thiostrepton to the medium, the *tipA* promoter could be strongly induced, leading to overexpression of the gene of interest. As such, the construction of this strain will enable us to study the effect of anionic phospholipid cardiolipin on growth and development in *S. coelicolor* under normal growth conditions without any form of stress.

7.2. Construction of the strains.

The plasmid pCLS113A was constructed by amplifying *SCO1389* from pCLS105 using *Pfu* DNA polymerase and primers CL102 and CL103 (Table 9), digesting the product with *XbaI* and *NdeI*, and cloning the 673 bp fragment (Fig. 40 C) in the *XbaI* and *NdeI* site of pIJ8600. In plasmid pCLS113A *SCO1389* was was placed under the control of the thiostrepton-inducible promoter *tipA*. The vector was verified by restriction and digestion (Fig. 41 B). By conjugation from *E. coli* strain ET12567 containing the driver plasmid pUZ8002 (Kieser *et al*., 2000), pCLS113A was transferred into M145 where it integrated into the ΦC31 attachment site. The resulting strain, RJ110 (Table 1), contain the functional copy of *SCO1389*. Transconjugants were screened for am^r, and propagated on a medium containing apramycin (50 μg/ml).

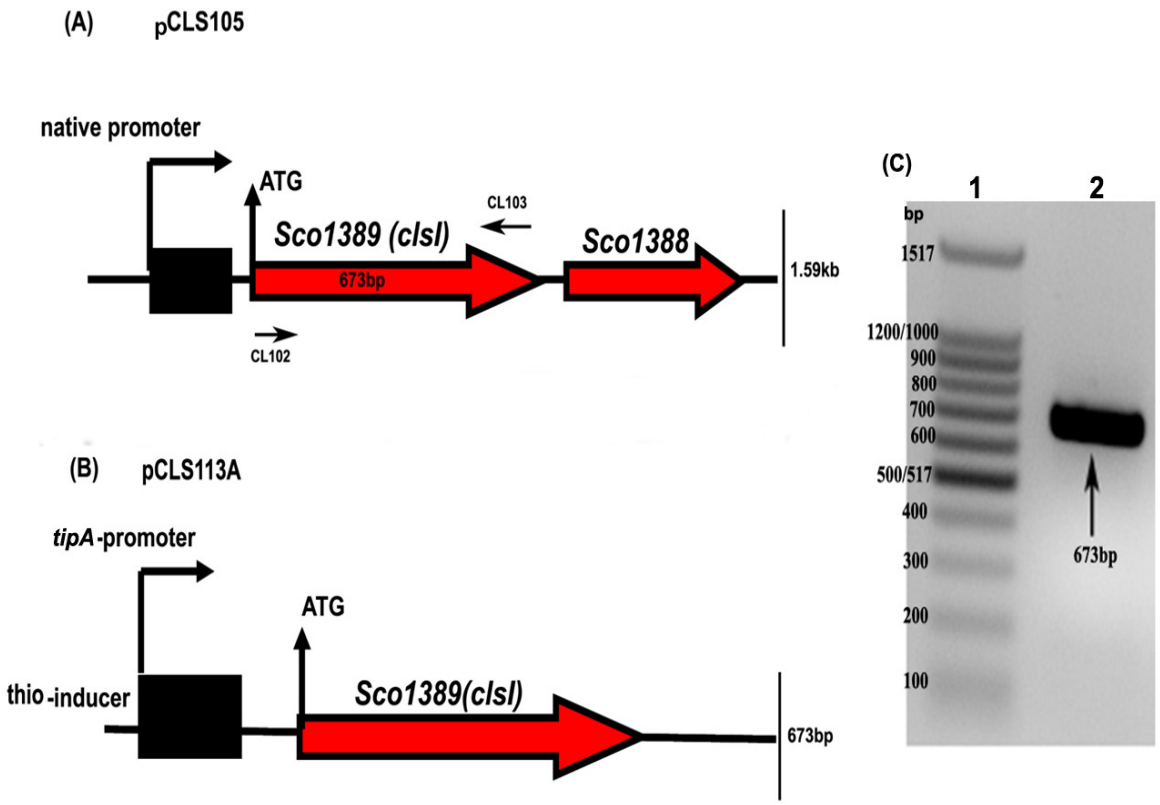

Figure 40: Diagram of *SCO1389* over-expression vector:

A- Represents the expression of *SCO1389* on native promoter, which acts as the template for the primers CL102 and CL103. C- Shows the PCR product 673bp, containing only *SCO1389* with start codon. B- Represents the *SCO1389* on *tipA* promoter.

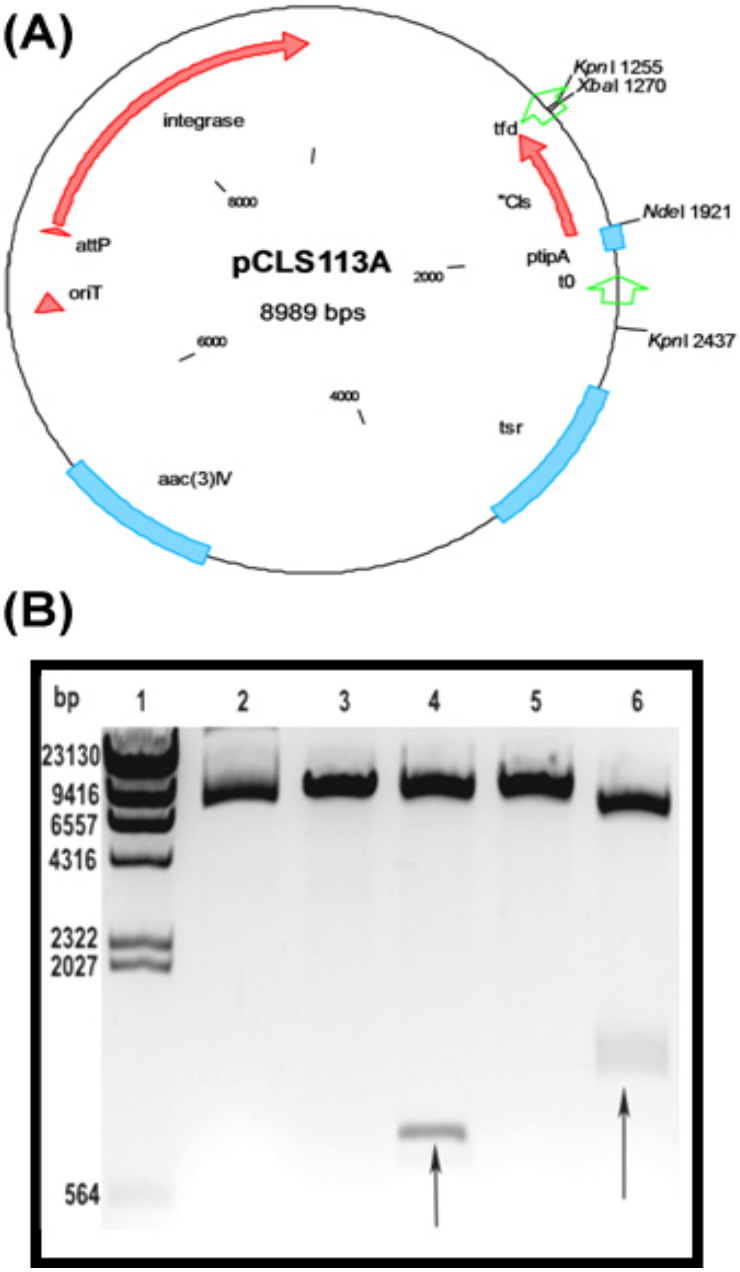

Figure 41: Confirmation of pCLS113A over expression vector of *SCO1389*.

(A) pCLS113A was constructed by ligation of 673bp PCR fragment to pIJ8600, carryies *SCO1389* under *tipA* control and codes for apramycin resistant. (B) Confirmation of the plasmid pCLS113A by restriction analysis. Lane 1-λ *HindIII* marker; lanes 2 - Uncut plasmid DNA, lane 3 - *XbaI*; lane 4 – *NdeI* and *XbaI*; lane 5- *NdeI* and lane 6- *KpnI*. The black arrow shows the lane 4-673bp PCR product and lane 6-1.118 Kb fragment that contain a functional copy of *SCO1389*.

7.3. Over expression of *SCO1389* dramatically alters cell shape and the growth pattern in *S.coelicolor*.

By adding 10 μg/ml of thiostrepton to the medium, the *tipA* promoter could be strongly induced (Ali *et al.*, 2002) of the gene of interest. (Fig.44). *S. coelicolor* pIJ8600, grown in the absence or presence of thiostrepton were indistinguishable from the normal hyphae produced by the parent strain M145. Overexpression of *SCO1389* gave rise to a very different cell type (Fig. 44). These cells had an oval and swollen shape and were much shorter and thicker than normal hyphae (a field of representative cells is shown in Fig. 44 B2). They were able to grow, branch, and form relatively dense cultures, although these cultures grew more slowly and delayed in sporulation than normal. Using a cover slip, cultures were grown on MS agar medium. The slides for microscopic examination were prepared by methanol fixation of the cover slips. To the cover slip 8μl 40% (w/v) glycerol was added and the slides were prepared. Then the slides were analysed under the microscope Nikon TE-2000 eclipse. On observation there was clear evidence that RJ110 was severely affected following over expression of *SCO1389* during its growth and development (Fig. 46). A similar phenotype has been described in overexpression of $DivIVA_{sc}$ which strongly perturbed cell shape determination, which largely took place at the tips in apically growing hyphae. Overexpression of $DivIVA_{sc}$ protein has also shown to affect cell wall assembly at the tips. This observation was similar to overexpression phenotype of *SCO1389* which can be speculated that CL may be required to localize $DivIVA_{sc}$ for apical extension in *S. coelicolor*. Overexpression of *SCO1389* produced swollen tips in hyphae (Fig. 40-B2) similar to the reminiscent of the effects of lysozyme or certain antibiotics on hyphal actinomycetes (Gray *et al*., 1990). On prolonged *SCO1389* overexpression frequent cell lysis was observed (Fig. 41A).

7.4. NAO staining of mutant cells overexpressing *SCO1389*.

A similar protocol was followed from previous chapter 6 to use fluorescent probe (NAO) to stain cardiolipin. The partial depletion of *SCO1389* appeared to cause growth arrest with no erection of aerial hyphae, short substrate mycelial growth with reduced in thickness, less branching, less frequency of curved hyphae, which are unusual in *Streptomyces*. This showed alteration in *SCO1389* expression affects streptomycete morphology. Overexpression of *SCO1389* gave rise to a very different cell type (Fig. 43D). These cells had an oval and swollen shape and were much shorter and thicker than normal hyphae (a field of representative cells is shown in Fig. 43 D2). They were able to grow, branch, and form relatively dense cultures, although these cultures grew more slowly and are delayed in sporulation. On the basis of this finding, these mutants were subjected to staining with NAO, to observe the localization of cardiolipin within the swollen membranes and Syto 42 staining of the nucleoids within the hyphae. The exposure times used for the fluorescence and phase-contrast images were 0.3 and 0.02 s, respectively. The arrows indicated in A3 and B3 show the normal cardiolipin distribution in anucleated regions and hyphal tips; A4 and B4 shows the fluorescent foci in aerial hyphae. On induction with thiostrepton, C3, 4 shows normal distribution in *S. coelicolor* pIJ8600, D4 and 5 the arrows shows swollen substrate hyphae and swollen tips, strong fluorescent cardiolipin domains with irregular distribution of the nucleoids. D6 shows aerial hyphae with empty spores with no nucleoids and irregular distribution of fluorescent foci of cardiolipin. The fluorescent foci was counted from hyphal tips, branch points and anucleated regions from the substrate hyphae and expressed in percentage distribution using a dot plot graph (Fig. 42). RJ110 and *S. coelicolor* pIJ8600 on an average show more than 90 percent of cardiolipin fluorescent foci at the tips and in branch points in induced and uninduced states. But, in RJ110 on induction there was significant 15 percent increase in anucleated regions compared to 40 percent in *S. coelicolor* pIJ8600 during both induced and uninduced states. We speculate that this may be the reason for swollen substrate hyphae, spores and tips.

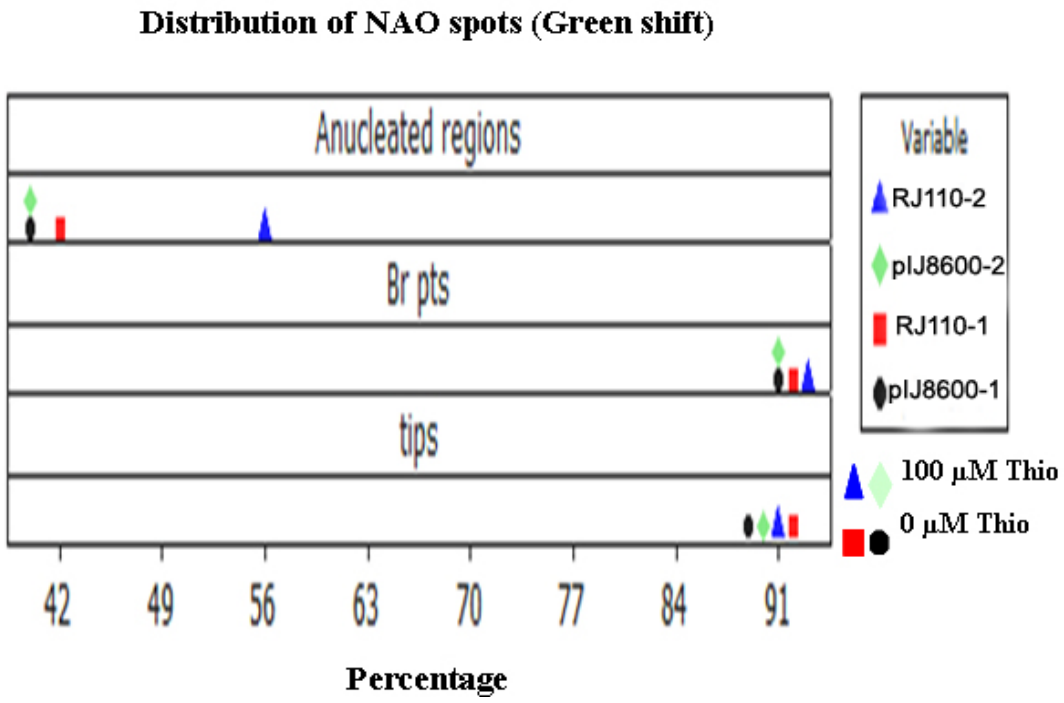

Figure 42: Percentage distribution of cardiolipin NAO spots.

The graph shows the dot plot distribution of cardiolipin NAO spots in hyphal tips, branch points and anucleated regions (within substrate hyphae) in RJ110 and *S. coelicolor* on induction with thiostrepton.

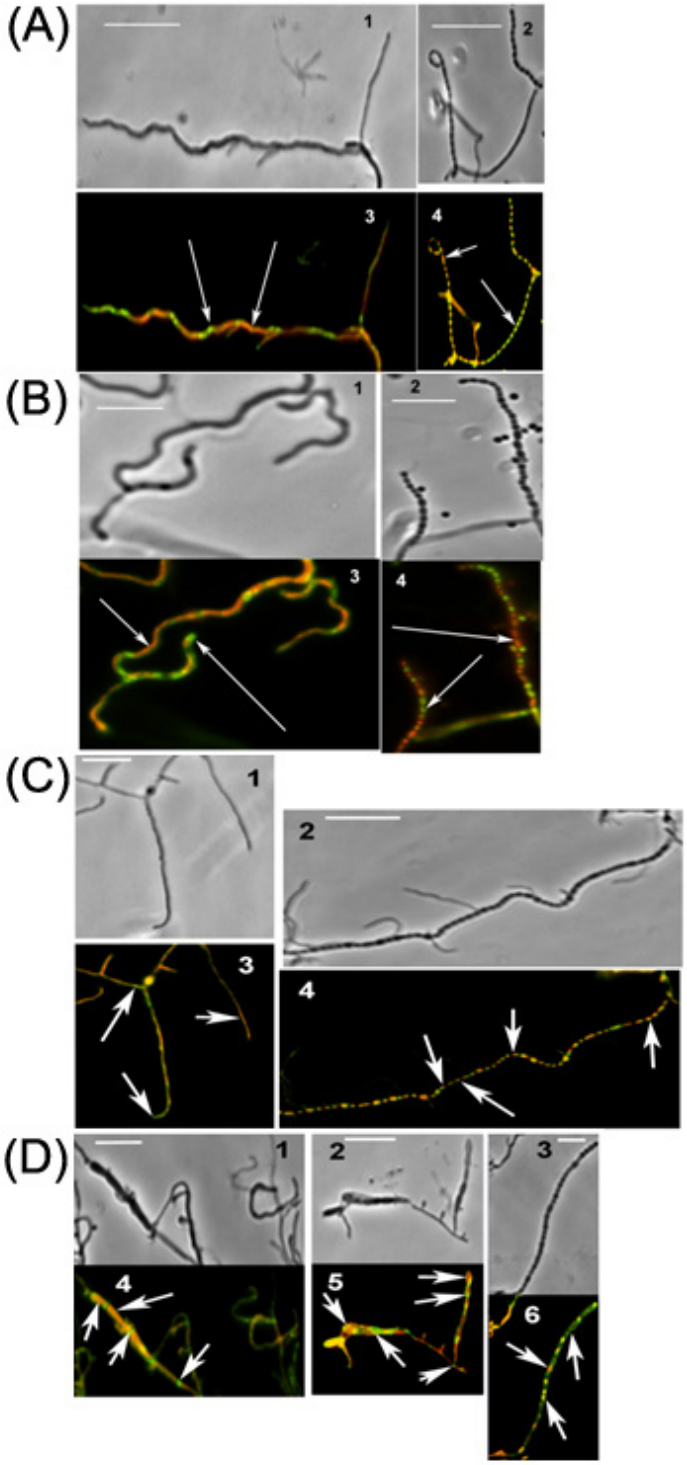

Figure 43: Effect of thiostrepton on distribution of cardiolipin

The strains marked A and C-*S. coelicolor* pIJ8600, B and D- RJ110. Both A and B are grown in absence of thio, C and D in presence of thio. The fluorescent images are shown in, A (3, 4), B (3, 4), C (3, 4) and D (4-6) are captured in both DAPI and FITC filters, RED highlights DNA and GREEN shows cardiolipin. Corresponding phase-contrast images, A (1, 2), B (1, 2), C (1, 2) and D (1-3) are also shown. Size bar, 10 μm.

7.5 Over expression of CL causes altered morphology in growth.

To study the effects of over expression of *SCO1389*, spores of RJ110 were allowed to germinate and grow on the plate of thiostrepton for 3 days. The parameters used in this study were also used in chapter 6, studying the depletion of *SCO1389*. P1-branch angles; P2-branch/μm; P3-width of branch points; P4-width of substrate hyphae (sectioned at every 1μm) ; P5- width of the tips ; P6- spore size distribution; P7- spore chain length (μm) ; P8-width of aerial hyphae.

Using two sample‘t’-test with 95% confidence limit the statistical analysis was analysed and tested for null hypothesis. Total of 5 different field were considered, and each of them was tested for the significance difference of ‘p’ value <0.05. In the absence of inducer thiostrepton no significant effect was seen in RJ110 and *S. coelicolor* pIJ8600, expect for width of the substrate P4 (Fig. 44 A1 and 2). This change may be due to the leaky nature of the *tipA* promoter (Ali N *et al*., 2002). However, in the presence of thiostrepton, *SCO1389* was strongly induced under *tipA* promoter which strongly affected the cell morphology. The average branching angle was reduced from 100.82° in *S. coelicolor* pIJ8600 to 82.46° in RJ110 in the presence of the inducer thiostrepton. Hyper branching was observed on addition of the inducer thiostrepton in RJ110, intra branch distances were reduced to 2.75 μm compared to 12.64 μm in *S. coelicolor* pIJ8600. An average increased substrate width 1.214 μm (Fig. 44 B2) and tip width 0.727 μm was observed compared to presence and absence of inducer in *S. coelicolor* pIJ8600. Altering the expression of *SCO1389* suggested that increased CL content in *S. coelicolor* could affect the direction of extended hypha and branching.

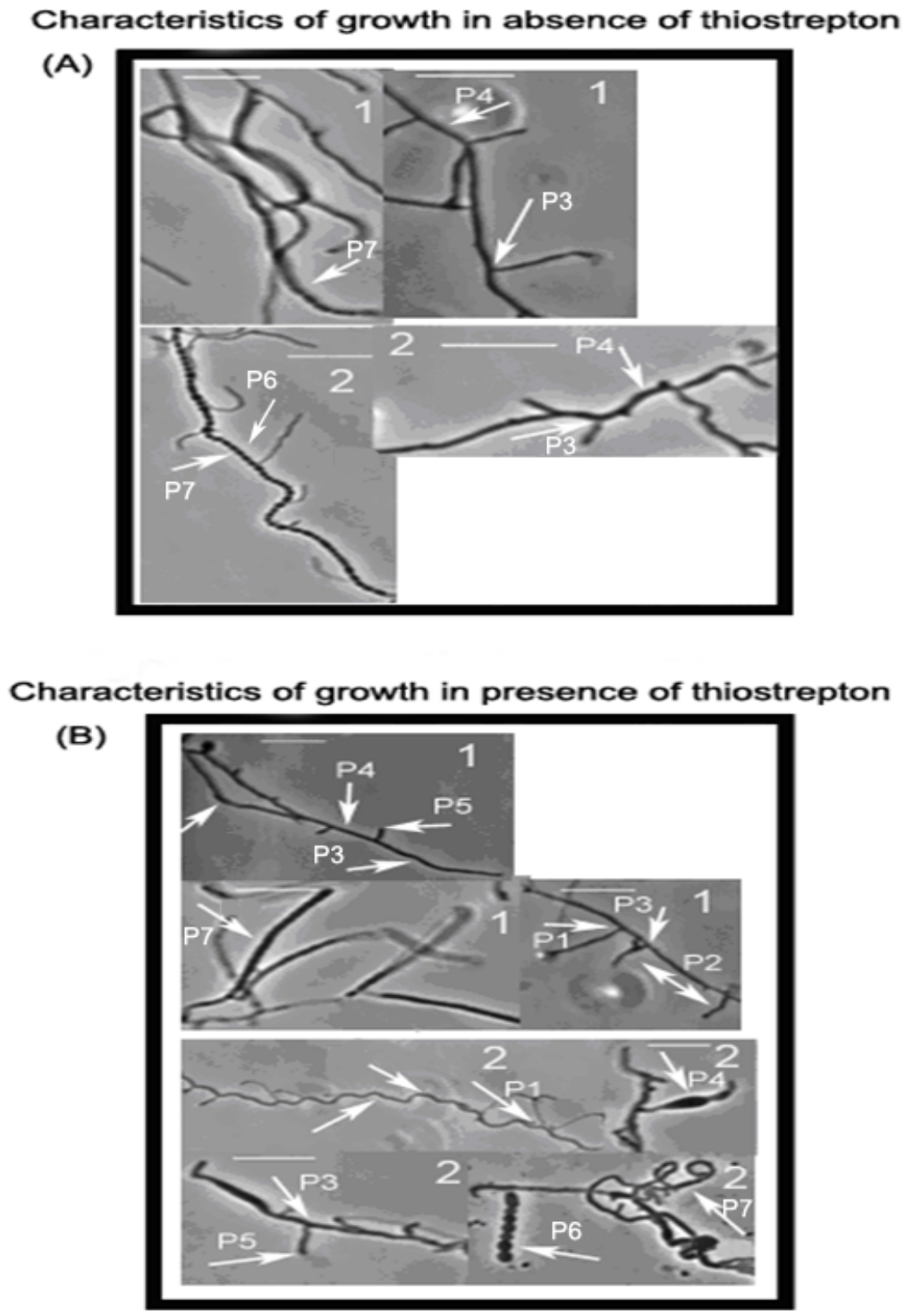

Figure 44: Increase in CL content affects the morphology of the cell.

In A and B, 1-*S. coelicolor* pIJ8600 and 2-RJ110. The white arrows show the parameters that show significant difference in absence and presence of atc. P1-branch angles; P2-branch/µm; P3-width of branch points; P4-width of substrate hyphae (sectioned at every 1µm) ; P5- width of the tips ; P6- spore size; P7- spore chain length (µm) ; P8-width of aerial hyphae.

P	Characteristics'	0-µM Thio		100µM Thio	
		pIJ8600[1]	RJ110[2]	pIJ8600[3]	RJ110[4]
1	Branching angles	100.82 (8.33)	97.55 (2.96)	100.82 (8.33)	82.46 (8.80)
2	Branch/µm	12.98 (3.52)	12.10 (1.49)	12.64 (3.99)	2.75 (1.00)
3	Branch pt width	0.5597 (0.0653)	0.5995 (0.0371)	0.5279 (0.0285)	0.6020 (0.0390)
4	Substrate width(for every µm)	0.5696 (0.0554)	0.6896 (0.0445)	0.5368 (0.0182)	1.214 (0.255)
5	Tip width	0.5342 (0.0443)	0.5546 (0.0302)	0.5156 (0.0292)	0.727 (0.137)
6	Spore size	0.9675 (0.0237)	1.0069 (0.0596)	0.9606 (0.0149)	1.889 (0.396)
7	Spore chain length	6.32 (1.31)	6.82 (1.54)	5.93 (1.05)	6.224 (0.474)
8	Aerial hyphae width	0.4747 (0.0288)	0.4990 (0.0216)	0.4788 (0.0361)	0.5436 (0.0264)

Table 16: Effect of thio on growth parameters.

The table shows the average mean and standard deviation of each parameter in presence and absence of thiostrepton.

P	Characteristics'	Over-expression strain-*tipA*/thio			
		1,2	3,4	1,3	2,4
1	Branching-angles	NS	S	NS	S
2	Branch/µm	NS	S	NS	S
3	Branch pt width	NS	S	NS	S
4	Substrate width(for every µm)	S	S	NS	S
5	Tip width	NS	S	NS	S
6	Spore size	NS	S	NS	S
7	Spore chain length	NS	NS	NS	NS
8	Aerial hyphae width	NS	S	NS	S

Table 17: Distribution of 'P' value during growth defects.

The 'P'-value table, when P<0.05 it is significant (S) and P>0.05 it is non-significant (NS).

7.6 Over expression of *SCO1389* lead to bursting and swelling of the hyphal tip.

To observe the effects of overexpression of *SCO1389* on growing hyphae, spores from RJ110 were allowed to germinate and grow in the presence of thiostrepton. Time-lapse microscopy was set up as explained in chapter 3, and the images were captured every 10 minutes by phase contrast microscopy. Figure 45 shows after induction of *tipA*, hyphal tips had become swollen and rounded, and then burst (Fig. 45A). The bursting tendencies of hyphal tips are reported in fungi as a result from delicate balance between cell wall synthesis and wall lysis in apical growth (Garcia *et al*., 1972). From the present observation we constitute circumstantial evidence to support the following assumptions: (i) the apices of *S. coelicolor* hyphae have a large potential of wall lytic activity; (ii) the release of this activity during growth must be a gradual process delicately co-ordinated with wall synthesis; (iii) the balance between synthesis and lysis of wall polymers can be easily disturbed and shifted in favour of lysis by the over production of anionic phospholipid, CL resulting in violent disintegration of the hyphal apex (Fig. 47A) or, formation of large apical swellings (Fig. 44 B2). We also speculate that during an increase CL production it might activate the osmotic stress proteins (Romantsov *et al*., 2007) which might be recruited at the tips and interfere with the proteins (Flardh, 2003) involved in normal apical extension. These changes may allow the tips to sense the growth medium, and the presence of a hydrostatic pressure difference between the interior of the tip and its environment (Park. and Robinson, 1966) this may result in bursting of hyphal tips.

The frames 8 to 12, the black arrows clearly indicate the bursting tip (Fig. 45B). Using the same set up, it was possible to visualize the effect of *SCO1389* overexpression on tip growth. Without induction of *tipAp*, hyphae of strain RJ110 showed normal tip growth. After addition of the inducer, the tip regions were broadend and swollen (Fig. 45B). This lead to a unique phenomenon that's usually seen only fungi, multiplying or dividing tips.

Time-lapse videos on RJ110 in the presence of thiostrepton showed that apical extension of hyphae with dividing tips mimicking the growth of fungi (Fig. 45B). It showed a broad tip joint where the dividing starts. Genetic studies in fungi have identified genes involved in these processes, and shown that microtubules, F-actin and a number of other proteins (including kinesin and dynein) are critical for tip growth and nuclear migration (Fischer, 1999; Xiang and Morris, 1999; Momany, 2002). In comparison to the situation in fungi, the mechanism underlying apical growth in *Streptomyces* is taken over by $DivIVA_{sc}$. This protein is required for creating or maintaining the cell polarity that is needed for tip extension. Because $DivIVA_{sc}$ can specifically localize to the tips, it might be interacting with cardiolipin at the curvature (Huang *et al.*, 2006) along with other proteins that are needed for growth polarity (Tseng *et al*., 2006; Flradh, 2003; Noens *et al*., 2007). The evidence of dividing tips and swollen hyphae in RJ110 may be the visible signs for control the growth polarization in *S. coelicolor* (Fig.45B), and the apparent hyperbranching caused by SCO1389 overexpression (Fig.44 B2) are consistent with the model established for the role DivIVAsc localization in *S. coelicolor* (Flardh, 2003) . Consequently, it seems that *SCO1389* is required for tip growth, branch formation and erection aerial hyphae. It appears that proteins involved during apical growth and cell division may be lapidated and anchored into cell membranes.

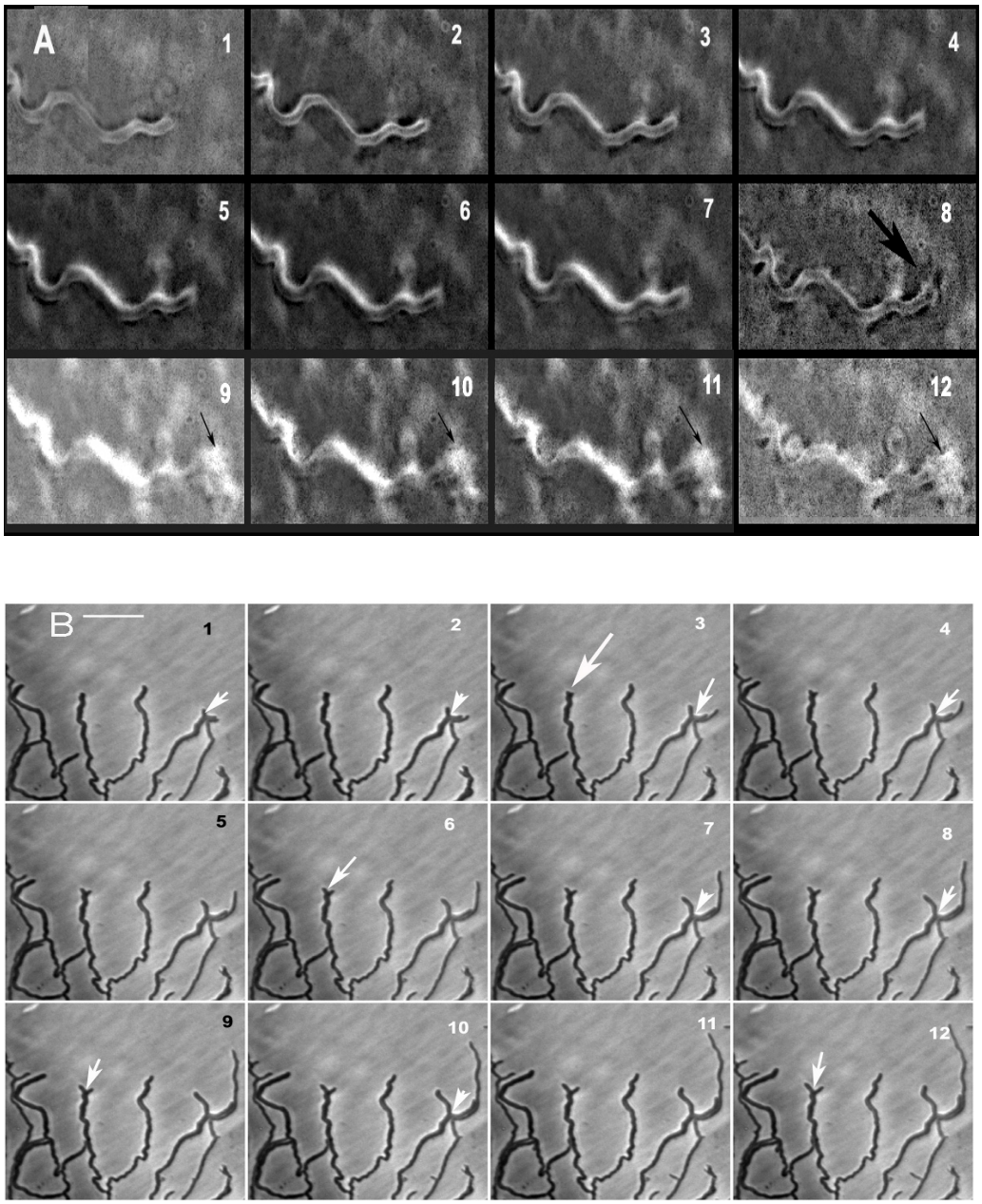

Figure 45: Induction of SCO1389 causes cell death and abornormal dividing tips in *S. coelicolor.*

Time-lapse microscopy shows bursting hyphal tips and swollen multiplying tips when *SCO1389* is over expressed. RJ110 was grown in the presence of thiostrepton and observed by time lapse microscopy. Black arrows indicate bursting (A) and white arrows showing multiplication of tips (B).

7.7 Effect of NaCl and thiostrepton gradient on the overexpression strains.

Previous studies showed that NaCl and sucrose had effects on the fatty acid compositions of cells (McGarrity *et al*., 1975). Both salinity and osmolality are important since the ionic strength will influence the structures of membranes comprised of lipids with ionic head groups. In *E. coli*, cardiolipin dominates the increase in the proportion of anionic lipid on high salinity conditions (Romantsov *et al*., 2009). Based from these observations, we made an attempt to see whether an increase in NaCl concentration (0 to 0.7M NaCl) along with a increase in thiostrepton gradient (0 to 100µg/ml) will show any specific phenotypic changes in growth. The strains RJ110 (Fig. 48 [b, d]), *S. coelicolor* pIJ8600 (Fig. 46 c) and M145 (Fig. 46 a) were grown in a gradient distribution of NaCl (0M to 0.7M) and thiostrepton (0-100µg/ml) on minimal media agar plates. The growth was monitored for a week.

The plates A1 (0.0M NaCl) and B1 (0.7M NaCl) contained no thiostrepton the growth seems to unaffected on high osmolarity conditions (Fig. 46). The only difference was the production of antibiotics seen in B1, this may be a result of activation of the osmo response regulator gene, *osaB* (Bishop *et al*., 2004). However, in A2 (0.0M NaCl) and B2 (0.7M NaCl) contain 100µg/ml thiostrepton again the growth was unaffected , in B2 on high osmolarity conditions and thiostrepton, the growth of the strains was slowed down but none of them showed any growth defects (the plates were monitored for a week , but no change was noticed). These results contradict the relation between cardiolipin and NaCl, studied in *E. coli*. (Romantsov *et al*., 2009). Although there were mixed results from the experiment it would interesting to see the relation between osmoadpation and lipid profiling in *S.coelicolor*.

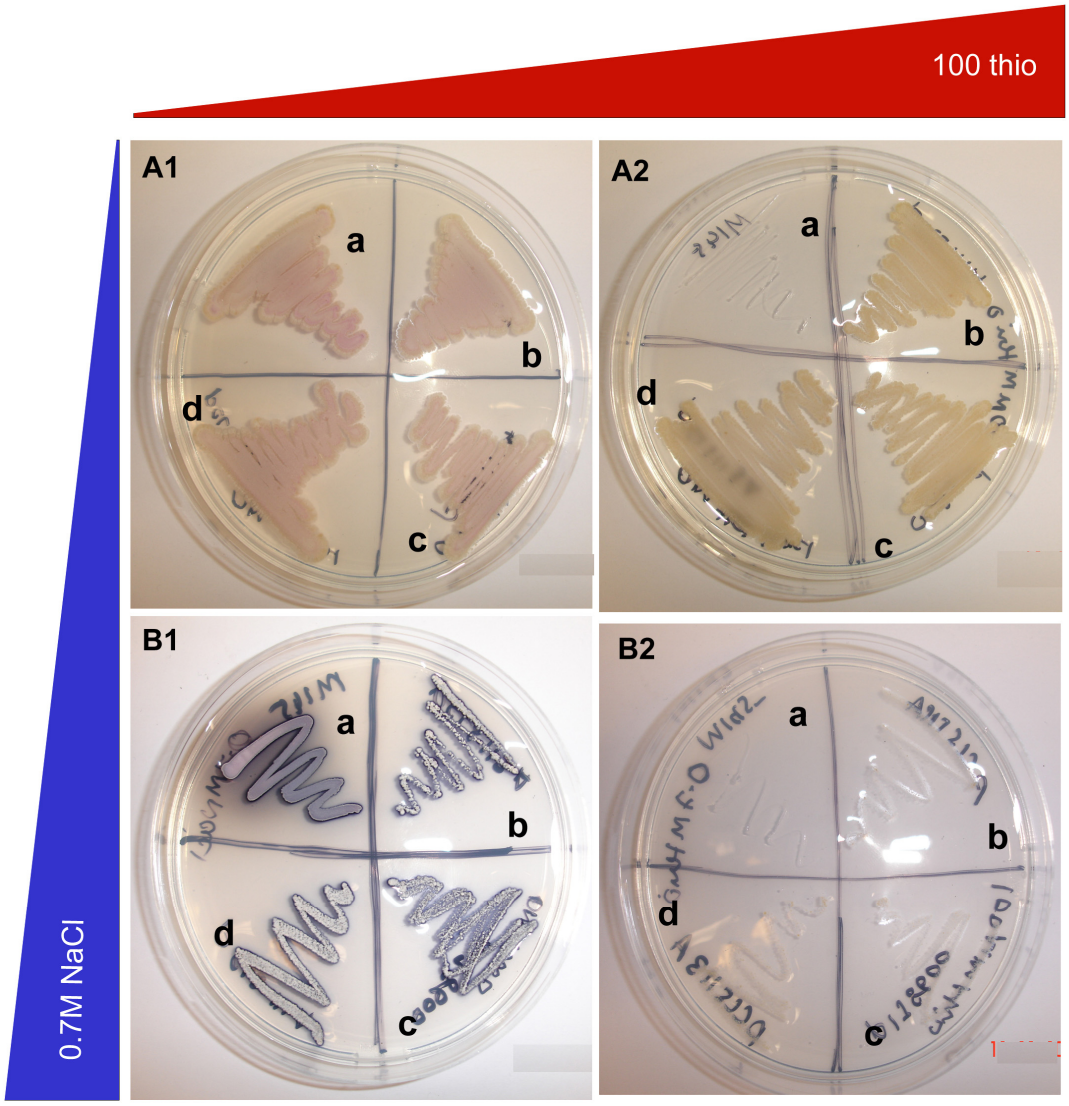

Figure 46: No growth defects seen in RJ110 and *S. coelicolor* pIJ8600 on minimal media agar.

A1 and A2 have 0mM and 100mM thiostrepton with constant 0mM NaCl. B1 and B2 have 0mM and 100mM thiostrepton with 0.7M NaCl constant, a-M145, b & d-RJ110, c-*S. coelicolor pIJ8600*. The plates show the gradient of thiostrepton in red and NaCl in blue. The plates were incubated at 30° C for three days.

7.8 Conclusions

Overexpression of SCO1389 strongly perturbed cell shape, which largely affected the tips of apically growing hyphae. A similar phenotype has been described showing overexpression of $DivIVA_{sc}$ which strongly perturbed cell shape. These observations are very similar to *SCO1389* overexpression phenotype which suggests that cardiolipin may be required to localize $DivIVA_{sc}$ for apical extension and recruiting cell- division, other cell shape determining proteins and targeting them to the respective regions within the cell. Statistical analysis showed that an increase of cardiolipin on induction with thiostrepton affected the cell architecture. In Figure 42 A2 shows RJ110 without thiostrepton, which resembled more to the control strain *S. coelicolor* pIJ8600. However, it did affect the P4-width of substrate hyphae (sectioned at every 1μm) and P7- change in degree of angles in direction of substrate hyphae. This may be due to the leakiness of the strong *tipA* promoter. On the contrary, on over expression of *SCO1389* of RJ110 with pCLS113A showed strong abnormal growth and swollen tips, hyphae, swollen spores and cell death (Fig. 44 B2; 43 D 4-6). The erection of aerial hyphae was normal, but infrequently showed irregular sized spores. In addition, bursting of hyphal tips and dividing tips was observed after prolonged *SCO1389* Overexpression (Fig. 45A & B). This conclusion is based on time-lapse observations.

Chapter 8

Localization of SCO1389 EGFP in *S. coelicolor*.

8.1. Introduction.

The localization of cardiolipin-rich domains at branch points, hyphal tips, and aerial hyphae, directed our interest to the subcellular localization of the enzyme involved in cardiolipin synthesis. The committed step in cardiolipin synthesis in *S. coelicolor* is catalyzed by cardiolipin synthase (*clsI*, the gene product of *SCO1389*) (Sandova *et al.*, 2009). For microscopic analysis the strain RJ113 was constructed, with a EGFP fusion at the N terminus, SCO1389-EGFP, the expression of which was controlled from the native promoter.

8.2. Construction of SCO1389 GFP fusion.

SCO1389 was fused with *egfp* from its own promoter. The EGFP was fused to the 'N' terminal end of *SCO1389*. The plasmid pCLS105 (Table 3), was used as the template for PCR reaction. Two consecutive PCR reaction was carried out, initial reaction was set up for the construction of plasmid pCLS107, which was constructed by amplifying *SCO1389* from plasmid pCLS105 using *Pfu* DNA polymerase and primers CL100 and CL102 (Table 11), digesting the product with *BamHI* and *XbaI*, and cloning the 1005 bp fragment in the *BamHI and NheI* site of pEGFPN1 (Table 3).The plasmid pCLS107 was verified by restriction and digestion (Fig. 47). PCR reaction conditions that was followed for amplifying the *SCO1389* gene was; denaturation at 94°C for 2 min, then 10 cycles with denaturation at 94°C for 45 s, annealing at 42.4°C for 45 s, and extension at 72°C for 1 min 30 s, were followed by 15 cycles with the annealing temperature increased to 44.6°C. A last elongation step was done at 72°C for 5 min. The PCR product was analyzed by gel electrophoresis and purified using a PCR Purification kit.

The expected sizes were 1005 bp. In pCLS107, the hexamer 'TGAACT' (containing 'TGA' stop codon) was replaced with 'TGGATCC' (containing *BamHI* site) which then fused to the EGFP of pEGFPN1, resulting in SCO1389-EGFP fusion. The resulting plasmid pCLS107 acts as the precursor vector for next set of cloning reaction.

Subsequent cloning reaction was carried out digesting pMS82 with *VspI* and *EcoRV* and ligating to the 1.5 Kb VspI/PvuII fragment (carrying *SCO1389-egfp*) from pCLS107 and selecting the resulting plasmid pCLS108B for hygromycin resistance. By conjugation from *E. coli* strain ET12567 containing the driver plasmid pUZ8002 (Kieser *et al*., 2000), pCLS108B was transferred into M145 strain where it integrated into the ΦBT1 attachment site. The resulting strain, RJ113 (Table 1), contain the copy of *SCO1389-egfp* from native promoter. The exconjugants were screened for hyg^r and was propagated on a medium containing hygromycin (50 µg/ml).

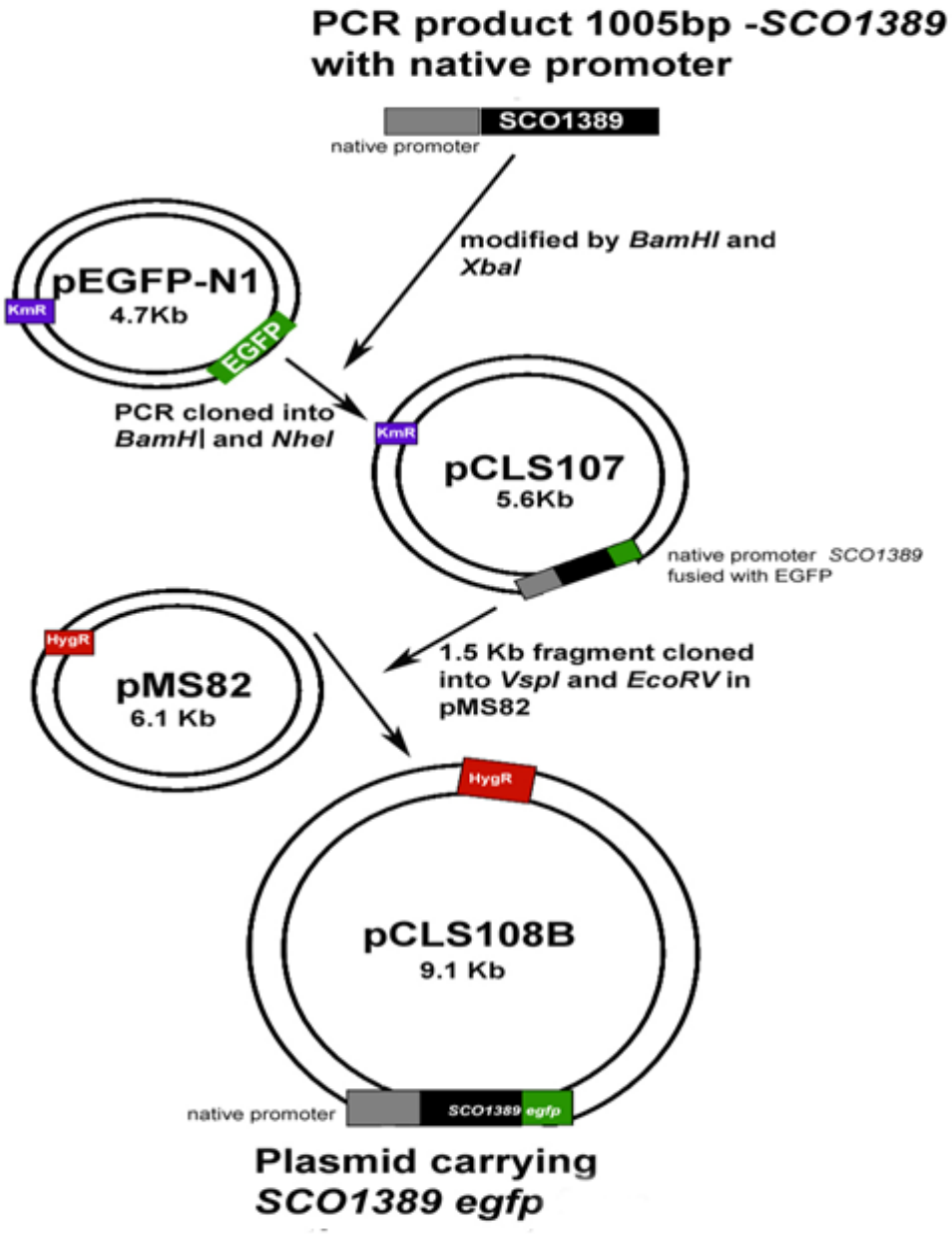

Figure 47: Cloning steps involved in construction of *SCO1389 egfp* fusion vector pCLS108B.

pCLS105 was used as the template for PCR reaction, the product carries SCO1389 from native promoter with stop codon removed. pEGFN1 the source for EGFP-N terminal fusion vector generated pCLS107 which was further, sub-cloned onto pMS82 an integrating vector (attPΦBT1, hyg^r) in the *S.coelicolor* chromosome.

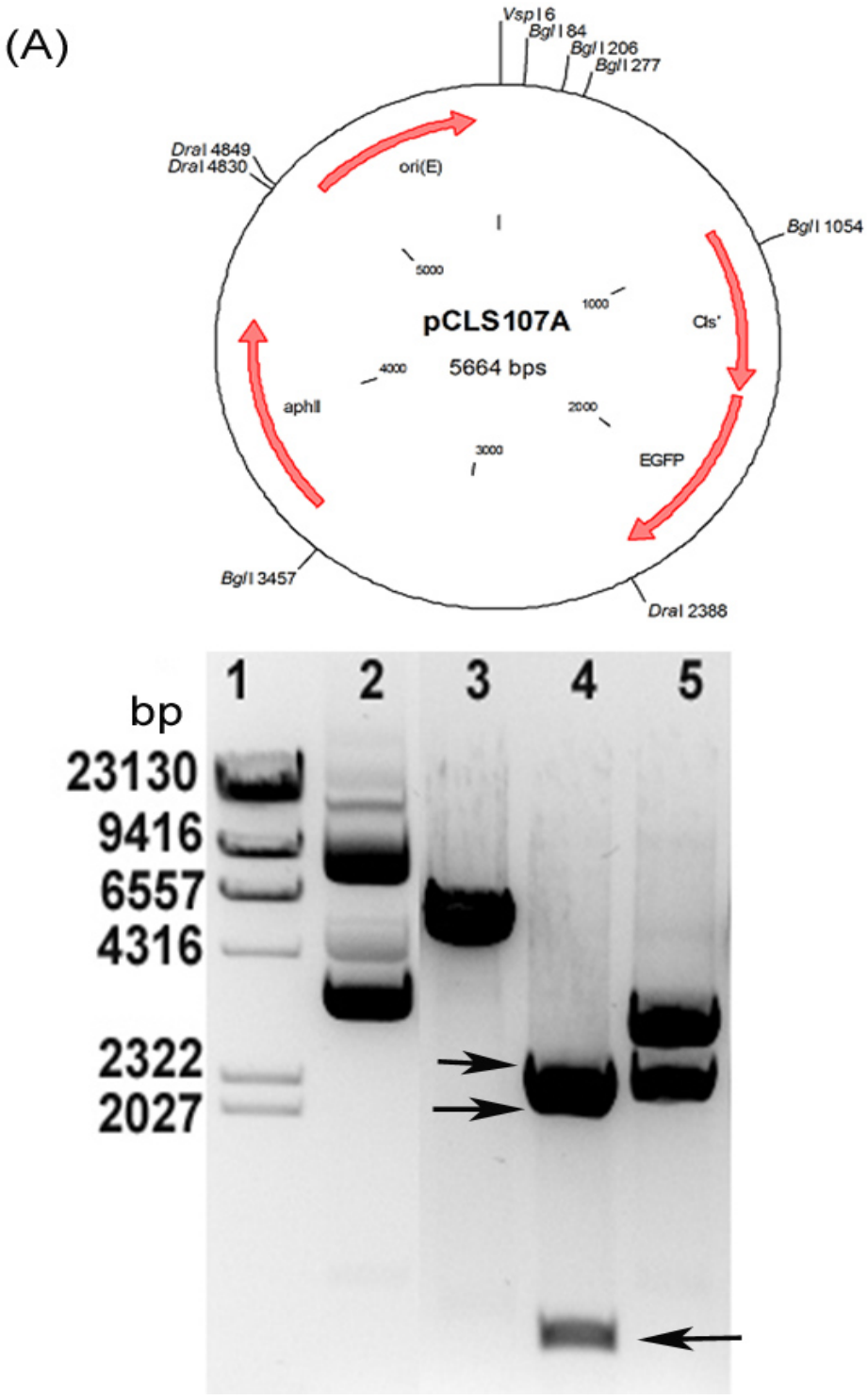

Figure 48: Confirmation of pCLS107 .

(A) pCLS107 plasmid map was constructed by ligating 4.2 Kb *EcoRI* fragment into pALTERI **,** the clone carries functional copy of *SCO1389* with native promoter. (B) Confirmation of the plasmid pCLS102 by restriction analysis. Lane 1-λ *HindIII* marker; lanes 2 - Uncut plasmid DNA, lane 3 – *VspI* ; lanes 4 – *BglI*; lane 5- *DraI*. The black arrow shows in lane 4 confirms the presence of the inserts.

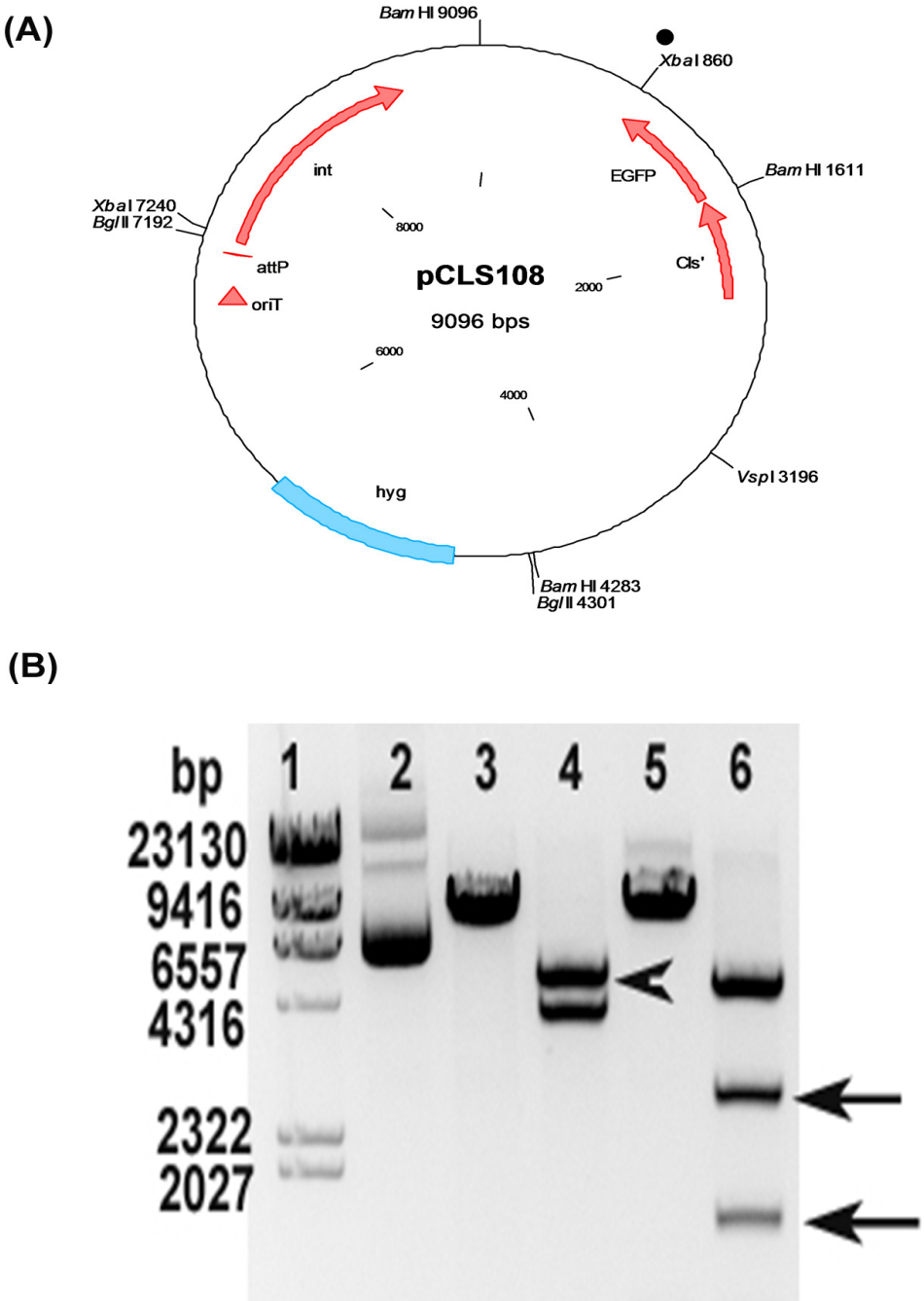

Figure 49: Confirmation of pCLS108B .

(A) pCLS108B plasmid map was constructed by ligating 1.5 Kb *VspI and EcoRV* fragment into pMS82 **,** the clone carries functional copy of *SCO1389* fused with *egfp* from native promoter. (B) Confirmation of the plasmid pCLS108B by restriction analysis. Lane 1-λ *HindIII* marker; lanes 2 - Uncut plasmid DNA, lane 3 – *VspI* ; lanes 4 – *VspI/XbaI*; lane 5- *XbaI;* lane 6-*BamHI* .The black arrow shows in lane 4 and 6 confirms the presence of the insert.Black circle shows that *XbaI* is blocked by methylation.

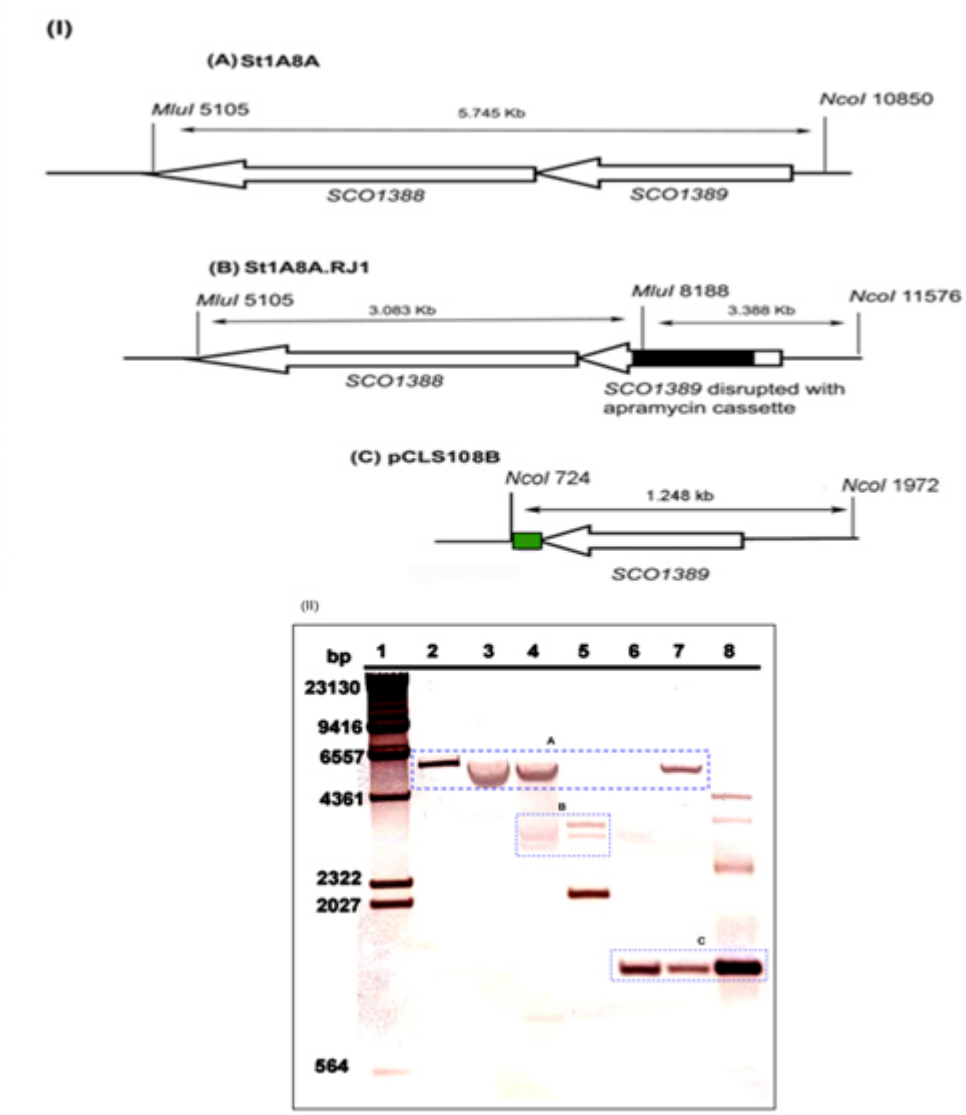

Figure 50: Southern blot confirmation of pCLS108B

(I) Schematic sketch of the cosmid and plasmid maps with restriction sites that supports the grid boxes in the Southern blot. **(II)** Lane 1-λHindIII marker-wt DNA, lane 2- StA8A cosmid ,lane 3-gDNA M145,lane 4-gDNA RJ111 ,lane 5- StA8A.RJ1 cosmid, lane 6-gDNA RJ113,lane 7-gDNA RJ107,lane 8-pCLS108 plasmid DNA. Samples were treated with *MluI*, *HindIII* and *NcoI*. Blue Box (A) highlights the fragment size 5.745 bp (*SCO1389)* in lanes 2, 3, 4 and 7; lane 5-disrupted cosmid StA8A.RJ1 and lane 6 -conditional double cross over mutant (RJ114); Box (B) highlights the fragment size 3.388 bp and 3.083 bp in lanes 4 (single crossover RJ111) and 5 represents the disrupted cosmid (StA8A.RJ1); Box (C) highlights the fragment size 1.248 bp in lanes 6 (RJ114) , 7(RJ113-M145 carrying the extra copy of *SCO1389* gene) and 8 (pCLS105 vector carrying *SCO1389*gene). 1.59 Kb fragment of pCLS105 is the gene probe.The other bands in the blot correspond to λ DNA probe.

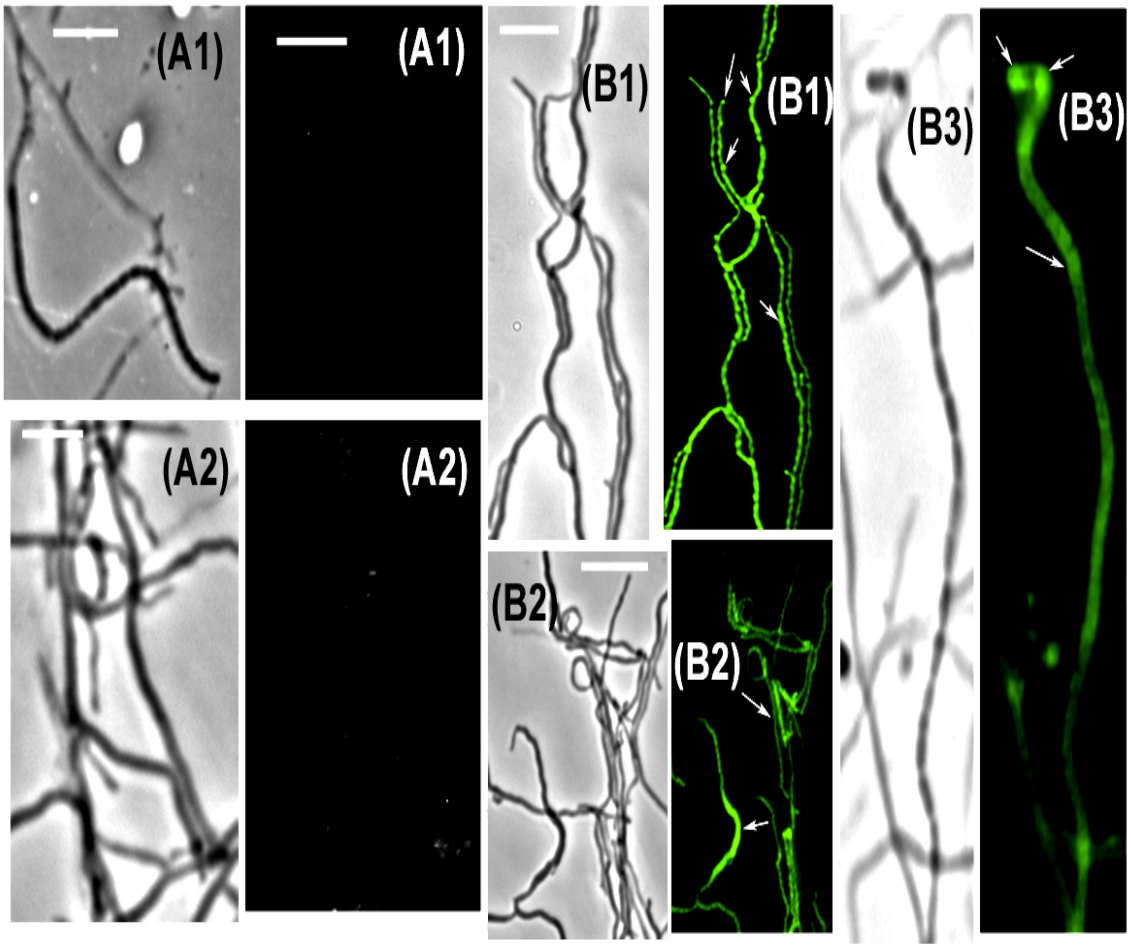

Figure 51: Subcellular localization of SCO1389EGFP.

The strains were M145 (A1 and A2), RJ113 carrying an *SCO1389-egfp* fusion integrated at *attB*ΦBT1 (B1, B2 and B3). A1, A2, B1, B2 and B3 in white lettering show the fluorescence images with pseudocoloring green to clearly visualize the EGFP signals. In B1 the white arrows highlight the strong fluorescence at hyphal tip and in substrate hyphae. In B3 white arrows indicate examples of faint fluorescent foci at aerial hyphae. Phase-contrast images are shown to the left of each fluoresecent images, and all marked in black lettering. Size bar, 10 mm.

8.3. Cardiolipin localizes to different parts of the hyphae, but not cardiolipin synthase.

Plasmid pCLS108B had the entire *SCO1389* fused in frame to *egfp*, and were integrated ΦBT1 *attB* site within the chromosome. Plasmid pCLS108B was identical to the native *SCO1389*, such that upon integration it disrupted the chromosomal copy of *SCO1389*, leaving only the *SCO1389 egfp* fusion active. The chromosomal disruption of *SCO1389* was confirmed through Southernblots (Fig. 50) and restriction analysis (Fig. 49). A background of faint fluorescence was often seen in vegetative hyphae of M145 carrying no EGFP fusion and exposure conditions were adjusted so that this was barely visible. Strikingly, RJ113 showed distinctive regions of strong fluorescence mostly in the substrate hyphae and in few young aerial hyphae. Faint signals in the form of spots of fluorescence were occasionally observed in RJ113 at matured aerial hyphae and spore chains, but such signals were weak and inconsistent in comparison to the strong fluorescence at substrate hyphae. This suggested that *Streptomyces SCO1389* may transiently associate with aerial hyphae erection and spore maturation. In summary, *SCO1389* was predominantly located in substrate hyphae (Fig 51).

Chapter 9

General Discussion & future work.

9.1. Summary of discussion.

CL is a membrane lipid present in all organisms except archaea. The precursor of CL is phosphatidylglycerol which is universally synthesized from CDP-DAG and glycerolphosphate with phosphatidylglycerolphosphate as intermediates. However, *S. coelicolor* employs a eukaryotic metabolism to form CL, CDP-DAG as the donor for the phosphatidyl group which is transferred to a molecule of PG to form CL. In most of the bacteria, a phosphatidyl group is transferred from one PG to another PG to form CL; it is generally thought that Cls in prokaryotes belong to the PLD superfamily, whereas in eukaryotes they come under CDP-alcohol phosphatidyltransferase superfamily. *S. coelicolor* contains a gene belonging to the PLD superfamily, *SCO7081*. A recent study shows that, two *cls* homologs from *E. coli* have been identified, YmdC and YbhO (Guo *et al*., 2000). From BLAST search in *S. coelicolor* genome, one gene was showing a strong hit for YmdC and YbhO was identified, as *SCO7081*, which is annotated as putative phospholipase D (PLD), which might be the alternative pathway for synthesis of CL. However, this is just a speculation, unless a complete biochemical characterization of this gene is studied, we cannot draw a conclusion on the existence of alternative pathway for CL in *S. coelicolor*. In contrast, eight genes encoding for putative CDP-alcohol phosphatidyltransferases were identified in the genome of *S. coelicolor*. The function of four of these eight genes has been assigned a role in phospholipid metabolism in *S. coelicolor* (Sandoval *et al.,* 2009), phosphatidylinositol synthase (*SCO1527*), type II phosphatidylserine synthase (*SCO6467*), phosphatidylglycerolphosphate synthase (*SCO5753*), and CL synthase (*SCO1389*). Interestingly, the gene *SCO1389* is present in most actinobacteria, implying a broad occurrence of a eukaryote-like Cls in this family of organisms. Lipids until recently have been considered an inert hydrophobic environment for the action of membrane proteins. Recent, evidence shows that amphitropic protein MinD from Min system undergoes dynamic oligomerization with membrane phospholipids (section 1.7.6). This shows the involvement of lipids interacting with proteins during dynamic cellular processes.

The primary objective of the work described in this thesis was to determine the functions of gene encoded by *SCO1389* from *S. coelicolor*. To deduce the function of the gene *SCO1389*, a strategy for chromosomal deletion of the gene was investigated. Deletion within the chromosome was achieved, by providing a second copy of *SCO1389* within the chromosome of *S. coelicolor*. Genetic evidence shows that *SCO1389* may be essential for the growth and development. However, a precise function of this gene was speculated to be having a major role in phospholipid biosynthesis. Analysis from TLC (James Roxburgh, unpublished data) shows that CL was not detectable in the *SCO1389* disruptants. However, the mutants are severely affected on their growth and sporulation. On rich media, MS it was observed that the cells did not grow, indicating that *SCO1389* is an essential gene. However, on minimal media, the mutants of *SCO1389* grew weakly and were very slow growing; implying *SCO1389* may be sharing some regulatory role apart from the structural nature of producing CL in membranes. As discussed previously (Sandoval *et al.,* 2009), *SCO1389* is the only gene found that is related to CL synthesis.

SCO1389 is the first bacterial CL synthase protein of eukaryotic origin that has been identified in a prokaryotic mycelial organism. *SCO1389* is particularly interesting as it is an essential protein with a new and unknown function that is shown here to have a profound impact on tip and aerial growth. Partial depletion of *SCO1389* interfered with polar growth and lead to abnormal hyphal shapes. The distorted hyphae, with very less branching and no erection of aerial hyphae were striking feature of Δ *SCO1389* mutants. This phenotype to our knowledge has not been previously discussed in *Streptomyces*. Depletion of *SCO1389* appeared to cause a deficiency in growth and development of the cells. However, there was enough genetic evidence that *SCO1389* is essential for growth and development; it was not clear why cells cannot grow in the absence of this gene. Increase and decrease CL content of the cells are considerably affected giving rise to abnormal growth or no growth.

Following, statistical analysis it showed altered CL content within cells affected the mycelial architecture. Decreased CL content affected the, branch angles; branch/μm; width of substrate hyphae (sectioned at every 1μm); change of direction in substrate hyphae (measured in μm); change in degree of angles in direction of substrate hyphae; width of aerial hyphae. However, average number of branchs/tip, width of branch points and tip width was not affected. On the contrary, on complementation of RJ118b it restored aerial hyphae erection and normal sporulation. However, due to the strong induction of *tcp830* few parameters was affected like branch angles; branch/μm; width of substrate hyphae (sectioned at every 1μm) ; change of direction in substrate hyphae (measured in μm) and change in degree of angles in direction of substrate hyphae . This may be due to increased CL content by the inducer, atc. In parallel, RJ117 showed no significant difference in statistical analysis in the presence of atc.

Overexpression of *SCO1389* was brought about by addition of thiostrepton that affected cell shape, sporulation and produced swollen hyphae, dividing tips (similar to fungi), hyper branching and cell death. Increase CL accumulation within substrate hyphae, was revealed by staining with fluorescently labelled 10-nonyl acridine orange. Through time-lapse microscopy in addition to swollen and dividing tips, for the first time spontaneous lysis of hyphal tips was seen. The erection of aerial hyphae was normal, but showed irregular sized spores.

From statistical analysis the following parameters was severely affected, branch angles; branch/μm; width of branch points; width of substrate hyphae (sectioned at every 1μm); width of the tips; change of direction in substrate hyphae (measured in μm); change in degree of angles in direction of substrate hyphae; spore size distribution and width of aerial hyphae. In parallel, RJ108 in the presence and absence of inducer thiostrepton showed no significant difference.

Using the fluorescent CL specific probe 10-nonyl acridine orange (NAO) has shown a great difference in the staining pattern between the CL deficient cells (RJ118b) and M145 wild type cells. From the staining pattern, it was very clear that CL localizes at the tips, branch points and selective anucleated domains within hyphae. However, to localize SCO1389, translational fusion with EGFP was constructed to monitor the expression of CL synthase during the growth. A background of faint fluorescence was often seen in vegetative hyphae of M145 carrying no EGFP fusion and exposure conditions were adjusted so that this was barely visible. RJ113 showed distinctive regions of strong fluorescence mostly in the substrate hyphae and in few young aerial hyphae. Faint signals in the form of spots of fluorescence were occasionally observed in RJ113 at matured aerial hyphae and spore chains, but such signals were weak and inconsistent in comparison to the strong fluorescence at substrate hyphae. This suggested that *Streptomyces SCO1389* may transiently associate with aerial hyphae erection and spore maturation. In summary, *SCO1389* was predominantly located in substrate hyphae. Using fluorescent reporter studies, it is clearly evident that CL localizes in the cell and not Cls.

In the presence of inducer, anhydrotetracycline it rescued the mutant RJ118b and produced a spot similar to the control CL spot with same rentention factor on TLC analysis (James Roxburgh, unpublished data). Highest level of CL was produced in RJ110 induced by thiostrepton and there was an increase in CL spot appeared at the same position as CL reference standard.

Time-lapse microscopy of *S. coelicolor* presents many challenges through its oxygen dependence, focal depth, mycelial heterogeneity, and agar-dependent sporulation. Compared to other streptomycetes, *S. coelicolor* is more adaptable to imaging system and capable of producing movies, which is essential for understanding the cell biology of this model organism. However, we could track down most of the growth and development in *S. coelicolor*, we were still unable to image the erection of aerial hyphae and we expect this problem to remain constant due to repressive effects of the agar plug on the formation of aerial hyphae and the stimulatory effect on substrate hyphae following the transfer of cover-slip-grown cultures to imaging chambers. We have also shown the application of fluorescent probes like FM4 64, Syto 42, and NAO in live cell staining of *S. coelicolor*. FM4 64 staining revealed the distinct lipid domains within *S. coelicolor*, which persuaded us to move on to use more specific marker, stain NAO to localize anionic phospholipid CL within mycelium. Although the VJ101 mutant showed a normal distribution of CL, this may be due to the fact that *ftsksc* in *S. coelicolor* has been shown not essential for the growth but contribute genetic instability due to irregular nucleoids arrangement (Wang, *et al*.,2007). Since, no major results were further obtained in this study we decided to focus on the phospholipid metabolisms in *S. coelicolor*. The ability of lipids to promote formation of membrane sub domains with unique protein and lipid composition provides a mechanism to compartmentalize and regulate biological processes.

9.2. Future work.

The anionic phospholipid CL has now attracted the curiosity of researchers from diverse fields, including membrane biogenesis, lipid protein interaction, lipidomics and apoptosis. The recent advances in CL study in bacterial model *E. coli*, has opened a new gateway in addressing the fundamental role of CL in cell growth and protein translocations. Much of the work presented in this thesis identifies areas of future work. These are discussed in this section.

9.2.1. Sizing and volume distribution of the spores.

Using a coulter counter Multisizer 3 (Beckman Coulter, High Wycombe, U.K) the spore volume and size of *S. coelicolor* can be was measured. Spore sizes, given as sphere diameters, were calculated using the MS-Multisizer 3 software (Buhr, T.L *et al*., 2008). This reference counter provides number, volume and surface area distribution information in the overall size range of 0.4 μm to 1200 μm. Based on digital pulse processing technology (DPP) makes the Multisizer 3 the instrument of choice for sizing and counting.

Harvesting RJ110 and *S. coelicolor* pIJ8600 in the presence of thiostrepton, the spores volume and size can be measured using Multisizer 3. This will show the effect of CL on spore size distribution in *S. coelicolor*.

9.2.2 Transcriptional studies.

S1 nucleases mapping experiments need to be carried out to confirm the transcriptional start point of the *SCO1389* gene. These experiments should investigate the RNA produced before CL synthase production at different stages of life cycle. This will guide to more detail information about the biosynthetic pathway of phospholipids, mainly of *SCO1389* during the growth and development in *S.coelicolor*.

9.2.3 Protein studies.

Over expressing and purification of *SCO1389* would allow protein/DNA interaction complexes studies. With the pure form of *SCO1389*, *in vitro* biochemical assays can be carried out. Using site-directed mutagenesis, truncated version of the *SCO1389* gene products can be expressed and analysed. Since, this is a novel eukaryotic like protein found in bacteria; protein crystallization studies would elucidate the detail structural comparison between the other CLS from higher organisms.

9.2.4 Lipidomics studies.

From the earlier evidence and information based on putative of functions of phospholipids showed that they collectively or individually participate in and influence cellular processes. The genetic approach has limitation of being indirect and pleiotropic effect in the cellular processes. However, with biochemical experiments a significant progress can be achieved to define at the molecular requirements of phospholipids in several processes. Using electron spray mass spectrophotometeric, TLC the lipids profile can be formulated for *S.coelicolor*.

9.2.5 RT-PCR.

Present studies have showed that *SCO1389* was essential for growth and development of *Streptomyces coelicolor*. However, to understand the expression profiles of *SCO1389* and other related phospholipid metabolism genes during cell cycle, RT-PCR can be used to measure and monitor the expression in basal and vegetative mycelium during growth.

Chapter 10

References

Adamsi Lowell, S., And Norman N. Durham. (1979) Simple agar block slide culture suitable for varying the environment of bacteria during time-Lapse cinephotomicrography. *Applied Enviro Microbiol* : 740-741.

Addinall, S. G., Cao, C., & Lutkenhaus, J. (1997) Temperature shift experiments with an ftsZ84(Ts) strain reveal rapid dynamics of FtsZ localization and indicate that the Z ring is required throughout septation and cannot reoccupy division sites once constriction has initiated. *J Bacteriol* 179(13): 4277-84.

Agnieszka Kois, Magdalena Swiatek, Dagmara Jakimowicz, and Jolanta Zakrzewska-Czerwinska1. (2009) SMC Protein-Dependent Chromosome Condensation during Aerial Hyphal Development in *Streptomyces. J Bacteriol* 191: 310–319.

Ainsa, J.A., Parry, H.D., and Chater, K.F. (1999) A response regulator like protein that functions at an intermediate stage of sporulation in *streptomyces coelicolor* A(3)2. *Mol.Microbiol* 34: 607-619.

Ainsa, J.A., Ryding, N.J., Hartley, N., Findlay, K.C., Bruton, C.J., & Chater, K.F. (2000) WhiA, a protein of unknown function conserved among gram-positive bacteria, is essential for sporulation in *Streptomyces coelicolor* A3(2). *J Bacteriol* 182: 5470–5478.

Alam, M.S., S.K. Garg, and P. Agrawal. (2007) Molecular function of WhiB4/Rv3681c of *Mycobacterium tuberculosis* H37Rv: a [4Fe-4S] cluster co-ordinating protein disulphide reductase. *Mol. Microbiol* 63: 1414–1431.

Ali Nasima., Paul R. Herron, Meirwyn C. Evans, and Paul J. Dyson. (2002) Osmotic regulation of the *Streptomyces lividans* thiostrepton-inducible promoter, *ptipA Microbiology* 148: 381–390.

Allan Eunice J., and J. I. Prosser. (1983) Mycelial Growth and Branching of *Streptomyces coelicolor* A3(2) on Solid Medium. *J Gen Microbio* 129: 2029-2036.

Altschul Stephen F., Thomas L. Madden, Alejandro A. Schäffer1, Jinghui Zhang, Zheng Zhang, Webb Miller, and David J. Lipman. (1997) Gapped BLAST and PSI-BLAST: a new generation of protein database search programs *Nucleic Acids Research ,* 25:17 3389–3402.

Anderson, A.S., Wellington, E.M.H. (2001) The taxonomy of *Streptomyces* and related genera. *Inter.J. Sys.Evol.Microbiol* 51: 797-814.

Ausmees Nora,1 Helene Wahlstedt,1 Sonchita Bagchi,1 Marie A. Elliot,2 Mark J. Buttner3 and Klas Flärdh. (2007) SmeA, a small membrane protein with multiple functions in *Streptomyces* sporulation including targeting of a SpoIIIE/FtsK-like protein to cell division septa. *Mol. Microbiol.* 65: 1458–1473.

Ausmees, N., Wahlstedt, H., Bagchi, S., Elliot, M.A., Buttner, M.J., Flärdh K. (2007) SmeA, A small membrane protein with multiple functions in *Streptomyces* sporulation including targeting of a SpoIIIE/FtsK-like protein to cell division septa. *Mol Microbiol* 65(6): 1458-73.

Aussel, L., Barre, F.X., Aroyo, M., Stasiak, A., Stasiak, A.Z., and Sherratt, D. (2002) FtsK Is a DNA Motor protein that activates chromosome dimer resolution by switching the catalytic state of the XerC and XerD recombinases. *Cell* 108: 195–205.

Barak I., Katarína Muchova, Anthony J. Wilkinson, Peter J. O'Toole and Nada Pavlendova. (2008) Lipid spirals in *Bacillus subtilis* and their role in cell division. *Mol Microbiol* 68(5), 1315–1327.

Barak, I., and Wilkinson, A.J. (2007) Division site recognition in *Escherichia coli* and *Bacillus subtilis*. *FEMS Microbiol Rev* 31: 311–326.

Bath, J., Wu, L. J., Errington, J., & Wang, J. C. (2000) Role of *Bacillus subtilis* SpoIIIE in DNA transport across the mother cell-prespore division septum. *Science* 290(5493): 995-7.

Baumgart, T., Das, S., Webb, W.W., Jenkins, J.T. (2005) Membrane elasticity in giant vesicles with fluid phase coexistence. *Biophys J* 89: 1067–1080.

Baumgart, T., Hess, S.T., Webb, W.W. (2003) Imaging coexisting fluid domains in biomembrane models coupling curvature and line tension. *Nature* 425: 821–824.

Begg, K.J., Dewar, S.J., and Donachie, W.D. (1995) A New *Escherichia coli* Cell Division Gene, *ftsK*. *J Bacteriol* 177: 6211–6222.

Bentley, S.D., Chater, K.F., Tarraga, C., A.M., Challis, G.L., Thompson, N.R., James, K.D., Harris, D.E., Quail, M.A., Kiesser, H., Harper, D., *et al.* (2002) Complete genome sequence of the model actinomycete *Streptomyces coelicolor* A3 (2). *Nature* 417: 141-147.

Berardo Christina Di, David S. Capstick, Maureen J. Bibb, Kim C. Findlay, Mark J. Buttner, and Marie A. Elliot,1. (2008) Function and Redundancy of the Chaplin Cell Surface Proteins in Aerial Hypha Formation, Rodlet Assembly, and Viability in *Streptomyces coelicolor*. *J Bacteriol*, p: 5879–5889.

Bergelson, L.D., S.G. Batrakov, and T.V. Pilipenko. (1970) A new glycolipid from *Streptomyces. Chem.Phycs.Lipids* 4:181-190.

Bernal, P., J. Munoz-Rojas, A. Hurtado, J. L. Ramos, and A. Segura. (2007) A *Pseudomonas putida* cardiolipin synthesis mutant exhibits increased sensitivity to drugs related to transport functionality. *Environ. Microbiol* 9: 1135–1145.

Beth A. Rowan, Delene J. Oldenburg, and Arnold J. Bendich. (2007) A high-throughput method for detection of DNA in chloroplasts using flow cytometry. *Plant Methods* 35: 1746- 4811.

Bibb Maureen, J., Virginie Molle, and Mark J. Buttner. (2000) σBldN, an extracytoplasmic function RNA polymerase sigma factor required for aerial mycelium formation in *Streptomyces coelicolor* A3(2). *J. Bacteriol*, p. 4606–4616.

Bibb Mervyn, J., George H. Jones, Richard Joseph, Mark J. Buttner and Judy M. Ward. (1987) The agarase gene *(dagA)* of *Streptomyces coelicolor* A3 (2): affinity purification and characterization of the cloned gene product *J Gen Microbiol* 1 133: 2089-2096.

Bierman,M., Logan,R., O'Brien,K., Seno,E.T., Rao,R.N., and Schoner, B.E. (1992) Plasmid cloning vectors for the conjugal transfer of DNA from *Escherichia coli* to Streptomyces spp. *Gene*, 116: 43–49.

Bignell, D.R.D., Lau, L.H., Colvin, K.R., & Leskiw, B.K. (2003) The putative anti-anti-sigma factor BldG is post-translationally modified by phosphorylation in *Streptomyces coelicolor*. *FEMS Microbiol Lett* 225: 93–99.

Bignell, D.R.D., Warawa, J.L., Strap, J.L., Chater, K.F., & Leskiw, B.K. (2000) Study of the bldG locus suggests that an anti-anti-sigma factor and an anti-sigma factor may be involved in *Streptomyces coelicolor* antibiotic production and sporulation. *Microbiology* 146: 2161–2173.

Bigot, S., Saleh, O.A., Lesterlin, C., Pages, C., Karoui, M.E., Dennis, C., Grigoriev, M., Allemand, J.F., Barre, F.X., and Cornet, F. (2005) KOPS: DNA motifs that control *E.coli* chromosome segregation by orienting the FtsK Translocase. *EMBO J* 24:3770-3780.

Binenbaum, Z., Parola, A.H., Zaritsky, A., and Fishov, I. (1999) Transcription- and translation-dependent changes in membrane dynamics in bacteria: testing the transertion model for domain formation. *Mol Microbiol* 32: 1173–1182.

Bruce Hudsont William, B. Upholt, Joseph Devinny, and Jerome Vinograd. (1969) The use of an ethidium analogue in the dye-buoyant density procedure for the isolation of closed circular DNA: the variation of the superhelix density of mitochondrial DNA. Proc Natl Acad Sci; 62(3): 813–820.

Buddelmeijer N., Beckwith, J. (2002). Assembly of cell division proteins at the *E. coli* cell center. *Current opinion in Microbiology* 5(6): 553-7.

Burn, P. (1988) Amphitropic proteins: a new class of membrane proteins. *Trends Biochem Sci* 13: 79-83.

Burne, R.A., Z.T. Wen, Y.Y. Chen, and J.E. Penders. (1999) Regulation of expression of the fructan hydrolase gene of *Streptococcus mutans* GS-5 by induction and carbon catabolite repression. *J Bacteriol* 181: 2863–2871.

Buhr, T.L, McPherson D.C. and Gutting B.W, (2008) Analysis of broth-cultured Bacillus atrophaeus and Bacillus cereus spores. *Journal of App Microbio*: 1364-5072.

Calderon Mario Sandoval, Otto Geiger, Ziqiang Guan, Francisco Barona-Gomez, and Christian Sohlenkamp. (2009) A Eukaryote-like cardiolipin synthase is present in *Streptomyces coelicolor* and in most actinobacteria. *J Biol Chem* 284:26, pp: 17383–17390.

Campo, N., Tjalsma, H., Buist, G., Stepniak, D., Meijer, M., Veenhuis, M., *et al.* (2004) Subcellular sites for bacterial protein export. *Mol Microbiol* 53: 1583–1599.

Capiaux, H., Lesterliin, C., Perals, K., Louarn, J.M., and Cornet, F. (2002) A dual role for the FtsK protein in *Escherichia coli* chromosome segregation. *EMBO* 3: 532–536.

Capstick David, S., Joanne M. Willey, Mark J. Buttner3., and Marie A. Elliot. (2007) SapB and the chaplins: connections between morphogenetic proteins in *Streptomyces coelicolor. Mol Microbiol* (2007) 64(3): 602–613.

Carballido-Lopez, R. (2006) The bacterial actin-like cytoskeleton. *Microbiol Mol Biol Rev* 70: 888–909.

Castuma, C.E., Crooke, E., and Kornberg, A. (1993) Fluid membranes with acidic domains activate DnaA, the initiator protein of replication in *Escherichia coli. J Biol Chem* 268: 24665–24668.

Catakli, S., Andrieux, A., Decaris, B., & Dary, A. (2005) Sigma factor WhiG and its regulation constitute a target of a mutational phenomenon occurring during aerial mycelium growth in *Streptomyces ambofaciens* ATCC23877. *Res Microbiol* 156: 328–40.

Cerdeno-Tarraga, A.M., A. Efstratiou, L.G. Dover, M.T.G. Holden, M. Pallen, S.D. Bentley, G.S. Besra, C. Churcher, K.D. James, A. De Zoysa, T. Chillingworth, A. Cronin, L. Dowd, T. Feltwell, N. Hamlin, S. Holroyd, K. Jagels, S. Moule, M.A. Quail, E. Rabbinowitsch, K.M. Rutherford, N.R. Thomson, L. Unwin, S. Whitehead, B.G. Barrell, and J. Parkhill. (2003) The complete genome sequence and analysis of *Corneybacterium diptheriae* NCTC13129. *Nucleic Acids Res* 31: 6516-6523.

Challis, G.L. and Hopwood, D.A. (2003) Synergy and contingency as driving forces for the evolution of multiple secondary metabolite production by *Streptomyces species*. *PNAS* 100: 14555-14561.

Champness Wendy, C. (1988) New loci required for *Streptomyces coelicolor* morphological and physiological differentiationt. *J Bacteriol*, p: 1168-1174.

Chater Keith, F., & Govind Chandra. (2006) The evolution of development in *Streptomyces* analysed by genome comparisons. *FEMS Microbiol Rev.* 30: 651–672.

Chater, K.F. (1993) Genetics of differentiation in *Streptomyces. Annu.Rev.Microbiol* 47: 685-713.

Chater, K.F. (1972) A morphological and genetic mapping study of white colony mutants of *Streptomyces coelicolor*. *J Gen Microbiol* 72: 9-28.

Chater, K.F. (1998) Taking a genetic scalpel to the *Streptomyces* colony. *Microbiol* 144: 1465-1478.

Chater, K.F. (2001) Regulation of sporulation in *Streptomyces coelicolor* A3(2):a check point multiplex?. *Curr Opin Microbiol* 4: 667-673.

Chater, K.F., and Horinouchi, S. (2003) Signalling early developmental events in two highly diverged *Streptomyces species*. *Mol Microbiol* 48:9-15.

Chater, K.F., Bruton, C,J., Plaskitt, K.A., Buttner, M.J., Mendez, C., & Helmann, J.D. (1989) The developmental fate of *S. coelicolor* hyphae depends upon a gene-product homologous with the motility sigma-factor of *B.subtilis. Cell* 59: 133–143.

Chen, C.W., C.H. Huang, H.H. Lee, H.H. Tsai, and R.Kirby. (2002) Once the circle has been broken: dynamics and evolution of *Streptomyces* chromosomes. *Trends Genet* 18: 522–529.

Chiu, M.L., Folcher, M., Griffin, P., Holt, T., Klatt, T., & Thompson, C.J. (1996). Characterization of the covalent binding of thiostrepton to a thiostrepton-induced protein from *Streptomyces lividans*. *Biochemistry* 35: 2332-2341.

Chiu, M.L., Folcher, M., Katoh, T., Puglia, A.M., Vohradsky, J., Yun, B.S., Seto, H. & Thompson, C.J. (1999) Broad spectrum thiopeptide recognition speci®city of the *Streptomyces lividans* TipAL protein and its role in regulating gene expression. *J Biol Chem* 274: 20578-20586.

Cho, Y.H., Lee, E.J., Ahn, B.E., and Roe, J.H. (2001) SigB, an RNA polymerase sigma factor required for osmoprotection and proper differentiation of *Streptomyces coelicolor*. *Mol Microbiol* 42: 205–214.

Choi, K.H., R.J. Heath, and C.O. Rock. (2000) β-Ketoacyl-acyl carrier protein synthase III (FabH) is a determining factor in branchd-chain fatty acid biosynthesis. *J Bacteriol* 182: 365–370.

Claessen Dennis, Ietse Stokroos, Heine J. Deelstra, Nynke A. Penninga, Christiane Bormann, Jose A. Salas, Lubbert Dijkhuizen, and Han A.B. Wosten. (2004) The

formation of the rodlet layer of *Streptomycetes* is the result of the interplay between rodlins and chaplins. *Mol Microbiol,*53 (2): 433–443.

Claessen, D., Rink, R., de Jong, W., Siebring, J., de Vreugd, P., Boersma, F.G.H., Dijkhuizen, L., and Wosten, H.A.B. (2003) A novel class of secreted hydrophobic proteins involved in aerial hyphae formation in *Streptomyces coelicolor* by forming amyloiod-like fibrils. *Gene Dev.* 17: 1714-1726.

Claessen, Dennis Han A.B. Wosten, Geertje Van Keulen, Onno G. Faber, Alexandra M.C.R. Alves, Wim G. Meijer, and Lubbert Dijkhuizen. (2002) Two novel homologous proteins of *Streptomyces coelicolor* and *Streptomyces lividans* are involved in the formation of the rodlet layer and mediate attachment to a hydrophobic surface. *Mol. Microbiol* 44(6): 1483–1492.

Clark, D., Lightner, V., Edgar, R., Modrich, P., Cronan, J.E. Jr, Bell, R.M. (1980). Regulation of phospholipid biosynthesis in *Escherichia coli*. Cloning of the structural gene for the biosynthetic *sn*-glycerol-3-phosphate dehydrogenase. *J Biol Chem* 255: 714–17.

Cole, S.T., R. Brosch, J. Parkhill, T. Garnier, C. Churcher, D. Harris, S.V. Gordon, K. Eiglmeier, S. Gas, C.E. Barry III, F. Tekaia, K. Badcock, D. Basham, D. Brown, T. Chillingworth, R. Connor, R. Davies, K. Devlin, T. Feltwell, S. Gentles, N. Hamlin, S. Holroyd, T. Hornsby, K. Jagels, A. Krogh, J. McLean, S. Moule, L. Murphy, K. Oliver, J. Osborne, M.A. Quail, M.A. Rajandream, J. Rogers, S. Rutter, K. Seeger, J. Skelton, R. Squares, S. Squares, J.E. Sulston, K. Taylor, S. Whitehead & B.G. Barrell. (1998) Deciphering the biology of *Mycobacterium tuberculosis* from the complete genome sequence. *Nature* 393:537-544.

Coleman, J. (1990). Characterization of *Escherichia coli* cells deficient in 1-acyl*sn*-glycerol-3-phosphate acyltransferase activity. *J Biol Chem* 265: 17215–21.

Coleman, J. (1992) Characterization of the *Escherichia coli* gene for 1-acyl-sn-glycerol-3-phosphate acyltransferase (*plsC*). *Mol Gen Genet* 232: 295–303.

Corre, J., and Louarn, J.M. (2002) Evidence from terminal recombination gradients that FtsK uses replichore polarity to control chromosome terminus positioning at division in *Escherichia coli*. *J Bacteriol* 184:3801–3807.

Crick, F. (1966) Codon–anticodon pairing: the Wobble hypothesis. *J Mol Biol* 19:548–555.

Crooke, E., Hwang, D.S., Skarstad, K., Thony, B., and Kornberg, A. (1991) *Escherichia coli* minichromosome replication: regulation of initiation at oriC. *Res Microbiol* 142: 127–130.

Crooke S. Elliott, Celina E. Castumag, and Arthur Kornberg. (1992) The Chromosome Origin of *Escherichia coli* Stabilizes DnaA Protein during Rejuvenation by Phospholipid. *J Biochem* Vol. 267, 24, pp: 16779-16782.

Dalton, K.A., Thibessard, A., Hunter, J.I., and Kelemen, G.H. (2007) A novel compartment, the 'subapical stem' of the aerial hyphae, is the location of a sigN-dependent, developmentally distinct transcription in *Streptomyces coelicolor*. *Mol Microbiol* 64: 719–737.

Daniel, R.A., and Errington, J. (2003) Control of cell morphogenesis in bacteria: two distinct ways to make a rodshaped cell. *Cell* 113: 767–776.

Datta Pratik, Arunava Dasgupta, Anil Kumar Singh, Partha Mukherjee, Manikuntala Kundu, and Joyoti Basu. (2006) Interaction between FtsW and penicillin-binding protein 3 (PBP3) directs PBP3 to mid-cell, controls cell septation and mediates the formation of a trimeric complex involving FtsZ, FtsW and PBP3 in Mycobacteria. *Mol. Microbiol* 62(6): 1655–1673.

Datta Pratik, Arunava Dasgupta, Sanjib Bhakta, and Joyoti Basu. (2002) Interaction between FtsZ and FtsW of *Mycobacterium tuberculosis*. *J Biol Chem*. 77:28, p: 24983–24987.

Datsenko, K.A. & Wanner, B.L. (2000) One-step inactivation of chromosomal genes in *Escherichia coli* K-12 using PCR products. *PNAS* 97(12): 6640.

David E. Anderson, Frederico J. Gueiros-Filho, and Harold P. Erickson. (2004) Assembly dynamics of FtsZ rings in *Bacillus subtilis* and *Escherichia coli* and effects of FtsZ-regulating proteins. *J Bacteriol* 186: 5775-5781.

David S. Capstick, et al., (2007) SapB and the chaplins: connections between morphogenetic proteins in *Streptomyces coelicolor*. *Mol Microbiol* 64(3): 602–613.

Davis, J. (1990) What are antibiotics? Archaic functions for modern activities. *Mol Microbio* 4: 1227-1232.

Davis, N.K., & Chater, K.F. (1990) Spore colour in *Streptomyces coelicolor* A3(2) involves the developmentally regulated synthesis of a compound biosynthetically related to polyketide antibiotics. *Mol Microbiol* 4: 1679–1691.

De Boer, P., Crossley, R. & Rothfield, L. (1992) The essential bacterial cell-division protein FtsZ is a GTPase. *Nature* 359(6392): 254-6.

De Kruijff, B., Killian, J.A., Rietveld, A.G., and Kusters, R. (1997) Phospholipid structure and *Escherichia coli* membranes. *Curr Topics Membr* 44: 477–515.

Del Sol, R., Pitman, A., Herron, P., & Dyson, P. (2003) The product of a developmental gene, crgA, that coordinates reproductive growth in Streptomyces, belongs to a novel family of actinomycete-specific proteins. *J Bacteriol* 185: 6678–6685.

Den Hengst Chris D., and Mark J. Buttner. (2008) Redox control in Actinobacteria. *Biochimica et Biophysica Acta (BBA) - General Subjects* 1780, 11: 1201-1216.

Den Blaauwen, T., Buddelmeijer, N., Aarsman, M.E., Hameete, C.M., & Nanninga, N. (1999) Timing of FtsZ assembly in *Escherichia coli*. *J Bacteriol* 181(17): 5167-75.

Derouaux, A., Halici, S., Nothaft, H., Neutelings, T., Moutzourelis, G., Dusart, J., et al. (2004a) Deletion of a cyclic AMP receptor protein homologue diminishes germination and affects morphological development of *Streptomyces coelicolor*. *J Bacteriol* 186: 1893–1897.

Derouaux, A., Dehareng, D., Lecocq, E., Halici, S., Nothaft, H., Giannotta, F., Moutzourelis, G., Dusart, J., Devreese, B., Titgemeyer, F. (2004b) Crp of Streptomyces coelicolor is the third transcription factor of the large CRP-FNR superfamily able to bind cAMP. *Biochem Biophys Res Commun* 325: 983-990.

Dillon, D.A., Wu WI, Riedel, B., Wissing, J.B., Dowhan, W., Carman, G.M. (1996) The *Escherichia coli* pgpB gene encodes for a diacylglycerol pyrophosphate phosphatise activity. *J Biol Chem* 271: 30548–53.

Donachie, W.D. (2001). Co-ordinate regulation of the *Escherichia coli* cell cycle or the cloud of unknowing. *Mol Microbiol* 40(4): 779-85.

Dowhan, W. (1997a) CDP-diacylglycerol synthase of microorganisms. *Biochem. Biophys. Acta* 1348: 157–65.

Dowhan, W. (1997b) Molecular basis for membrane phospholipid diversity: Why are there so many lipids? *Annu Rev Biochemistry*, 66: 199-232.

Dowhan, W. (1997c) Molecular basis for membrane phospholipid diversity: why are there so many lipids? *Annu Rev Biochem* 66: 199–232.

Dowhan, W., Mileykovskaya, E., Bogdanov, M. (2004) Diversity and versatility of lipid-protein interactions revealed by molecular genetic approaches. *Biochem Biophys Acta* 1666: 19-39.

Draper, G.C., and Gober, J.W. (2002) Bacterial chromosome segregation. *Annu Rev Microbiol* 56: 567-597.

Draper, G.C., McLennan, N., Begg, K., Masters, M., and Donachie, W.D. (1998) Only the N-terminal domain of FtsK functions in cell division. *J Bacteriol* 180: 4621–4627.

Eaton, D., and J.C. Ensign. (1980). *Streptomyces viridochromogenes* spore germination initiated by calcium ions. *J Bacteriol* 143: 377–382.

Edwards, D.H., and Errington, J. (1997) The *Bacillus subtilis* DivIVA protein targets to the division septum and controls the site specificity of cell division. *Mol Microbiol* 24: 905– 915.

Elliot, M., F. Damji, R. Passantino, K. Chater, and B. Leskiw. (1998) The *bldD* gene of *Streptomyces coelicolor* A3(2): a regulatory protein involved in morphogenesis and antibiotic production. *J Bacteriol* 180: 1549–1555.

Elliot, M.A., & Leskiw, B.K. (1999) The BldD protein from *Streptomyces coelicolor* is a DNA-binding protein. *J Bacteriol* 181: 832–6835.

Elliot, M.A., Bibb, M.J., Buttner, M.J., & Leskiw, B.K. (2001) BldD is a direct regulator of key developmental genes in *Streptomyces coelicolor* A3(2). *Mol Microbiol* 40: 257–269.

Emoto, K., and Umeda, M. (2001) Membrane lipid control of cytokinesis. *Cell Struct Funct* 26: 659–665.

Eoin Fahy, et al., (2005) A comphrensive classification of system for lipids. *J Lipid Res:* 46.

Erickson, H., Taylor, D., Taylor, K., Bramhill, D. (1996) Bacterial cell division protein FtsZ assembles into protofilament sheets and minirings, structural homologs of tubulin polymers. Proc *Natl Acad Sci USA* 93: 519-523.

Errington, J., Daniel, R.A., and Scheffer, D.J. (2003) Cytokinesis in Bacteria. *Microbiol. Mol Biol Rev* 67: 52-65.

Fernandez-Moreno, M.A., J.L. Caballero, D.A. Hopwood, and F. Malpartida. (1991) The act cluster contains regulatory and antibiotic export genes, direct targets for translational control by the *bldA* tRNA gene of *Streptomyces*. *Cell* 66: 769–780.

Fischer, R. (1999) Nuclear movement in filamentous fungi. *FEMS Microbiol Rev* 23: 39–68.

Fishov, I., and C.L. Woldringh. (1999) Visualization of membrane domains in *Escherichia coli. Mol Microbiol* 32: 1166–1172.

Firshein, W. (1989) Role of the DNA/membrane complex in prokaryotic DNA replication. *Annu Rev Microbiol* 43: 89-120.

Flardh, K. (2003a) Essential role of DivIVA in polar growth and morphogenesis in *Streptomyces coelicolor* A(3)2. *Mol Microbiol* 49:1523-1536.

Flardh, K. (2003b) Growth polarity and cell division in *Streptomyces*. *Curr Opin Microbiol* 6: 564–571.

Flardh, K., Findlay, K.C., & Chater, K.F. (1999) Association of early sporulation genes with suggested developmental decision points in *Streptomyces coelicolor* A3(2). *Microbiol* 145: 2229–2243.

Flardh, K., Leibovitz, E., Buttner, M.J., & Chater, K.F. (2000) Generation of a non-sporulating strain of *Streptomyces coelicolor* A3(2) by the manipulation of a developmentally controlled ftsZ promoter. *Mol Microbiol* 38: 737–749.

Flärdh, K., and Buttner, M.J. (2009) *Streptomyces* morphogenetics: dissecting differentiation in a filamentous bacterium. *Nat. Rev. Microbiol.* **7:** 36-49.

Florova, G., Kazanina, G., Reynolds, K.A. (2002) Enzymes involved in fatty acid and polyketide biosynthesis in Streptomyces glaucescens: role of FabH and FabD and their acyl carrier protein specificity. *Biochem* 41(33):10462-71.

Frederic L. Hoch. (1991) Cardiolipins and biomembrane function. *Biochimica et Biophysica Acta 1113*: 71-133.

Fuglsang, A. (2005) Intragenic position of UUA codons in streptomycetes. *Microbiol* 151: 3150–3152.

Funnell, B.E. (1993) Participation of the bacterial membrane in DNA replication and chromosome partition. *Trends Cell Biol* 3: 20–24.

Galina Florova, Galina Kazanina, and Kevin A. Reynolds. (2002) Enzymes involved in fatty acid and polyketide biosynthesis in *Streptomyces glaucescens*: Role of FabH and FabD and their acyl carrier protein specificity. *Biochem* 41: 10462-10471.

Garcia Bartnicki, and Eleanor Lippman. (1972) The bursting tendency of hyphal tips of fungi: presumptive evidence for a delicate balance between wall synthesis and wall lysis in apical growth. *J Gen Microbio* 73: 487-500.

Gossen, M., Freundlieb, S., Bender, G., Muller, G., Hillen, W, and Bujard, H. (1995) Transcriptional activation by tetracyclines in mammalian cells. *Science* 268: 1766–1769.

Granozzi, C., et al., (1990) A breakdown in macromolecular synthesis preceeding differentiation in *Streptomyces coelicolor*. *J Gen Microbiol* 136: 713-716.

Granozzri, C., R. Billetta, R. Passantino, M. Sollazzo and A.M. Pugli. (1990) A breakdown in macromolecular synthesis preceding differentiation in *Streptomyces coelicolor*. A3(2) *J Gen Microbiol* 136: 713-716.

Grantcharova Nina, Wimal Ubhayasekera, Sherry L. Mowbray, Joseph R. McCormick and Klas Flärdh. (2003) A missense mutation in ftsZ differentially affects vegetative and developmentally controlled cell division in *Streptomyces coelicolor* A3(2). *Mol Microbiol* 47 (3): 645–656.

Grantcharova Nina., Lustig, U., and Flardh, K. (2005) Dynamics of Fts Z assembly during Sporulation in *Streptomyces coelicolor* A3 (2). *J Bacteriol* 187: 3227-3237.

Graumann, P.L. (2004) Cytoskeletal Elements in bacteria. *Curr Opin Microbiol* 7: 565-571.

Gray, D.I., Gooday, G.W., and Prosser, J.I. (1990) Apical hyphal extension in *Streptomyces coelicolor* A3 (2). *J Gen Microbiol* 136: 1077–1084.

Gray, D.I., Gooday ,G.W., and J.I. Prosser. (1990) Apical hyphal extension in *Streptomyces coelicolor* A3(2) *J Gen Microbiol* 136: 1077-1084.

Green, P.R., Merrill, A.H., Jr., and Bell, R.M. (1981) Membrane phospholipid synthesis in *Escherichia coli*: purification, reconstitution, and characterization of sn-glycerol-3-phosphate acyltransferase. *J Biol Chem* 256: 11151–11159.

Gregory, L. Challis, and David A. Hopwood. (2003) Synergy and contingency as driving forces for the evolution of multiple secondary metabolite production by Streptomyces species, *PNAS* 100 (2).

Gullbrand, B., & Nordström, K. (2000) FtsZ ring formation without subsequent cell division after replication runout in *Escherichia coli*. *Mol Microbiol* 36(6): 1349-59.

Guo, D., Tropp, B.E. (1998) Cloning of the *Bacillus firmus* OF4 cls gene and characterization of its gene product. *Biochim Biophys Acta* 1389(1): 34-42.

Guo, D., Tropp, B.E. (2000) A second *Escherichia coli* protein with CL synthase activity. *Biochim. Biophys. Acta* 1483: 263–74.

Gust, B., Kiesser, T., and Chater, K.F. (2002) PCR targeting sytem in *Streptomyces coelicolor. Norwich: the John Innes Foundation.*

Han, L., A. Khetan, W.S. Hu, and D.H. Sherman. (1999). Time-lapsed confocal microscopy reveals temporal and spatial expression of the lysine ε-aminotransferase gene in *Streptomyces clavuligerus*. *Mol Microbiol* 34: 878–886.

Han, L., S. Lobo, and K.A. Reynolds. (1998) Characterization of β-ketoacylacyl carrier protein synthase III from *Streptomyces glaucescens* and its role in initiation of fatty acid biosynthesis. *J Bacteriol* 180: 4481–4486.

Hardisson Carlos, Manuel-Benjamin Manzanal, Josl-Antonio Salas, And Juan-Evaristo Suarez. (1978) Fine Structure, Physiology and Biochemistry of Arthrospore Germination in *Streptomyces antibioticus*. *J Gen Microbiol* 105:203-214.

Harry, E.J. (2001) Bacterial cell division: regulating Z-ring formation. *Mol Microbiol* 40: 795–803.

Haruo Ikeda, Jun Ishikawa, Akiharu Hanamoto, Mayumi Shinose, Hisashi Kikuchi, Tadayoshi Shiba, Yoshiyuki Sakaki, Masahira Hattori & Satoshi omura. (2003) Complete genome sequence and comparative analysis of the industrial microorganism *Streptomyces avermitilis*. *Nature Biotechnology* 21: 526 – 531.

Heath, R.J., Goldfine, H., Rock, C.O. (1997) A gene (plsD) from *Clostridium butyricum* that functionally substitutes for the sn-glycerol-3-phosphate acyltransferase gene (plsB) of *Escherichia coli*. *J Bacteriol* 179: 7257–63.

Heath, R.J., Jackowski, S., and Rock, C.O. (1994) Guanosine tetraphosphate inhibition of fatty acid and phospholipid synthesis in *Escherichia coli* is relieved by overexpression of glycerol-3-phosphate acyltransferase (plsB). *J Biol Chem* 269: 26584–26590.

Heath, R.J., and Rock, C.O. (1996) Roles of the FabA and FabZ β-hydroxyacyl-acyl carrier protein dehydratases in *Escherichia coli* fatty acid biosynthesis. *J Biol Chem* 271: 26538-26542.

Heath, R.J., Rock, C.O. (1998) A conserved histidine is essential for glycerolipid acyltransferase catalysis. *J Bacteriol* 180: 1425–30.

Hempel, A.M., Wang, S., Letek, M., Gil, J.A., and Flardh, K. (2008) Assemblies of DivIVA mark sites for hyphal branching and can establish new zones of cell wall growth in *Streptomyces coelicolor*. *J Bacteriol* 90: 7579–7583.

Hempel Antje Marie, Sheng-bing Wang, Michal Letek, Jose A. Gil, and Klas Flard. (2008) Assemblies of DivIVA Mark Sites for Hyphal Branching and Can Establish New Zones of Cell Wall Growth in *Streptomyces coelicolor*. *J Bacterio*, p: 7579–7583.

Hersch, G., Burton, R., Bolon, D., Baker, T., Sauer, R. (2005) Asymmetric interactions of ATP with the AAA+ClpX6 unfoldase: allosteric control of a protein machine. *Cell* 121: 1017-1027.

Hesketh, A.R., Chandra, G., Shaw, A.D., Rowland, J.J., Kell, D.B., Bibb, M.J., & Chater, K.F. (2002) Primary and secondary metabolism, and post-translational protein modifications, as portrayed by proteomic analysis of *Streptomyces coelicolor. Mol Microbiol* 46: 917–932.

Hett Erik, C., and Eric J. Rubin. (2008) Bacterial Growth and Cell Division: a Mycobacterial Perspective. *Microbiol and MolBiol Rev*, p: 126–156.

Hiraoka Shuichi, Hiroshi Matsuzaki, Isao Shibuya. (1993) Active increase in cardiolipin synthesis in the stationary growth phase and its physiological significance in *Escherichia coli. FEBS:* 336. pp: 221-224.

Hodgson, D.A. (2000) Primary metabolism and its control ion streptomycetes: a most unusual group of bacteria. *Adv Microbial Physiol* 42: 47-238.

Holmes, D.J., Caso, J.L. & Thompson, C.J. (1993) Autogenous transcriptional activation of a thiostrepton-induced gene in *Streptomyces lividans*. *EMBO J* 12: 3183-3191.

Holt, T.G., Chang, C., Laurent-Winter, C., Murakami, T., Garrels, J.I., Davies, J.E., and Thompson, C.J. (1992) Global changes in gene expression related to antibiotic biosynthesis in *Streptomyces hygroscopicus*. *Mol Microbiol* 6: 969– 980.

Hopwood, D.A. (1960) Phase contrast observation on *Streptomyces coelicolor*. *J Gen Microbio* 22: 1-295-302.

Hopwood, D.A., H. Wildermuth and Helen M. Palmer. (1970) Mutants of *Streptomyces coelicolor* defective in sporulation. *J Gen Microcbiol* 61: 397-408.

Hsiao Nai-Hua, Johannes So ding, Dirk Linke, Corinna Lange,Christian Hertweck,3 Wolfgang Wohlleben, and Eriko Takano. (2007) ScbA from *Streptomyces coelicolor* A3(2) has homology to fatty acid synthases and is able to synthesize c-butyrolactones. *Microbiol* 153: 1394–1404.

Hu, Z.L., and Lutkenhaus, J. (1999) Topological regulation of cell division in *Escherichia coli* involves rapid pole to pole oscillation of the division inhibitor MinC under control of MinD and MinE. *Mol Microbiol* 34: 82–90.

Huang, K.C., R. Mukhopadhyay, and N.S. Wingreen. (2006) A curvature-mediated mechanism for localization of lipids to bacterial poles. *PLOS Comput Biol*: 2-11 - 1357-1364

Hunt, A.C., Servin-Gonzalez, L., Kelemen, G.H., & Buttner, M.J. (2005) The bldC developmental locus of *Streptomyces coelicolor* encodes a member of a family of small DNA-binding proteins related to the DNA-binding domains of the MerR family. *J Bacteriol* 187: 716–728.

Imrich Barak, Katarína Muchova, Anthony J. Wilkinson, Peter J. O'Toole, and Nada Pavlendova. (2008) Lipid spirals in *Bacillus subtilis* and their role in cell division. *Mol Microbiol.*; 68(5): 1315–1327.

Iyer, L.M., K.S. Makarova, E.V. Koonin, and L. Aravind. (2004) Comparative genomics of the FtsK-HerA superfamily of pumping ATPases: implications for the origins of chromosome segregation, cell division and viral capsid packaging. *Nucleic Acids Res*. 32: 5260–5279.

Jackson Mary, Dean C. Crick, and Patrick J. Brennan. (2000) Phosphatidylinositol is an essential phospholipid of mycobacteria. *J Biol Chem* 275, 39, p: 30092–30099.

Jacobs, M.A., Alwood, A., Thaipisuttikul, I., Spencer, D., Haugen, E., Ernst, S.,Will, O., Kaul, R., Raymond, C., Levy, R. (2003) Comprehensive transposon mutant library of *Pseudomonas aeruginosa*. *Proc Natl Acad Sci* 100: 14339–14344.

Jakimowicz, D., Mouz, S., Zakrzewska-Czerwinska, Z., & Chater, K.F. (2006) Regulation of developmentally controlled parAB promoter leading to formation of ParB complexes in *Streptomyces coelicolor* aerial hyphae. *J Bacteriol* 188: 1710–1720.

Jakimowicz, D., Zydek, P., Kois, A., Zakrzewska- Czerwinska, J. & Chater, K.F. (2007) Alignment of multiple chromosomes along helical ParA scaffolding in sporulating Streptomyces hyphae. *Mol Microbiol* 65: 625–641.

Jakimowicz, P., Cheesman, M.R., Bishai, W.R., Chater, K.F., Thomson, A.J., & Buttner, M.J. (2005) Evidence that the Streptomyces developmental protein WhiD, a member of the WhiB family, binds a 4Fe-4S cluster. *J Biol Chem* 280: 8309–8315.

Ji, Y., B. Zhang, S.F. Van Horn, P. Warren, G. Woodnutt, M.K. Burnham, and M. Rosenberg. (2001) Identification of critical *staphylococcal* genes using conditional phenotypes generated by antisense RNA. *Science* 293:2266– 2269.

Jiang, H., & Kendrick, K.E. (2000) Characterization of ssfR and ssgA, two genes involved in sporulation of *Streptomyces griseus*. *J Bacteriol* 182: 5521–5529.

Ji, Y., Zhang, B., Van, S. F., Horn, Warren, P., Woodnutt, G., Burnham, M. K. & Rosenberg, M. (2001). Identification of critical staphylococcal genes using conditional phenotypes generated by antisense RNA. *Science* 293(5538): 2266-9.

Jianghong Rao, and George M. Whitesides. (1997) Tight Binding of a Dimeric Derivative of Vancomycin with Dimeric L-Lys-D-Ala-D-Ala. *J Am Chem Soc.,* 119: 10286-10290.

John E. Cronan, J.R., and Robert M. Bell. (1974) Mutants of *Escherichia coli* Defective in Membrane Phospholipid Synthesis: Mapping of the Structural Gene for L-Glycerol 3-Phosphate Dehydrogenase. *J Bacteriol,* p 598-605.

Johnson, J.E. and Cornell, R.B. (1999) Amphitropic proteins: regulation by reversible membrane interactions. *Mol Membr Biol* 16: 217-235.

Jong Wouter de, Angel Manteca, Jesus Sanchez, Giselda Bucca, Colin P. Smith, Lubbert Dijkhuizen, Dennis Claessen, and Han A.B. Wösten. (2009) NepA is a structural cell wall protein involved in maintenance of spore dormancy in *Streptomyces coelicolor*. *Mol Microbiol* 71(6): 1591–1603.

Joseph C. Aub, Barbara H. Sanford, and Marilyn N. Cote. (1965) Studies on reactivity of tumor and Normal cells to a wheat germ agglutinin. *Physiology* 54: 396-399.

Joseph C. Aub, Carol Tieslau, and Ann Lankester. (1963) Reactions of normal and tumor cell surfaces to enzymes, in wheat-germ lipase and associated mucopolysaccharides. *Physiology* 50:613-619.

Jyothikumar Vinod, Emma J. Tilley, Rashmi Wali, and Paul R. Herron. (2008) Time-Lapse Microscopy of *Streptomyces coelicolor* Growth and Sporulation. *Appl. Environ. Microbiol*., p: 6774–6781.

Kaneda, T. (1991) Iso- and anteiso-fatty acids in bacteria: biosynthesis, function, and taxonomic significance. *Microbiol Rev* 55: 288–302.

Kates, M. (1960). Chromatographic and radioisotopic investigations of the lipid components of runner bean leaves. *Biochim Biophys Acta* 41: 315-28.

Kates, M., Syz, J.Y., Gosser, D., Haines, T.H. (1993) pH-dissociation characteristics of cardiolipin and its 2'-deoxy analogue. *Lipids* 28(10): 877-82.

Katharine A. Michie, Jan Lowe. (2006) Dynamic filaments of the bacterial cytoskeleton. *Annu Rev Biochem* 75: 467-492.

Kato, J., Suzuki, A., Yamazaki, H., Ohnishi, Y., & Horinouchi, S. (2002) Control by A-factor of a metalloendopeptidase gene involved in aerial mycelium formation in *Streptomyces griseus*. *J Bacteriol* 184: 6016–6025.

Kato, J.Y., Ohnishi, Y., & Horinouchi, S. (2005) Autorepression of AdpA of the AraC/XylS family, a key transcriptional activator in the A-factor regulatory cascade in *Streptomyces griseus*. *J Mol Biol* 350: 12–26.

Kawai, F., Hara, H., Takamatsu, H., Watabe, K., and Matsumoto, K. (2006) Cardiolipin enrichment in spore membranes and its involvement in germination of *Bacillus subtilis* Marburg. *Genes Genet Syst* 81: 69–76.

Kawai, F., Shoda, M., Harashima, R., Sadaie, Y., Hara, H., and Matsumoto, K. (2004) Cardiolipin domains in *Bacillus subtilis* Marburg membranes. *J Bacteriol* 186: 1475– 1483.

Kawamoto, S., Watanabe H., Hesketh A., Ensign, J.C., & Ochi, K. (1997) Expression analysis of the ssgA gene product, associated with sporulation and cell division in *Streptomyces griseus*. *Microbiol* 143: 1077–1086.

Keijser, B., Noens, E., Kraal, B., Koerten, H., & VanWezel, G. (2003) The *Streptomyces coelicolor* ssgB gene is required for early stages of sporulation. *FEMS Microbiol Lett* 225: 59–67.

Keijser, B.J., Van Wezel, G.P., Canters, G.W., Kieser, T., Vijgenboom, E. (2000) The ram-dependence of *Streptomyces lividans* differentiation is bypassed by copper. *J Mol Microbiol Biotechnol* 2(4): 565-574.

Kelemen Gabriella, H., and Mark J. Buttner. (1998) Initiation of aerial mycelium formation in Streptomyces. *Curr. Opin. Microbiol* 1: 656-662.

Kelemen, G.H., G.L. Brown, J. Kormanec, L. Potuckova, K.F. Chater, and M.J. Buttner. (1996). The positions of the sigma-factor genes, whiG and sigF, in the hierarchy controlling the development of spore chains in the aerial hyphae of *Streptomyces coelicolor* A3(2). *Mol Microbiol* 21: 593–603.

Khodakaramian, G., Lissenden, S., Gust, B., Moir, L., Hoskisson, P.A., Chater, K.F., and Smith, M.C.M. (2006) Expression of Cre recombinase during transient phage infection permits efficient marker removal in Streptomyces . *Nucleic Acids Res*. 34,No.3 e20.

Kiesser, T., Bibb, M.J., Buttner, M.J., Chater, K.F., and Hopwood, D.A. (2000) Practical Streptomyces genetics. Norwich: the John Innes Foundation. *J Mol Microbiol Biotechnol* 2(4): 565-74.

Kim, H.J., Calcutt, M.J., Schmidt, F.J. & Chater, K.F. (2000) Partitioning of the linear chromosome during sporulation of *Streptomyces coelicolor* A3(2) involves an oriC-linked parAB locus. *J Bacteriol* 182: 1313–1320.

Kodani Shinya, Michael E. Hudson, Marcus C. Durrant, Mark J. Buttner, Justin R. Nodwell, and Joanne M. Willey. (2004) The SapB morphogen is a antibiotic-like peptide derived from the product of the developmental gene ramS in *Streptomyces coelicolor. PNAS* 101: 31-11448–11453.

Kois, A., Swiatek, M., Jakimowicz, D.& Zakrzewska-Czerwińska, J.(2009) SMC protein-dependent chromosome condensation during aerial hyphal development in *Streptomyces*. *Bacteriology* 191(1): 310-9.

Koppelman, C., Aarsman, M., Postmus, J., Pas, E., Muijsers, A., Scheffers, D., Nanninga, N., Den Blaauwen, T. (2004) R174 of *Escherichia coli* FtsZ is involved in membrane interaction and protofilament bundling, and is essential for cell division. *Mol Microbiol* 51: 645-657.

Koppelman, C.M., T. Den Blaauwen, M.C. Duursma, R.M.A. Heeren, and N. Nanninga. (2001) *Escherichia coli* minicell membranes are enriched in cardiolipin. *J Bacteriol* 183: 6144–6147.

Kormanec, J., Homerova, D., Potuckova, L., Novakova, R., & Rezuchova, B. (1996) Differential expression of two sporulation-specific sigma factors of *Streptomyces aureofaciens* correlates with the developmental stage. *Gene* 181: 19–27.

Kormanec, J., Potuckova, L., & Rezuchova, B. (1994) The *Streptomyces aureofaciens* homologue of the whiG gene encoding a putative sigma factor essential for sporulation. *Gene* 143: 101–103.

Labes, G., Bibb, M. and Wohlleben,W. (1997) Isolation and characterization of a strong promoter element from the Streptomyces ghanaensis phage I19 using the gentamicin resistance gene (aacC1) of Tn1696 as reporter. *Microbiol* 143: 1503–1512.

Lamothe Reyes, R., C. Possoz, O. Danilova, and D.J. Sherratt. (2008) Independent positioning and action of *Escherichia coli* replisomes in live cells. *Cell* 133: 90–102.

Larson, T.J., Ludtke, D.N., and Bell, R.M. (1984) sn-Glycerol-3- phosphate auxotrophy of plsB strains of *Escherichia coli* evidence that a second mutation, plsX, is required. *J Bacteriol* 160: 711–717.

Lawlor, E.J., H.A. Baylis, and K.F. Chater. (1987) Pleiotropic morphological and antibiotic deficiencies result from mutations in a gene encoding a tRNA like product in *Streptomyces coelicolor* A3(2). *Genes Dev* 1: 1305–1310.

Lee, E.J., Cho, Y.H., Kim, H.S., Ahn, B.E., and Roe, J.H. (2004) Regulation of σB by an anti- and anti-anti-sigma factor in *Streptomyces coelicolor* in response to osmotic stress. *J Bacteriol* 186: 8490–8498.

Leskiw, B.K., E.J. Lawlor, J.M. Fernandez-Abalos, and K.F. Chater (1991a) TTA codons in some genes prevent their expression in a class of developmental, antibiotic-negative Streptomyces mutants. *Proc Natl Acad Sci. USA* 88: 2461–2465.

Leskiw, B.K., M.J. Bibb, and K.F. Chater. (1991b) The use of a rare codon specifically during development. *Mol Microbiol* 5:2861–2867.

Letek Michal, Efren Ordonez, Jose Vaquera, William Margolin, Klas Flardh,4 Luis M. Mateos,1 and Jose A. Gil1. (2008) DivIVA is required for polar growth in the MreB-lacking rod-shaped Actinomycete *Corynebacterium glutamicum*. J Bacteriology, p: 3283–3292.

Lechevalier, H.A., Lechevalier, M.P. & Gerber, N.N. (1971). Chemical composition as a criterion in the classification of actinomycetes. *Adv Appl Microbiol* 1(14): 47-742.

Levy, O., Ptacin, J.L., Pease, P.J., Cost, G.J., Gore, J., Sherratt, D., Bustamante, C., Cozzarelli, N.R. (2005) Identification of oligonuleotide sequences that direct the movement of the *Escherichia coli* FtsK translocase. *PNAS* 102: 49-17618-17623.

Lightner, V.A., Larson, T.J., Tailleur, P., Kantor, G.D., Raetz, C.R.H., Bell, R.M., and Modrich, P. (1980). Membrane phospholipid synthesis in *Escherichia coli:* cloning of a structural gene (plsB) of the sn-glycerol-3-phosphate acyltransferase. *J Biol Chem* 255: 9413–9420.

Liu, G., Draper, G.C., Donachie, W.D. (1998) FtsK is a bi-functional protein involved in cell division and chromosome localization in *E. coli. Mol Microbiol* 29: 893-903.

Liu, N.J.L., Duntton, R.J., and Pogliano, K. (2006) Evidence that the SpoIIIE DNA Trnaslocase participates in membrane fusion during cytokinesis and engulfment. *Mol Microbiol* 59: 1097-1113.

Lopez, C.S., A. F. Alice, H. Heras, E.A. Rivas, and C. Sanchez-Rivas. (2006) Role of anionic phospholipids in the adaptation of *Bacillus subtilis* to high salinity. *Microbiol* 152: 605–616.

Lowe, J., and Amos, L.A. (1998) Crystal structure of the bacterial cell division protein FtsZ. *Nature* 391: 203 – 206.

Lu Ying-Jie, Yong-Mei Zhang, Kimberly D. Grimes, Jianjun Qi, Richard E. Lee, and Charles O. Rock. (2006) Acyl-Phosphates initiate membrane phospholipid synthesis in gram-positive pathogens. *Mol Cell*: 23: 765–772.

Luijsterburg, M.S., M.C. Noom, G.J. Wuite, and R. . Dame. (2006) The architectural role of nucleoid-associated proteins in the organization of bacterial chromatin: a molecular perspective. *J. Struct. Biol* 156: 262-272.

Luijsterburg, M.S., M.F. White, R. van Driel, and R.T. Dame. (2008). The major architects of chromatin: architectural proteins in bacteria, archaea and eukaryotes. *Crit Rev Biochem Mol Biol* 43: 393-418.

Lutkenhaus, J. (2002) Dynamic proteins in bacteria. *Curr Opin Microbiol* 5: 548–552.

Ma Hongtao, and Kevin Kendall . (1994) Cloning and analysis of a gene cluster from *Streptomyces coelicolor* that causes accelerated aerial mycelium formation in *Streptomyces lividans*. *J Bacteriol*,p: 3800-3811.

Margolin, W. (2000) Themes and variations in prokaryotic cell division. *FEMS Microbiol Rev* 24: 531-548.

Marston, A.L., Thomaides, H.B., Edwards, D.H., Sharpe, M.E. & Errington, J. (1998) Polar localization of the MinD protein of *Bacillus subtilis* and its role in selection of the mid-cell division site. *Genes Dev* 12(21): 3419-30.

Marie A. Elliot, Troy R. Locke, Claire M. Galibois, Brenda K. Leskiw. (2003) BldD from *Streptomyces coelicolor* is a non-essential global regulator that binds its own promoter as a dimmer. *FEMS Microbiol Letters* 225: 35-40.

Mary C. Pangborn. (1942) Isolation and purification of a serologically active phospholipid from Beef heart. *J Biol Chem* 143: 247-256.

Matsumoto Kouji, Jin Kusaka, Ayako Nishibori, and Hiroshi Hara. (2006) Lipid domains in bacterial membranes. *Mol Microbiol* 61(5): 1110–1117.

Mattila, K.J., Valle, M.S., Nieminen, M.S., Valtonen, V.V., Hietaniemi, K.L. (1993) Dental infections and coronary atherosclerosis. *Atherosclerosis* 103(2): 205-11.

Matthew A. Gregory, Rob Till, and Margaret C.M. Smith. (2003) Integration Site for Streptomyces Phage ΦBt1 and development of site-specific integrating vectors. *J Bacteriol,* P: 5320–5323.

Mazza, P., Noens, E.E., Schirner, K., Grantcharova, N., Mommaas, A.M., Koerten, H.K., Muth, G., Flärdh, K., Wezel, G.P.V., Wohlleben, W. (2006) MreB of *Streptomyces coelicolor* is not essential for vegetative growth but is required for the integrity of aerial hyphae and spores. *Mol Microbiol* 60:4: 838-852.

McAuley Katherine E., Paul K. Fyfe, Justin P. Ridge, Neil W. Isaacs, Richard J. Cogdell, and Michael R. Jones. (1999) Structural details of an interaction between cardiolipin and an integral membrane protein. *PNAS* 96, 26: 14706–14711.

McCormick, J. R. and Losick, R. (1996) Cell division gene ftsQ is required for efficient sporulation but not growth and viability in *Streptomyces coelicolor* A3(2). *J Bacteriol* 178: 5295–5301.

McGarrity J.T., J.B. Armstrong, (1975) The effect of salt on phospholipid fatty acid composition in *Escherichia coli* K-12, *Biochim Biophys Acta* 398: 258–264.

McMurray, W.C., Jarvis, E.C. (1980) Partial purification of diphosphatidylglycerol synthetase from liver mitochondrial membranes. *Can J Biochem* 58(10): 771-6.

McVittie, A. (1974) Ultrastructural studies on sporulation in wild-type and white colony mutants of *Streptomyces coelicolor*. *J Gen Microbiol* 81: 291–302.

Mendez, C., & Chater, K.F. (1987) Cloning of whiG, a gene critical for sporulation of *Streptomyces coelicolor* A3(2). *J Bacteriol* 169: 5715–5720.

Merrick, M.J. (1976) A morphological and genetic mapping study of bald colony. J *Gen Microbiol* 96: 299-315.

Miguelez, E.M., Martín, C., Manzanal, M.B., and Hardison, C. (1992) Growth and morphogenesis in *Streptomyces*. *FEMS Microbiol Lett* 100: 351–360.

Mileykovskaya, E., and Dowhan, W. (2000) Visualization of phospholipid domains in *Escherichia coli* by using the cardiolipin-specific fluorescent dye 10-N-nonyl acridine orange. *J Bacteriol* 182: 1172–1175.

Mileykovskaya, E., and Dowhan, W. (2005) Role of membrane lipids in bacterial division-site selection. *Curr Opin Microbiol* 8: 135–142.

Mileykovskaya, E., and William Dowhan. (2005) Role of lipids in bacterial divison-site selection. *Curr Opin Microbiol* 8: 135-142.

Mileykovskaya, E., Dowhan, W. (2009) Cardiolipin membrane domains in prokaryotes and eukaryotes. *Biochimica at Biophysica Acta* (Article in Press).

Mileykovskaya, E., Dowhan, W., Birke, R.L., Zheng, D., Lutterodt, L., and Haines, T.H. (2001) Cardiolipin binds nonyl acridine orange by aggregating the dye at exposed hydrophobic domains on bilayer surfaces. *FEBS Lett* 507: 187– 190.

Mileykovskaya, E., Dowhan, W., Birke, R.L., Zheng, D., Lutterodt, L., Haines, T.H. (2001) Cardiolipin binds nonyl acridine orange by aggregating the dye at exposed hydrophobic domains on bilayer surfaces. *FEBS Lett* 507(2): 187-90.

Mileykovskaya, E., Fishov, I., Fu, X., Corbin, B., Margolin, W., and Dowhan, W. (2003) Effects of phospholipid composition on MinD–membrane interactions in vitro and in vivo. *J Biol Chem* 278: 22193–22198.

Mileykovskaya, E., Sun, Q., Margolin, W., and Dowhan, W. (1998) Localization and function of early cell division proteins in filamentous *Escherichia coli* cells lacking phosphatidylethanolamine. *J Bacteriol* 180: 4252–4257.

Mistry Bhavesh V,1 Ricardo Del Sol,1 Chris Wright,2 Kim Findlay,3 and Paul Dyson,1. (2008) FtsW Is a dispensable cell division protein required for Z-Ring stabilization during sporulation septation in *Streptomyces coelicolor*. *J Bacteriol,* p: 5555–5566.

Mizushima, T., Ishikawa, Y., Obana, E., Hase, M., Kubota, T., Katayama, T., Kunitake, T., Watanabe, E., Sekimizu, K. (1996) Influence of cluster formation of acidic phospholipids on decrease in the affinity for ATP of DnaA protein. *J Biol Chem* 271: 3633-3638.

Molle Virginie, and Mark J. Buttner. (2000) Different alleles of the response regulator gene bldM arrest *Streptomyces coelicolor* development at distinct stages Mol Microbiol 36(6): 1265-1278.

Molle Virginie, Wendy J. Palframan,1 Kim C. Findlay,2 and Mark J. Buttner,1. (2000) WhiD and WhiB, homologous proteins required for different stages of sporulation in *Streptomyces coelicolor* A3(2) *J Bacteriol*, p: 1286–1295.

Momany, M. (2002) Polarity in filamentous fungi: establishment, maintenance and new axes. *Curr Opin Microbiol* 5: 580–585.

Moore, B.S., & Piel, J. (2000) Engineering biodiversity with type II polyketide synthase genes. *Antonie van Leeuwenhoek* 78: 391–398.

Murakami, T., Holt, T.G. & Thompson, C.J. (1989) Thiostreptoninduced gene expression in *Streptomyces lividans*. *J Bacteriol* 171: 1459-1466.

Nanninga, N. (1998) Morphogenesis of *Escherichia coli*. *Microbiol Mol Biol Rev* 62: 110–129.

Neumann, T., Piepersberg, W., and Distler, J. (1996) Decision phase regulation of streptomycin production in *Streptomyces griseus*. *Microbiol* 142: 1953–63.

Nguyen Kien, T., Joanne M. Willey, Liem D. Nguyen, Lieu T. Nguyen, Patrick H. Viollier, and Charles J. Thompson. (2002) A central regulator of morphological differentiation in the multicellular bacterium *Streptomyces coelicolor. Mol Microbiol* 46(5): 1223–1238.

Nguyen Liem, Nicole Scherr, John Gatfield, Anne Walburger, Jean Pieters, and Charles J. Thompson. (2007) Antigen 84, an effector of pleiomorphism in *Mycobacterium smegmatis. J Bacteriol*, p: 7896–7910.

Nishibori A., J. Kusaka, H. Hara, M. Umeda, K. Matsumoto. (2005) Phosphatidylethanolamine domains and localization of phospholipid synthases in *Bacillus subtilis* membranes. *J Bacteriol* 187: 2163–2174.

Nishida Hiromi, Yasuo Ohnishi, Teruhiko Beppu, and Sueharu Horinouchi. (2007) Evolution of γ-butyrolactone synthases and receptors in *Streptomyces. Environmental Microbiol* 9-8: 1986 – 1994.

Nishijima, S., Asami, Y., Uetake, N., Yamagoe, S., Ohta, A., Shibuya, I. (1988) Disruption of the *Escherichia coli cls* gene responsible for cardiolipin synthesis. *J Bacteriol* 170: 775–80.

Nodwell, J.R., and R. Losick. (1998) Purification of an extracellular signalling molecule involved in production of aerial mycelium by *Streptomyces coelicolor*. *J Bacteriol* 180: 1334–1337.

Nodwell, J.R., M. Yang, D. Kuo, and R. Losick. (1999) Extracellular complementation and the identification of genes involved in aerial mycelium formation in *Streptomyces coelicolor*. *Genetics* 151: 569–584.

Nodwell, J.R., McGovern, K., Losick R. (1996) An oligopeptide permease responsible for the import of an extracellular signal governing aerial mycelium formation in *Streptomyces coelicolor. Mol Microbiol* 22: 881-893.

Noens, E.E., Mersinias, V., Traag, B.A., Smith, C.P., Koerten, H.K, & Van Wezel, G.P. (2005) SsgA-like proteins determine the fate of peptidoglycan during sporulation of *Streptomyces coelicolor*. *Mol Microbiol* 58: 929–944.

Noens, E.E., Mersinias, V., Willemse, J., Traag, B.A., Laing, E., Chater, K.F., *et al.* (2007) Loss of the controlled localisation of growth stage-specific cell wall synthesis pleiotropically affects developmental gene expression in an *ssgA* mutant of *Streptomyces coelicolor*. *Mol Microbiol* 64: 1244–1259.

Nora Ausmees, Helene Wahlstedt, Sonchita Bagchi, Marie A. Elliot, Mark J. Buttner, and Klas Flardh. (2007) SmeA, a small membrane protein with multiple functions in *Streptomyces* sporulation including targeting of a SpoIIIE/FtsK- like protein to cell division septa. *Mol Microbiol* 65(6): 1458–1473.

Norris, V. (1992) Phospholipid domains determine the spatial organization of the *Escherichia coli* cell cycle: the membrane tectonics model. *J Theor Biol* 154: 91–107.

Norris, V. (1995) Hypothesis: chromosome separation in *Escherichia coli* involves autocatalytic gene expression, transertion and membrane-domain formation. *Mol Microbiol* 16: 1051–1057.

O'Connor Tamara, J., Pamela Kanellis, and Justin R. Nodwell. (2002) The *ramC* gene is required for morphogenesis in *Streptomyces coelicolor* and expressed in a cell type-specific manner under the direct control of RamR. *Mol Microbiol* 45(1): 45–57.

O'Connor Tamara, J., and Justin R. Nodwell. (2005) Pivotal Roles for the Receiver Domain in the Mechanism of Action of the Response Regulator RamR of *Streptomyces coelicolor*. *J. Molecular Biology* 351(5): 1030-1047.

Ohnishi, T., Yamazaki, H., Kato, J.Y., Tomono, A., and Horinouchi, S. (2005) AdpA,a central transcriptional regulator in the A-factor regulatory cascade that leads to morphological development and secondary metabolism in *Streptomyces griseus*. *Biosci Biotechnol Biochem* 69: 431-439.

Okadat Masahiro Hiroshi Matsuzaki, Isao Shibuya, and Kouji Matsumoto. (1994) Cloning, sequencing, and expression in *Escherichia coli* of the *Bacillus subtilis* gene for phosphatidylserine synthase. *J Bacteriol*, p: 7456-7461.

Osmiałowska Beata Ruban, Dagmara Jakimowicz, Aleksandra Smulczyk-Krawczyszyn, Keith F. Chater, and Jolanta Zakrzewska-Czerwin´ska1. (2006) Replisome localization in vegetative and aerial hyphae of *Streptomyces coelicolor*. *J Bacteriol*, p: 7311–7316.

Paget, M.S., Chamberlin, L., Atrih, A., Foster, S.J., & Buttner, M.J. (1999) Evidence that the extracytoplasmic sigma factor, sigmaE, is required for normal cell wall structure in *Streptomyces coelicolor* A3(2) *J Bacteriol* 181: 204–211.

Parish, T., and N. G. Stoker. (1997) Development and use of a conditional antisense mutagenesis system in Mycobacteria. *FEMS Microbiol Lett* 154: 151–157.

Park David, and Peter M. Robinson. (1966) Internal pressure of hyphal tips of fungi, and its significance in morphogenesis. *Annals of Botany* 30: 119- 425-437.

Parton S. Fischer, R.M. Parton, P. C. Hickey, J. Dijksterhuis, H.A. Atkinson, & N.D. Read. (2000) Confocal microscopy of FM4-64 as a tool for analysing endocytosis and vesicle trafficking in living fungal hyphae. *J Microscopy* 198: 246-259.

Patrick H. Viollier, Wolfgang Minas, Glenn E. Dale, Marc Folcher, and Charles J. Thompson. (2001) Role of acid metabolism in *Streptomyces coelicolor* morphological differentiation and antibiotic biosynthesis. *J Bacteriol*: 3184–3192.

Pease, P.J., Levy, O., Cost, G.J., Gore, J., Ptacin, J.L., Sherratt, D., Bustamante, C., Cozzarelli, N.R. (2005) Sequence –directed DNA translocation by purifies by Ftsk. *Science* 307: 586-590.

Peters, P.C., Migocki, M.D., Thoni, C., and Harry, E.J. (2007) A new assembly pathway for the cytokinetic Z ring from a dynamic helical structure in vegetatively growing cells of *Bacillus subtilis*. *Mol Microbiol* 64: 487–499.

Petit, J.M., Huet, O., Gallet, P.F., Maftah, A., Ratinaud, M.H., Julien, R. (1994) Direct analysis and significance of cardiolipin transverse distribution in mitochondrial inner membranes. *Eur J Biochem* 220(3): 871-9.

Petit, J.M., Maftah, A., Ratinaud, M.H., Julien, R. (1992) 10N-nonyl acridine orange interacts with cardiolipin and allows the quantification of this phospholipid in isolated mitochondria. *Eur J Biochem* 209(1): 267-73.

Piette, A., Derouaux, A., Gerkens, P., Noens, E.E., Mazzucchelli, G., Vion, S., et al. (2005) From dormant to germinating spores of *Streptomyces coelicolor* A3(2): new perspectives from the crp null mutant. *J Proteome Res* 4: 1699–1708.

Pichoff, S., & Lutkenhaus, J. (2002) Unique and overlapping roles for ZipA and FtsA in septal ring assembly in *Escherichia coli*. *EMBO* 21(4): 685-93

Pirett Jacqueline, M., and Keith, F. Chater. (1985) Phage-mediated cloning of bidA, a region involved in *Streptomyces coelicolor* morphological development, and its analysis by genetic complementation. *J Bacteriol,*p: 965-972.

Pogliano Kit, Joe Pogliano, and Eric Becker. (2003) Chromosome segregation in Eubacteria. *Curr Opin Microbiol* 6: 586–593.

Pope Margaret, K., Brian D. Green, and Janet Westpheling. (1996) The bld mutants of *Streptomyces coelicolor* are defective in the regulation of carbon utilization, morphogenesis and cell–cell signalling. *Mol Microbiol* 19(4): 747–756.

Pope Margaret, k., Brian green, and Janet Westpheling. (1998) The bldB gene encodes a small protein requiredfor morphogenesis, antibiotic production, and catabolite control in *Streptomyces coelicolor*. *J Bacteriology, p*: 1556–1562.

Possoz, C., Ribard, C., Gagnat, J., Pernodet, J.L., Guerineau, M. (2001) The integrative element pSAM2 from Streptomyces: Kinetics and mode of conjugal transfer. *Mol Microbiol* 42: 159–166.

Potuckova, L., G.H. Kelemen, K.C. Findlay, M.A. Lonetto, M.J. Buttner, and J. Kormanec. (1995) A new RNA polymerase sigma factor, σF, is required for the late stages of morphological differentiation in *Streptomyces sp*. *Mol Microbiol* 17: 37–48.

Prosser, J.I., and Tough, A.J. (1991) Growth mechanics and growth kinetics of filamentous microorganism. *Crit Rev Biotechnol* 10: 253-274.

Raskin, D.M., and de Boer, P.A.J. (1999) Rapid pole-to-pole oscillation of a protein required for directing division to the middle of *Escherichia coli*. *Proc Natl Acad Sci USA* 96: 4971–4976.

Raychaudhuri, D. (1999) ZipA is a MAP-Tau homolog and is essential for structural integrity of the cytokinetic FtsZ ring during bacterial cell division. *EMBO J* 18: 2372-2383.

Rebekah M. Dedrick, Hans Wildschutte, and Joseph, R., McCormick. (2009) Genetic interactions of *smc*, *ftsK*, and *parB* genes in *Streptomyces coelicolor* and their developmental genome segregation phenotypes. *J Bacteriol*, p: 320–332.

Redenbach, M., Kieser, H.M., Denapaite, D., Eichner, A., Cullum, J., Kinashi, H. & Hopwood, D.A. (1996). A set of ordered cosmids and a detailed genetic and physical map for the 8 Mb *Streptomyces coelicolor* A3(2) chromosome. *Mol Microbiol* 21(1): 77-96.

Revill W. Peter, Maureen J. Bibb, and David A. Hopwood. (1996) Relationships between fatty acid and polyketide synthases from *Streptomyces coelicolor* A3(2): characterization of the fatty acid synthase acyl carrier protein. *J Bacteriol*, p: 5660–5667.

Revill W. Peter, Maureen J. Bibb, Ann-Karolin Scheu, Helen J. Kieser, and David A. Hopwood. (2001) β-Ketoacyl acyl carrier protein synthase III (FabH) is essential for fatty acid biosynthesis in *Streptomyces coelicolor* A3(2). *J Bacteriol*, p: 3526–3530.

Revill, W. Peter, et *al*., (2001) beta-Ketoacyl acyl carrier protein synthase III (FabH) is essential for fatty acid biosynthesis in *Streptomyces coelicolor* A3(2). *J Bacteriol*: 3526–3530.

Revill, W.P., and P.F. Leadlay. (1991) Cloning, characterization, and high level expression in *Escherichia coli* of the *Saccharopolyspora erythraea* gene encoding an acyl carrier protein potentially involved in fatty acid biosynthesis. *J Bacteriol* 173: 4379–4385.

Revill, W.P., M.J. Bibb, and D.A. Hopwood. (1995) Purification of a malonyltransferase from *Streptomyces coelicolor.* A3(2) and analysis of its genetic determinant. *J Bacteriol* 177: 3946–3952.

Rock, C.O., Cronan, J.E., Jr., and Armitage, I.M. (1981) Molecular properties of acyl carrier protein derivatives. *J Biol Chem* 256: 2669–2674.

Rodrıguez Antonio -Garcıa, Patricia Combes, Rosario Perez-Redondo, Matthew C. A. Smith, and Margaret C.M. Smith, (2005) Natural and synthetic tetracycline-inducible promoters for use in the antibiotic-producing bacteria *Streptomyces Nucleic Acids Research*: 33: 9-1-8.

Romantsov Tatyana, Stephan Helbig, Doreen E. Culham, Chad Gill, Leanne Stalker and Janet M. Wood. (2007) Cardiolipin promotes polar localization of osmosensory transporter ProP in *Escherichia coli. Mol Microbio* 64(6): 1455–1465.

Romberg, L., and Levin, P.A. (2003) Assembly Dynamics of the Bacterial cell Division protein FtsZ: Poised at the Edge of stability. *Annu Rev Microbiol.* 57: 125-154.

Rowan Beth, A., Delene J. Oldenburg, and Arnold J. Bendich. (2007) A high-throughput method for detection of DNA in chloroplasts using flow cytometry. *Plant Methods* 3:5: 1746-4811

Rudner, D.Z., Pan, Q., & Losick, R.M. (2002). Evidence that subcellular localization of a bacterial membrane protein is achieved by diffusion and capture. *Proc Natl Acad Sci USA* 99: 8701–8706.

Rueda, B., Miguelez, E.M., Hardisson, C., Manzanal, M.B. (2001) Changes in glycogen and trehalose content of *Streptomyces brasiliensis* hyphae during growth in liquid cultures under sporulating and non-sporulating conditions. *FEMS Microbiol Lett* 194(2): 181-5.

Rut Carballido-Lopez. (2006) The bacterial actin-like cytoskeleton. *Microbiol Mole biol Rev* 888–909.

Rut, L.C. (2006) Orchestrating bacterial cell morphogenesis. *Mol Microbiol* 60: 815-819.

Ryding, N.J., G.H. Kelemen, C.A. Whatling, K. Flardh, M.J. Buttner, and K.F. Chater. (1998) A developmentally regulated gene encoding a repressorlike protein is essential for sporulation in *Streptomyces coelicolor* A3(2). *Mol Microbiol* 29: 343–357.

Ryding, N.J., M.J. Bibb, V. Molle, K.C. Findlay, K.F. Chater, and M.J. Buttner. (1999) New sporulation loci in *Streptomyces coelicolor* A3(2). *J Bacteriol* 181: 5419–5425.

Sandova Mario-Calderon, Otto Geiger, Ziqiang Guan Francisco Barona-Gomez, and Christian Sohlenkamp. (2009) A eukaryote-like cardiolipin synthase is present in *Streptomyces coelicolor* and in most actinobacteria. *J Biol Chem* 284,26: 17383-17390.

Satomi Nishijima, Yukio Asami, T. Nobuyuki Uetake, Satoshi Yamagoe, Akinori Ohta Isao Shibuya (1988) Disruption of the *Escherichia Coli* Cls gene responsible for cardiolipin synthesis. *J Bacteriol* 170(2): 775-780.

Schaechter, M., Polaczek, P., and Gallegos, R. (1991) Membrane attachment and DNA bending at the origin of the *Escherichia coli* chromosome. *Res Microbiol* 142: 151-154.

Scheffers, D.J., Pinho, M.G. (2006) Bacterial cell wall synthesis: New insights from localization studies. *Microbiol Molec Biol Rev* 69: 585–607.

Schlame Michael, Diego Rua, Miriam L. Greenberg. (2000) The biosynthesis and functional role of cardiolipin. *Progress in Lipid Research* 39: 257-288.

Schneider, D., Bruton, C.J., & Chater, K.F. (2000) Duplicated gene clusters suggest an interplay of glycogen and trehalose metabolism during sequential stages of aerial mycelium development in *Streptomyces coelicolor* A3(2). *Mol Gen Genet* 263: 543–553.

Schweddock, J., J.R.McCormick, E.R. Angert, J.R.Nodwell, and Losick.R. (1997) Assembly of the cell division protein FtsZ into ladder like structures in the aerial hyphae of *Streptomyces coelicolor*. *Mol Microbio* 25(5): 847-858.

Sevcikova, B., and Kormanec, J. (2002) Activity of the *Streptomyces coelicolor* stress-response sigma factor sigmaH is regulated by an anti-sigma factor. *FEMS Microbiol Lett* 209: 229–235.

Sevcikova, B., Benada, O., Kofronova, O., and Kormanec, J. (2001) Stress-response sigma factor sigma(H) is essential for morphological differentiation of *Streptomyces coelicolor* A3(2). *Arch Microbiol* 177: 98–106.

Shaw, N., Stead, A. (1974) The reaction of phosphoglycolipids and other lipids with hydrofluoric acid. *J Biochem* 143(2): 461-465.

Shen, Y., Yoon, P., Yu TW, Floss, H.G., Hopwood, D., & Moore, B.S. (1999) Ectopic expression of the minimal whiE polyketide synthase generates a library of aromatic polyketides of diverse sizes and shapes. *Proc Natl Acad Sci* USA 96: 3622–3627.

Shibuya, I., C. Miyazaki, and A. Ohta. (1985) Alteration of phospholipid composition by combined defects in phosphatidylserine and cardiolipin synthases and physiological consequences in *Escherichia coli*. *J Bacteriol* 161: 1086-1092.

Shih, Y.L., Le, T., and Rothfield, L. (2003) Division site selection in *Escherichia coli* involves dynamic redistribution of Min proteins within coiled structures that extend between the two cell poles. *Proc Natl Acad Sci USA* 100: 7865– 7870.

Simona Lobasso, Matilde Sublimi Saponetti, Francesco Polidoroa, Patrizia Lopalco, Jasna Urbanija, Veronika Kralj-Iglic, Angela Corcelli. (2009) Archaebacterial lipid membranes as models to study the interaction of 10-*N*-nonyl acridine orange with phospholipids. *Chemistry and Physics of Lipids* 157: 12–20.

Soliveri, J., Brown, K.L., Buttner, M.J., & Chater, K.F. (1992) Two promoters for the whiB sporulation gene of *Streptomyces coelicolor* A3(2) and their activities in relation to development. *J Bacteriol* 174: 6215–6220.

Soliveri, J.A., Gomez, J., Bishai, W.R., & Chater, K.F. (2000) Multiple paralogous genes related to the *Streptomyces coelicolor* developmental regulatory gene whiB are present in *Streptomyces* and other actinomycetes. *J Microbiol* 6: 333–343.

Stahlberg, H., Kutejova, E., Muchova, K., Gregorini, M., Lustig, A., et al. (2004) Oligomeric structure of the Bacillus subtilis cell division protein DivIVA determined by transmission electron microscopy. *Mol Microbiol* 52: 1281–1290.

Stebbins, M.J., Urlinger, S., Byrne, G., Bello, B., Hillen, W. and Yin, J.C.P. (2001) Tetracycline-inducible systems for Drosophila. *Proc Natl Acad Sci* 98: 10775–10780.

Steven A. Short, and David C. White. (1972) Biosynthesis of cardiolipin from phosphatidylglycerol in *Staphylococcus aureus*. *J Bacteriol,*p: 820-826.

Suefuji, K., R. Valluzzi, and D. Ray Chaudhuri. (2002) Dynamic assembly of MinD into filament bundles modulated by ATP, phospholipids, and MinE. *Proc Natl Acad Sci* USA 99: 16776–16781.

Summers, R.G., A. Ali, B. Shen, W.A. Wessel, and C.R. Hutchinson. (1995) Malonyl-coenzyme A:acyl carrier protein acyltransferase of *Streptomyces glaucescens*: a possible link between fatty acid and polyketide biosynthesis. *J Biochem* 34: 9389–9402.

Sun, J., Kelemen, G.H., Fernandez-Abalos, J.M., and Bibb, M.J. (1999) Green fluorescent protein as a reporter for spatial and temporal gene expression in *Streptomyces coelicolor* A3 (2). *J Microbiol* 145: 2221– 2227.

Susstrunk, U., Pidoux, J., Taubert, S., Ullmann, A., and Thompson, C.J. (1998) Pleiotropic effects of cAMP on germination, antibiotic biosynthesis and morphological development in *Streptomyces coelicolor*. *Mol Microbiol* 30: 33–46.

Szeto, T.H., Rowland, S.L., Rothfield, L.I., and King, G.F. (2002) Membrane localization of MinD is mediated by a C-terminal motif that is conserved across eubacteria, archaea, and chloroplasts. *Proc Natl Acad Sci USA* 99: 15693–15698.

Takano Eriko. (2006) γ-Butyrolactones: *Streptomyces* signalling molecules regulating antibiotic production and differentiation. *Curr Opin Microbiol* 9: 287-294.

Takano, E., White, J., Thompson, C.J. & Bibb, M.J. (1995) Construction of thiostrepton-inducible, high-copy-number expression vectors for use in *Streptomyces* spp. *Gene* 166: 133-137.

Tan, H.R., Yang, H.H., Tian, Y.Q., Wu Whatling, C.A., Chamberlin, L.C., Buttner, M.J., Nodwell, J., & Chater, K.F. (1998) The *Streptomyces coelicolor* sporulation-specific sigma (WhiG) form of RNA polymerase transcribes a gene encoding a ProXlike protein that is dispensable for sporulation. *Gene* 212: 137–146.

Thanbichler M., and L. Shapiro. (2006) Chromosome organization and segregation in bacteria. *J Struct. Biol* 156: 292-303.

Thanbichler Martin, & Lucy Shapiro. (2008) Getting organized - how bacterial cells move proteins and DNA. *Nat Rev Microbiol* 6: 28-40.

Thomas Vanden, Boom, and John E. Cronan, Jr. (1989) Genetics and regulation of bacterial lipid metabolism. *Annu Rev Microbiol* 43: 317-343.

Tian,Y., Fowler, K., Findlay, K., Tan, H., & Chater, K.F. (2007) An unusual response regulator influences sporulation at early and late stages in *Streptomyces coelicolor*. *J Bacteriol* 189: 2873-2885.

Traag, B.A., Gilles, P., Van Wezel. (2008) The SsgA-like proteins in actinomycetes: small proteins up to a big task. *Antonie van Leeuwenhoek* 94: 85–97.

Traag, B.A., Kelemen, G.H., & Van Wezel, G.P. (2004) Transcription of the sporulation gene ssgA is activated by the IclR-type regulator SsgR in a whi-independent manner in *Streptomyces coelicolor* A3 (2) *Mol Microbiol* 53: 985–1000.

Tropp, B.E. (1997) Cardiolipin synthase from *Escherichia coli*. *Biochim Biophys Acta* 1348: 192–200.

Tropp, B.E., Louis Ragolia, Weiming Xia, William Dowhan, Roger Milkman, Kenneth E. Rudd, Radmila Ivanis Evic, and Dragutin J. Savic. (1995) Identity of the *Escherichia coli cls* and *nov* genes. *J bacteriol,*p: 5155–5157.

Tsay, J.T., W. Oh, T.J. Larson, S. Jackowski, and C.O. Rock. (1992) Isolation and characterization of the b-ketoacyl-acyl carrier protein synthase III gene (fabH) from *Escherichia coli* K-12. *J Biol Chem* 267: 6807–6814.

Tseng Shun-Fu a, Tzu-Wen Huang b, Carton W. Chen b, Ming-Kai Chern c, Ming F. Tam c, Shu-Chun Teng. (2006) ShyA, a membrane protein for proper septation of hyphae in *Streptomyces*. *Biochemical and Biophysical Research Communications* 343: 369–377

Tung T. Hoang, and Herbert P. Schweizer. (1997) Fatty acid biosynthesis in *Pseudomonas aeruginosa*: cloning and characterization of the *fabAB* operon encoding b-Hydroxyacyl- acyl carrier protein dehydratase (FabA) and b-Ketoacyl-acyl carrier protein synthase I (FabB). *J Bacterol,* p: 5326–5332.

Ueda Kenji,1 Ken-Ichi Oinuma, Go Ikeda, Kuniaki Hosono, Yasuo Ohnishi, Sueharu Horinouchi, and Teruhiko Beppu. (2002) AmfS, an Extracellular Peptidic Morphogen in *Streptomyces griseus. J Bacteriol*, p: 1488–1492.

Van Keulen, G., J. Alderson, J. White, and R.G. Sawers. (2007) The obligateaerobic actinomycte *Streptomyces coelicolor* A3(2) survives extended periodsof anaerobic stress. *Environ Micobiol* 9: 3143–3149.

Vaughan, S., Wickstead, B., Gull, K. & Addinall, S.G. (2004) Molecular evolution of FtsZ protein sequences encoded within the genomes of archaea, bacteria, and eukaryota. *J Mol Evol* 58(1): 19-29.

Van Wijk, G.M.T., Hostetler, K.Y., Schlame, M., Van Den Bosch, H. (1991) Cytidine diphosphate diglyceride analogs of antiretroviral dideoxynucleosides: evidence for release of dideoxynucleoside-monophosphates by phospholipid biosynthetic enzymes in rat liver subcellular fractions. *Biochim Biophys Acta* 1086: 99-105.

Verma, J.N. & Khuller, G.K. (1982) Pathways of phosphatidylethanolamine catabolism in *Streptomyces griseus*. *Indian journal of Biochemistry and Biophysics* 19(3): 191-4.

Vida Thomas, A., and Scott D. Erm. (1995) A new vital Stain for visualizing vacuolar membrane dynamics and endocytosis in Yeast *J Cell Biol* 128(5): 779-792.

Viollier, P.H., Kelemen, G.H., Dale, G.E., Nguyen, K.T., Buttner, M.J., and Thompson, C.J. (2003a) Specialized osmotic stress response systems involve multiple SigB-like sigma factors in *Streptomyces coelicolor*. *Mol Microbiol* 47: 699–714.

Viollier, P.H., Weihofen, A., Folcher, M., and Thompson, C.J. (2003b) Post-transcriptional regulation of the *Streptomyces coelicolor* stress responsive sigma factor, SigH, involves translational control, proteolytic processing, and an anti-sigma factor homolog. *J Mol Biol* 325: 637–649.

Volff, J.N., and J. Altenbuchner. (1998) Genetic instability of the *Streptomyces* chromosome. *Mol Microbiol* 27: 239–246.

W. Firshein. (1989) Role of the DNA/membrane complex in prokaryotic DNA replication. *Ann Rev Microbio* 43:pp: 89-120.

Wallace, K.K., B. Zhao, H.A. McArthur, and K.A. Reynolds. (1995) *In vivo* analysis of straight-chain and branchd-chain fatty acid biosynthesis in three Actinomycetes. *FEMS Microbiol Lett* 131: 227–234.

Wachtler, V., Rajagopalan, S. & Balasubramanian, M.K. (2003) Sterol-rich plasma membrane domains in the fission yeast *Schizosaccharomyces pombe*. *Journal Cell Science* 116(5): 867-74.

Wang Bing, and Howard K. Kuramitsu. (2005) Inducible antisense RNA expression in the characterization of gene functions in *Streptococcus* mutans *Infection. Imm*, p: 3568–3576.

Wang Lei, Yanfei Yu, Xinyi He, Xiufen Zhou, Zixin Deng, Keith F. Chater, and Meifeng Tao. (2007) Role of an FtsK-like protein in genetic stability in *streptomyces coelicolor* A(3)2. *J Bacteriol*,p: 2310-2318.

Wang Sheng-Bing, Stuart Cantlay, Niklas Nordberg, Michal Letek, Jose A. Gil and Klas Flardh. (2009) Domains involved in the *in vivo* function and oligomerization of apical growth determinant DivIVA in *Streptomyces coelicolor. FEMS Microbiol Lett* 297: 101–109.

Wang Sheng-Lan, Ke-Qiang Fan, Xu Yang, Zeng-Xi Lin, Xin-Ping Xu, and Ke-Qian Yang. (2008) CabC, an EF-Hand calcium-binding protein, is involved in Ca^{2+} mediated regulation of spore germination and aerial hypha formation in *Streptomyces coelicolor. J Bacteriol,*p: 4061–4068.

Wang, L., and Lutkenhaus, J. (1998) FtsK is an essential cell division protein that is localized to the septum and induced as part of the SOS response. *Mol Microbiol* 29: 731-740.

Wenner Thomas, Virginie Roth, Gilles Fischer, Celine Fourrier, Bertrand Aigle, Bernard Decaris, and Pierre Leblond. (2003) End-to-end fusion of linear deleted chromosomes initiates a cycle of genome instability in *Streptomyces ambofaciens*. *Mol Microbiol* 50: 11–425.

Wezel Van, G.P., J. White, P. Young, P.W. Postma, and M.J. Bibb. (1997) Substrate induction and glucose repression of maltose utilization by *Streptomyces coelicolor* A3(2) is controlled by *malR*, a member of the *lacI-galR* family of regulatory genes. *Mol Microbiol* 23: 537–549.

Weiss, D.S. (2004) Bacterial cell division and the septal ring. *Mol Microbiol* 54(3): 588-97.

Willey, J., R. Santamaria, J. Guijarro, M. Geislich, and R. Losick. (1991) Extracellular complementation of a developmental mutation implicates a small sporulation protein in aerial mycelium formation by *Streptomyces coelicolor*. *Cell* 65: 641–650.

Willey, J., Schwedock, J., Losick, R. (1993) Multiple extracelluler signals govern the production of a morphogenetic protein involved in aerial mycelium formation by *Streptomyces coelicolor. Genes Dev* 7: 895-903.

Williams, S.T., Goodfellow, M., Alderson, G. (1989) Genus *Streptomyces Watkman* and Hendrici 1943. In *Bergey's Manual of Determinative Bacteriology*, 4.

Williams, S.T., Sharpe, M.E., Holt, J.G. Baltimore, Wachtler, V., Rajagopalan, S., and Balasubramanian, M.K. (2003) Sterol-rich plasma membrane domains in the fission yeast *Schizosaccharomyces pombe*. *J Cell Sci* 116: 867– 874.

Woldringh, C.L., Jensen, P.R., and Westerhoff, H.V. (1995) Structure and partitioning of bacterial DNA: determined by a balance of compaction and expansion forces? *FEMS Microbiol Lett* 131: 235–242.

Xiang, X., and Morris, N.R. (1999) Hyphal tip growth and nuclear migration. *Curr Opin Microbiol* 2: 636–640.

Xie Pengfei, Ana Zeng, and Zhongjun Qin. (2009) cmdABCDEF, a cluster of genes encoding membrane proteins for differentiation and antibiotic production in *Streptomyces coelicolor* A3 (2). *BMC Microbiology* 9: 157.

Xie Zhoujie, Wenli Li1, Yuqing Tian, Gang Liu, and Huarong Tan. (2007) Identification and characterization of sawC, a whiA -like gene, essential for sporulation in *Streptomyces ansochromogenes. Arch Microbiol.* 188(6): 575-82.

Xu Hongbin,1 Keith, F., Chater,2 Zixin Deng,3 and Meifeng Tao,1. (2008) A Cellulose Synthase-Like Protein Involved in Hyphal Tip Growth and Morphological Differentiation in *Streptomyces*. *J Bacteriol*, p: 4971–4978.

Yamazaki Haruka, Yasuo Ohnishi, and Sueharu Horinouchi. (2000) An A-Factor-dependent extracytoplasmic function sigma factor (sAdsA) that is essential for morphological development in *Streptomyces griseus. J Bacteriol*, p: 4596–4605.

Yamazaki Haruka, Yasuo Ohnishi, and Sueharu Horinouchi. (2003a) Transcriptional switch on of *ssgA* by A-Factor, which is essential for spore septum formation in *Streptomyces griseus. J Bacteriol*, p: 1273–1283.

Yamazaki Haruka, Yuji Takano, Yasuo Ohnishi, and Sueharu Horinouchi. (2003b) *amfR,* an essential gene for aerial mycelium formation, is a member of the AdpA regulon in the A-factor regulatory cascade in *Streptomyces griseus. Mol Microbiol* 50 (4): 1173–1187.

Yamazaki, H., Tomono, A., Ohnishi, Y., & Horinouchi, S. (2004) DNA binding specificity of AdpA, a transcriptional activator in the A-factor regulatory cascade in *Streptomyces griseus*. *Mol Microbiol* 53: 555–572.

Yasuo Ohnishi, Jun Ishikawa, Hirofumi Hara,1 Hirokazu Suzuki, Miwa Ikenoya, Haruo Ikeda, Atsushi Yamashita, Masahira Hattori, and Sueharu Horinouchi, (2008) The Genome Sequence of the Streptomycin-Producing Microorganism *Streptomyces griseus*. *IFO 13350 J Bacteriol*, p: 4050–4060.

Yehuda, S.B., Rudner, D.Z., and Losick, R. (2003) Assembly of SpoIIIE DNA Translocase on chromosome trapping in *Bacillus subtilis*. *Curr Biol* 13: 1296-2200.

Yeo, M., & Chater, K. (2005) The interplay of glycogen metabolism and differentiation provides an insight into the developmental biology of *Streptomyces coelicolor*. *Microbiol* 151: 855–861.

Yim, L., Vandenbussche, G., Mingorance, J., Rueda, S., Casanova, M., Ruysschaert, J.M., *et al.* (2000) Role of the carboxy terminus of *Escherichia coli* FtsA in self interaction and cell division. *J Bacteriol* 182: 6366–6373.

Yong-Mei Zhang and Charles O. Rock. (2008) Membrane lipid homeostasis in bacteria. *Nat Rev* 6: 222-233.

Yoshiho Nagata, and Max M. Burger. (1974) Wheat Germ Agglutinin. *J Biol Chem* 249: 10, PP: 3116-3122.

Yu, T.W. & Hopwood, D.A. (1995) Ectopic expression of the *Streptomyces coelicolor whiE* genes for polyketide spore pigment synthesis and their interaction with the *act* genes for actniorhodin biosynthesis. *J Microbiol* 141: 2779-2791.

Yu, X.U., Weihe, E.K., and Margolin, W. (1998) Role of the C terminus of FtsK in *Escherichia coli* chromosome segregation. *J Bacteriol* 180: 6424–6428.

Zhang, L., F. Fan, L.M. Palmer, M.A. Lonetto, C. Petit, L.L. Voelker, A. St. John, B. Bankosky, M. Rosenberg, and D. McDevitt. (2000) Regulated gene expression in *Staphylococcus aureus* for identifying conditional lethal phenotypes and antibiotic mode of action. *Gene* 255: 297–305.

Zhiwei Shen, and David M. Dyers. (1996) Isolation of *vibrio harveyi* acyl carrier protein and the *fabG*, *acpP*, and *fabF* genes involved in fatty acid biosynthesis. *J Bacteriol*, p: 571–573.

Zhou, P., Florova, G., Reynolds, K.A. (1999) Polyketide synthase acyl carrier protein (ACP) as a substrate and a catalyst for malonyl ACP biosynthesis. *Chem biol* 6(8): 577-84.

Publications

Applied and Environmental Microbiology, Nov. 2008, p. 6774–6781 Vol. 74, No. 21
0099-2240/08/$08.00+0 doi:10.1128/AEM.01233-08

Time-Lapse Microscopy of *Streptomyces coelicolor* Growth and Sporulation▽†

Vinod Jyothikumar, Emma J. Tilley, Rashmi Wali, and Paul R. Herron*

Strathclyde Institute of Pharmacy and Biomedical Science, University of Strathclyde, Royal College, 204 George Street, Glasgow G1 1 XW, United Kingdom

Received 3 June 2008/Accepted 25 August 2008

Bacteria from the genus *Streptomyces* are among the most complex of all prokaryotes; not only do they grow as a complex mycelium, they also differentiate to form aerial hyphae before developing further to form spore chains. This developmental heterogeneity of streptomycete microcolonies makes studying the dynamic processes that contribute to growth and development a challenging procedure. As a result, in order to study the mechanisms that underpin streptomycete growth, we have developed a system for studying hyphal extension, protein trafficking, and sporulation by time-lapse microscopy. Through the use of time-lapse microscopy we have demonstrated that *Streptomyces coelicolor* germ tubes undergo a temporary arrest in their growth when in close proximity to sibling extension sites. Following germination, in this system, hyphae extended at a rate of ~20 μm h^{-1}, which was not significantly different from the rate at which the apical ring of the cytokinetic protein FtsZ progressed along extending hyphae through a spiraling movement. Although we were able to generate movies for streptomycete sporulation, we were unable to do so for either the erection of aerial hyphae or the early stages of sporulation. Despite this, it was possible to demonstrate an arrest of aerial hyphal development that we suggest is through the depolymerization of FtsZ-enhanced green fluorescent protein (GFP). Consequently, the imaging system reported here provides a system that allows the dynamic movement of GFP-tagged proteins involved in growth and development of *S. coelicolor* to be tracked and their role in cytokinesis to be characterized during the streptomycete life cycle.

Fluorescence microscopy has revolutionized our understanding of the bacterial cell and provided new opportunities to investigate the behavior of cell division proteins and chromosome dynamics in bacteria (25). Central to this research is the application of time-lapse microscopy to study bacterial cell division, which has revealed the complexity with which bacteria coordinate cellular growth and division. For example, the rod-shaped bacteria *Escherichia coli* and *Bacillus subtilis* incorporate new peptidoglycan into their cell wall along their lateral walls, while coccoid bacteria such as *Staphylococcus aureus* do so at mid-cell (4). Actinobacteria, such as *Corynebacterium* and members of the mycelial, antibiotic-producing genus *Streptomyces*, incorporate peptidoglycan at the cell poles (4). In the case of streptomycetes, this allows them to adopt a hyphal growth strategy through peptidoglycan incorporation at the hyphal tip (9). This is ideally suited to the colonization of their particulate habitat, the soil, through the generation of a mycelium that permits nutrients to be transported from a nutrient reservoir to the actively growing tip. As such, streptomycetes represent a group of organisms that grow in a fashion distinct from other, better understood bacteria. The knowledge base associated with morphological and physiological differentiation in the model organism *Streptomyces coelicolor*, coupled with the viability of cell division mutants, means that a greater understanding of streptomycete growth and sporulation may provide important clues to understanding bacterial growth in general (18, 21). Perhaps one reason why an understanding of streptomycete cell division has lagged behind that for other bacteria is the technical difficulty associated with imaging this complex bacterium. To date, microscopic studies of cell division in streptomycetes have generated snapshot images of hyphae or spores. Such images can give only limited information on protein and nucleoid movement in space and time, and, as a result, the exact order of intracellular events during hyphal growth and sporulation in *Streptomyces* is still largely obscure (5, 6). The multinucleate nature of streptomycete hyphae means that time-lapse microscopy is likely to prove a key tool in understanding patterns in nucleoid and protein trafficking during hyphal growth, and although it was used to demonstrate spatial and temporal localization of cephamycin C biosynthesis in *Streptomyces clavuligerus* (11), so far it has not been used to study growth and development. Perhaps the main reasons for this are the technical challenges associated with carrying out time-lapse microscopy of the model organism, *S. coelicolor*. These include oxygen dependence, a developmentally heterogeneous mycelium, the three-dimensional pattern of hyphal growth, and an inability to sporulate in the absence of a solid support. Consequently, we set out to design an imaging system that could overcome at least some of these technical problems and support time-lapse microscopy of hyphal growth and sporulation. In order to do this, we exploited the design features of an inverted microscope coupled with rendering of three-dimensional representations of phase-contrast images and the availability of oxygen-permeable imaging chambers.

* Corresponding author. Mailing address: Strathclyde Institute of Pharmacy and Biomedical Science, University of Strathclyde, Royal College, 204 George Street, Glasgow G1 1 XW, United Kingdom. Phone: 44-141-5482531. Fax:. 44-141-5484924. E-mail: paul.herron@strath.ac.uk.

† Supplemental material for this article may be found at http://aem.asm.org/.

▽ Published ahead of print on 12 September 2008.

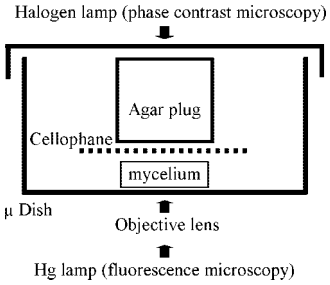

FIG. 1. Imaging chamber for capturing streptomycete growth on solid medium. Spores were germinated for an appropriate length of time on cellophane disks on agar before being inverted and transferred to the μ-dish imaging chamber. Subsequently, a cylinder of 3MA was applied to the cellophane dish and the imaging chamber transferred to the incubation chamber set to 30°C and allowed to equilibrate for 1 hour before commencement of imaging.

MATERIALS AND METHODS

Bacterial strains and cultivation conditions. *S. coelicolor* M145 and *S. coelicolor* K113 (a derivative of *S. coelicolor* M145 containing a second copy of *ftsZ* translationally fused to the enhanced green fluorescent protein [EGFP] gene [7]; generously supplied by Klas Flärdh, Lund University, Sweden) were grown on MS agar and supplemented with apramycin (100 μg ml^{-1}) when necessary at 30°C (16). For time-lapse microscopy, minimal agar (16) containing 5% (wt/vol) mannitol (3MA) or tap water agar (1% [wt/vol]) was used as circumstances required. For time-lapse microscopy of germination or growth of substrate hyphae, spores were germinated on 0.5-cm^2 sterile cellophane squares, placed on 3MA, and incubated at 30°C. Cellophane was removed after appropriate time intervals and transferred to imaging chambers. Time-lapse microscopy of sporulation was carried out by placing cellophane squares on sterile coverslips and inserting the coverslip into 3MA at an acute angle before inoculation with around 1×10^7 *S. coelicolor* spores (26). After 36 h, the cellophane was peeled away from the coverslip and transferred to imaging chambers.

Imaging chambers. Cellophane squares were placed, hyphal side down, in uncoated μ-dishes (Ibidi GmbH, Munich, Germany), and a plug of agar cut with a number 4 cork borer was placed on top of the cellophane. 3MA was used for germination or hyphal growth, and water agar was used for sporulation (Fig. 1). The microscope stage was heated to 30°C using an Ibidi heating system with a heated lid (Ibidi GmbH, Munich, Germany). In order to minimize focal drift, the microscope stage and imaging chamber were allowed to equilibrate for 60 min with respect to temperature before imaging commenced.

Fluorescence microscopy. Samples were studied using a Nikon TE2000S inverted microscope and observed with a CFI Plan Fluor DLL-100X oil N.A. 1.3 objective lens, and images were captured using a Hamamatsu Orca-285 Firewire digital charge-coupled device camera. Captured images were processed using IPlabs 3.7 image processing software (BD Biosciences Bioimaging, Rockville, MD). Briefly, 0.5-μm Z sections of both phase-contrast and fluorescent images were captured at 15-min intervals and used to render three-dimensional images. FtsZ-EGFP in *S. coelicolor* K113 was visualized with a fluorescein isothiocyanate filter set at an exposure time of 100 ms. Measurements of hyphal growth and Z-ring movement were made using IPlabs 3.7 image processing software and analyzed statistically using Microsoft Excel 2003; equality of variance between data sets was first determined using F tests and then subjected to the appropriate Student *t* test depending on the outcome of the F test. Multiple data sets were analyzed by analysis of variance. Where appropriate, means are supplemented by standard deviations in parentheses.

RESULTS

Germination of *S. coelicolor* M145 is heterogeneous and displays apical dominance. Although *S. coelicolor* is able to survive in the absence of oxygen for long periods of time (28), despite several attempts to grow *S. coelicolor* on agar sandwiched between glass coverslips and slides using a variety of imaging chambers, we were unable to do so. Presumably this was due to poor oxygen availability. As a result, we took advantage of the oxygen permeability and optically high quality of the plastic used in μ-dish manufacture in order to carry out time-lapse microscopy of hyphal growth. Spores of *S. coelicolor* M145 were inoculated onto a cellophane disk on 3MA, allowed to air dry for 30 min at 30°C, transferred to the imaging chamber (Fig. 1), and allowed to equilibrate for 1 hour before initiation of time-lapse microscopy. We analyzed the development of 90 spores individually. A total of 85% of spores swelled and became phase dark prior to germ tube emergence; this is characteristic of spore germination before germ tube emergence (27). A total of 15% of spores did not germinate, at least until hyphal growth made observation of individual spores difficult. It was impossible to describe accurately the germination pattern of 26% of the spores because of the difficulty of attributing individual hyphae to a parental spore due to spore clumping and hyphal overgrowth. However, we were able to track and describe the germination and early branching behavior of the remaining spores (59%). Emergence of a primary germ tube occurred between 2.25 and 6 h after initiation of imaging (3.75 and 7.5 h, respectively, after the original plating out), and 63.3% of spores produced one hypha and 36.7% produced two hyphae (Table 1). No spores that produced more than two hyphae were observed, in contrast to the results of Noens et al. (24), who observed as many as four germ tubes per spore.

Two classes of microcolonies developed in those spores that produced one germ tube: when a branch emerged from the primary germ tube, 7 (14.3%) primary germ tubes ceased growth for an average of 3.1 (±2.16) hours (Fig. 2A; see Movie S2A in the supplemental material), while the remaining 20 (49%) primary germ tubes showed no growth cessation (Fig. 2C; see Movie S2C in the supplemental material). Where growth of the primary germ tube was arrested, it was apparent that, following branch emergence, the branching occurred relatively soon after germination. Germ tubes that displayed growth arrest did so when a branch emerged on average 2.7

TABLE 1. Heterogeneity of *S. coelicolor* microcolonies following germination

Germination class[a]	No. of hyphae emerging from each spore	Growth arrest of primary hypha	% of germinations	$e_2 - e_1$[b] (h)	e_1 arrest[c] (h)
A	1	Yes	14.3	2.7 (1.45)	3.1 (2.16)
C	1	No	49.0	5.7 (1.62)	
B	2	Yes	20.4	1.4 (1.46)	4.9 (2.44)
D	2	No	16.3	3.5 (2.23)	

[a] Germination of a random selection of spores was observed by time-lapse microscopy, and four classes of spore germinations were observed: one or two hyphae, with or without growth arrest.

[b] Time difference between emergence of primary hypha at time e_1 from a spore and appearance of a second extension site at time e_2; the latter was the first hyphal branch (class A or C) or the emergence of a second hypha from the spore (class B or D). $e_2 - e_1$ values were compared statistically by the Student *t* test with respect to arrested (class A) and non arrested spores (class C) with one germ tube ($P < 1 \times 10^{-4}$), arrested (class B) and non arrested (class D) spores with two germ tubes ($P < 0.013$), arrested spores with one (class A) or two (class B) germ tubes ($P < 0.048$), and nonarrested germ tubes with one (class C) or two (class D) spores ($P < 0.004$). All four comparisons showed significant differences between the two populations in each individual test. Standard deviations are shown in parentheses.

[c] Time between cessation of growth of primary hypha and subsequent restart of growth. Standard deviations are shown in parentheses.

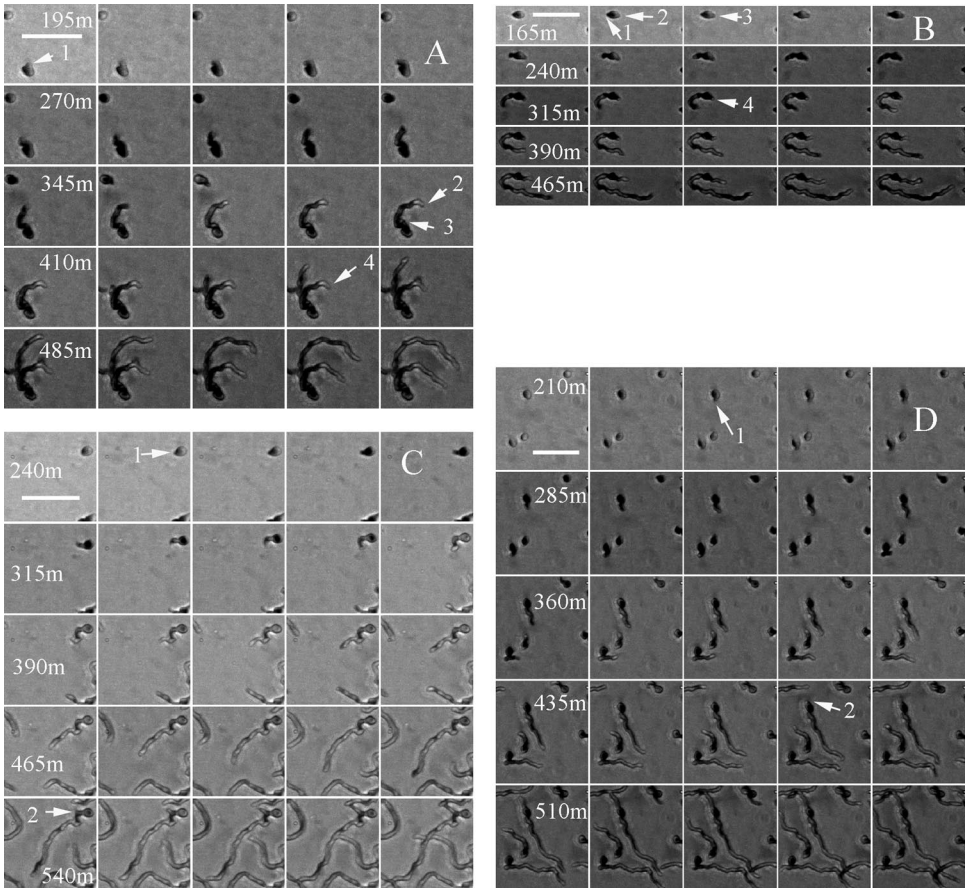

FIG. 2. Heterogeneity of *S. coelicolor* microcolonies following germination. Numbers represent minutes after initiation of time-lapse microscopy (see Movies S2A, S2B, S2C, and S2D in the supplemental material). Horizontal white bars represent 10 μm. The four observed classes of *S. coelicolor* germination are displayed. (A) Class A germination, showing emergence of the primary hypha (1), growth arrest of the primary hypha (2) following branch emergence (3), and growth restoration of the primary hypha (4). (B) Class B germination, showing two hyphae emerging from the spore (1 and 2), growth arrest by one hypha (3), and growth restoration of the arrested hypha (4). (C) Class C germination, showing hyphal emergence (1) and branch appearance (2) (no growth arrest of the primary hypha). (D) Class D germination, showing emergence of the primary hypha (1) and emergence of the secondary hypha (2) from the spore (no growth arrest of the primary hypha).

(±1.45) hours after germination, when the mean primary germ tube length was 2.3 μm, and these were termed class A germinations (Fig. 2A; see Movie S2A in the supplemental material). When no growth arrest was observed, the first branch emerged on average 5.7 (±1.62) hours after germination, when the mean primary germ tube length was 5.1 μm; these were termed class C germinations (Fig. 2C; see Movie S2C in the supplemental material). The time interval ($e_2 - e_1$) between the emergence of the first (germination) and the second (branch) growing tip was significantly longer in class C germinations than in class A germinations (Table 1).

Two classes of hyphal morphology were also generated from those spores that produced two germ tubes; 10 (20.4%) primary germ tubes ceased growth for an average of 4.9 (±2.44) hours following the emergence of a second germ tube from the same spore (Fig. 2B; see Movie S2B in the supplemental material). Meanwhile another eight primary germ tubes (16.3%) showed no growth arrest (Fig. 2D; see Movie S2D in the supplemental material). As was the case with branching in class A germinations, it was apparent that where growth of a primary germ tube was arrested following the emergence of a second germ tube, the latter occurred relatively soon after the primary germination. Primary germ tubes that displayed growth arrest did so when a second tube emerged on average 1.4 (±1.46) hours after germination; these were termed class B germinations (Fig. 2B; see Movie S2B in the supplemental material). Occasionally, two germ tubes emerged simultaneously from a spore; one always ceased growth for a period of time (Fig. 2B; see Movie S2A in the supplemental material). When no growth arrest was observed, the secondary germ tube emerged on average 3.5 (±2.23) h after emergence of the primary germ tube; these were termed class D germinations (Fig. 2D; see Movie S2D in the supplemental material). The time interval ($e_2 - e_1$) between the emergence of the first and the second growing tip was significantly longer in class D germinations than in class B germinations (Table 1), although the length of arrest caused by branching (class A) or appearance of a second germ tube (class B) was not significantly different (Table 1). However, the time intervals between emergence of a primary and a secondary growth site were significantly longer when the second extending tip was derived from a branch (class A or C) rather than a germ tube (class B or D), irre-

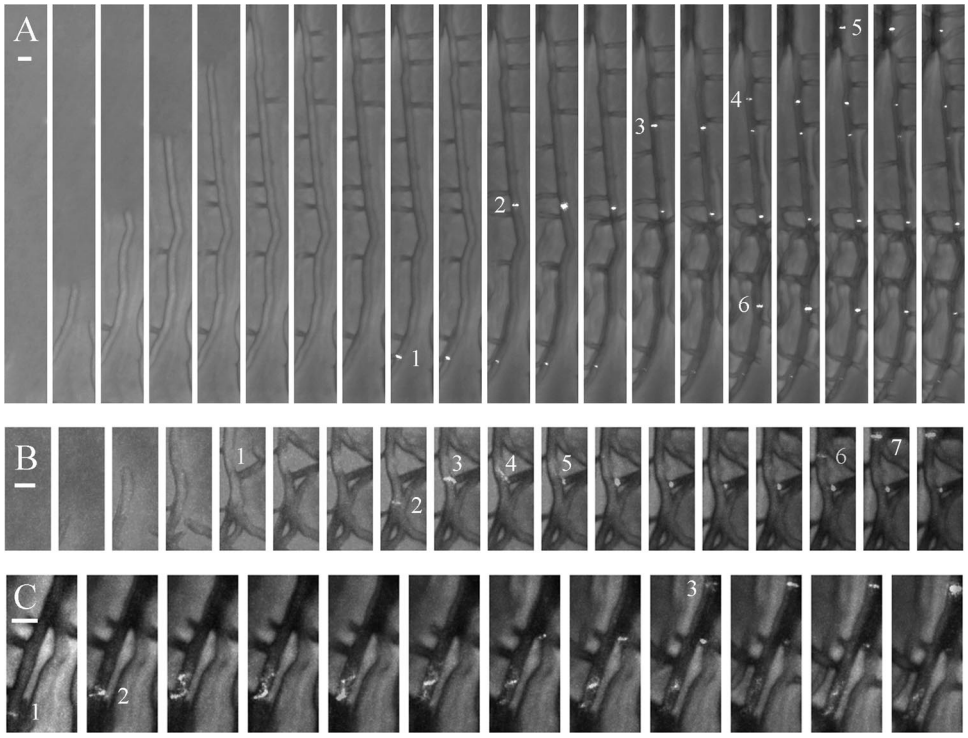

FIG. 3. Localization of FtsZ rings in growing *S. coelicolor* K113 substrate hyphae. Spores were germinated overnight before being transferred to an imaging chamber and allowed to equilibrate for 1 hour before commencement of imaging. The mosaic images are composed of images taken at 30-min intervals, while images taken at 15-min intervals are shown in Movies S3, S3A, S3B, and S3C in the supplemental material. Horizontal white bars represent 2 μm. (A) Hyphal branching and progression of FtsZ rings (1 to 6) toward the growing hyphal tip; it is not clear if FtsZ ring 6 is located in the primary hypha or a parallel hypha. (B) Progression (2 to 7) and division of an FtsZ ring (3) at a hyphal branch (1). (C) Extended FtsZ spiral (2) as FtsZ rings progress toward the hyphal tip (1 to 3).

spective of whether growth was arrested or not (Table 1). The timing of the initial germination had no effect either on the appearance of a second germ tube or on whether the primary germ tube underwent growth arrest (data not shown). Consequently, in a young *S. coelicolor* microcolony, and irrespective of whether one or two germ tubes emerge from a spore, if two young hyphal tips are located close to each other, one is able to exert an apical dominance over the other and arrest the latter's growth for a period of time.

FtsZ follows the extending hyphal tip and is not required for branching. *S. coelicolor* K113 spores failed to germinate when illuminated with light of a wavelength of 492 nm, which was necessary to excite EGFP. Despite this, we were able to visualize the movement of FtsZ-EGFP in substrate hyphae. K113 spores were inoculated onto 3MA as described previously and incubated overnight at 30°C. The next day, the cellophane square was transferred to an imaging chamber (Fig. 1), the tips of the radially extending mycelium identified by phase-contrast microscopy, and images captured as described above. This allowed us to visualize FtsZ-EGFP ring progression in growing substrate hyphae. Ten individual hyphae were observed with respect to their patterns of branching and Z-ring formation (see Movie S3 in the supplemental material). Hyphae grew across the field at an average tip extension rate of 19.58 (±2.67) μm h^{-1}, and branches formed on average 10.94 (±2.85) μm behind the hyphal tip. The average distance between branches was 7.63 (± 6.68) μm; this relatively large standard deviation associated with branch-to-branch distances suggests that *S. coelicolor* shows great variability in branch placement with respect to the location of other branches. These values were in broad agreement with those of Allan and Prosser (1). However, the relatively low standard deviation associated with the tip-to-branch distance suggests that branch placement is tightly linked to the distance from the hyphal tip. Taken together, the differences in the standard deviations of the tip-to-branch and branch-to-branch distances suggest that although *S. coelicolor* did not branch every time the tip-to-branch distance reached 10.94 μm, when it did so, the branch was placed close to 10.94 μm from the hyphal tip. A cessation of growth was seen in 82 (73.2%) branches that emerged from the 10 primary hyphae examined, while the remaining 30 branches (26.8%) displayed no growth arrest. It was apparent that when growth arrest occurred, the branch emerged in close proximity to a neighboring hypha (see Movie S3 in the supplemental material). In those branches where the tip displayed growth arrest, the tip-to-branch distance was significantly longer ($P < 0.02$), at 11.29 (±2.76) μm, than in those that displayed no growth arrest (10.06 [±2.93] μm). Rings of FtsZ-EGFP appeared at discrete locations after branching on average 56.06 (±16.96) μm behind the hyphal tip (Fig. 3A; see Movies S3 and S3A in the supplemental material) and presumably went on to initiate the formation of septa. Z rings formed on average 20.1 (±10.37) μm apart, and by measuring the distance between the apical and subapical Z rings and relating

this to the time difference between their appearances, we were able to calculate the rate of progression of the apical Z ring as 17.11 (±8.45) μm h^{-1}. Although rate of Z ring progression showed more variation than the rate of hyphal tip of extension (coefficients of variation were 51.6% and 13.6%, respectively), there was no significant difference between the two rates, which suggests either a direct or indirect association between Z-ring progression and peptidoglycan incorporation at the hyphal tip.

This reinforces the genetic evidence that FtsZ is not required for tip extension or branching in *S. coelicolor* (26), and although Z rings formed at some hyphal branch points (Fig. 3B; see Movies S3 and S3B in the supplemental material), this was not the case with many branches. Following the formation of a discrete Z ring, there was a transient increase in brightness of the ring (Fig. 3A; see Movies S3 and S3A in the supplemental material). The reason for this is unclear; perhaps it is due to movement of the ring out of the plane of the perpendicular, although a transient expansion of a compacted Z-ring spiral to produce apparent higher levels of fluorescence seems a more likely explanation. Z rings remained visible at the same location throughout the course of our observations, although many eventually faded to some degree. Occasionally, FtsZ spirals were seen (Fig. 3C; see Movies S3 and S3C in the supplemental material) and also moved toward the hyphal tip. Clearly the visible spiral displayed in Fig. 3C and in Movie S3C in the supplemental material moved much more slowly than Z-ring progression, and it took around 2 hours for the spiral to move through a 4-μm section of hyphae, before coalescing to form a discrete ring. The reason for this is not clear; although many other faintly fluorescing FtsZ spirals were observed distal to the apical Z ring (see Movie S3 in the supplemental material), suggesting that the progression of FtsZ behind the hyphal tip proceeds in a spiral manner.

Rehydration of aerial hyphae causes FtsZ-EGFP ring disassembly. *S. coelicolor* K113 was used to image the movement of Z rings by time-lapse microscopy in order to study the positioning and movement of FtsZ-EGFP in aerial hyphae. Coverslip-cellophane-grown cultures of *S. coelicolor* K113 were transferred to an imaging chamber, and aerial hyphae were identified by phase-contrast microscopy and subjected to time-lapse microscopy at 15-min intervals. In the absence of an agar plug, no further hyphal growth or development of aerial hyphae was seen, presumably due to hyphal dehydration or phototoxicity (data not shown). In order to maintain viability of aerial hyphae, it was necessary to apply a plug of tap water agar (Fig. 1). Despite this, the presence of tap water agar blocked the development of young aerial hyphae into spore chains and stimulated growth of substrate hyphae; we believe that the former was due to the premature disassembly of FtsZ-EGFP (Fig. 4; see Movie S4 in the supplemental material). If this is true, then it suggests that aerial hyphae have a means of sensing conditions inappropriate for sporulation and prevent its completion, either directly or indirectly, through the depolymerization of FtsZ-EGFP spirals. In older *S. coelicolor* K113 aerial hyphae, where there were no visible FtsZ-EGFP rings, presumably because they had already disassembled and initiated the laying down of divisional septa, is was possible for those aerial hyphae to complete the sporulation process and germinate (Fig. 5; see Movie S5 in the supplemental material).

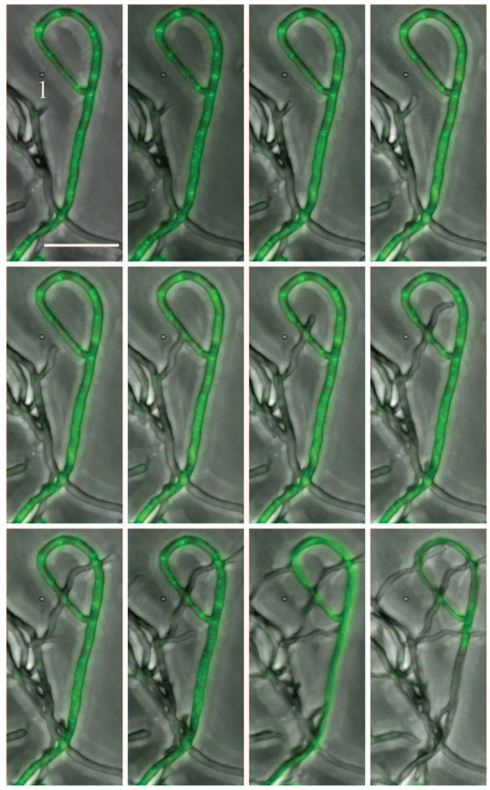

FIG. 4. Disassembly of FtsZ rings in aerial hyphae. Aerial hyphae of *S. coelicolor* K113 were grown on cellophane-covered coverslips for 36 h and transferred to imaging chambers. The mosaic image is composed of images taken at 30-min intervals, while Movie S4 in the supplemental material is composed of images taken at 15-min intervals. The horizontal white bar represents 10 μm. A hyphal tip activated for growth by transfer of the mycelium to the imaging chamber is labeled (1).

Septation, indicated by the regular invaginations, occurred simultaneously along the nascent spore chain proceeding through to the generation of mature spores that were subsequently able to undergo germination (Fig. 5; see Movie S5 in the supplemental material).

DISCUSSION

Time-lapse microscopy of *S. coelicolor* presents many challenges through its oxygen dependence, focal depth, mycelial heterogeneity, and agar-dependent sporulation. We have developed an imaging system allowing tracking of individual hyphae and proteins in conjunction with GFP that has overcome most of these difficulties through the use of an inverted microscope and agar plugs to flatten the mycelium as well as the provision of nutrients (13). Cellophane prevents hyphae from penetrating the agar plug and maintains the hyphae within a relatively narrow focal range, while the use of a motorized focus drive and the generation of Z sections means that phase-contrast images can be rendered in three dimensions to overcome the large focal depth required to image a mycelium. Finally, Ibidi μ-dishes allow the provision of oxygen to the mycelium.

In response to environmental and nutritional signals, *S.*

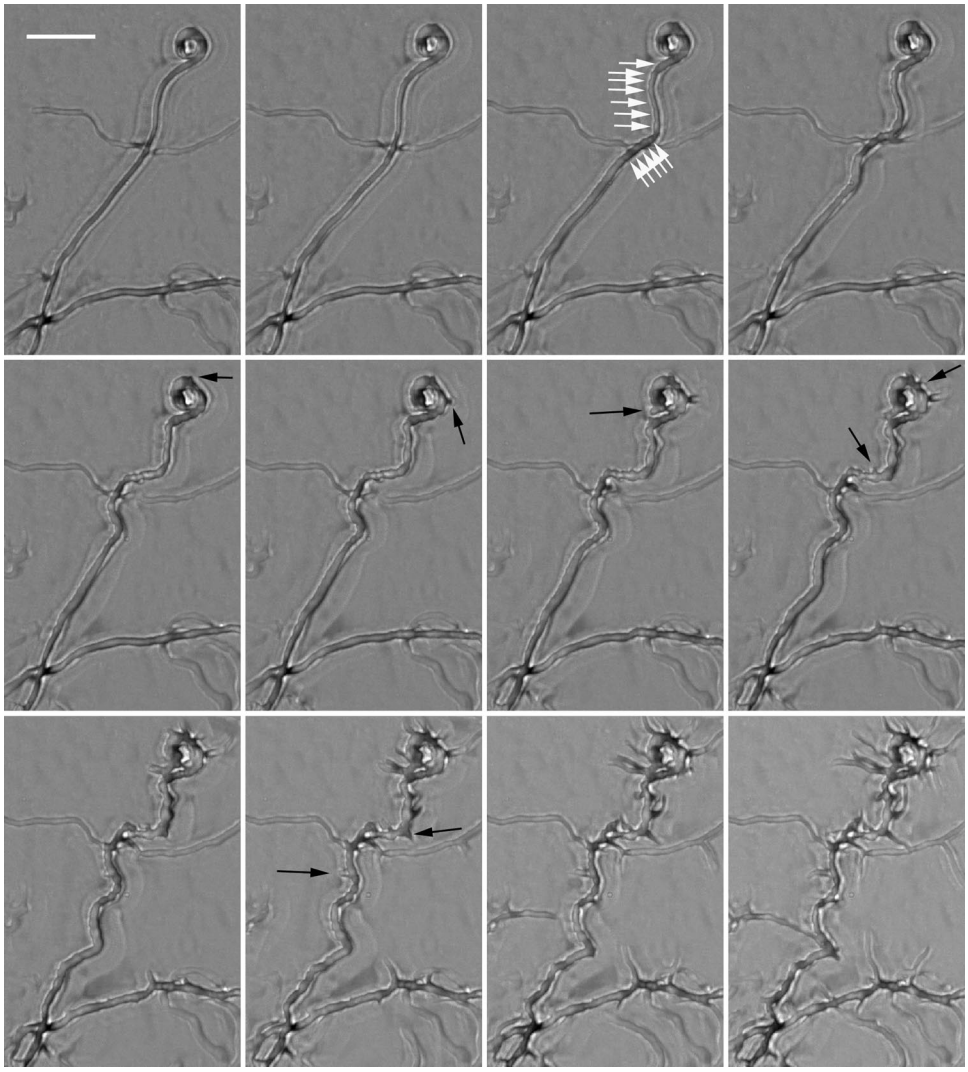

FIG. 5. Sporulation of *S. coelicolor* K113 aerial hyphae. Aerial hyphae of *S. coelicolor* K113 were grown on cellophane-covered coverslips for 36 h and transferred to imaging chambers. The mosaic image is composed of images taken at 30-min intervals while Movie S5 in the supplemental material is composed of images taken at 15-min intervals. The horizontal white bar represents 10 μm. White arrows show appearance of regular invaginations in the hyphal wall, characteristic of a forming spore chain. Black arrows show germinating spores.

coelicolor spores germinate following an initial increase in spore volume and differentiation of spore walls into an outer layer and an inner layer (14). The outer layer ruptures at the point(s) of germ tube emergence, while the inner layer forms the hyphal wall (27). The germ tube emerges to form an apical cell that grows by elongation through peptidoglycan synthesis, primarily at the hyphal tip (4, 6) but also to a lesser extent in subapical regions (9, 22), and is thought to be driven by hydrostatic pressure (23). The work reported here shows that if a second extension site develops close to the first, one of the extension sites is arrested for a period of time irrespective of whether the spore produces one or two germ tubes. The mechanism by which this arrest is achieved is not known; perhaps hyphal extension requires the presence of a nucleoid close to the tip and, as such, it is necessary for chromosome replication to take place before both tips possess an associated nucleoid and subsequently extend. Either chromosome replication or partitioning is associated with the earliest events of spore germination (12). Miguélez et al., (23) showed that in the presence of the peptidoglycan synthesis inhibitor vancomycin, DNA synthesis was arrested following the current round of replication, which suggests a close relationship between cell wall synthesis and chromosome replication. Even though Yang and Losick (30) were unable to find any evidence that DNA replication activity is concentrated at the apex, it seems likely that chromosome replication and segregation are linked with peptidoglycan incorporation, although the mechanisms by which this is achieved are unknown. The germinating spores of some *Streptomyces* species produce germination inhibitors (10) in order to inhibit extension of sibling germ tubes. It is thought that this provides a mechanism by which mass spore germination is prevented in order that potentially lethal mistakes in germination decisions are limited. *S. coelicolor* spores contain endogenous sources of nutrients such as trehalose (19, 20), and

it may be that growth arrest is a manifestation of a switch by the extending tip from an endogenous to an exogenous energy source or even a redeployment of nutrient resources within the microcolony. We were unable to generate movies of FtsZ-EGFP during germination, which is perhaps due to the inhibitory effects of light during spore germination seen in some streptomycete species (15). Following germination, hyphal extension occurred at a rate of ~20 μm h^{-1} and FtsZ-EGFP rings were laid down ~56 μm behind the growing tip. *Streptomyces granaticolor* lays down septa 28 μm from the hyphal tip (17), and as septum formation is dependent on the initial formation of a ring of FtsZ (26), it appears that either there is some variability in the frequency of septum formation between these two species or cultivation conditions affect septal frequency. It was thought that the subapical daughter compartment created a new extension site through branching (14) and this new apical cell was eventually partitioned from the subapical cell by a new septum. However, the movies presented here clearly show that branching occurs before rings of FtsZ-EGFP are laid down and septa form. While some branches do form FtsZ-EGFP rings at their bases, many do not. It may be that septa form at the bases of hyphal branches independently of FtsZ, but the movies presented here indicate that there is cytoplasmic continuity between many primary hyphae and their branches. Snapshot images of substrate hyphae stained with vancomycin-FL or FM4-64 show that many branches do not possess a septum at their base (data not shown). FtsZ-EGFP follows the extending hyphal tip at approximately the same speed (~20 μm h^{-1} in this system), which suggests that there is some form of association between the protein and extension site. Previous workers have shown that *ftsZ* mutants of *S. coelicolor*, although unable to sporulate, are able to support the growth and branching of substrate hyphae (7, 8, 21, 26). Both growth and branching of substrate hyphae occur before visible FtsZ-EGFP rings form, and it seems likely that the role of FtsZ in *S. coelicolor* substrate hyphae is to mark sites for septation. Perhaps the role of septa is to prevent cytoplasmic leakage in the event of a breach of the hyphal walls following a trauma such as phage lysis.

Although some streptomycetes can sporulate in liquid culture (14), the knowledge infrastructure available for *S. coelicolor* means that an imaging system capable of producing movies is essential for understanding the cell biology of this model organism. The system described here provides a means to do this to some degree. We were unable to image the erection of aerial hyphae and expect this to remain a recalcitrant problem due to repressive effects of the agar plug on the formation of aerial hyphae and the stimulatory effect on substrate hyphae following the transfer of coverslip-grown cultures to imaging chambers. Presumably the nutrients that supported growth of substrate hyphae in tap water agar came from action of the Dag protein that allows *S. coelicolor* to use agar as a nutrient source (2). Breaking of the surface tension by the action of SapB (29) is required for the erection of aerial hyphae by *S. coelicolor*, and it is not known whether aerial hyphae can be formed when they are trapped within the liquid phase; we have been unable to observe this. We believe that, as it was possible to image hyphae by phase-contrast microscopy, liquid from the agar plug permeated the cellophane and trapped any emerging aerial hyphae in the liquid phase. This prevented their further development and suggests that the ability of *S. coelicolor* to complete sporulation was dependent on the absence of hydration; if visible FtsZ-EGFP rings were seen in an aerial hypha at the time of their transfer to imaging chambers, hyphal maturation was blocked and FtsZ-EGFP rings disassembled (Fig. 4; see Movie S4 in the supplemental material). The simplest explanation for this is that aerial hyphae sense transfer from an aerial to a hydrated environment and signal FtsZ ring disassembly and developmental arrest. It is tempting to suggest that sensing of aerial growth may be through the sky pathway (3), where it is proposed that a signal molecule accumulates in the aerial hyphal wall and binds a sensor so that it can no longer diffuse into the medium and stimulates the expression of rodlin and chaplin genes. Perhaps, when aerial hyphae are transferred to an aqueous environment, diffusion of the signaling molecule not only prevents stimulation of *rdl* and *chp* expression, but also signals FtsZ ring disassembly. Despite this, in older hyphae, sporulation was able to proceed at least to the point where discrete, visible spores were visible (Fig. 5; see Movie S5 in the supplemental material), indicating the existence of point of no return beyond which sporulation cannot be blocked. Septation occurred simultaneously along the nascent spore chain, proceeding through to the generation of mature spores that were subsequently able to undergo germination (Fig. 5; see Movie S5 in the supplemental material). Understanding of this hyphal aging process, coupled with identification of the proteins that facilitate it, is essential to understanding the sequence of events during sporulation. In order to increase our understanding of the complex processes that underpin development of this complex bacterium, we will go on to refine this imaging system in order to "close the circle" with the aim of studying growth and protein trafficking during all stages of the *S. coelicolor* life cycle.

ACKNOWLEDGMENTS

This work was supported by BBSRC grant BB/D521657/1 and a University of Strathclyde Ph.D. studentship.

We are grateful to Klas Flärdh (Lund University, Sweden) for the provision of *S. coelicolor* K113. Helpful discussions with Nick Read (University of Edinburgh, United Kingdom) during development of the imaging system are gratefully acknowledged.

REFERENCES

1. **Allan, E. J., and J. I. Prosser.** 1983. Mycelial growth and branching of *Streptomyces coelicolor* A3(2) on solid medium. J. Gen. Microbiol. **129:**2029–2036.
2. **Bibb, M. J., G. H. Jones, R. Joseph, M. J. Buttner, and J. M. Ward.** 1987. The agarase gene (*dagA*) of *Streptomyces coelicolor* A3(2): affinity purification and characterization of the cloned gene product. J. Gen. Microbiol. **133:**2089–2096.
3. **Claessen, D., W. de Jong, L. Dijkhuizen, and H. A. B. Wösten.** 2006. Regulation of *Streptomyces* development: reach for ths sky! Trends Microbiol. **14:**313–319.
4. **Daniel, R. A., and J. Errington.** 2003. Control of cell morphogenesis in bacteria: two distinct ways to make a rod-shaped cell. Cell **113:**767–776.
5. **Elliot, M. A., M. J. Buttner, and J. R. Nodwell.** 2008. Multicellular development in *Streptomyces*, p. 419–438. *In* D. E. Whitworth (ed.), Myxobacteria: multicellularity and differentiation. ASM Press, Washington, DC.
6. **Flärdh, K.** 2003. Growth polarity and cell division in *Streptomyces*. Curr. Opin. Microbiol. **6:**564–571.
7. **Grantcharova, N., U. Lustig, and K. Flärdh.** 2005. Dynamics of FtsZ assembly during sporulation in *Streptomyces coelicolor* A3(2). J. Bacteriol. **187:**3227–3237.
8. **Grantcharova, N., W. Ubhayasekera, S. L. Mowbray, J. R. McCormick, and K. Flärdh.** 2003. A missense mutation in *ftsZ* differentially affects vegetative and developmentally controlled cell division in *Streptomyces coelicolor* A3(2). Mol. Microbiol. **47:**645–656.

9. **Gray, D. I., G. W. Gooday, and J. I. Prosser.** 1990. Apical hyphal extension in *Streptomyces coelicolor* A3(2). J. Gen. Microbiol. **136:**1077–1084.
10. **Grund, A. D., and J. C. Ensign.** 1985. Properties of the germination inhibitor of *Streptomyces viridochromogenes* spores. J. Gen. Microbiol. **131:**833–847.
11. **Han, L., A. Khetan, W.-S. Hu, and D. H. Sherman.** 1999. Time-lapsed confocal microscopy reveals temporal and spatial expression of the lysine ε-aminotransferase gene in *Streptomyces clavuligerus.* Mol. Microbiol. **34:** 878–886.
12. **Hardisson, C., M.-B. Manzanal, J.-A. Salas, and J.-E. Suàrez.** 1978. Fine structure, physiology and biochemistry of arthrospore germination in *Streptomyces antibioticus*. J. Gen. Microbiol. **105:**203–214.
13. **Hickey, P. C., D. J. Jacobson, N. D. Read, and N. L. Glass.** 2002. Live-cell imaging of vegetative hyphal fusion in *Neurospora crassa*. Fungal Genet. Biol. **37:**109–119.
14. **Hodgson, D. A.** 1992. Differentiation in actinomyctes. Soc. Gen. Microbiol. Symp. **47:**407–440.
15. **Imbert, M., and R. Blondeau.** 1999. Effect of light on germinating spores of *Streptomyces viridosporu*s. FEMS Microbiol. Lett. **181:**159–163.
16. **Kieser, T., M. J. Bibb, M. J. Buttner, K. F. Chater, and D. A. Hopwood.** 2000. Practical *Streptomyces* genetics. The John Innes Foundation, Norwich, United Kingdom.
17. **Kretschmer, S.** 1982. Dependence of the mycelial growth pattern of the individually regulated cell cycle in *Streptomyces granaticolor*. Z. Allg. Mikrobiol. **22:**335–347.
18. **Mazza, P., E. E. Noens, K. Schirner, N. Grantcharova, A. N. Mommaas, H. K. Koerten, G. Muth, K. Flärdh, G. P. van Wezel, and W. Wohlleben.** 2006. MreB of *Streptomyces coelicolor* is not essential for vegetative growth but is required for the integrity of aerial hyphae and spores. Mol. Microbiol. **60:**838–862.
19. **McBride, M. J., and J. C. Ensign.** 1987. Metabolism of endogenous trehalose by *Streptomyces griseus* spores or cells of other actinomycetes. J. Bacteriol. **169:**5002–5007.
20. **McBride, M. J., and J. C. Ensign.** 1990. Regulation of trehalose metabolism by *Sreptomyces griseus* spores. J. Bacteriol. **172:**3637–3643.
21. **McCormick, J. R., E. P. Su, A. Driks, and R. Losick.** 1994. Growth and viability of *Streptomyces coelicolor* mutant for the cell division gene *ftsZ*. Mol. Microbiol. **14:**243–254.
22. **Miguélez, E. M., C. Hardisson, and M. B. Manazanal.** 1993. Incorporation and fate of *N*-acetyl-D-glucosamine during hyphal growth in Streptomyces. J. Gen. Microbiol. **139:**1915–1920.
23. **Miguélez, E. M., C. Martín, M. B. Manazanal, and C. Hardisson.** 1992. Growth and morphogenesis in Streptomyces. FEMS Microbiol. Lett. **100:** 351–360.
24. **Noens, E. E., V. Mersinias, J. Willemse, B. A. Traag, E. Laing, K. F. Chater, C. P. Smith, H. K. Koerten, and G. P. van Wesel.** 2007. Loss of the controlled localization of growth stage-specific cell-wall synthesis pleiotropically affects developmental gene expression in an *ssgA* mutant of *Streptomyces coelicolor*. Mol. Microbiol. **64:**1244–1259.
25. **Reyes-Lamothe, R., C. Possoz, O. Danilova, and D. J. Sherratt.** 2008. Independent positioning and action of *Escherichia coli* replisomes in live cells. Cell **133:**90–102.
26. **Schwedock, J., J. R. McCormick, E. R. Angert, J. R. Nodwell, and R. Losick.** 1997. Assembly of the cell division protein FtsZ into ladder like structures in the aerial hyphae of *Streptomyces coelicolor*. Mol. Microbiol. **26:**847–858.
27. **Sharples, G. P., and S. T. Williams.** 1976. Fine structure of spore germination in actinomycetes. J. Gen. Microbiol. **96:**233–332.
28. **Van Keulen, G., J. Alderson, J. White, and R. G. Sawers.** 2007. The obligate aerobic actinomycte *Streptomyces coelicolor* A3(2) survives extended periods of anaerobic stress. Environ. Micobiol. **9:**3143–3149.
29. **Willey, J. M., A. Willems, S. Kodani, and J. R. Nodwell.** 2006. Morphogenetic surfactants and their role in the formation of aerial hyphae in Streptomyces coelicolor. Mol. Microbiol. **59:**731–742.
30. **Yang, M. C., and R. Losick.** 2001. Cytological evidence for association of the ends of the linear chromosome in *Streptomyces coelicolor*. J. Bacteriol. **183:** 5180–5186.